543865

Department of Spatial Sciences

Strategies for Estimating Atmospheric Water Vapour using Ground-based GPS Receivers in Australia

Agustan

This thesis is presented for the Degree of
Master of Science (Surveying and Mapping)
Curtin University of Technology

2004

Declaration

This thesis contains no material which has been accepted for the award of any other degree or diploma in any university.

To the best of my knowledge and belief this thesis contains no material previously published by any other person except where due acknowledgment has been made.

Date: 9th June 2004

ABSTRACT

The Global Positioning System (GPS) of navigation satellites was first developed for global navigation and position determination purposes. Signals from satellites are delayed by the Earth's neutral atmosphere on propagating to ground-based receivers, termed the tropospheric delay. Although an unwanted term for precise positioning, the tropospheric delay may be converted to atmospheric water vapour, which is a vital parameter for weather forecasting.

This research investigates the optimum GPS processing strategy to estimate atmospheric water vapour derived from ground-based GPS receivers particularly in the Australian region. For this purpose, GPS data observations from GPS permanent stations across Australia, mainly from the Australian Regional GPS Network, will be processed using scientific GPS software in post-processed mode and near real-time mode.

This research shows that by applying high accuracy GPS data processing, the tropospheric delay could be estimated precisely. The quality of GPS data processing is indicated by the station coordinates repeatability since the coordinates can gauge at least a coarse assessment of the ability of the processing method to estimate the tropospheric delay.

The precipitable water can be estimated from the wet component after separating the tropospheric delay into dry and wet components. High accuracy GPS data processing is dependent on the best choice of processing strategies, and the correct application of error-correction models and a priori constraints. This research finds that the GPS-PW estimation agrees with Radiosonde-PW estimation with an average of standard deviation at 2.5mm level for post-processed strategy and 2.8mm for near real-time strategy. The standard deviation of tropospheric parameter estimates is 1.1mm for post-processed strategy and 1.5mm for near real-time strategy.

ACKNOWLEDGEMENTS

First of all I would like to express my gratitude to Dr. Nigel Penna, my supervisor for his guidance, support and supervision whilst undertaking this research. From him, I have learnt so many things especially the techniques of estimating atmospheric water vapour by using ground-based GPS receivers.

Special thanks also go to A/Prof. Mike Stewart, my co-supervisor, who always gave me valuable advice; Prof. Will Featherstone, from whom I learnt many things about GPS data processing and 'research and scientific spirits'; Mrs. Lori Peterson and Mrs. Pam Kapica, for their help during my time in the Department of Spatial Sciences, and the Australian Bureau of Meteorology (BoM) for data permission enabling me to conduct this research

I would like to thank members of the Geodesy Group, whom I will never forget for we always met together every Friday afternoon; my fellow students in Geodesy laboratory: Sten, Simon, Irek and Xiaoli for the basket time; my fellow student, Deavi Purnomo for her friendship, help and badminton. The Bishopsgate family especially for Mr. Wahyudi and Mr. Monza Sukadis; Mr. Iwan Fals, Mr. Kho Ping Hoo and Mr. Jin Yong for entertainment during my research. Special thanks also go to Pak Swas and Joe for their valuable support.

Finally, I would like to thank my wife Devi Roza Krisnandhi, my son Almukantar Fikriansyah La Tinulu, my family: Bapak dan Ibu H. Kausar AS, Ayah dan Mammi di Rappocini, Ria Bunbun, Cece, Cici, Atto, Ana, Keluarga di Bogor, Jakarta dan Sulawesi. Thanks for all your support.

TABLE OF CONTENTS

Page

ABSTRACT i

ACKNOWLEDGEMENTS ii

TABLE OF CONTENTS iii

LIST OF FIGURES vii

LIST OF TABLES x

Chapter

1. INTRODUCTION 1

2. ATMOSPHERIC WATER VAPOUR AND ITS MEASUREMENT 5

2.1 The Atmosphere 5

2.2 Atmospheric Water Vapour Definition 7

2.3 The Importance of Measuring Water Vapour 8

2.4 Atmospheric Water Vapour Quantification 9

2.5 Techniques for Atmospheric Water Vapour Observation 10

2.5.1 Upward looking observations 12

2.5.2 Downward looking observations 15

2.5.3 Comparison of water vapour observation techniques 17

2.6 Summary 19

3. GPS FOR ESTIMATING ATMOSPHERIC WATER VAPOUR 21

3.1 Background of GPS for Meteorology 21

3.2 GPS Meteorology Initiatives Worldwide 24

3.3 Estimating Water Vapour from Ground-based GPS Observations 25

3.3.1 Tropospheric delay 26

3.3.2 Conversion from zenith wet delay to precipitable water 30

3.4 Error Sources and Processing Strategies for GPS Water Vapour Estimation 31

3.4.1 GPS orbit 31

3.4.2 Station coordinates 32

Chapter **Page**

3.4.3 Multipath and cycle slip errors 32
3.4.4 Tropospheric estimation interval and relative constraints 33
3.4.5 Antenna height 33
3.4.6 Antenna phase centre variations 33
3.4.7 Elevation mask 34
3.4.8 Mapping function and elevation-dependent weighting 34
3.4.9 Data processing overlap 35
3.4.10 Ocean tide loading effect 36
3.4.11 Atmospheric pressure loading 38
3.4.12 Earth body tides 39
3.4.13 Ambiguity resolution 39
3.4.14 Surface meteorological sensors 40
3.4.15 Error budget of PW estimates 40
3.5 The International GPS Service (IGS) 41
3.6 The International Terrestrial Reference Frame (ITRF) 44
3.7 Summary 45

4. GPS ESTIMATION OF ATMOSPHERIC WATER VAPOUR IN AUSTRALIA: METHOD, DATA SETS AND SOFTWARE 47
4.1 The Methodology 47
4.2 The Data Sets 48
4.2.1 The GPS data 49
4.2.2 Meteorological data 51
4.2.3 Co-location of GPS, Surface Meteorological and Radiosonde Stations 53
4.2.4 Precise satellite orbits 56
4.2.5 The ITRF coordinates 56
4.2.6 The ocean tide loading data 58
4.3 The Software 58
4.3.1 ADDNEQ Program in Bernese GPS Software 60
4.4 Summary 62

Chapter **Page**

5. STRATEGY TESTING FOR POST-PROCESSED GPS PRECIPITABLE WATER VAPOUR ESTIMATION 63
5.1 Post-Processed GPS-Water Vapour Estimation 63
5.1.1 Network configuration 65
5.1.2 Station coordinate constraints 68
5.1.3 Tests on observation sampling interval 69
5.1.4 Tests on elevation mask, weighting observation and mapping function 71
5.1.5 Ocean tide loading 76
5.1.6 Tropospheric interval and relative constraint estimates 79
5.1.7 Troposphere gradient parameter 82
5.1.8 Ambiguity resolution 83
5.1.9 Combination of best strategy in GPS data processing 85
5.2 Validation of Post-Processed Strategy with Radiosonde Data 86
5.2.1 Validation of GPS-PW estimation with radiosondes-PW estimation 86
5.3 Analysis 91
5.4 Summary 97

6. STRATEGY TESTING FOR NEAR REAL-TIME GPS PRECIPITABLE WATER VAPOUR ESTIMATION 98
6.1 Near Real-Time GPS-Water Vapour Estimates 98
6.1.1 Real-time ephemeris 99
6.1.2 Removing low accuracy satellites 105
6.1.3 Down-weighting low accuracy satellites 108
6.1.4 Estimating orbits strategy 110
6.2 Validation of Near Real-Time Strategy with Radiosonde Data 115
6.3 Analysis 116
6.4 Summary 118

7. CONCLUSIONS AND RECOMMENDATIONS 119

Page

REFERENCES 122
APPENDIX A: POST-PROCESSED GPS-PW ESTIMATES 133
APPENDIX B: NEAR REAL-TIME GPS-PW ESTIMATES 145
APPENDIX C: SATELLITE APRIORI SIGMA FOR DOWN-WEIGHTING STRATEGY 158
APPENDIX D: VISUALISATION OF GPS-PW ESTIMATES INTERPOLATION 162

LIST OF FIGURES

		Page
Figure 2.1	The Atmosphere	5
Figure 2.2	The Structure of the Atmosphere	6
Figure 2.3	Phase Changes of Water	8
Figure 2.4	The Hydrological Cycle	9
Figure 2.5	Classification of Water Vapour Observation Techniques	11
Figure 2.6	Radiosonde with a Balloon Instrument Platform	13
Figure 2.7	Water Vapour Radiometer	14
Figure 3.1	GPS Techniques for Estimating Atmospheric Water Vapour	23
Figure 3.2	Satellite-Satellite Based Method	23
Figure 3.3	Refracted GPS Signal by Atmospheric Delays	26
Figure 3.4	Zenith Total Delay Illustration	29
Figure 3.5	Summary of Estimating Precipitable Water Vapour	46
Figure 4.1	The GPS Station Configuration	50
Figure 4.2	The GPS Station Data Availability	51
Figure 4.3	The Configuration of GPS and RCS around Australia	52
Figure 4.4	Data Processing Steps in the Bernese GPS Software	60
Figure 5.1	Ausclus-1 Configuration	67
Figure 5.2	Ausclus-2 Configuration	67
Figure 5.3	Baseline Lengths	68
Figure 5.4	Comparison of Height Recoveries for Darwin and Hobart on Applying a 180 second Sampling Interval Observation	71
Figure 5.5	Comparison of Height Recoveries for Darwin on Applying Elevation-dependent Weigting	75
Figure 5.6	Comparison of Height Recoveries for Hobart on Applying Elevation-dependent Weigting	75
Figure 5.7	The Effects of the OTL models for the Height Recovery at Darwin	78
Figure 5.8	The Effects of the OTL models for the Height Recovery at Karratha	78

Page

Figure 5.9	Detail Effects of the OTL models for the Height Recovery at Karratha	79
Figure 5.10	The Effect of the Tropospheric Estimation Interval and Relative Constraint to the Mean Repeatability of the Height Component	82
Figure 5.11	GPS-PW Estimates for Perth from Different Fixed Station Configurations	89
Figure 5.12	GPS-PW Estimates for Darwin from Different Fixed Station Configurations	89
Figure 5.13	GPS-PW Estimates and Radiosonde-PW Estimates for Alice Springs	91
Figure 5.14	Horizontal Distance between GPS stations to Surface Meteorological Stations, Radiosonde Stations and the σ of GPS-Radiosonde PW Estimates	94
Figure 5.15	Vertical Differences between GPS stations to Surface Meteorological Stations, Radiosonde Stations and the σ of GPS-Radiosonde PW Estimates	95
Figure 6.1	Coordinates Recovery for Ceduna	101
Figure 6.2	Coordinates Recovery for Darwin	101
Figure 6.3	Coordinates Recovery for Hobart	102
Figure 6.4	Coordinates Recovery for Karratha	102
Figure 6.5	Coordinates Recovery for Perth	103
Figure 6.6	Coordinates Recovery for Townsville	103
Figure 6.7	The Accuracy Code of the IGU Orbits	106
Figure 6.8	The Percentage of the Average Satellite's Accuracy Code in 120 Days	106
Figure 6.9	The Height Improvement for Townsville by Removing Low Accuracy Satellites	107
Figure 6.10	The Height Improvement for Townsville by Down-Weighting Strategy	110
Figure 6.11	The Set of the Orbital Elements	111
Figure 6.12	The Process of Estimating Orbits Strategy	112

Page

Figure 6.13 Example of the Difference of the Satellite Position at the Particular Epoch between the Original IGU Orbit and the Updated IGU Orbit 113

Figure 6.14 The Height Improvement for Townsville by Estimating Orbit Strategy 114

Figure 6.15 Comparisons of Strategies for Improving Orbital Quality 114

LIST OF TABLES

		Page
Table 2.1	Average Composition of the Atmosphere	7
Table 2.2	Characteristics of Radiosonde type Vaisala RS80 Sensors	12
Table 2.3	Summary of Radiosonde Platforms	13
Table 2.4	Summary of Atmospheric Water Vapour Observation	18
Table 3.1	Main Tidal Constituents	37
Table 3.2	Ocean Tide Loading Models	38
Table 3.3	Error Budget for Ground-based GPS-PW Estimates	41
Table 3.4	The IGS Analysis Centres	43
Table 3.5	The IGS Products	43
Table 4.1	The GPS Stations Site Equipment	50
Table 4.2	Co-location of GPS Stations and Surface Meteorological Stations	53
Table 4.3	Distance between GPS Stations and Radiosonde Stations	55
Table 4.4	The ITRF2000 Station Coordinates and Velocities	57
Table 5.1	Summary of GPS Post-Processed Strategies for PW Estimation	64
Table 5.2	Tests on Sampling Interval Observation	70
Table 5.3	The Repeatability of Tests on 5 Degrees Elevation Mask with No Elevation-Dependent Weighting	72
Table 5.4	The Repeatability of Tests on 5 Degrees Elevation Mask with Elevation-Dependent Weighting	72
Table 5.5	The Repeatability of Tests on 10 Degrees Elevation Mask with No Elevation-Dependent Weighting	73
Table 5.6	The Repeatability of Tests on 10 Degrees Elevation Mask with Elevation-Dependent Weighting	73
Table 5.7	The Repeatability of Tests on 15 Degrees Elevation Mask with No Elevation-Dependent Weighting	74
Table 5.8	The Repeatability of Tests on 15 Degrees Elevation Mask with Elevation-Dependent Weighting	74
Table 5.9	The Repeatability of the Northing Component from OTL Tests	76
Table 5.10	The Repeatability of the Easting Component from OTL Tests	77

		Page
Table 5.11	The Repeatability of the Height Component from OTL Tests	77
Table 5.12	The Height Repeatability of the Tests on 15 Minutes Tropospheric Estimation Interval and Relative Constraint	80
Table 5.13	The Height Repeatability of the Tests on 30 Minutes Tropospheric Estimation Interval and Relative Constraint	80
Table 5.14	The Height Repeatability of the Tests on 60 Minutes Tropospheric Estimation Interval and Relative Constraint	81
Table 5.15	The Height Repeatability of the Tests on 120 Minutes Tropospheric Estimation Interval and Relative Constraint	81
Table 5.16	The Height Repeatability of the Tests on 180 Minutes Tropospheric Estimation Interval and Relative Constraint	81
Table 5.17	The Effect of the Troposphere Gradient Estimates	83
Table 5.18	Ambiguity Test Results	84
Table 5.19	The Average Baseline Length and the Height Repeatability	84
Table 5.20	The Improvement of the Station Coordinates Repeatability	86
Table 5.21	Tests on Different Fixed Station Configurations	88
Table 5.22	Comparison of GPS-PW Estimates and Radiosonde-PW Estimates	90
Table 5.23	The Quality of Tropospheric Parameter Estimates	92
Table 5.24	Summary of Post-Processed GPS-PW Estimates	93
Table 5.25	Statistics of Conversion Factor	96
Table 6.1	The Repeatability from GPS Data Processing by Using IGU Orbits	100
Table 6.2	Bad Sessions for Non-Fixed GPS Stations	104
Table 6.3	The Repeatability after Removing the Outliers	104
Table 6.4	Comparison of Original IGU Orbits and Removing Low Accuracy Satellites	107
Table 6.5	Value of Sigma Weight Based on the Kruse Formula	109
Table 6.6	Comparison of Original IGU orbits and Weighting Low Accuracy Satellites	109
Table 6.7	Comparison of Original IGU orbits and Estimating Orbits	113
Table 6.8	Station Coordinates Repeatability in Near Real-Time Mode	115

		Page
Table 6.9	Comparison of NRT-GPS-PW and Radiosonde-PW	116
Table 6.10	The Quality of the Tropospheric Parameter Estimates in Near Real-Time Mode	117

Chapter 1

INTRODUCTION

The Global Positioning System (GPS) can now be used to determine the location of an object on the Earth's surface to millimetre accuracy using differential techniques. This is possible due to hardware developments and much research in GPS data processing techniques. Such research includes the ability to mitigate errors that can otherwise reduce the accuracy of data processing results.

One of the error sources in GPS positioning comes from the atmosphere through which GPS signals propagate from GPS satellites to GPS receivers. However, since the atmosphere consists of different gases, which have the ability to affect the GPS signal propagation, it is one of the error contributors in GPS data, and is known as the atmospheric delay. Therefore, much GPS data processing research has dealt with the treatment of atmospheric delay. At GPS signal frequencies, it can be considered as two parts, the ionospheric delay and neutral atmospheric delay.

The ability to estimate neutral atmospheric delay brings GPS into use in the field of meteorology, since its estimated delay may be converted to determine atmospheric water vapour. The atmospheric water vapour is the element that determines humidity and is also related to precipitation. Therefore, atmospheric water vapour plays an important role in meteorology. In addition, atmospheric water vapour itself is a major greenhouse gas, which is related to global warming. This research aims to assess the ability of GPS to measure water vapour in the Australian atmosphere.

Traditionally, atmospheric water vapour has been measured using radiosondes, water vapour radiometers (WVRs) and a special sensor microwave / imager (SSM/I) (Brock and Richardson, 2001). Radiosondes provide in-situ measurements and good vertical resolution (Bevis *et al.*, 1992), however they are expensive and offer limited global coverage (Liou *et al.*, 2001). The advantages of WVRs are their high accuracy and continuous temporal resolution. However, they are costly and not portable (Dodson *et al.*, 1996), provide poor spatial coverage and are unable to operate during moderate to heavy rain (Liou *et al.*, 2001). As an alternative, ground-based GPS

receivers can be used (Bevis *et al.*, 1992; Duan *et al.*, 1996; Ware *et al.*, 1997; Tregoning *et al.*, 1998; and Liou *et al.*, 2001). Ground-based GPS receivers have the capacity to provide continuous water vapour estimates in all weathers, at relatively low cost, and with a spatial resolution based on the number of GPS receivers and their configuration.

Since the 1990s, much research around the world has been conducted to determine the best strategy of estimating atmospheric water vapour from GPS. For example, GPS/MET (Global Positioning System/Meteorology) and GPS-IPW (Global Positioning System-Integrated Precipitable Water) projects in the USA, WAVEFRONT (Water Vapour Experiment For Regional Operational Network) project in Europe, MAGIC (Meteorological Applications of GPS Integrated Column Water Vapor Measurement) in the Western Mediterranean, GASP (GPS Atmospheric Sounding Project) in Germany, and the GPS Meteorology project in Japan. On the other hand, little work has been done on estimating atmospheric water vapour from GPS in Australia, with the first research detailed by Tregoning *et al.* (1998) and Feng *et al.* (2001).

The neutral atmospheric delay, which affects the GPS signals, is the total delay that is caused by the atmospheric layers that are electrically neutral at GPS signal frequencies. The troposphere is the lowest layer of the atmosphere which extends from the Earth's surface to a height of approximately 14km. This layer contributes approximately 75 to 80 percent of the total neutral atmospheric delay and is often simply known as the tropospheric delay.

GPS data processing can estimate the tropospheric delay and by using surface temperature and pressure data, this quantity can be converted to total precipitable water (PW). Total PW can be defined as the integral of absolute humidity along the vertical direction and it is used in meteorology and hydrology to quantify atmospheric water vapour (Pugnaghi *et al.*, 2002).

Initial studies showed that total PW could be estimated from GPS to an accuracy of 1-2mm (Rocken *et al.*, 1995). It was demonstrated that GPS networks can estimate PW with a temporal resolution of 30 minutes or better and the root mean square

(RMS) differences between GPS-derived PW and WVR-derived PW, varied between 1.15 and 1.45 mm (Duan *et al.*, 1996). In Europe, the suitability of GPS for routinely estimating PW during varying climatic conditions was tested in the WAVEFRONT project. The results showed that PW could be routinely estimated in a post-processed mode to an accuracy of 1-2mm (Dodson *et al.*, 1999). However, such quality estimates were obtained from temperate climates, and may not be entirely valid in Australia that has a range of climates including tropical, desert, temperate, Mediterranean and polar (in the Australian Antarctic Territory).

In order to benefit meteorological forecasting, the GPS-PW estimates must be available within near real-time (Baker *et al.*, 2001). Hence studies are now focusing on this issue. For example, the 'SuomiNet Project' (Ware *et al.*, 2000) in USA was developed to estimate PW continuously, accurately, in all weathers, and in near real-time. This project also has potential applications in coastal meteorology, providing ground truth for satellite radiometry.

The major problem in near real-time estimation is the quality of the satellite orbital data. Post-processed studies have been conducted using post-processed satellite orbits available through the International GPS Service (IGS), which are known as IGS final orbits. These have an accuracy of 5cm, however they are available after 2 weeks (IGS, 2002). To address real-time work, the IGS produce an orbit that is available in near real-time called the IGS Ultra Rapid (IGU) orbit which is delivered twice a day. However its accuracy is about 25cm (IGS, 2002).

Previous studies found that some strategies can be applied to improve the quality of real-time orbits, such as the IGU orbits. These strategies are the removal of data for the low accuracy ('bad') satellites from the solution (Dodson and Baker, 1998); using a down-weighting strategy for 'bad' satellites rather than removing them (Kruse *et al.*, 1999); and by improving satellite orbital parameters from GPS data (Ge *et al.*, 2001). Currently, in the USA, Europe and Japan, the GPS-PW estimates in near real-time mode are ready to be used in weather forecasting.

This research investigates the possibility of applying GPS as a technique to estimate PW in the Australian region, by using a continuous GPS data set from January 2001

until April 2001, from 20 GPS permanent stations distributed across the Australian region. The data set was processed using Bernese Version 4.2 software (Hugentobler *et al.*, 2001). Most of these GPS stations are part of the Australian Regional GPS Network (ARGN), maintained by the National Mapping Division of Geoscience Australia and other GPS stations around Australia whose data are freely available. These data were used to determine the optimum GPS post-processed strategy for estimating PW from ground-based GPS receivers across Australia, and also to determine the techniques for estimating atmospheric water vapour in near real-time mode derived from ground-based GPS receivers across Australia.

This thesis is composed of seven chapters. Chapter 1 is the introduction and an overview of the atmosphere. Details of the importance and the role of water vapour is given in Chapter 2. Some water vapour terminology and atmospheric water vapour observation techniques are also described. In Chapter 3, fundamental concepts of GPS estimation of atmospheric water vapour are introduced, focusing on the zenith tropospheric delay and its relation to atmospheric water vapour. A literature review is provided to show the development of GPS for estimating atmospheric water vapour to date.

Chapter 4 describes the methodology, the data sets and the software used in this research to estimate atmospheric water vapour using ground-based GPS receivers in Australia. The post-processed tests are then described in Chapter 5 and present the results of a post-processed strategy for estimating atmospheric water vapour using ground-based GPS receivers. This chapter also presents the validation of atmospheric water vapour estimates from GPS data processing with atmospheric water vapour estimates from radiosondes.

Chapter 6 presents the results of a near real-time strategy for estimating atmospheric water vapour using ground-based GPS receivers. Similar to Chapter 5, this chapter also presents the validation of atmospheric water vapour estimates from near real-time GPS data processing with atmospheric water vapour estimates from radiosondes. Finally, Chapter 7 summarises the research with conclusions and recommendations for further work.

Chapter 2

ATMOSPHERIC WATER VAPOUR AND ITS MEASUREMENT

This chapter describes aspects of atmospheric water vapour including the atmospheric structure and composition, water vapour definition and why it should be measured. Several water vapour observation techniques that have been developed are also reviewed.

2.1. The Atmosphere

The atmosphere can be considered the whole mass of air surrounding the Earth. It lies from the Earth's surface to approximately 10,000km above it. (See Figure 2.1)

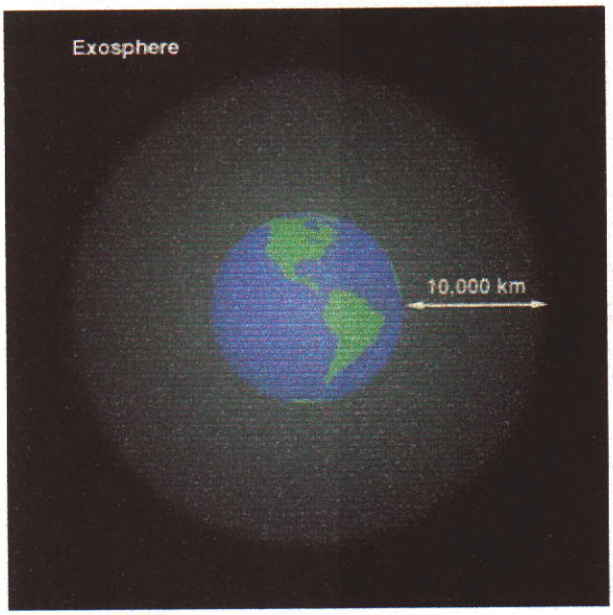

Figure 2.1 The Atmosphere (Kempler, 2000)

According to its temperature structure, the atmosphere is divided into four layers, namely the troposphere, stratosphere (including ozone layer), mesosphere, and ionosphere (thermosphere). The temperature profile depends on the altitude and is different for each layer. Between each layer, there is a zone where the temperature profile is relatively constant. These in-between zones are named after the layer below

with some modification from the word -sphere to -pause. For example, between the troposphere and the stratosphere, ie above the troposphere, there is a zone called the tropopause. Figure 2.2 illustrates the structure of the atmosphere.

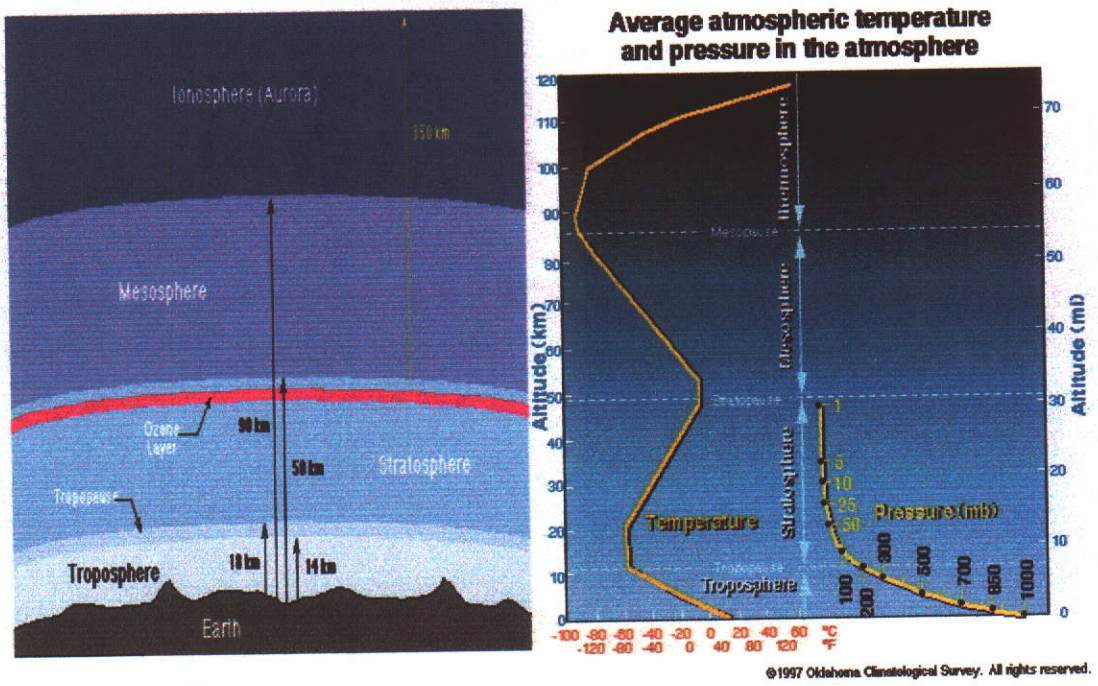

Figure 2.2 The Structure of the Atmosphere
(Guidry *et al.*, 2001 and Droegemeier, 2002)

The atmosphere has an electrically active part contained in the ionosphere and mesosphere; and an electrically neutral part contained in the troposphere and the stratosphere (Gabor, 1997). Because around 75 percent of the total molecular and gaseous masses of the atmosphere, including the atmospheric water vapour (Barry and Chorley, 1989), are found in the troposphere layer, the neutral part of the atmosphere is therefore often simply referred to as the troposphere. This research from now on will use this term (i.e. the troposphere as the neutral atmosphere which consists of the troposphere and the stratosphere).

2.2. Atmospheric Water Vapour Definition

In simple terms, the atmospheric water vapour can be defined as water in a gaseous state, especially when diffused as a vapour in the atmosphere and at a temperature

below boiling point. Water vapour enters the air by the evaporation and sublimation processes. Soil, lakes, streams, rivers and ocean surfaces are the contributors to the evaporation process, whereas ice in glaciers and transpiration from plant leaves are the contributors to the sublimation process. The main contribution for water vapour in the atmosphere comes from evaporation from ocean surfaces, which accounts for approximately 85 percent of the process (Jacobson, 1999).

By volume, about 4 percent of the atmosphere is water vapour, but it is not evenly distributed around the globe. Table 2.1 shows that the volume of water vapour is not fixed. Its distribution depends on pressure, density and air temperature, which vary with latitude, longitude and season.

Gas	Per cent by volume
Fixed Gases	
Nitrogen	78.08
Oxygen	20.95
Argon	0.93
Neon	0.0015
Helium	0.0005
Krypton	0.0001
Xenon	0.000005
Variable Gases	
Water Vapour	0.00001 to 4.0
Carbon dioxide	0.029 to 0.036
Methane	0.00009 to 0.00017
Ozone	0.000003 to 0.001

Table 2.1 Average Composition of the Atmosphere (Jacobson, 1999)

2.3. The Importance of Measuring Water Vapour

Water can be found in three different states: liquid, solid and gas. Water vapour in the atmosphere is a presentation of water in gaseous form and plays an important role in the greenhouse effect because it absorbs infra-red radiation. Jacobson (1999) also

states that water vapour is one of the chemical reactants and a carrier of latent heat. Previous studies concluded that water vapour could not be separated from the hydrological cycle and climate of the Earth's system (American Geophysical Union, 1995). Moreover, the Infrared Measurements and Water Vapour Studies Group at NASA (National Aeronautics and Space Administration) found that detailed water vapour observations are essential to the improved analysis and prediction of convective storms (Infrared Measurements Group, 2002).

As a chemical reactant and latent heat carrier, water vapour operates by its changing phases. It can change to liquid or solid, conversely liquid or solid water in the atmosphere can also change to a vapourised state. Latent heat is a kind of energy, which is produced from energy released during condensation, freezing and deposition of a substance; or energy absorbed during evaporation, melting and sublimation (Jacobson, 1999). Figure 2.3 shows the phase changes of water in the atmosphere.

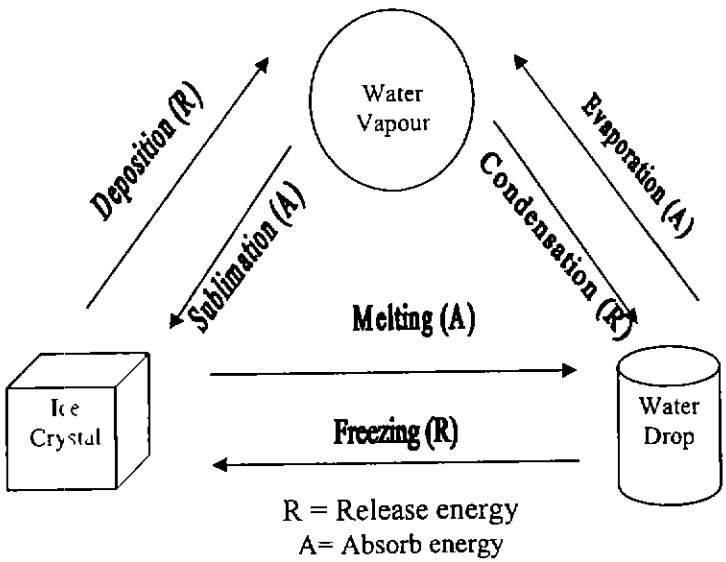

Figure 2.3 Phase Changes of Water (Summarised from Jacobson, 1999)

Water vapour also plays an important role in the hydrological cycle (illustrated in Figure 2.4) which may be defined as the sequence of conditions through which water passes from vapour in the atmosphere through precipitation upon land or water surfaces and ultimately back into the atmosphere as a result of evaporation and

transpiration (Merriam-Webster, 1936). Water vapour maintains the balance of the water cycle through the processes shown in Figure 2.3. The hydrological cycle supplies fresh water from the salty water of the oceans through evaporation. Therefore, water vapour has a direct benefit to mankind as a fresh water supplier. Unfortunately however, according to the Infrared Measurements and Water Vapour Studies Group at NASA, water vapour is poorly measured on a global scale, particularly in the upper-troposphere (altitude 2-8km) (Jaegle *et al.*, 1999).

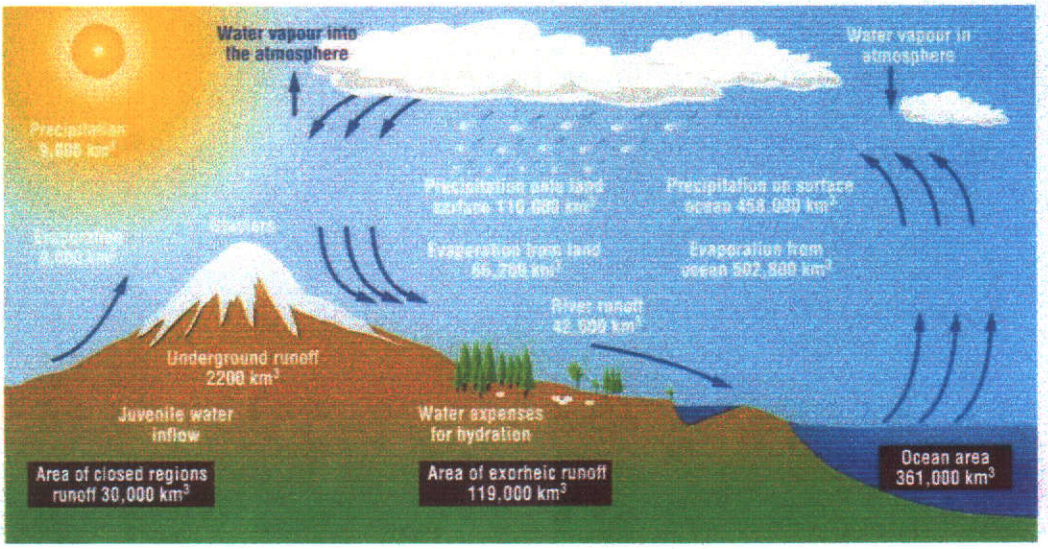

Figure 2.4 The Hydrological Cycle
(Source: http://www.unesco.org/science/waterday2000/Cycle.htm)

2.4. Atmospheric Water Vapour Quantification

For meteorological studies, atmospheric water vapour is usually quantified by measuring the total atmospheric water vapour contained in a vertical column of unit cross-sectional area, extending from the Earth's surface to the top of the atmosphere. This parameter is known as total precipitable water (PW). PW is commonly expressed in terms of the height at which that water substance would stand if completely condensed and collected in a vessel of the same unit cross section. Similarly, Bevis *et al.* (1992) quantified the atmospheric water vapour above the Earth's surface as the vertical integrated mass of water vapour per unit area, or as the height of an equivalent column of liquid water. In addition, Pugnaghi *et al.* (2002) also quantified the PW as the integral of the absolute humidity ρ_v (or water vapour

density) along the vertical direction. The water vapour density is defined as the mass of water vapour in a unit volume of air. It is a measure of the actual water vapour content of the air and generally expressed in grams per cubic metre or kg/m^3 (Linacre and Geerts, 1997 and Crowder, 2000). This term is usually known as Integrated Water Vapour (IWV).

PW is usually expressed in mm whereas IWV is usually expressed in kg/m^2. Therefore to convert IWV to PW, simply divide the amount of water vapour content by the density (ρ) of water (Bevis *et al.*, 1992). In practice, 1 kg/m^2 of IWV corresponds to 1 mm of PW (Pugnaghi *et al.*, 2002).

2.5. Techniques for Atmospheric Water Vapour Observation

Basically, there are two types of atmospheric water vapour observation: in-situ observation techniques and remote sensing observation techniques. Remote sensing observation techniques consist of two different observation sensors, namely active and passive sensors. The difference between them is the active sensor is designed to transmit and receive radiation, whereas the passive sensor is designed only to receive radiation emitted by objects.

For in-situ water vapour measurement techniques, all instruments are placed on the ground surface. However, for upper air observations, (the portion of the atmosphere that is above the lower troposphere, generally 850 hPA or about 1500m above sea level (NetCent Communication, 2003)), all sensor instruments are carried by different platforms, for example, balloons, rockets and aeroplanes. The radiosonde is an example of an in-situ observation technique and uses a balloon as the instrument carrier platform.

Remote sensing techniques use imaging (scanning) and sounding as a principal method for observing water vapour in the atmosphere. Sounding can be defined as a plot of the vertical variations of observed weather elements made above a station, from energy radiation, whether it comes from active or passive sensors. These variations come from the abilities of gases to absorb radiation, which differ from one to another. All weather satellite systems, for example the NOAA (National Oceanographic and Atmospheric Administration) satellite system, are examples of remote sensing observation techniques. Figure 2.5 illustrates the classification of water vapour observation techniques.

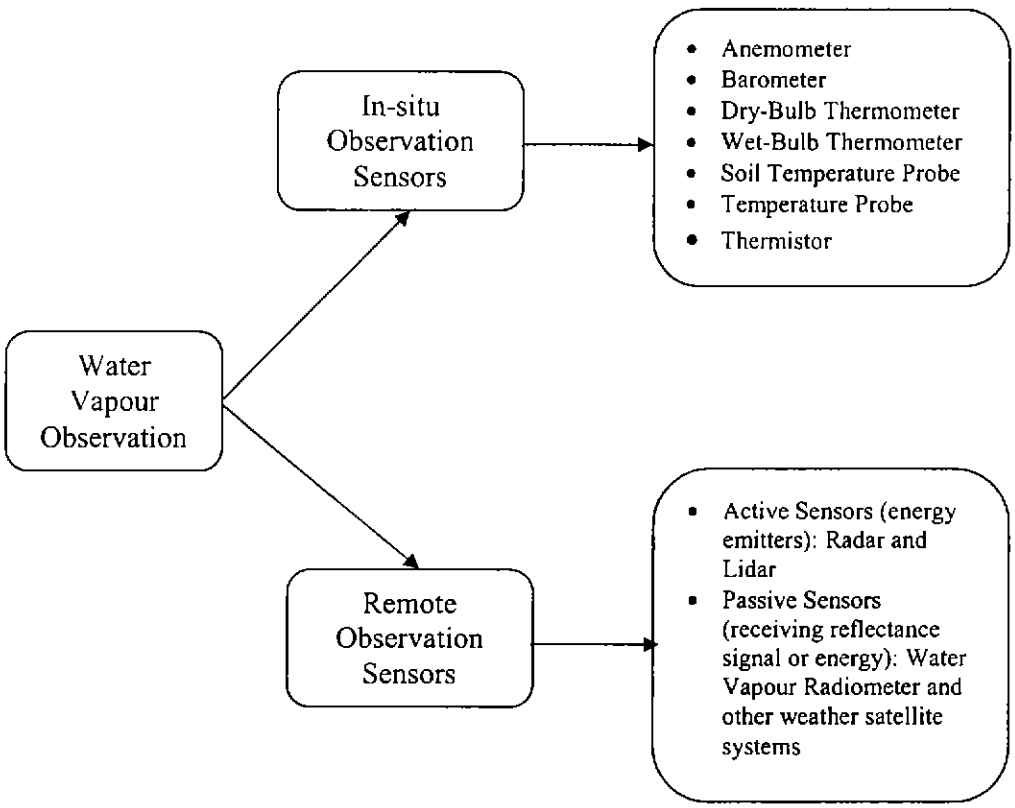

Figure 2.5 Classification of Water Vapour Observation Techniques

Another classification of water vapour observation techniques is the perspective approach. There is the 'upward looking' approach, which measures the water vapour from the Earth's surface upward. Secondly, there is the 'downward looking' approach, which measures the water vapour from a satellite or other instrument in the atmosphere, to the Earth's surface or ground station.

2.5.1 Upward looking observations

Radiosondes

The radiosonde is one of the most popular water vapour in-situ observation techniques. It comprises a group of instruments for simultaneous measurement and radio transmission of meteorological data, including temperature, pressure and humidity in the atmosphere. Usually, these instruments are carried into the atmosphere by a balloon filled with helium or hydrogen.

The radiosonde contains instruments capable of making direct in-situ measurements of air temperature, humidity and pressure, with changing height, typically to altitudes of approximately 27,400m. Therefore, there are three main components in the radiosonde: the pressure, temperature and humidity sensors. A radio transmitter located within the instrument package transmits observed data immediately to the ground station. The ascent of a radiosonde also provides an indirect measure of the wind speed and direction at various levels throughout the troposphere.

The characteristics and configuration of the instruments comprising the radiosonde depend on its type. An example of radiosonde characteristics (type Vaisala RS80 that is operated by the British Atmospheric Data Centre) can be seen in Table 2.2, and Figure 2.6 shows an example of a radiosonde package.

Sensor	***Measuring Range***	***Resolution***	***Accuracy***	***Lag***
Pressure Sensor	3mb to 1060mb	0.1mb	+/- 0.5mb	-
Temperature Sensor	-90^0C to $+60^0$C	0.1^0C	+/- 0.2^0C	< 2.5s (with conditions: velocity 6ms^{-1}, and pressure 1000mb)
Humidity Sensor	0% to 100% relative humidity (RH)	1% RH	+/- 2% RH	< 1s (with conditions: velocity 6ms^{-1}, pressure: 1000mb, and temperature 20^0C)

Table 2.2 Characteristics of the Vaisala RS80 Radiosonde

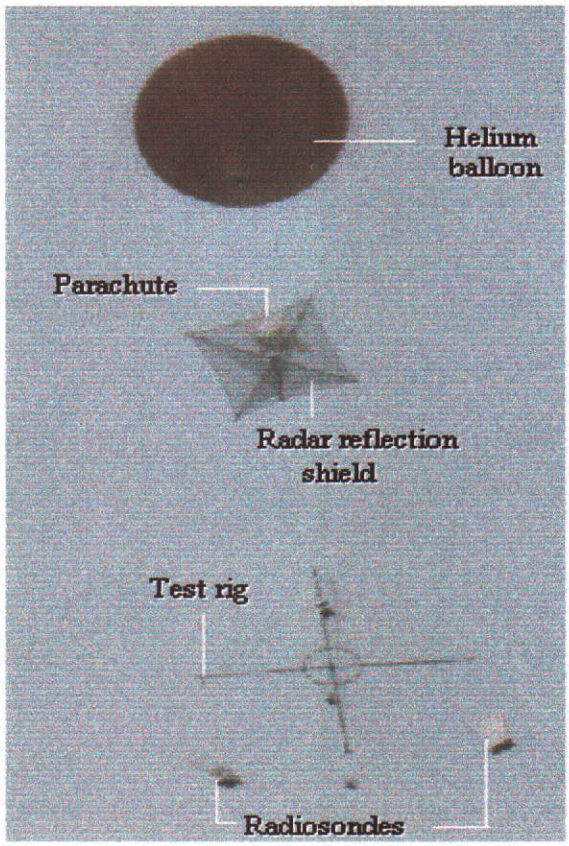

Figure 2.6 Radiosonde with a Balloon Instrument Platform
(British Atmospheric Data Centre, 2002)

Other platforms used to carry the instrument package are aeroplanes and rockets. Each platform has advantages and disadvantages which are summarised in Table 2.3.

Observation Platform	*Advantages*	*Disadvantages*
Balloons	The least expensive in-situ measurement	Very poor temporal and spatial resolution
Aeroplanes	Excellent in spatial and temporal resolution. The paths are fully controlled	Vertical profile data are not obtained if commercial aeroplanes are used, since there is no observation during take off and landing.
Rockets	Can achieve higher altitudes compared to balloons and aeroplanes.	Expensive

Table 2.3 Summary of Radiosonde Platforms (Brock and Richardson, 2001)

Water Vapour Radiometer

Radiometers passively measure the intensity of electromagnetic energy at certain frequencies. By scanning and measuring the brightness temperature, which depends on the surface temperature, sky temperature and surface dielectric constant (index of refraction), water vapour can be observed. A water vapour radiometer uses energy radiation at high frequencies, usually between 23.8 and 31.4 GHz, and consists of an antenna or scanning mechanism, a receiver, and a data handling system. Figure 2.7 shows a water vapour radiometer.

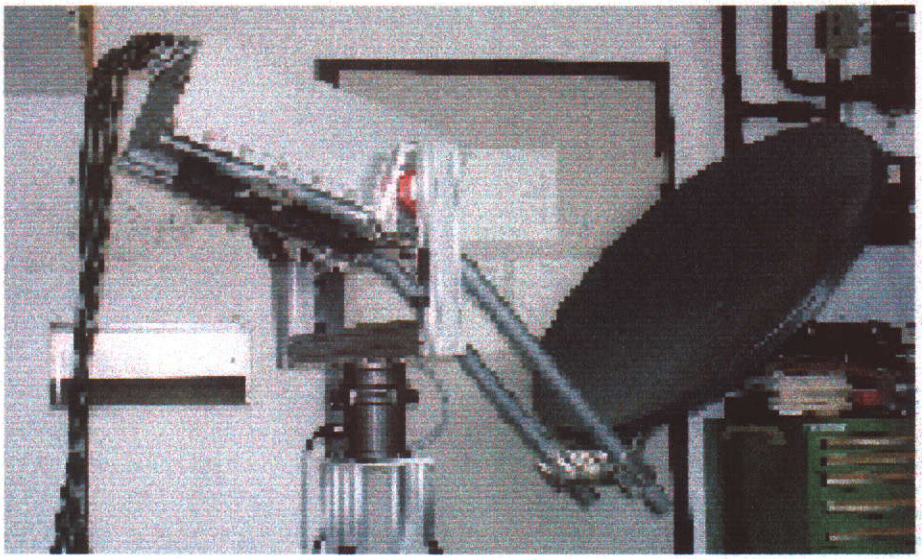

Figure 2.7 Water Vapour Radiometer (Roy, 2002)

Global Positioning System

Another upward looking atmospheric water vapour observation technique is the Global Positioning System (GPS). GPS is a satellite-based radio positioning system which has been developed and operated by the U.S. Department of Defense (DoD), and mainly used for positioning and navigation. The GPS consists of three segments (Kaplan, 1996), namely:

- The space segment; comprising the satellites and transmitted signals
- The control segment; ground facilities that maintain and control the space segment
- The user segment; including equipment, computational techniques and users

GPS can be used to determine positions anywhere on Earth to millimetric accuracy given sufficient data and data processing techniques. One of the important factors that determines the accuracy of position is the quality of GPS signals. These signals transmitted by GPS satellites and recorded by GPS receivers have been delayed when they propagate through the atmosphere. This delay is known as the atmospheric delay, which can be considered as 2 parts, ionospheric delay (about 10 – 100 m of delay) and neutral atmospheric delay (about 2.3 – 30 m of delay). About 75 to 80 percent of the neutral atmospheric delay is due to the troposphere layer. Therefore, as mentioned in Chapter 1, in this research, the neutral atmospheric delay is simply known as the tropospheric delay. The tropospheric delay is caused by a non-dispersive effect from the atmospheric molecular and gaseous, including the water vapour. Therefore, by assessing the tropospheric delay, the atmospheric water vapour can be quantified.

2.5.2 Downward looking observations

Downward looking water vapour observations are mainly based on weather satellite systems. A weather satellite is an orbiting platform upon which instruments are placed for the observation of weather systems and the measurement of atmospheric properties (weather elements) from space (Hopkins, 1996). The weather satellites are equipped with radiance sensors, which are radiometers that measure the emitted radiance in a series of discrete spectral intervals of the electromagnetic spectrum. Therefore, the advantages of the weather satellites depend on the sensitivity of the sensors to determine the emitted radiance.

There are four different sensors usually found on weather satellites (Hopkins, 1996):

1. Visible sensors, which detect the visible portion of the sunlight reflected back to space from the clouds, the Earth's surface and the atmosphere. These sensors have a spectral range of between 0.55 and 0.99 μm.
2. Infrared Sensors, which respond to the upwelling infrared radiation emitted by the clouds, the Earth's surface and the atmosphere. These sensors have a spectral range of between 10.3 and 12.6 μm.
3. Water vapour sensors, which respond to observe the water vapour in the near infrared spectrum (6.7 μm).

4. Microwave sensors, which sense the microwave (far infrared) radiation emitted by the Earth with wavelengths of about 1.5cm. These sensors can penetrate clouds and distinguish between ground and ice or snow surfaces.

For the infrared spectrum, various sensors have been developed that are useful to sense the infrared radiation including atmospheric water vapour. For example Television Infrared Observation Satellites (TIROS), TIROS Operational Vertical Sounder (TOVS), Medium-Resolution Infrared Radiometer (MRIR), Temperature Humidity Infrared Radiometer (THIR), and High Resolution Infrared Radiation Sounder (HIRS). On the other hand, Scanning Multichannel Microwave Radiometer (SMMR) and Special Sensor Microwave Imager (SSM/I) are examples of microwave sensors.

Based on satellite orbits, there are two basic types of weather satellite, polar-orbiting satellites, which have an altitude of approximately 850km, and geostationary satellites, which have an altitude of approximately 36,000km over the equator (Crowder, 2000). NOAA (USA) and Meteor (Russia) satellite systems are examples of polar-orbiting satellites, whereas Meteorological Satellite (METEOSAT, Europe), Geostationary Operational Meteorological System (GOMS, Russia), Geostationary Meteorological Satellite (GMS, Japan) and Geostationary Operational Environmental Satellite (GOES, USA) are examples of geostationary satellites.

The polar-orbiting satellites can observe all around the Earth whereas the geostationary satellites are limited to the area between 70 degrees North and 70 degrees South in latitude. The geostationary satellites can observe the Earth's phenomena from a stationed position above the equator and provide information in a short time. On the other hand, the polar-orbiting satellites need more time to observe the same point at middle and low latitudes compared to geostationary satellites. However, for meteorological purposes, the World Meteorological Organisation (WMO) combines both of these satellite systems into Global Observing System (GOS) to enhance the quality of meteorological data.

2.5.3 Comparison of water vapour observation techniques

A brief comparison of the water vapour observation techniques discussed previously is now summarised in Table 2.4, highlighting the advantages and disadvantages of each technique.

Observing Platform	Measurement System	Advantages	Problems
Earth's surface	Routine surface meteorological observations. Instruments include wet- and dry-bulb psychrometer (an instrument to measure humidity) and dew point hygrometer (an instrument which measures the dew point temperature by cooling or heating a front-surface mirror until condensation just appears on the mirror surface).	Long records of reasonably high quality global data are available. Observations are made at least daily and often more frequently.	Spatial coverage is non-uniform. Data are on the Earth's surface only.
Balloons	Routine radiosonde (weather balloon) observations. Humidity sensors include carbon and lithium chloride hygristors (a humidity element used in radiosondes), capacitive sensors, goldbeater's skin, and human hair.	Method in use since 1930s, so long data records are available. Global network of about 800 stations making one to four observations per day at each station. Data have relatively good vertical resolution in lower troposphere.	Data quality is variable for regions with altitude 8-12km and poor for regions with altitude above 12km. Quality of observations is poor at very high and low humidities. Differences in instruments and practices between countries, and changes over time, make data interpretation difficult. Spatial coverage is limited.
	Research soundings (using, e.g., frost point hygrometers)	Quality of humidity observations is high. Data extend beyond altitude limits of radiosondes.	Instruments are expensive, so soundings are made infrequently at limited locations.

	Reference radiosondes	High-quality observations could be used for comparison with operational measurement systems and for field experiments.	In developmental stage. Instruments are more expensive than expendable radiosondes.
Satellites	Infrared sensors (e.g., TOVS)	Sensors provide total column water vapour and some vertical profile information over large areas.	Data are limited to cloud-free regions and can exhibit regional biases. Vertical resolution is poor.
	Microwave sensors (e.g., SMMR, SSM/I)	Sensors provide total column water vapour data over large regions and are not heavily influenced by clouds.	Data are limited to ice-free ocean regions, and vertical resolution is poor.
	Solar occultation methods e.g., SAGE (Stratospheric Aerosol and Gas Experiment) II	Global humidity data at very high altitudes in the stratosphere and above. High accuracy and vertical resolution.	Coverage is limited by clouds. Sampling is poor in tropical regions.
	Global Positioning System	Provides continuous water vapour estimates in all weathers, at relatively low cost and portable.	Methods are in research and developmental stage.
Aircraft	Instruments mounted on special research aeroplanes or commercial aircraft. The research instruments include dew point and lyman alpha hygrometers, differential absorption lidars, capacitive sensors	Research aircraft can make measurements in almost any location at any time desired. Measurements with commercial aircraft could provide good data coverage over much of the globe.	Research missions are expensive, so data collection is limited. Programs involving commercial aircraft have not been widely implemented.
Ground-based remote sensors	Raman lidar, Differential absorption lidar	Sensors provide high-quality data with high vertical and temporal resolution.	The systems are expensive and require highly skilled operators. Usefulness is limited in the daytime and in cloudy conditions.

Table 2.4 Summary of Atmospheric Water Vapour Observation
(American Geophysical Union, 1995)

From Table 2.4, it can be seen that the major considerations in selecting a water vapour observation technique are resolution (spatial, vertical and temporal), cost, flexibility and accuracy. The best spatial resolution is given by weather satellites since they work based on images. However, they have poor temporal resolution because they must rotate in their own orbits with a fixed time frame and cloud constraint for a system which is not equipped with low frequency sensors. Recently, ground-based remote sensors gave the best vertical and temporal resolution. However they are expensive and sometimes not flexible. The radiosondes are the most common because they give relatively high accuracy in the lower atmosphere. However the quality of data is reduced for regions with an altitude above 8km, since 'icing problems' arise. This causes the balloon to fluctuate in the freezing altitude and produces unrepresentative wind and thermodynamic data.

As an additional technique, GPS can provide high temporal resolution, since GPS signals are transmitted continuously. This technique is flexible because the GPS receivers are designed to be portable, and have the ability to observe in the upper atmosphere by virtue of GPS providing an integrated quantity. However, the system only usually provides the total amount of water vapour above the site in the zenith direction, since slant direction estimates are still in the development stage by many researchers and projects around the world.

2.6. Summary

Water vapour in the atmosphere has an important role because it is one of the gases that can contribute to the greenhouse effect, as a chemical reactant and carrier of latent heat. It is a fundamental element in the hydrological cycle and has an essential role in the improved analysis and prediction of convective storms.

The atmospheric water vapour is quantified by measuring the total atmospheric water vapour contained in a vertical column of unit cross-sectional area extending from the Earth's surface to the top of the atmosphere. There are two terms related to atmospheric water vapour quantification, namely precipitable water (PW) and integrated water vapour (IWV). The unit of IWV is kg/m^2 whereas mm for the PW

therefore to define the relation between the IWV and the PW, simply divides the amount of water vapour content by the density (ρ) of liquid water.

The water vapour density (ρ_v) is the same as the absolute humidity which is defined as the mass of water vapour in a unit volume of air. The atmospheric water vapour can be observed by different techniques, however, spatial resolution, temporal resolution, vertical resolution, accuracy, cost and flexibility are the main considerations in selecting a water vapour observation technique.

Chapter 3

GPS FOR ESTIMATING ATMOSPHERIC WATER VAPOUR

As mentioned in Chapter 2, the ability of GPS to sense the atmospheric water vapour is still in the research stage, therefore this chapter describes the principles of estimating atmospheric water vapour using ground-based GPS receivers. It is not an attempt to describe the basic theory of GPS. It is assumed that the reader has a general understanding of high precision GPS positioning principles. Otherwise, some comprehensive references such as Hofmann-Wellenhof *et al.* (2001) and Leick (1995) are recommended. However, literature covering GPS for estimating atmospheric water vapour is reviewed, to show the development of GPS for meteorological applications around the world.

3.1 Background of GPS for Meteorology

The role of water vapour and its measurement techniques have been described in Chapter 2. As mentioned, one water vapour measurement technique is GPS. Bevis *et al.* (1992) used "GPS meteorology" as a term to present a new approach in remote sensing of the troposphere and stratosphere, by measuring the refraction of GPS signals that propagate through the atmosphere. Otherwise, this term can also be understood as the use of GPS for meteorological purposes, especially in estimating atmospheric water vapour content. The term "GPS meteorology" in this research focuses on estimating atmospheric water vapour content only.

Some reasons why GPS is used for estimating atmospheric water vapour have been stated in Chapter 2. For example, it can provide continuous water vapour estimates in all weathers, at low cost, and with a spatial resolution limited only by the number of receivers deployed. Moreover, Yunck *et al.* (2000) list the attractions of GPS as a tool for atmospheric sensing not found in established space techniques:

- Compact, low power and economical
- Ability to sound the atmosphere from the stratopause to the Earth's surface

- A vertical resolution of a few hundred meters in the troposphere compared with several kilometres or more for other space instruments
- The prospect of concurrently sampling the full global atmosphere at low cost

These advantages will likely lead to other meteorological purposes which Jerret and Nash (2001) and Businger *et al.* (1996) briefly propose:

- Forecast verification. This can be obtained from the ability of GPS to economically provide continuous data with a high temporal resolution
- Climate verification. GPS can provide an accurate way to monitor long-term trends; good vertical resolution in the upper troposphere and stratosphere, and in all-weather monitoring through clouds and aerosols on a global scale. These factors are important in climate (Gradinarsky *et al.*, 2002) and global change research.

Basically, there are two different methods in meteorological studies using GPS which are illustrated in Figure 3.1. The first uses a ground-based GPS receiver and the second uses a satellite-mounted GPS receiver. Both methods are mainly based on the atmospheric refractivity, which can slow and change the direction of the GPS signal. The ground-based GPS receiver method is discussed in more detail in Section 3.3.

The radio occultation technique is used in the satellite to satellite method. The history of using GPS as a sounding tool for atmospheric studies based on radio occultation has clearly been described by Yunck *et al.* (2000). The satellite-based GPS receiver technique deploys a GPS receiver on a low Earth orbiting (LEO) satellite. The principle involved is that the atmosphere acts as a spherical lens, bending and slowing the propagation of signals, whereas the positions of the two satellites (GPS and LEO) are known, so the atmospheric delay can be determined (Gabor, 1997). Figure 3.2 illustrates atmospheric soundings by using a satellite-based GPS receiver.

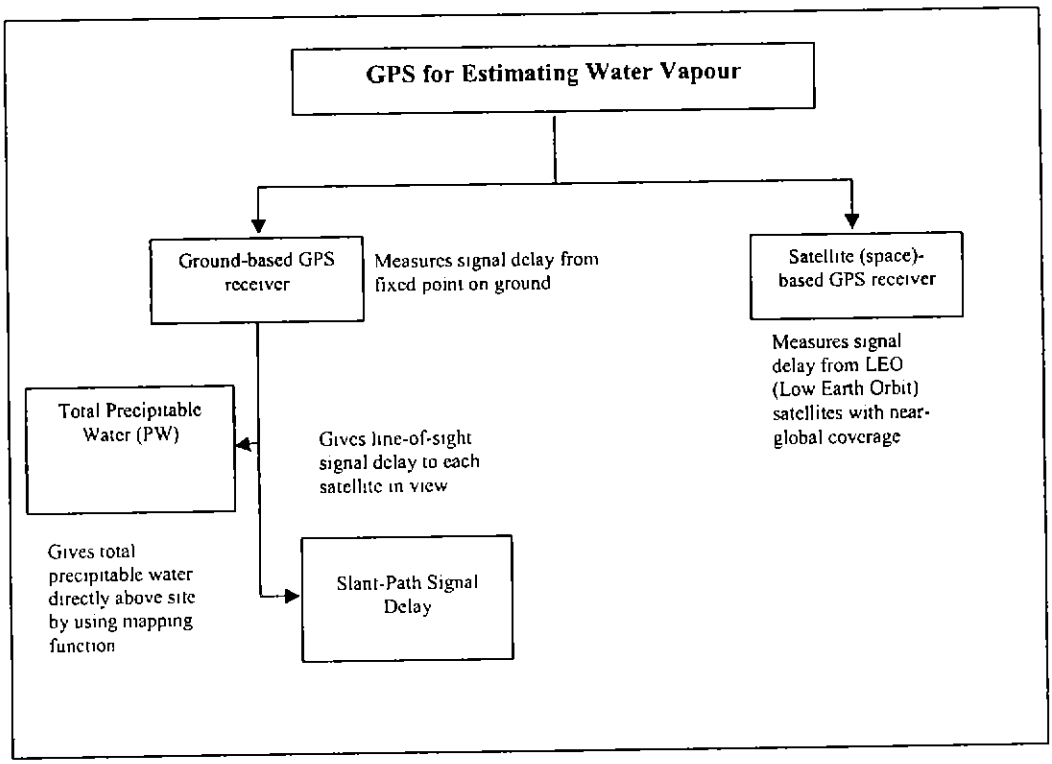

Figure 3.1 GPS Techniques for Estimating Atmospheric Water Vapour

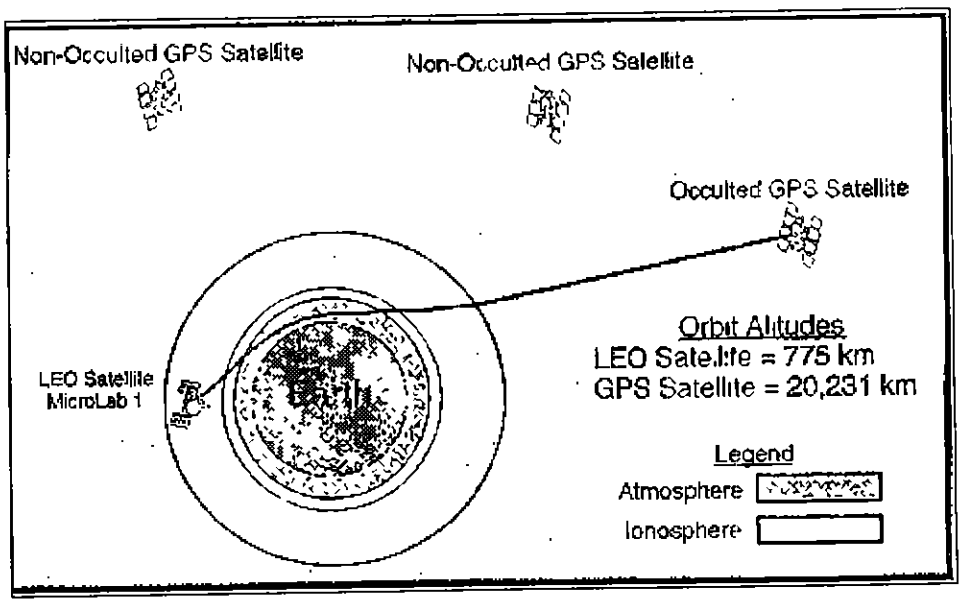

Figure 3.2 Satellite-Satellite Based Method (Gabor, 1997)

3.2 GPS Meteorology Initiatives Worldwide

The use of GPS for estimating atmospheric water vapour started in the 1990s when the 'wet' part of the tropospheric delay was successfully converted to PW (e.g., Bevis *et al.*, 1992; Rocken *et al.*, 1993; Duan *et al.*, 1996) and applied in the meteorology field (Yoshihara *et al.*, 2000). After testing in many pilot projects around the world, GPS is presently used to obtain additional information about water vapour that might not otherwise be available. Therefore many research institutes, especially in the USA, Europe and Japan have been involved in researching the use of GPS for meteorology.

In the USA, GPS/MET (Ware *et al.*, 1996; Rocken *et al.*, 1997; Marquardt *et al.*, 2001) assessed active limb sounding, based on the satellite-satellite occultation method. A major development in the use of the occultation approach is the COSMIC (Constellation Observing System for Meteorology, Ionosphere and Climate), a joint U.S.-Taiwan project (Lee *et al.*, 2001). The GPS Integrated Precipitable Water Vapour (GPS-IPW) project uses GPS as a tool in operational weather forecasting. This particular project was undertaken by NOAA, National Geodetic Survey (NGS), National Data Buoy Center, the Scripps Institution of Oceanography, the University of Hawaii at Manoa, the University Navstar Consortium (UNAVCO), and the U.S. Coast Guard Navigation Center (USCG). In addition, GPS/STORM experiment (Rocken *et al.*, 1995; Duan *et al.*, 1996) estimated the absolute value of precipitable water by using GPS data and comparing to radiosonde measurements during a time period which included more than 6 major storms to demonstrate the validity of the method.

In Europe, GPS meteorology initiatives have been conducted on regional (European continent) and local (individual country) scales. At the local scale, some European countries with permanent GPS networks undertook GPS meteorology initiatives. For example, Germany with the GASP project (Dick *et al.*, 2001; Gendt *et al* 2001); Sweden (Elgered *et al.*, 1997; Johansson *et al.*, 1998; Davis and Elgered, 1998; Bouma and Stoew, 2001); France and Italy (Paccione *et al.*, 2002). WAVEFRONT (Dodson *et al.*, 1999) and MAGIC (Haase *et al.*, 2001) projects are examples of regional scale initiatives. Recently, the European Cooperation in the field of

Scientific and Technical Research (COST) conducted an action called COST Action 716, entitled, Exploitation of Ground-based GPS for Climate and Numerical Weather Prediction Applications, signed by 15 countries including Austria, Belgium, the Czech Republic, Denmark, Finland, France, Germany, Hungary, Italy, the Netherlands, Norway, Spain, Sweden, Switzerland and the United Kingdom.

In Asia, Japan leads the campaign, having established over 1000 permanent GPS stations and uses GPS as networks for meteorological research (Tsuda *et al.*, 1998; Iwabuchi, 2000; Ohtani, 2001). This project now operates to estimate PW in near real-time. Previously, Liou *et al.* (2001) assessed the use of GPS to estimate total PW in a near tropical area (Taiwan), and compared their results with a microwave radiometer and radiosondes. Moreover, Thailand has assessed the use of GPS to estimate total PW to clarify the water and energy cycle system for hydrological applications, based on water vapour (Takiguchi *et al.*, 2000).

In Australia, the first GPS meteorology experiment was conducted by Tregoning *et al.* (1998). They proposed strategies in GPS data processing to estimate the total PW. In addition, Feng *et al.* (2001) estimated atmospheric water vapour by using GPS data from the Australian Regional GPS Network (ARGN).

3.3 Estimating Water Vapour from Ground-based GPS Observations

Atmospheric water vapour may be estimated using ground-based GPS receivers due to the radio signal refractivity (bent and slowed). The refractivity of the atmosphere causes a delay in the GPS signal compared with what would be expected if there were no intervening atmosphere. The ionosphere, a region of charged particles between 50 and ~1000km above the Earth's surface, is the largest source of atmospheric signal delays. However, since the refraction in a charged medium depends on frequency, it is possible to remove this effect by using dual-frequency GPS observations. Up to 50km above the Earth's surface, the atmosphere is electrically neutral (non-ionised). Temperature, pressure and water vapour changes are the main sources of signal delay, especially in the troposphere. The tropospheric delay (tropospheric refraction) can be estimated in high precision GPS data

processing and converted to atmospheric water vapour. Figure 3.3 illustrates the refraction of GPS signals in the atmosphere.

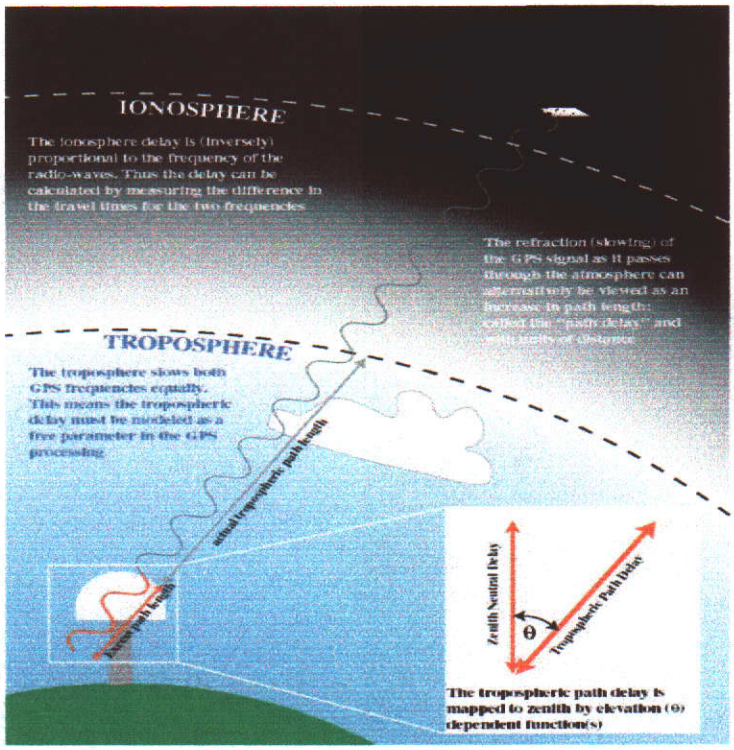

Figure 3.3 Refracted GPS Signal by Atmospheric Delays
(NOAA Forecast Systems Laboratory Demonstration Division, 2001)

3.3.1 Tropospheric Delay

As mentioned in Section 2.1, the atmosphere has an electrically active part and an electrically neutral part. The electrically active part contained in the ionosphere causes a delay, the ionospheric delay. In GPS data processing, the ionospheric delay can be eliminated if dual frequency data are available and is not discussed further in this research. The neutral atmosphere is often referred to as the troposphere in GPS research, therefore the delay which is caused by the neutral part, is known as the tropospheric delay.

The tropospheric delay is caused by the signal refraction due to the varying index of refraction of the air layers. Hofmann-Wellenhoff *et al.* (2001) define the tropospheric delay D^{Trop} of GPS signal propagation in zenith direction as:

$$D^{Trop} = \int (n-1)ds = 10^{-6} \int N^{Trop} ds \quad \text{.....(3-1)}$$

where n is the refractivity index, N^{Trop} is refractivity and ds is the dimension of length on a GPS signal along the receiver to satellite path. Related to the thermodynamic state variables of the air, the refractivity of the air is usually described by empirical formulae. It is a function of temperature (T), partial pressure of dry air (P_d) and partial pressure of water vapour (P_v) and can be expressed as (Thayer, 1974):

$$N^{Trop} = k_1 \left(\frac{P_d}{T} \right) Z_d^{-1} + k_2 \left(\frac{P_v}{T} \right) Z_v^{-1} + k_3 \left(\frac{P_v}{T^2} \right) Z_v^{-1} \quad \text{.....(3-2)}$$

where: k_1 (77.604 ± 0.014K/mbar), k_2 (64.79 ± 0.08K/mbar) and k_3 ($(3.776 \pm 0.004) \times 10^5$K^2/mbar) are the refractivity constants which are empirically determined, Z_d^{-1} and Z_v^{-1} are the inverse compressibility factors for dry air and water vapour, respectively. Rocken *et al.* (2001) define the first term in the right-hand side of Equation (3-2) as the dry refractivity N_{dry} and the sum of the remaining two terms on the right hand side of Equation (3-2) is defined as the wet refractivity N_{wet}. Hence:

$$N_{dry} = k_1 \left(\frac{P_d}{T} \right) Z_d^{-1} \quad \text{.....(3-3)}$$

$$N_{wet} = k_2 \left(\frac{P_v}{T} \right) Z_v^{-1} + k_3 \left(\frac{P_v}{T^2} \right) Z_v^{-1} \quad \text{.....(3-4)}$$

Therefore, the tropospheric delay can be expressed as:

$$D^{Trop} = D^{dry} + D^{wet} \quad \text{.....(3-5)}$$

where D^{dry} is the hydrostatic delay and D^{wet} is the wet delay.

Equation (3-1) and (3-5) can be written as:

$$D^{Trop} = D^{dry} + D^{wet} = 10^{-6}\int N_{dry}\,ds + 10^{-6}\int N_{wet}\,ds \quad \text{.....(3-6)}$$

where N_{dry} and N_{wet} are the refractivity caused by the dry and wet components along the signal path (s) respectively.

From Equations (3-2), (3-5) and (3-6), the tropospheric delay can be written as:

$$D^{Trop} = 10^{-6}\int\left(k_1 \frac{P_d}{T} Z_d^{-1}\right)ds + 10^{-6}\int\left(k_2 \frac{P_V}{T} Z_V^{-1} + k_3 \frac{P_V}{T^2} Z_V^{-1}\right)ds \quad \text{.....(3-7)}$$

$$D^{dry} = 10^{-6}\int\left(k_1 \frac{P_d}{T} Z_d^{-1}\right)ds \quad \text{.....(3-8)}$$

$$D^{wet} = 10^{-6}\int\left(k_2 \frac{P_V}{T} Z_V^{-1} + k_3 \frac{P_V}{T^2} Z_V^{-1}\right)ds \quad \text{.....(3-9)}$$

The total tropospheric delay on a GPS signal along the receiver to satellite path may be mapped to the zenith to result in the *zenith tropospheric delay* (ZTD), by means of a 'mapping function', which is a function of satellite elevation angle (E).

$$D^{Trop} = f(E)ZTD \quad \text{.....(3-10)}$$

Therefore, from Equations (3-5) and (3-10), the zenith tropospheric delay also consists of the hydrostatic and the wet components which are known as the *zenith hydrostatic delay* (ZHD) and the *zenith wet delay* (ZWD) respectively. Mendes and Langley, (1998) define the relation as:

$$D^{Trop} = f(E)ZTD = f^{dry}(E)ZHD + f^{wet}(E)ZWD \quad \text{.....(3-11)}$$

where $f^{dry}(E)$ and $f^{wet}(E)$ are hydrostatic and wet mapping functions respectively.

Figure 3.4 illustrates the concept of the zenith tropospheric delay.

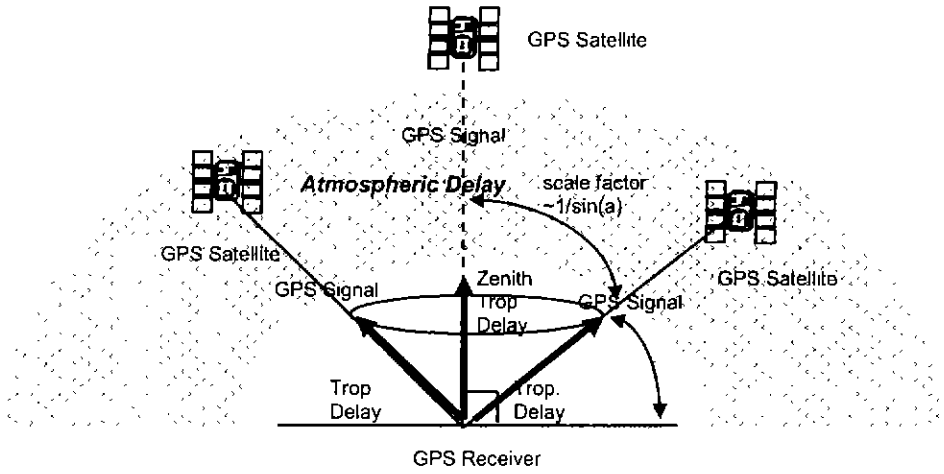

Figure 3.4 Zenith Total Delay Illustration

In practice, using scientific GPS data processing software, the ZTD is estimated by two different strategies (Bock and Doerflinger, 2001). These are *deterministic parameter estimation* (least squares adjustment) as used for example in the Bernese GPS Software (Hugentobler *et al.*, 2001) and *stochastic estimation* (Kalman filtering), used in GAMIT (King and Bock, 1997) and GIPSY (Webb and Zumberge, 1993) software for example.

ZHD can be estimated very accurately by using surface pressure measurement and has been modelled by Elgered *et al.* (1991) based on the Saastamoinen model as:

$$ZHD = 2.2779 \pm 0.0024\left(\frac{P}{\left(1 - 0.00266\cos(2\phi) - 0.00028H\right)}\right) \quad \text{.....(3-13)}$$

where ZHD is estimated in millimetres, H is the height above the ellipsoid in km; P is the total air pressure measurement in mbar and ϕ is station latitude. ZHD which makes up 90% of delay can be measured very accurately when pressure is known (to mm accuracy). On the other hand, ZWD which makes up 10% of delay is much more difficult to model since there are strong variations in the distribution of atmospheric water vapour in space and time. ZWD estimation error is commonly about 10-20% (Rizos, 1999).

Based on Equation (3-5), the ZWD is then determined by subtracting ZHD from ZTD. Finally zenith wet delay is converted to precipitable water, as is described in the next section.

3.3.2 Conversion from Zenith Wet Delay to Precipitable Water

ZWD may be converted to PW by using a conversion factor (Π), and can be expressed by the following equation (Liou *et al.*, 2001):

$$PW = \Pi . ZWD \quad \text{.....(3-14)}$$

where $$\Pi = \frac{10^8}{\rho R_v \left[\frac{k_3}{T_m} + k_2' \right]} \quad \text{.....(3-15)}$$

and $$T_m = \frac{\int \frac{P_v}{T} dz}{\int \frac{P_v}{T^2} dz} = 70.2 + 0.72 T_s \text{ (Bevis } et\ al.\text{, 1992)} \quad \text{.....(3-16)}$$

where ρ is the density of liquid water (1000 kg m^{-3}); R_v is the specific gas constant of water vapour (461.524 J kg^{-1} K^{-1}), k_3 and k_2' are atmospheric refractivity constants equal to 3.739.10^5 K^2 $mbar^{-1}$ and 22.1 K $mbar^{-1}$ respectively, T_m is the mean temperature of the atmosphere along the signal path in degrees Kelvin, and finally T_s is the surface temperature (at the GPS antenna) in degrees Kelvin.

Therefore, equation (3-14) can be rewritten as:

$$PW = ZWD \left[\frac{10^8}{1000 \times (461.524) \times \left[\frac{3.739 \times 10^5}{70.2 + 0.72 T_s} + 22.1 \right]} \right] \quad \text{.....(3-17)}$$

The accuracy of the conversion factor (Π) depends on the determination of the mean temperature (T_m). Bevis *et al.* (1992) derived a linear relationship between T_m and T_s as shown by Equation (3-16), with an accuracy of approximately 15%. Coarsely, Π has the value of about 0.15, while it is a function of season, location and weather (Liou *et al.*, 2001). Emardson *et al.* (1998) also concluded that Π must be determined by considering the local and regional situations, especially individual site situations.

3.4 Error Sources and Processing Strategies for GPS Water Vapour Estimation

High accuracy GPS water vapour estimation is dependent on the best choice of processing strategies, the correct application of error-correction models and a priori constraints (Baker, 1998). Factors that must be considered include ambiguity resolution, elevation mask, mapping functions, a priori tropospheric model, tropospheric estimation interval and amount of data processing overlap. The a priori constraints include station coordinate constraints, tropospheric interval and relative constraints. Error-correction models include GPS orbit errors, station coordinates errors, multipath and cycle slip errors, antenna errors, the ocean tide loading effect, the atmospheric pressure loading and the Earth body tide effect.

This section will describe the data processing strategies and error sources for GPS water vapour estimation.

3.4.1 GPS orbit

GPS orbit errors influence the calculation of the range between a satellite and a receiver. The information of satellite coordinates and their orbits are known as ephemerides. There are two basic types of GPS ephemeris: the broadcast and the precise. The broadcast ephemeris is available from GPS signals and is obtainable from a GPS receiver in real-time, whereas precise ephemerides are obtained after the time of observation usually and are computed either by the user or a third-party such as the International GPS Service (IGS). Further details about the IGS are described in Section 3.6.

High accuracy positioning, which is usually based on the relative positioning GPS technique, needs precise satellite orbits to minimise error which can affect the accuracy of GPS data processing results. Bauersima (1983) in Hugentobler *et al.* (2001) derived the relation of orbit error and baseline length from the relative technique as:

$$\Delta x(m) \approx \frac{l}{d}.\Delta X(m) \approx \frac{l(km)}{25000(km)}.\Delta X(m) \quad \text{.....(3-18)}$$

where: Δx is the baseline error, l is the baseline length, d is the approximate distance to satellites and ΔX is the orbit error. For example, with a 2.5m broadcasting orbit error over a 1000km baseline length, the resultant baseline error is around 100mm.

3.4.2 Station coordinates

A priori positional information is important in high accuracy GPS data processing. The most popular technique in estimating error corrections based on observation adjustment is least squares. The least squares estimates consist of the corrections and the parameters which depend on the residual quantities (the difference between the a priori values and the raw or observed values). Therefore, there is a linear mathematical model relationship between a priori coordinates and the error corrections.

In 'GPS meteorology', usually some stations are fixed or constrained in order to overcome the correlation between coordinates and ZTD estimates (MAGIC, 1999) and to eliminate network rank deficiency. Consequently, fixing to the wrong coordinates will directly propagate to unknown parameters. Errors in the height component will directly affect the ZTD estimations. Previous studies show that 1cm height error at the fixed station can cause a bias of the ZTD estimation of 1mm (Tregoning *et al.*, 1998) to 3mm (Rocken *et al.*, 1993). Therefore, it is necessary to provide precise coordinates for all GPS stations. This requirement can be provided by using data from IGS stations that have very accurately determined coordinates in a high precision reference system such as the International Terrestrial Reference Frame (ITRF) that will be described in Section 3.7.

3.4.3 Multipath and cycle slip errors

Multipath errors affect the measurement of the pseudorange and carrier phase in determining the satellite to receiver distance. Multipath occurs when a signal reflects off another surface, giving a false pseudorange or carrier phase measurement. Multipath can be mitigated by antenna design, site location and data processing. Rocken *et al.* (1993, 1995) found that multipath errors can contribute to PW estimation error by up to 1mm.

Cycle slips occur when the receiver loses lock on the satellite signal while collecting GPS data. The slip must be detected and repaired in order to obtain clean observation data and can be done by analysing the observational residuals, particularly effective when the double differencing technique is used.

3.4.4 Tropospheric estimation interval and relative constraints

Tropospheric constraints are applied to describe how much the delay is allowed to vary between consecutive estimates. In addition, the solution interval must be short enough to accommodate the time-scale of the variability of the water vapour signal. Rocken *et al.* (1995) suggest that little advantage is found in decreasing the interval to less than 15 minutes.

3.4.5 Antenna height

Estimating water vapour by using GPS is related to high accuracy positioning, especially height determination, it is therefore important to determine the height of the GPS antenna accurately since all measurements are referenced to it. The antenna height knowledge is also important if a priori coordinates are those of a ground mark and not the mean antenna phase centre.

3.4.6 Antenna phase centre variations

GPS measurements refer to the phase centre of the GPS antenna, therefore the position of the antenna phase centre is computed directly by GPS software. The phase centre is not a physical point, but its location with respect to a physical feature on the antenna which can be determined through a set of calibration measurements. In addition, the phase centre variation differs between different antenna types. Rothacher *et al.* (1995) found that the antenna phase centre variations can contribute an error of up to 10cm in height determination.

3.4.7 Elevation mask

Observations at low elevations are generally corrupted by tropospheric refraction which deteriorates the quality of GPS estimated parameters. The signals from low elevation satellites have been disturbed by the atmosphere and are generally noisier and therefore will affect the quality of the solution.

However, using low-elevation observations may improve estimations of the tropospheric zenith delays (Rothacher *et al.*, 1997) because low elevation data can improve the observation geometry, increase the amount of available data and contain interesting meteorological information (Rocken *et al.*, 2001). Therefore, in many GPS-PW projects, an elevation mask of between 5 degrees and 20 degrees (Bock *et al.*, 2001; Tregoning *et al.*, 1998) is used.

3.4.8 Mapping function and elevation-dependent weighting

As was mentioned in Section 3.3.1 and illustrated in Figure 3.4, mapping functions are used to map real tropospheric slant delays to zenith delays. They are derived from mathematical models for the elevation dependence of the respective delays, and depend on geographical position and time of year to estimate the most probable moisture profile (Jerrett and Nash, 2001).

Errors in the mapping functions, which increase at low elevation angles, can induce systematic errors in the estimation of the tropospheric delay (Mendes and Langley, 1994). Therefore, in estimating atmospheric water vapour using ground-based GPS receivers, the accuracy of mapping function is important since many observations are made at a low elevation angle.

A number of precise mapping functions have been developed and can be used in GPS data processing based on equations 3.10 and 3.11. A widely used formula for $f(E)$ is the continuous fraction which is proposed by Marini and can be written as (Marini, 1972):

$$f(E) = \frac{1}{\sin(E) + \dfrac{a}{\sin(E) + \dfrac{b}{\sin(E) + \dfrac{c}{\sin(E) + \ldots}}}} \quad \ldots\ldots(3\text{-}19)$$

where E is the elevation angle, $f(E)$ is mapping function, a, b, and c are the coefficients.

This continuous fraction model becomes the basis for the development of other mapping functions, such as: Chao mapping function (Chao, 1973), the CfA 2.2 (Harvard-Smithsonian Center for Astrophysics) mapping function (Davis *et al.*, 1985) Ifadis mapping function (Ifadis, 1986), the MTT (Massachusetts Institute of Technology Temperature) mapping function (Herring, 1992), and Niell mapping function (Niell, 1996). The variations come from the value of the coefficients a, b, and c, which are determined from different tests.

However, for high precision applications, Mendes and Langley (1998) recommend to use the Niell, Herring or Ifadis mapping functions.

In order to use low-elevation observation to improve the ZTD estimations, the elevation-dependent weighting of the observations is introduced and can be written as (Hugentobler *et al.*, 2001):

$$w(z) = \cos^2 z \quad \ldots\ldots(3\text{-}20)$$

where z is the zenith angle of the satellite.

3.4.9 Data processing overlap

Data processing overlap is an important strategy to estimate the atmospheric water vapour using GPS. It is related to the use of the IGS precise orbits, which have discontinuities at the day boundaries (Ray, 2000). Tregoning *et al.* (1998) found that these discontinuities led to PW estimates and have an error of up to 2mm.

In addition, Baker (1998) showed the jumps may either be due to 'edge effects' in the Kalman Filter or due to actual jumps in the orbit data between consecutive days. To eliminate these effects, a sufficient overlap is introduced in the processing strategy.

3.4.10 Ocean tide loading effect

The Earth's surface moves periodically in response to the periodic motion of the oceans (e.g. Baker *et al.*, 1995). Hence ocean tide loading can be defined as a time varying deformation of the solid Earth due to the weight of the oceans. It can cause a bias in position, especially for the height component. It means that the position estimates will vary dependent on when the data were collected due to the cyclical rise and fall of the surface of the oceans. It is caused by the gravitational attraction of the Moon and the Sun on the Earth. The ocean tide loading contributes more than 10cm for the vertical displacement in some parts of the world (Baker *et al.*, 1995) and the effect must be modeled and taken into account to minimise error and to achieve high accuracy positioning by GPS (Dach and Dietrich, 2001).

The ocean tide loading (OTL) effects in GPS data can be corrected by using OTL displacement coefficients (also termed OTL parameters), which model the different tidal constituents of displacement (Penna and Baker, 2002). The constituents can be defined as individual components which comprise the tides and arise either from a specific astronomical feature (mainly from the Moon and the Sun), or from the interaction between two or more constituents.

Based on the occurrence, the tidal constituents can be classified into three types: semi-diurnal tides which occur approximately twice a day; diurnal tides which occur approximately once a day; and long period tides which occur once in more than 10 days. The 11 main tidal constituents are listed in Table 3.1 with their Darwin symbols.

Darwin Symbol	Name	Type	Period (h = solar hours; d = days)
M_2	Principal Lunar	Semi-diurnal	12.42 h
S_2	Principal Solar	Semi-diurnal	12.00 h
N_2	Major Lunar Elliptical	Semi-diurnal	12.66 h
K_2	Luni-Solar Declinational	Semi-diurnal	11.97 h
O_1	Principal Lunar	Diurnal	25.82 h
K_1	Luni-Solar Declinational	Diurnal	23.93 h
P_1	Principal Solar	Diurnal	24.07 h
Q_1	1st Order Elliptic	Diurnal	26.87 h
M_f	Lunar Fortnightly	Long period	13.66 d
M_m	Lunar Monthly	Long period	27.55 d
S_{sa}	Solar Semiannual	Long period	182.62 d

Table 3.1 Main Tidal Constituents (Baker *et al.*, 1995)

In GPS data processing, the time varying displacement, which is caused by the individual tidal constituent, is computed based on the IERS 1996 Conventions (McCarthy, 1996). This displacement is estimated from the OTL parameter amplitudes, Greenwich phase lags and the time of observation. The total site displacement then is obtained by summarising the displacements caused by individual tidal constituent and can be applied to the approximate station coordinates as a correction model.

The OTL effects are modelled into the OTL model by summarising the series of harmonics of known amplitudes and phases of each constituent. The amplitude indicates the maximum displacement and the phase provides the time maximum displacement compared with the tide generating force. These parameters are computed for a particular ocean tide model. Various global OTL models can be applied to minimise errors which are caused by the OTL effects in GPS data processing. Since 1994, more than 20 global OTL models have been developed (Shum *et al.*, 1997). Some of these models are listed in Table 3.2.

OTL Model	Developer
Schwiderski	Schwiderski (PODAAC)
NAO99.b / ORI	Matsumoto Model (University of Tokyo)
FES (Finite Element Solutions) series: 94.1; 95; 98; 99	Le Provost Model (Grenoble-PODAAC)
CSR3.0; CSR4.0	Eanes Model (Texas University-Austin)
RSC94; GOT99.2b; GOT00.2	GSFC Ray-Sanchez-Cartwright Model (NASA Goddard Space Flight)
TPXO.2; TPXO.5	Egbert Model (Oregon State of University)
AG95.1	Andersen (KMS) - Grenoble Model
DW95.0/.1	Desai-Wahr Model (University of Colorado)
Kantha.1/.2	Kantha Model (University of Colorado)
SR95.0/.1	Schrama-Ray Model (Delft/GSFC)
GSFC94A	Sanchez-Pavlis Model (NASA Goddard Space Flight)

Table 3.2 Ocean Tide Loading Models
(Summarised from Shum *et al.*, 1997 and Schemeck, 1991)

3.4.11 Atmospheric pressure loading

Variations in atmospheric circulation above a particular site cause loading deformation on the land surface, which can vertically displace a point by up to 20mm (Petrov and Boy, 2004) and are dominated by periods of approximately 2 weeks and are associated with the passage of synoptic scale (order 1000-2000 km) pressure systems (van Dam *et al.*, 1994). The expression for the vertical displacement due to atmospheric pressure loading is (McCarthy, 1996):

$$\Delta r = -0.35p - 0.55\overline{p} \quad \text{(3-21)}$$

where: Δr is the vertical displacement (mm), p is the local pressure anomaly with respect to the standard pressure of 1013 mbar, and $\overline{p}$ is the pressure anomaly within the 2000km circular region. Equation 3-21 shows that the vertical displacement due to atmospheric pressure loading fully depends on the air pressure around the site observation.

Since the GPS-PW estimation is directly linked to the high accuracy of GPS height determination, therefore the site-induced atmospheric pressure loading may also affect the PW estimates.

3.4.12 Earth body tides

The Earth body tide can be defined as an elastic deformation of the Earth's shape due to the gravitational forces from the alignment of the Sun, Moon and other planets (Stewart, 1998). Similar to the OTL effects, the Earth body tides cause a time-dependent variation in the height component.

The height variation due to the Earth body tide effect varies from 2cm (Stewart, 1998) to more than 20cm (Schuler, 2001) dependent on location and time. Therefore, the Earth body tides need to be modelled and applied in high accuracy GPS data processing.

In GPS-PW estimation, the Earth body tides affect the solution due to the long wavelength effect that causes a problem in long baseline observations (Penna, 1997) since often observations are usually included from long baselines (more than 2000km) to obtain high accuracy ZTD estimates (Tregoning *et al.*, 1998). In GPS data processing, the Earth body tide effects may be computed based on the IERS 1996 Conventions (McCarthy, 1996), and then applied to the approximate station coordinates as a correction.

3.4.13 Ambiguity resolution

High accuracy GPS positioning is conducted using the GPS carrier phase measurements since the phase can be measured to millimetre precision compared with a few metres for code measurements. Unfortunately, GPS carrier phase measurements are ambiguous because the whole number of wavelengths between the satellite and receiver (the integer ambiguity) is unknown. Therefore, in order to use the carrier phase these ambiguities must be resolved. More details about ambiguity resolution can be found in GPS references such as Hofmann-Wellenhof *et al.* (2001) and Leick (1995).

There are three phase ambiguity treatments (Rizos, 1999) in GPS data processing:

- Adjustment of all ambiguities as free parameters together with station coordinates, known as an *ambiguity-free* or ambiguity-float solution.
- Resolve the ambiguities by estimating ambiguity parameters to their nearest integer values, and iterate the solution, known as an *ambiguity-fixed* solution.
- Eliminate the phase ambiguity bias by differencing data between consecutive epochs.

The ambiguity resolution strategy is generally based on three factors, namely signal availability (single or dual frequency), baseline length and session length (Hugentobler *et al.*, 2001). However, if the observation time is long enough (i.e. for permanent arrays tracking the whole day) and baselines are long (i.e. more than several hundred km), treating ambiguities as floating numbers instead of integers has proven to be an acceptable method (Schuler, 2001).

3.4.14 Surface meteorological sensors

Surface pressure and temperature data are needed to derive PW from the tropospheric delay estimated in GPS data processing. The surface pressure data is needed to model the hydrostatic delay. Obtained in GPS data processing is an estimate of the total tropospheric delay, so removal of the hydrostatic delay leaves the ZWD. The surface temperature data is needed to derive the mean temperature of the atmosphere, which is then used to convert the ZWD to PW. Therefore, the accuracy of the observation sensor is important to minimise errors in estimating atmospheric water vapour. For example, an error of 1mbar from pressure sensor errors can contribute to 2mm error in ZWD estimation (Rocken *et al.*, 1993).

3.4.15 Error budget of PW estimates

Schuler (2001) conducted experiments using 6 months GPS data from some GPS stations in Europe to estimate PW using ground-based GPS receiver and produced an error budget of PW estimation and it is summarised in Table 3.3.

Error Source	Error Budget of PW Estimates (mm)	Comments
Station coordinates, including the antenna height, the OTL and the Earth body tides effects	0.3 – 1.1	Fixed coordinates are only recommended if antenna position is known with superior accuracy.
Satellite orbit error	0.3 – 1.6	Depends on the baseline length and orbit product.
Antenna phase centre variations	0.1 – 0.5	Unmodelled phase centre variations of GPS antenna
Multipath Effects	0.3 – 0.6	Depend on local environment, antenna type, receiver firmware and not for carrier phase multipath (multipath mitigation software)
Hydrostatic delay	0.1 – 0.5	Depends on the accuracy of surface pressure.
Conversion factor	0.1 – 0.3	Depends on the accuracy of surface temperature.
Total budget	***0.5 – 2.2***	

Table 3.3 Error Budget for Ground-based GPS-PW Estimates (Schuler, 2001)

3.5 The International GPS Service (IGS)

As described in Sections 3.4.4 and 3.4.6, the GPS orbits and the station coordinates are important for high accuracy GPS data processing. Therefore, errors in satellite orbits and station coordinates must be minimised or eliminated by using precise satellite orbits and station coordinates. Such information is available through the IGS. This started when the International Union of Geodesy and Geophysics (IUGG), at its 20th General Assembly in 1991, recommended establishing 'an analysis centre of a globally GPS tracking network', which is the concept of the International GPS Service (IGS). A globally distributed GPS network provides a comprehensive and robust source of tracking data to produce precise GPS satellite orbits and a set of accurate station coordinates that function as a realisation of a global datum (Rizos, 1999). The official IGS service started on 1st January 1994.

The primary objective of the IGS is to provide a service to support geodetic and geophysical research activities through GPS data products. Its products are:

- High accuracy GPS satellite ephemerides such as the IGS final orbit (IGS), IGS rapid orbits (IGR) and the IGS ultra rapid orbit (IGU)
- Earth rotation parameters
- Coordinates and velocities of the IGS tracking stations
- GPS satellite and tracking station clock information
- Ionospheric and tropospheric information

The IGS consists of 6 organisations, which are tracking stations, data centres, Analysis and Associated Analysis Centres, the Analysis Centre Coordinator, the Central Bureau and the Governing Board. The network of tracking stations consists of 367 permanent GPS stations (as of 13 April 2004) around the world and provides continuous GPS tracking in order to compute the satellite ephemerides and other data products. The data centres, which consist of three different categories: operational, regional and global data centres, are the responsible organisations for raw data management and data flow. Raw data from tracking stations are collected by the nearest operational data centres (15 operational data centres) and then converted to the right format, archived and then sent to 6 regional data centres. These centres also manage, archive the data and then send them to 3 global data centres which are the main interfaces to the analysis centres and to other users. The global data centres are:

- Crustal Dynamics Data Information System (CDDIS). NASA Goddard Space Flight Centre, Greenbelt, USA
- Institut Geographique National (IGN), Paris, France
- Scripps Institution of Oceanography (SIO). University of California, San Diego, USA

The analysis centres process the tracking data to produce the IGS products (daily estimates of the satellite ephemerides, station coordinates and Earth rotation parameters) and deliver them to global data centres, to the Analysis Data Centre Coordinator and to other designated bodies. There are 7 analysis centres (See Table 3.4.)

Center for Orbit Determination in Europe (CODE)	Switzerland
European Space Operations Center (ESA)	Germany
GeoForschungsZentrum (GFZ)	Germany
Jet Propulsion Laboratory (JPL)	USA
National Oceanic and Atmospheric Administration (NOAA) / National Geodetic Survey (NGS)	USA
Natural Resources Canada (NRCan).	Canada
Scripps Institution of Oceanography (SIO)	USA

Table 3.4 The IGS Analysis Centres

The analysis centres' products are sent to the Analysis Centre Coordinator who uses an orbit combination technique to produce the official IGS orbits. The Coordinator then sends the generated products to Global Data Centres and the Central Bureau Information System (CBIS) for archiving and user access. The products of the Analysis Centre Coordinator are listed in Table 3.5.

	Accuracy	**Latency**	**Updates**	**Sample Interval**
GPS Satellite Ephemerides				
Broadcast	260 cm	real time	--	daily
Predicted (Ultra-Rapid)	25 cm	real time	twice daily	15'
Rapid	5 cm	17 hrs	daily	5' or 15'
Final	<5 cm	13 days	weekly	5' or 15'
Geocentric Coordinates of IGS Tracking Stations (>130 sites)				
Final horizontal/vertical positions	3 mm/6 mm	12 days	weekly	weekly
Final horizontal/vertical velocities	2 mm per yr/3 mm per yr	12 days	weekly	weekly
Earth Rotation Parameters (mas = milli angular second; ms = millisecond)				
Rapid polar motion/polar motion rates/length-of-day	0.2 mas/0.4 mas per day/0.030 ms	17 hrs	daily	daily
Final polar motion/polar motion rates/length-of-day	0.1 mas/0.2 mas per day/0.020 ms	13 days	weekly	daily
Atmospheric Parameters				
Final tropospheric	4 mm zenith path delay	< 4 weeks	weekly	2 hrs
Ultrarapid tropospheric	6 mm zenith path delay	2-3 hrs	every 3hrs	1 hr

Table 3.5 The IGS Products (IGS, 2002)

The Central Bureau, located at the Jet Propulsion Laboratory (JPL), California Institute of Technology, Pasadena, California, USA, is responsible for the overall coordination and management of the IGS. The last organisation in the IGS is the International Governing Board (GB) which exercises the activities and direction of the IGS.

3.6 The International Terrestrial Reference Frame (ITRF)

As mentioned in Section 3.4.6, GPS estimation of atmospheric water vapour uses a priori station coordinates which should be determined precisely. Since the tectonics, geodynamics, or extraterrestrial gravitational sources cause Earth movement, such crustal motion must be considered in high accuracy positioning. For that reason, it is necessary to have a frame that is sensitive to detect small displacements of the Earth's surface. There are two types of reference system, namely the *Celestial Reference System* (CRS) which is a space fixed system to which the positions of celestial objects are referred; and the *Conventional Terrestrial Reference System* (CTRS).

For Earth sciences such as geodesy and geophysics, where the main task is to measure and map the Earth's surface, a terrestrial reference system is most useful. Therefore, the *International Terrestrial Reference System* (ITRS), which has its origin at the centre of the mass of the whole Earth including the oceans and the atmosphere, was established and then represented by the *International Terrestrial Reference Frame* (ITRF). The ITRF is maintained by the *International Earth Rotation Service* (IERS), an interdisciplinary service that maintains key connections between astronomy, geodesy and geophysics.

The ITRF is realised through space based measurements at specific sites around the globe and is affected by factors in the observation and processing of both the station and satellite positions and their motions. These factors include:

- Relationship between the Celestial Reference System and the ITRS such as the rotation rate of the Earth
- A priori coordinates of the sites

- The tectonic plate motion model used to account for site velocities
- Adopted geopotential model for the Earth's gravity field
- Gravitational constant of the Earth's mass
- Value used for the speed of light
- Tidal influences and Solar radiation pressure
- Clock offsets and drift rates
- Atmospheric effects
- Antenna variations

These factors are considered to produce an ITRF as a set of station coordinates and velocities. These products are then redefined periodically. For example, the ITRF 2000 is determined using data up to and including 2000 to realise the ITRS as a set of station coordinates and their velocities at epoch 1 January 2000 (Boucher *et al.*, 2004). An ITRF is produced in its most raw form as the Earth centred Cartesian coordinates (X, Y, Z). Therefore a reference ellipsoid must be used to convert to ellipsoidal coordinates (latitude, longitude and ellipsoidal height). The reference ellipsoid associated with the ITRF is the Geodetic Reference System of 1980 (GRS80).

In relation to GPS estimation of atmospheric water vapour, the ITRF is needed in order to determine the a priori station coordinates precisely. It defines not only the station coordinates, but also their velocities due to continental and regional tectonic motion, which are not always determined in other global, regional or local datums.

3.7 Summary

Atmospheric water vapour can be measured using ground-based GPS receivers. The term precipitable water (PW) is used to quantify atmospheric water vapour. It is obtained from the conversion of zenith wet delay (ZWD) given surface temperature estimates. The ZWD is the result of subtracting zenith hydrostatic delay (ZHD) from zenith total delay (ZTD). The ZHD may be calculated using surface pressure data, whereas the ZTD is estimated using the GPS data via either deterministic parameter estimation or stochastic parameter estimation.

The data processing strategies used for high accuracy GPS height determination are used substantially for estimating atmospheric water vapour using GPS. Error sources that affect the accuracy of the estimated atmospheric water vapour such as GPS satellite orbits, station coordinates, multipath and cycle slips, phase noise, antenna height, antenna phase centre, ocean tide loading effect, the Earth's body tides and surface meteorological sensors, must be minimised. The process of GPS estimate PW is summarised in Figure 3.5.

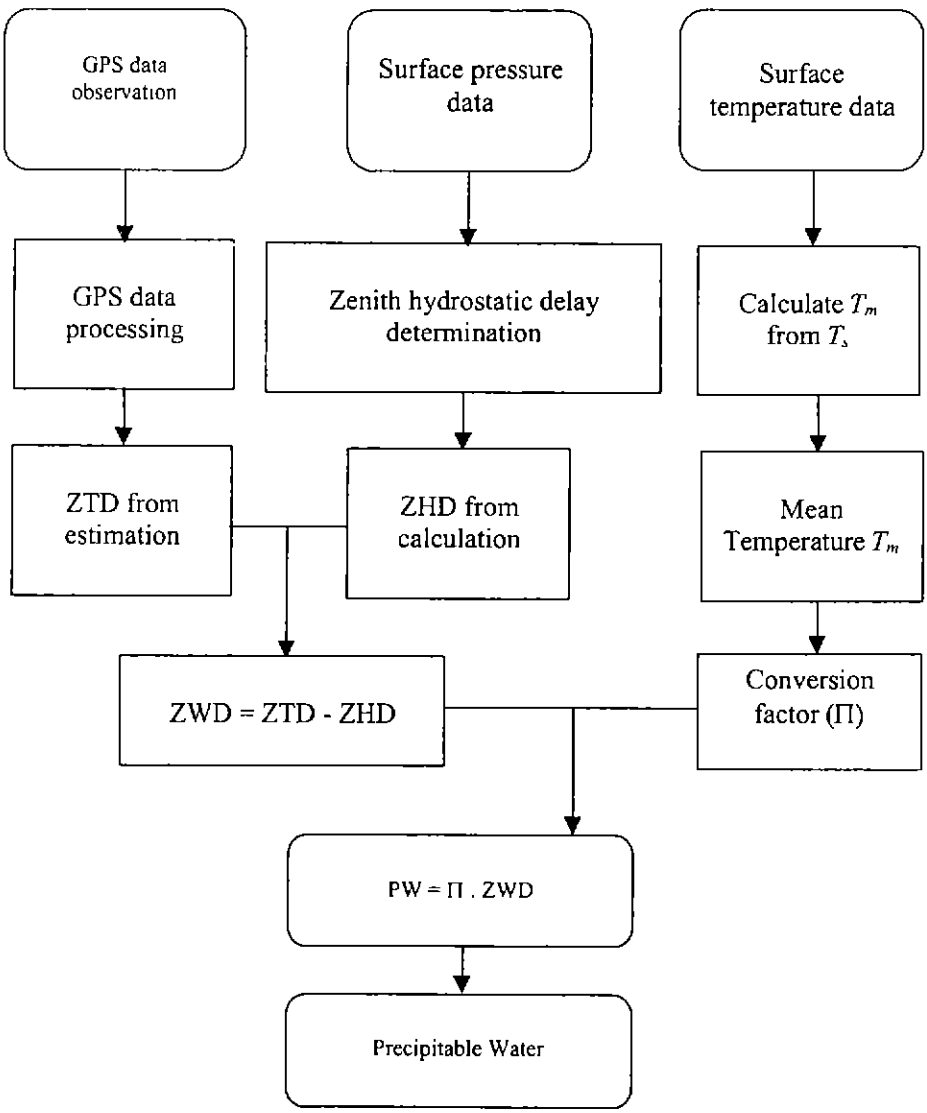

Figure 3.5 Summary of Estimating Precipitable Water from GPS

Chapter 4

GPS ESTIMATION OF ATMOSPHERIC WATER VAPOUR IN AUSTRALIA: METHOD, DATA SETS AND SOFTWARE

This chapter describes the estimation of atmospheric water vapour estimation using data from ground-based GPS receivers in and around Australia. The description includes the methodology, the data sets, and the software that is used. The methodology covers the technique of high accuracy GPS data processing and the strategy of data set selection. A brief description of the software used to process the GPS data is given in the last section of this chapter.

4.1 The Methodology

The technique of GPS estimation of atmospheric water vapour has been described in Chapter 3, and summarised in Figure 3.5. This research focuses on the strategies to process the GPS data to obtain high accuracy ZTD estimates using scientific GPS software. Using meteorological data, the ZWD is derived from the ZTD and then converted to PW. As discussed in Chapter 3, this requires the use of high accuracy carrier phase GPS data processing. These methods include the application of relative positioning in a network configuration and considering each error source and strategy discussed in Section 3.4.

The tropospheric delay estimation affects the quality of the coordinates, i.e. if the tropospheric delay estimation is wrong, then the coordinates will be wrong. Therefore the assessment of the coordinates can gauge at least a coarse assessment of the ability of the processing method to estimate the tropospheric delay. The quality of the coordinates is tested by using terms called the *repeatability* and the coordinate *recovery*. The repeatability is defined as the variability of the sessional solution about the mean coordinate. It is used in coordinate precision quality assessment. The coordinate recovery is the difference between the estimated coordinate and an assumed truth coordinate for each solution. In this case, the truth coordinates are the ITRF coordinates. It is used in coordinate accuracy assessment.

The tropospheric delay estimations are then converted to the PW using meteorological data. The GPS-PW estimates are assessed by comparing them with the radiosonde-PW estimates which are assumed as the 'truth PW estimates'.

The relative positioning technique is very effective at minimising or even eliminating GPS measurement biases, and hence is the basis for almost all high precision GPS positioning techniques (Rizos, 1999). It is used to eliminate the satellite and receiver clock errors by data differencing. However, data differencing also removes the atmospheric delay, the parameter that is required to be estimated. A large network is therefore needed to decorrelate the atmospheric delay at both ends of the baseline (Tregoning *et al.*, 1998). In addition, by using a GPS network in data processing, the random errors that are found in the observations can be minimised by the least-squares adjustment technique.

Most of the GPS estimation of atmospheric water vapour initiatives worldwide utilise GPS data from permanent GPS station networks and often these comprise IGS stations. GPS network examples for estimating the atmospheric water vapour are: SuomiNet (Ware *et al.*, 2001) in the USA, SAPOS (Dick *et al.*, 2001) in Germany, SWEPOS (Stoew *et al.*, 2001) in Sweden and GEONET (Ohtani, 2001) in Japan.

This research utilises dual-frequency GPS data from the Australian Regional GPS Network (ARGN), and other permanent GPS stations around Australia, whose data were obtainable, such as IGS stations. All the selected GPS stations have geodetic antenna types, are developed and placed in stable monumentation and have a continuous data flow. The meteorological data were provided by the Australian Bureau of Meteorology. More details of the data sets can be found in the next section.

4.2 The Data Sets

This research required a data set to conduct the tests to find the best strategy for GPS estimation of atmospheric water vapour in Australia. It included the investigation of the problems, the quality and other related issues. A data set from 1 January 2001

until 30 April 2001 was selected. This was chosen to provide a large sample (about 120 days), and also since at that time, the Australian atmosphere holds more water vapour due to the summer season and is more variable. The data sets are: the GPS data, the meteorological data, the precise satellite orbits, the a priori station coordinates and the ocean tide loading models. A description of each data set follows.

4.2.1 The GPS data

Most of the GPS data were collected from a permanent GPS station network named the *Australian Regional Geodetic Network* (ARGN), which consists of 15 GPS stations (Twilley and Digney, 2001) and is maintained by the National Mapping Division (formerly AUSLIG) of Geoscience Australia (GA). These GPS stations are located in Alice Springs, Casey (Antarctica), Ceduna, Cocos Island, Darwin, Davis (Antarctica), Hobart, Jabiru, Karratha, Macquarie Island (sub-Antarctic), Mawson (Antarctica), Stromlo, Tidbinbilla, Townsville, and Yaragadee.

The establishment of GPS stations in the ARGN started in 1990 (Yaragadee) and was completed in 1998 (Stromlo). All 15 GPS stations became fully operational in mid 1998, with a 30 second data collection interval. The ARGN is also included in the IGS network, therefore their coordinates are determined accurately because they are included in the ITRF solutions.

To enhance the network and increase the number of stations at which PW estimates could be obtained, other permanent GPS stations beside the ARGN that are located in and around Australia were selected. These GPS stations are Auckland (New Zealand), Bakosurtanal (Indonesia), Noumea (New Caledonia) and Perth (Australia), which are maintained by the IGS, and Burnie (Australia) which is maintained by GA for tidal observations in collaboration with the University of Tasmania. In total, there are 20 permanent and continuous GPS stations that are included in this research. The GPS station sites were selected to be free from any significant signal interference or multipath reflection, and high quality GPS receiver (L1/L2 carrier and code observation) and data transfer or communication facilities were present. The configuration of the GPS stations is illustrated in Figure 4.1.

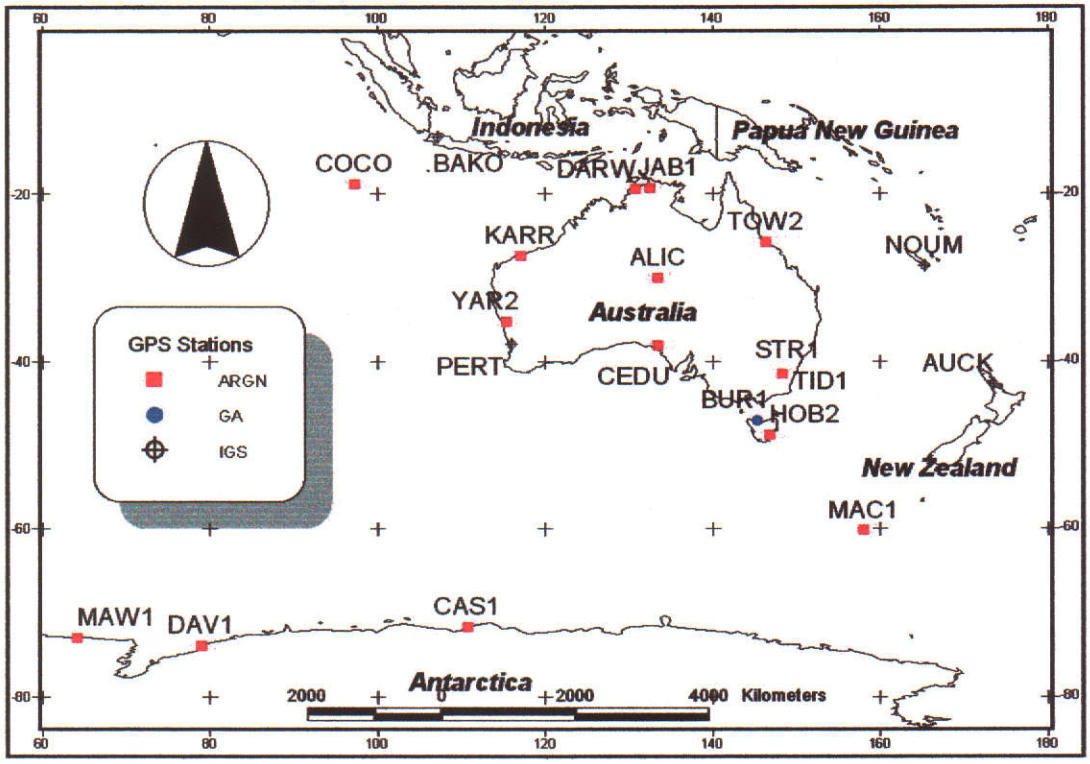

Figure 4.1 The GPS Station Configuration

Table 4.1 describes the equipment at the GPS station sites when the data sets were collected (from 1 January 2001-30 April 2001).

GPS Station	Station ID	GPS Receiver	Antenna Type
Alice Springs	ALIC	AOA ICS-4000Z ACT	AOA Dorne Margolin T
Auckland	AUCK	Rogue SNR-8000	AOA Dorne Margolin T
Bakosurtanal	BAKO	Trimble 4000SSI	TRM14532.00
Burnie	BUR1	Ashtech Z12	AOA Dorne Margolin T
Casey	CAS1	AOA ICS-4000Z ACT	AOA Dorne Margolin T
Ceduna	CEDU	AOA ICS-4000Z ACT	AOA Dorne Margolin T
Cocos Island	COCO	AOA SNR-12 ACT	AOA Dorne Margolin T
Darwin	DARW	AOA ICS-4000Z ACT	AOA Dorne Margolin T
Davis	DAV1	AOA ICS-4000Z ACT	AOA Dorne Margolin T
Hobart	HOB2	AOA ICS-4000Z ACT	AOA Dorne Margolin T
Jabiru	JAB1	Ashtech Z12	AOA Dorne Margolin T
Karratha	KARR	AOA ICS-4000Z ACT	AOA Dorne Margolin T
Macquarie Island	MAC1	AOA ICS-4000Z ACT	AOA Dorne Margolin T
Mawson	MAW1	AOA ICS-4000Z ACT	AOA Dorne Margolin T
Noumea	NOUM	Trimble 5700	TRM29659.00
Perth	PERT	Rogue SNR-8100 ACT	AOA Dorne Margolin T
Stromlo	STR1	AOA SNR-12 ACT	AOA Dorne Margolin T
Tidbinbilla	TID1	AOA ICS-4000Z ACT	AOA Dorne Margolin T
Townsville	TOW2	AOA ICS-4000Z ACT	AOA Dorne Margolin T
Yaragadee	YAR2	AOA ICS-4000Z ACT	AOA Dorne Margolin T

Table 4.1 The GPS Station Site Equipment

The summary of the GPS data availability for each station for the 120 days selected (1 January-30 April 2001) can be seen in Figure 4.2.

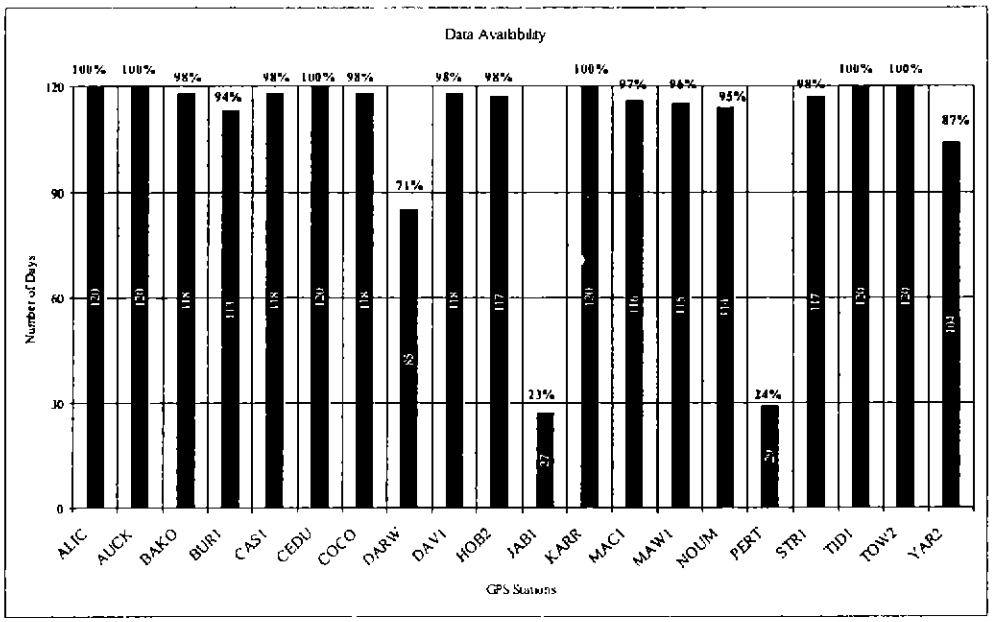

Figure 4.2 The GPS Station Data Availability

4.2.2 Meteorological data

In estimating atmospheric water vapour using ground-based GPS receivers, pressure and temperature data are needed to derive the PW from the estimated zenith total tropospheric delay. In addition, to control the quality of GPS-PW estimates, it is beneficial to obtain PW estimates from other measurement techniques. In this research, the quality of GPS-PW estimates was assessed by comparison with PW estimates from radiosondes.

All surface meteorological data (pressure and temperature) for estimating atmospheric water vapour using ground-based GPS receivers were obtained from the Australian Bureau of Meteorology. In addition, the Bureau of Meteorology observes atmospheric water vapour by using other instruments (for example, radiosondes) due to their responsibility for weather monitoring and research. Therefore, the atmospheric water vapour estimates obtained from ground-based GPS receivers can be compared to other instruments that have been established and used earlier.

In order to record and monitor climate data, Australia established meteorological observation stations around the mainland and in Antarctica. These observation stations were designed as national networks, land surface meteorological networks and upper air meteorological networks. The upper air can be defined as the area in the atmosphere which starts at levels above 850 millibars or approximately 1km above sea level (Glover, 2001). The land surface meteorological network includes 820 manual and automatic meteorological observing stations, more than 6,600 daily rainfall stations and about 780 rainfall intensity recorders; whereas there are 50 stations for upper air observations (Bureau of Meteorology, 2001). However, for climate change detection, Australia maintains 104 Reference Climate Stations (RCS) in its national network, which have the following criteria: continuous homogeneous records, high quality and long-term climate trends. Moreover, due to participation in the Global Climate Observing System (GCOS), Australia also maintains 68 stations from RCS as GCOS Surface Networks (GSN) and 16 stations as GCOS Upper Air Networks (GUAN). Figure 4.3 illustrates the configuration of the GPS and the RCS around Australia.

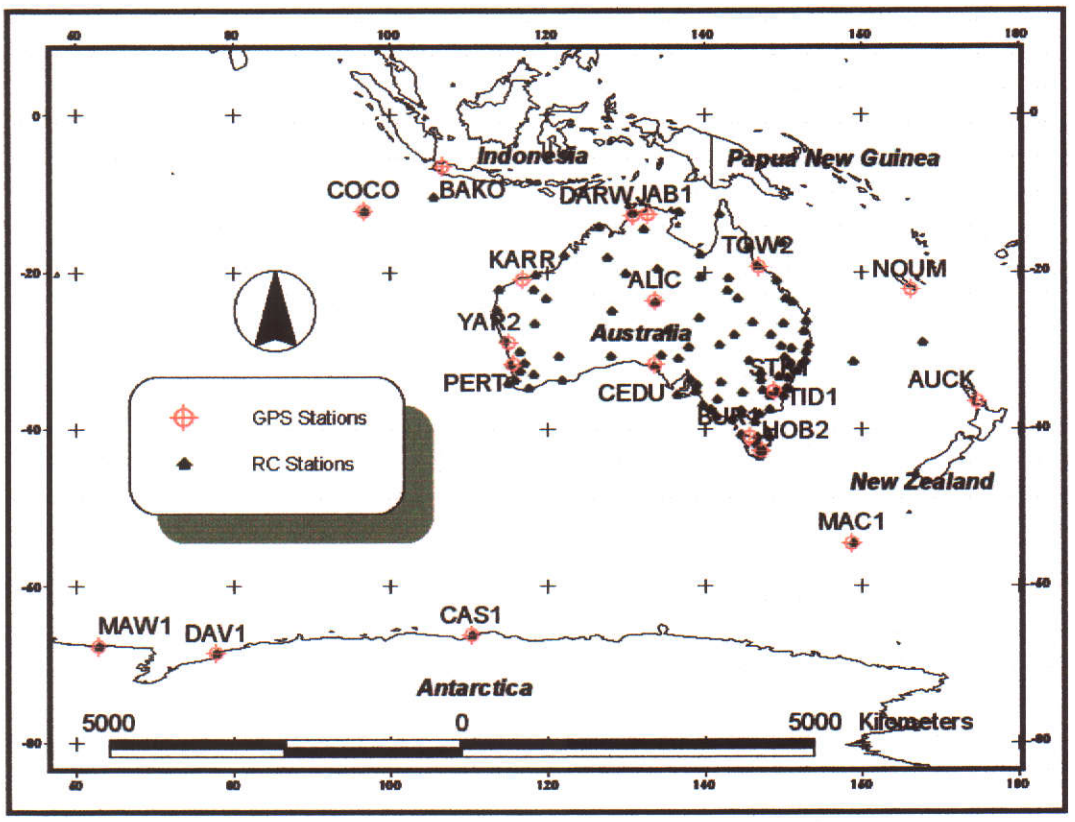

Figure 4.3 The Configuration of GPS and RCS around Australia

4.2.3 Co-location of GPS Surface Meteorological and Radiosonde Stations

Important aspects that must be taken into account in meteorological data are the location of meteorological stations and the distance between GPS stations and the stations. To derive water vapour estimates from GPS observations, temperature and air pressure at GPS locations (antennas) are needed. Therefore, temperature and pressure data at meteorological stations are mapped to GPS stations (antennas) by selecting the meteorological stations which are closest and have a similar altitude to the GPS station locations. The co-locations of GPS and surface meteorological stations are listed in Table 4.2.

GPS Station	*Australian Land Surface Station*		
	Name	*Distance*	*Height Difference*
Alice Springs	Alice Springs Airport	13.9km	41m
Casey	Casey	0.9km	3m
Ceduna	Ceduna AMO	30.46km	144m
Cocos Island	Cocos Island Airport	0.2km	1m
Darwin	Batchelor AWS	26.2km	30m
Davis	Davis	0.01km	5m
Hobart	Hobart Airport	6.2km	18m
Jabiru	Jabiru Airport AWS	0.43km	82m
Karratha	Roebourne	23.3km	104m
Macquarie Island	Macquarie Island	1.1km	6m
Mawson	Mawson	0.4km	14m
Perth	Perth Metro	13km	20m
Mt. Stromlo	Canberra Airport	17.4km	201m
Tidbinbilla	Tuggeranong	10.7km	59m
Townsville	Townsville Aero	30.4km	21m
Yaragadee	Morawa Airport	68km	4m

Table 4.2 Co-location of GPS Stations and Surface Meteorological Stations

As can be seen in Table 4.2, the distances and height differences between GPS stations to surface meteorological stations vary, therefore, the comparisons of PW estimates may also vary between each station.

Temperature and air pressure at meteorological stations were mapped into GPS antenna locations by using *World Meteorological Organisation* (WMO) technical note number 91 (1968) formula:

$$T_{gps} = (T_{met} - 0.0065) \times \Delta H_{gps-met} \quad (4.1)$$

$$P_{gps} = P_{met} . \times \exp\left[\frac{(0.034141 \times \Delta H_{gps-met})}{T_v}\right] \quad (4.2)$$

$$T_v = T_{met} + 0.5 \times 0.0065 \times \Delta H_{gps-met} + E \times C \quad (4.3)$$

$$E = \left(0.01 \times \exp\left(26.9348692 - \frac{\left(\frac{4914.0396 + 109218.53}{D_{met}}\right)}{D_{met}} - 0.0039015156 \times D_{met}\right)\right) \quad (4.4)$$

$$C = 0.107005 + H_{met} \times 0.0000250818 \quad (4.5)$$

where:

$T_{gps}; P_{gps}; H_{gps}$ are temperature, pressure and antenna height at GPS locations respectively; $T_{met}; P_{met}; H_{met}; D_{met}$ are temperature, pressure, barometer height and dew point temperature observation at meteorological stations respectively.

As the tropospheric estimation interval was set to every 15 minutes whereas surface pressure and temperature were observed every 3 hours, interpolation of pressure and temperature data were needed to synchronise the GPS and meteorological observations, to derive ZHD. Finally, ZWD was obtained by subtracting ZHD from TZD and converting the results to PW value, by using a conversion factor based on temperature data at GPS stations.

As listed in Table 4.2, only 16 GPS stations co-locate to the surface meteorological stations. It means only these stations can derive the PW estimates since the conversion from the tropospheric delay to PW needs the surface pressure and temperature data. These stations are: Alice Springs, Casey, Ceduna, Cocos Island, Darwin, Davis, Hobart, Jabiru, Karratha, Macquarie Island, Mawson, Perth, Stromlo, Tidbinbilla, Townsville and Yaragadee.

The GPS-PW estimates are validated to radiosonde-PW estimates from the GUAN Stations. However, there are only 14 GUAN stations that are co-located to GPS stations. Consequently only 14 GPS-PW estimates that can be validated with Radiosonde-PW estimates. The co-location between GPS stations and the GUAN stations are listed in Table 4.3.

GPS Stations	*Australian Upper Air Network*		
	Name	*Distance*	*Height Difference*
Alice Springs	Alice Springs Airport	13.9km	42m
Casey	Casey	0.9km	1m
Cocos Island	Cocos Island Airport	0.2km	2m
Darwin	Darwin Airport	53.9km	45m
Davis	Davis	0.01km	11m
Hobart	Hobart Airport	6.2km	41m
Karratha	Port Hedland Airport	173km	111m
Macquarie Island	Macquarie Island	1.1km	8m
Mawson	Mawson	0.4km	20m
Perth	Perth Airport	16.4km	30m
Mt. Stromlo	Wagga Wagga AMO	142km	569m
Tidbinbilla	Wagga Wagga AMO	141km	435m
Townsville	Townsville Aero	30km	23m
Yaragadee	Geraldton Airport	69km	235m

Table 4.3 Distances between GPS stations and Radiosonde stations

As can be seen in Table 4.3, the GPS stations and Radiosonde stations are separated by varying distances. For example, Karratha GPS station is located from about 173km away Port Hedland Airport where the radiosondes are launched. On the other hand, at Davis, the GPS station and the radiosonde station are separated by about 10 metres. Therefore, the quality of GPS-PW validation may be different for each station.

4.2.4 Precise satellite orbits

As mentioned in Section 3.4.1, precise satellite orbits are needed to minimise the orbit error in high accuracy GPS data processing, and such precise orbits are produced by the IGS. This research estimates PW using GPS data in a post-processed strategy and a near real-time strategy. For the post-processed strategy, the IGS Final (IGS) orbits were chosen because they are the most accurate satellite orbits now available. However, they cannot be used in a near real-time strategy because they are available only after 2 weeks. Therefore, the IGS Ultra Rapid (IGU) orbits were chosen for near real-time estimation because they are produced twice a day and provide real-time orbit data.

The IGS orbits are available 2 weeks after the time of observations, due to the time to undertake data collection, data analysis at the Analysis Centres and data combination by the IGS Analysis Centre Coordinator. The quality of the IGS orbits, as was shown in Table 3.5, is claimed to be about 5cm (IGS, 2002), based on the agreement between the 7 solutions from different Analysis Centres.

On the other hand, the IGU orbits were developed specifically for near real-time GPS meteorology applications and hence can be of use in practical weather forecasting. The IGU orbits are generated twice each day at 03:00 and 15:00 UTC and have a time-lag (time after the last observation used) of 3 hours (Springer, 2000). The IGU products contain 48 hours of orbital information. The first 24 hours contain a real orbit (an orbit based on actual observations) and the second 24 hours contain a predicted orbit. The quality of IGU orbits is claimed to about 20cm (IGS, 2002).

4.2.5 The ITRF coordinates

As described in Section 3.4.2, the quality of station coordinates plays an important role in high accuracy GPS data processing. Therefore, it is necessary to use the ITRF coordinates to ensure high accuracy a priori coordinates for the GPS stations.

Since this research utilises the GPS stations which are included in the IGS networks (except Burnie GPS station), the station coordinates and their velocity (station

movements) are included in the ITRF analysis. Unfortunately, the ITRF coordinates are not available for the Stromlo GPS station since only the Stromlo Satellite Laser Ranging (SLR) station is included in the ITRF solution. Moreover, the ITRF coordinates for GPS stations are assumed correct and will be used as a control to analyse the coordinate recovery of the estimated coordinates from GPS data processing.

This research used the ITRF2000 (Altamimi *et al.*, 2000) coordinates. Table 4.4 shows the ITRF2000 station coordinates and their velocities as used in this research.

Station ID	*X (m)*	V_X *(m/year)*	*Y (m)*	V_Y *(m/year)*	*Z (m)*	V_Z *(m/year)*
ALIC	-4052051.830	-0.0437	4212836.100	0.0009	-2545105.836	0.0497
AUCK	-5105681.003	-0.0253	461564.048	-0.0012	-3782181.752	0.0288
BAKO	-1836968.965	-0.0203	6065617.193	-0.0155	-716257.776	-0.0048
BUR1	-3989419.767	-	2699532.912	-	-4166619.774	-
CAS1	-901776.162	0.0001	2409383.419	-0.0077	-5816748.420	-0.0073
CEDU	-3753472.231	-0.0455	3912740.984	0.0066	-3347960.860	0.0461
COCO	-741950.006	-0.0436	6190961.630	0.007	-1337768.586	0.0479
DARW	-4091358.781	-0.0423	4684606.724	-0.0041	-1408580.460	0.0544
DAV1	486854.548	0.0008	2285099.302	-0.0032	-5914955.683	-0.0057
HOB2	-3950071.361	-0.0399	2522415.185	0.009	-4311638.362	0.0399
JAB1	-4236442.824	-0.0296	4559929.623	-0.0181	-1388624.653	0.0592
KARR	-2713832.258	-0.0458	5303935.087	0.0058	-2269515.012	0.0512
MAC1	-3464038.501	-0.0192	1334172.763	0.019	-5169224.323	0.0175
MAW1	1111287.166	0.0014	2168911.279	-0.0023	-5874493.595	-0.0036
NOUM	-5739971.535	-0.021	1387563.663	-0.0141	-2402123.551	0.0415
PERT	-2368686.968	-0.0483	4881316.517	0.0101	-3341796.161	0.049
STR1	-4467102.253	-	2683039.505	-	-3666949.947	-
TID1	-4460996.129	-0.0376	2682557.076	0.0011	-3674443.694	0.044
TOW2	-5054582.693	-0.0353	3275504.449	-0.012	-2091539.703	0.0496
YAR2	-2389025.536	-0.047	5043316.872	0.0079	-3078530.731	0.0488

Table 4.4 The ITRF2000 Station Coordinates and Velocities
(reference epoch 1997.00)

4.2.6 The ocean tide loading data

As described in Section 3.4.10, the OTL effects must be taken into account in high accuracy GPS data processing. Therefore, it is necessary to apply an OTL model to minimise these effects. In order to find the best OTL model that is suitable for Australian region, this research tested 10 different models computed by M.S. Bos and H.G. Scherneck from the Onsala Space Observatory (Swedish National Facility for Radio Astronomy). They are: Schwiderski (Schwiderski, 1980), FES94.1 (Le Provost *et al.*, 1994), FES95.2 (Le Provost *et al.*, 1998), FES99 (Lefevre *et al.*, 2000), GOT99.2b and GOT00.2 (Ray, 1999), CSR3.0 (Eanes and Bettadpur, 1996), CSR4.0 (Eanes and Shuler, 1999), NAO99.b (Matsumoto *et al.*, 2000) and TPXO.5 (Egbert *et al.*, 1994).

4.3 The Software

There are broadly two different types of GPS data processing software, namely commercial and scientific software (Seeber, 1993). Scientific software is needed to process GPS data for estimating atmospheric water vapour. There are a number of scientific softwares that can be used. For example: GAMIT (King and Bock, 1997), GIPSY (Webb and Zumberge, 1993) and Bernese (Hugentobler *et al.*, 2001). This research used Bernese GPS Software Version 4.2 which is available in the Western Australian Centre for Geodesy.

Bernese GPS software is designed for high accuracy positioning and is particularly well suited for ionosphere and troposphere modelling (Hugentobler *et al.*, 2001), and is already being used in GPS meteorology projects. These included the GPS meteorology project conducted in USA (UNAVCO, Rocken *et al.*, 1997), Japan (Tsuda *et al.*, 1998), and was also used in some of the WAVEFRONT project experiments (Dodson *et al.*, 1999).

The Bernese GPS software is scientific GPS data processing software developed and maintained by the Astronomical Institute, University of Berne, Switzerland, for high accuracy applications of GPS. This software consists of 5 parts:

1. Transfer part, which mainly generates files in Bernese specific format from GPS data in RINEX (Receiver Independent Exchange) format (Gurtner, 2001).
2. Orbit part, which generates a source-independent orbit representation, updates orbits, generates orbits in precise orbit format and compares orbits. Uses as input SP3 (Spofford and Remondi, 1999) format orbits.
3. Processing part, which is the main software module and is used to estimate the parameters based on GPS data.
4. Simulation part, which can generate simulated GPS data.
5. Service part, which mainly focuses on management of data and data representation.

Figure 4.4 on the next page illustrates the steps of data processing using Bernese GPS Software Version 4.2 (Hugentobler *et al.*, 2001).

For this research, not all of the steps which are illustrated in Figure 4.4 were used. The post-processed (Chapter 5) and near real-time (Chapter 6) strategies implemented in this research involved two different processing steps.

The post-processed strategy starts with the transfer part to convert the GPS RINEX data to Bernese format (activity number 1), and then to the generation of standard orbits (activity number 5) since the IGS precise orbits have been obtained. The next step is the processing part (activity number 6, 7 and 8) to estimate the ZTD through high accuracy GPS data processing strategies.

The near real-time strategy uses the same GPS data as the post-processed strategy but different orbit files. Therefore the main difference is with the standard orbits generation (activity number 5), before proceeding to the processing.

However, one of the near real-time strategies is the estimation of orbits (more detail in Section 6.1.4), which estimates the orbital parameters to improve the quality of IGU orbits based on the GPS data observations. Therefore, for this strategy, after the activity number 8, the process continues to the update orbits (activity number 9) and then back to the processing part (activity number 7) to estimate the ZTD.

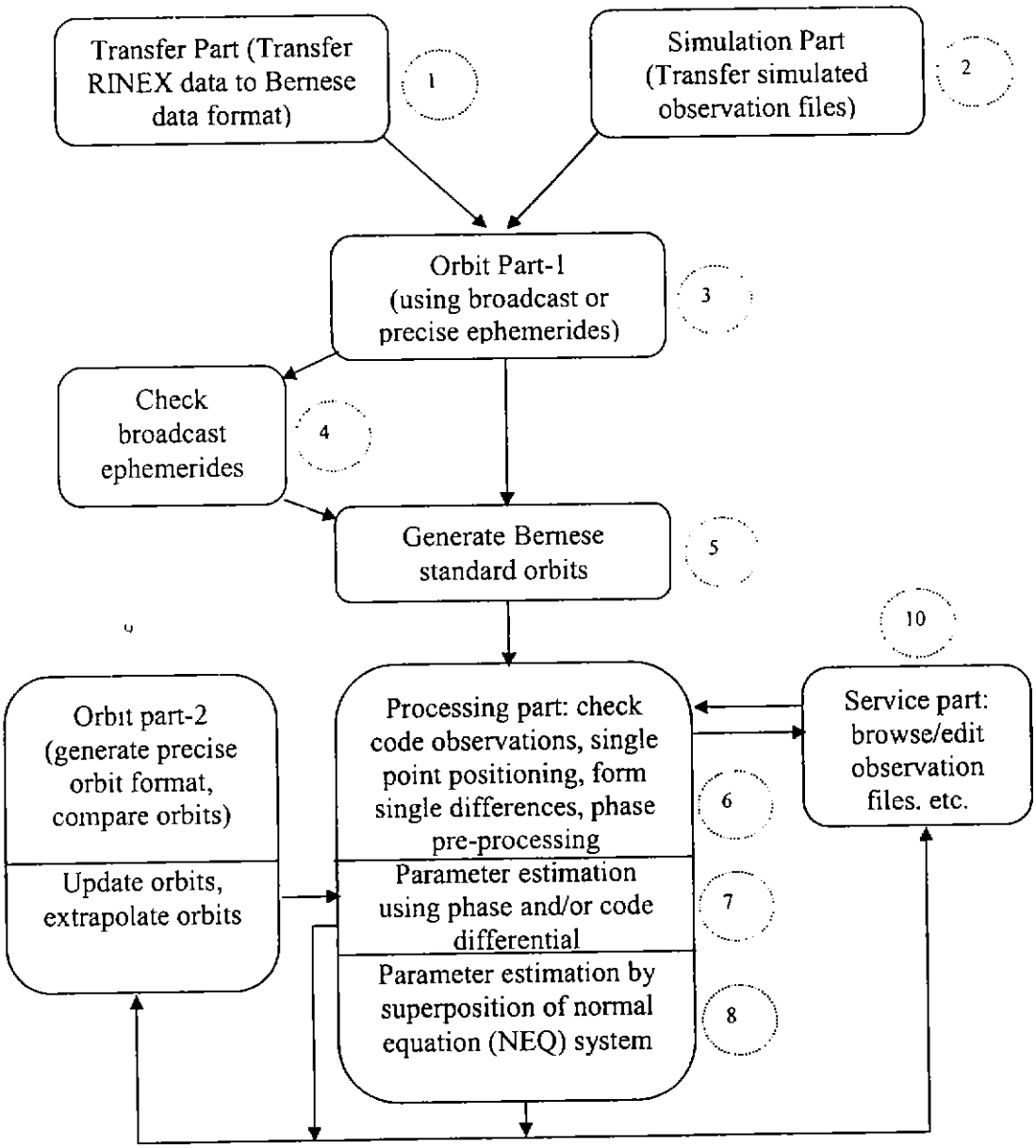

Figure 4.4 Data Processing Steps in the Bernese GPS Software
(The rectangle shapes illustrate the activity part (processing steps) which are inter-connected by flow lines. The number in the dashed circle illustrates the identity for each activity).

4.3.1 The ADDNEQ program in Bernese GPS Software

The ADDNEQ program in Bernese GPS Software was developed to handle the increased number of observations collected from permanent GPS arrays (Brockmann, 1996). This program utilises the normal equations (NEQ) which are

formed by least squares estimates since Bernese GPS Software estimates the parameters based on this method (Bock and Doerflinger, 2001).

The dimension of NEQ becomes much larger since the number of observation has increased. However, Brockman (1996) found that pre-elimination of parameters is a basic procedure to reduce the dimension of the NEQ system without losing the information. In addition, by performing some operations to NEQ matrices, the ADDNEQ progran. has advantages in (Becker *et al.*, 2000):

- Changing the auxiliary parameter information
- Scaling the normal equation systems
- Applying a priori transformations of the coordinates into different reference frame
- Changing the a priori values
- Changing the validity interval of the parameters (it means if any time-dependent parameter is modeled by a piecewise linear function, it is possible to join two or more intervals together, which reduces the number of parameters)
- Parameter stacking
- Constraining of the parameters

As this research works on a large number of parameters running from different data processing strategies, the ADDNEQ program is useful in terms of reducing time consumption, especially for different fixed station configuration tests since the program introduces parameter constraints based on the parameter transformation rules of NEQs. However, the ADDNEQ program also has some limitations, which are (Hugentobler *et al.*, 2001):

- Model modifications which are highly time-dependent, for example: different tropospheric mapping function, different a priori tide model,
- Ambiguity resolution,
- Different basic observation types, for example to change the observation frequency (L_1 and L_2 to L_3).

4.4 Summary

Data from 20 permanent GPS stations operating in the Australian region have been obtained from 1 January 2001 to 30 April 2001. These consist of 15 in the Australian GPS network (ARGN), maintained by the National Mapping Division of Geoscience Australia (formerly AUSLIG), 4 stations from the IGS network, and 1 station (Burnie) used for tidal observation by Geoscience Australia and the University of Tasmania.

The meteorological data needed to derive the PW from the estimated zenith total tropospheric delay were provided by the Australian Bureau of Meteorology (BoM). The meteorological data consist of surface meteorological data, used to derive GPS-PW estimates, and Radiosonde-PW estimates to validate the estimation results. The meteorological data were selected only from stations which are co-located with the GPS stations. Therefore, only 16 surface meteorological stations and 14 radiosonde stations were selected. The distance and the height difference between the surface meteorological station and the GPS station may affect the quality of GPS-PW estimates, whereas the distance and the height difference between the radiosonde launch site and the GPS station may give different quality of GPS-PW estimates for validation.

Other external data resources are also needed to perform high accuracy GPS data processing. The International GPS Service (IGS) provides precise GPS ephemerides and the International Earth Rotation Service (IERS) provides accurate ITRF station coordinates. The Onsala Space Observatory (Swedish National Facility for Radio Astronomy) provides various OTL models to be applied.

This research has used Bernese GPS Software Version 4.2 to process the GPS data to obtain high accuracy ZTD estimates.

Chapter 5

STRATEGY TESTING FOR POST-PROCESSED GPS PRECIPITABLE WATER VAPOUR ESTIMATION

This chapter describes the GPS data processing strategy for estimating the atmospheric water vapour around Australia. As was mentioned in Section 3.7, data processing strategies used for high accuracy GPS height determination are used substantially for estimating atmospheric water vapour using GPS. Therefore, different strategies in high accuracy data processing, which have been described in Section 3.4, are tested to find the best strategy that gives the highest quality of solution. The quality of the solution is assessed by using the coordinate repeatability and the coordinate recovery of each station, especially the height component. The GPS-PW estimates are derived based on the techniques which have been described in Chapter 3. In the last section of this chapter, the GPS-PW estimates are validated with radiosonde-PW estimates.

5.1 Post-Processed GPS-Water Vapour Estimation

The strategies for high accuracy GPS data processing have been described in Section 3.4, therefore, this research was mainly conducted based on those strategies, and considering the GPS data processing options that are available in the Bernese 4.2 GPS software. This applies standard models for Earth body tides and corrects the ionospheric delay by using the 'ionospherically free' linear combination. Therefore these two strategies are not considered further. As was mentioned in Chapter 4, this research uses the ITRF2000 as the reference frame since it is the latest version of ITRF and it is also compatible with the IGS ephemerides, which are held fixed.

This research used as a start point the findings from previous projects for the GPS estimation of PW which have been conducted around the globe The recommendation strategies from *GPS Water Vapour Experiment For Regional Operational Network Trials* (WAVEFRONT) and *Meteorological Applications of GPS Integrated Column Water Vapor Measurements in the Western Mediterranean*

(MAGIC) projects were considered as a guide to conduct this research. The summary of recommended GPS processing strategies to estimate the atmospheric water vapour from those projects can be seen in Table 5.1 (MAGIC, 1999; WAVEFRONT, 1999).

Strategy Options	***WAVEFRONT Recommendations***	***MAGIC Recommendations***
Satellite ephemeris	IGS precise final ephemeris (fixed)	IGS precise final ephemeris (fixed)
Differencing strategy	Ionospherically free observable	Ionospherically free observable
Data sampling rate	180 and 30 seconds	60 seconds
Elevation cut off angle	5 degrees	10 degrees
Weighting	Apply Elevation dependent weighting	Apply Elevation dependent weighting
Mapping function	Niell Mapping Function	Niell Mapping Function
Ocean tide loading (OTL)	Apply OTL model	Apply OTL model
Earth body tide	Apply Earth body tide model	Apply Earth body tide model
Antenna treatments	Apply antenna phase centre model	Apply antenna phase centre model
Tropospheric estimation interval	15 minutes	15 minutes
Tropospheric relative constraint	2mm/15 minutes	2cm/60 minutes
Data processing overlap	Minimum 6 hours	Minimum 4 hours
Ambiguity resolution	Ambiguities fixed solution	Ambiguities free solution
Station fixed	Fixed for well-established stations and high accuracy station coordinates from ITRF	Tightly constrain to well-established stations and high accuracy station coordinates from ITRF

Table 5.1 Summary of GPS Post-Processed Strategies for PW Estimation from Previous Projects

These recommendation strategies are refined to find the best strategies for the GPS estimation of PW around Australia. The quality of solution from different GPS data processing strategies is assessed by looking at the best estimation of station coordinates, since the tropospheric delay is highly correlated with coordinates especially the height component. Bock and Doerflinger (2001) state that 1mm error in zenith tropospheric delay can result in a bias in the vertical coordinate of the GPS station of 2-6mm. High accuracy GPS data processing produces the best quality of

estimated station coordinates, which means that the systematic errors have been mitigated as best as possible and therefore, the tropospheric delay is also estimated to good quality. The best quality tropospheric delay estimates are then used to derive PW.

As was illustrated in Figure 4.4, the steps of GPS data processing in a post-processed strategy start with the transfer part from the RINEX format to the Bernese format, and generate precise standard orbits from IGS final orbits. These two steps are included in the data preparation. The next step is data processing which includes network configuration; data pre-processing to eliminate clock errors, multipath and cycle slips; forms single differences to determine baselines; and then estimates the station coordinates and tropospheric delay based on high accuracy GPS data processing strategies. Since GPS data pre-processing strategies have been described in many GPS references such as Rizos (1999) and Hofmann-Wellenhof *et al.* (2001), this chapter focuses only on the network configuration and the strategies for estimating parameters of interest (station coordinates and tropospheric delay).

The following sections describe the strategies to construct the GPS network to process GPS data followed by the results of the GPS data processing strategies outlined in Table 5.1. These include: tests on observation sampling intervals, tests on elevation cut off angles, mapping functions and elevation dependent weighting, tests on ocean tide loading models, tests on tropospheric estimation interval and relative constraints, tests on ambiguity resolution and tests on different fixed station configurations.

5.1.1 Network Configuration

As was described in Chapter 4, 20 permanent GPS stations around Australia were used in this research. These collect GPS data every 30 seconds and the data are archived on a daily basis. The consequence of this situation is that the number of parameters are large, for example: station coordinate parameters, ambiguity parameters and tropospheric parameters. Moreover, the Bernese 4.2 GPS software is limited in the number of parameters that can be handled due to memory constraints. For example, with 20 GPS stations, there will be 60 station coordinate parameters

(X, Y, Z), more than 1000 ambiguity parameters (assuming 24 satellites in 480 observation epochs) and up to 1920 tropospheric delay parameters (assuming the tropospheric delay is estimated every 15 minutes). Therefore there will be more than 2200 parameters which are more than the maximum number that can be handled by the Bernese 4.2 GPS software.

To address this problem, the GPS stations in this research are divided into two groups, called Ausclus-1 and Ausclus-2. The Ausclus-1 is designed to accommodate the GPS stations which are maintained by the GA. The Ausclus-1 consists of 12 GPS stations which are distributed mainly on the Australian mainland: Alice Springs, Ceduna, Cocos Island, Darwin, Hobart, Jabiru, Karratha, Macquarie Island, Perth, Tidbinbilla, Townsville and Yaragadee.

On the other hand, the Ausclus-2 is designed to accommodate the GPS stations surrounding the Australian mainland, especially in the Polar region. These GPS stations are maintained by the GA and other survey institutions in other countries included in the IGS organisations. The Ausclus-2 consists of 13 stations: Alice Springs, Auckland, Bakosurtanal, Burnie, Casey, Darwin, Davis, Hobart, Mawson, Noumea, Perth, Mount Stromlo and Tidbinbilla.

Five stations have been selected to be included in both networks for quality control purposes. These stations are: Alice Springs, Darwin, Hobart, Perth and Tidbinbilla. The Ausclus-1 and the Ausclus-2 networks are illustrated in Figures 5.1 and 5.2 on page 67.

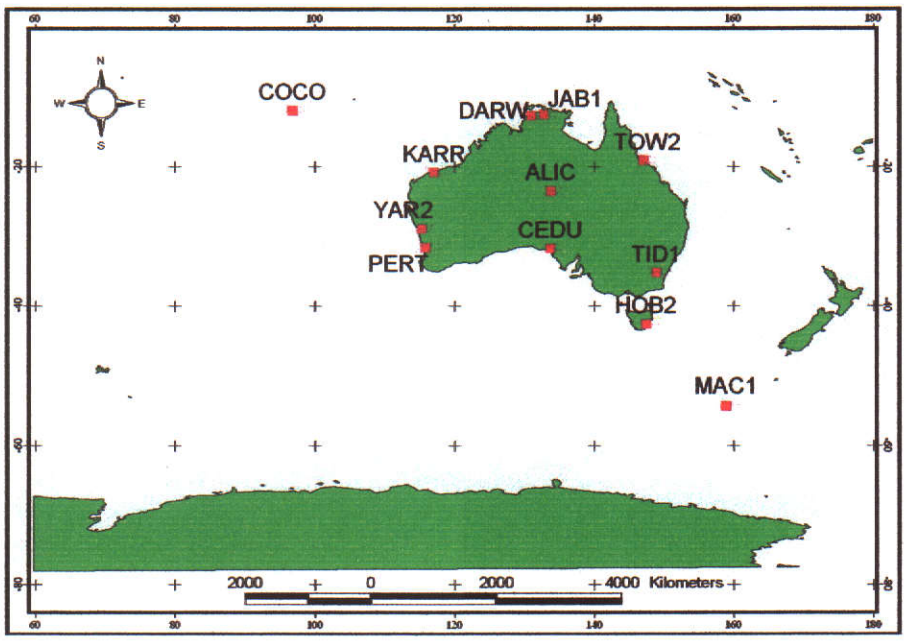

Figure 5.1 Ausclus-1 Configuration

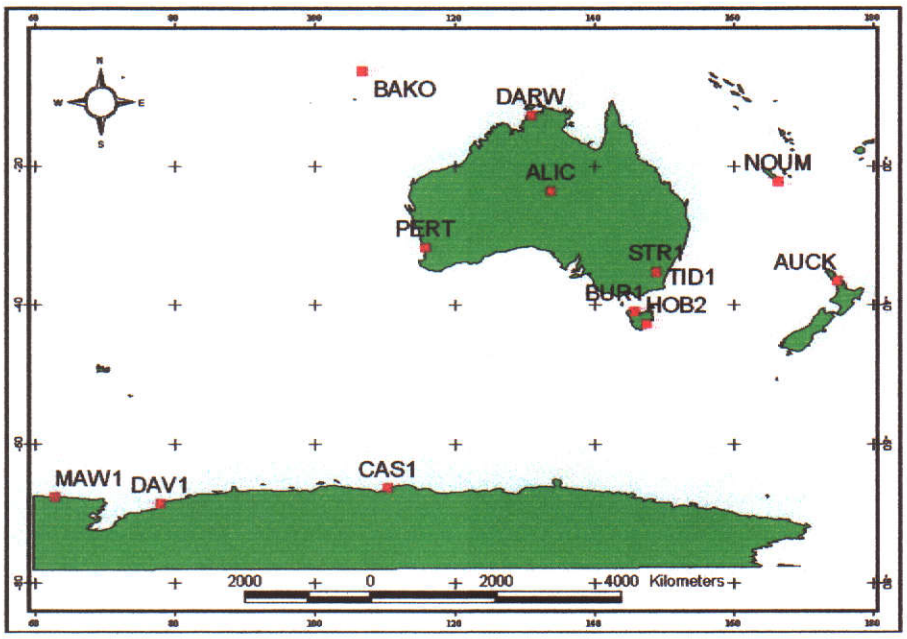

Figure 5.2 Ausclus-2 Configuration

The single difference observations between stations are formed based on the maximum number of observations common to both stations. Bernese 4.2 GPS software builds totally 25 different baselines for Ausclus-1 and 26 for Ausclus-2 during 120 sessions of data processing. The distances between stations (the baseline lengths) for both networks are shown in Figure 5.3.

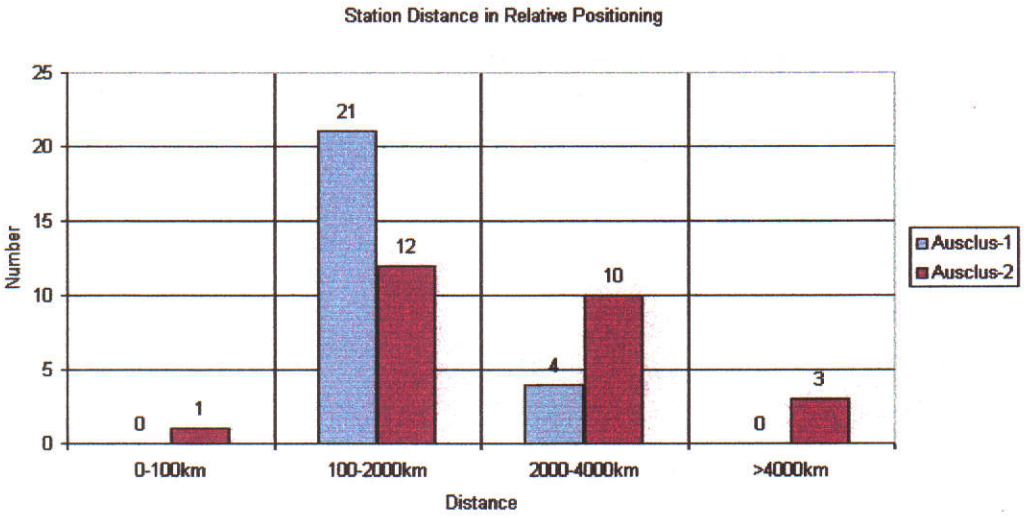

Figure 5.3 Baseline Lengths

5.1.2 Station Coordinate Constraints

In order to remove the datum defect in a least squares network solution, stations that have very accurately known coordinates were selected to be constrained. This strategy is one of the MAGIC recommendations. Moreover, Hugentobler *et al.* (2001) recommend setting up small a priori sigma values as a station coordinate constraint that corresponds to a fixed station. Since this research uses GPS data from ARGN and IGS networks whose station coordinates are precisely determined in the ITRF, the a priori station coordinates may be tightly constrained, and therefore the a priori sigma of station coordinates is set to 0.1mm.

This research mainly deploys Alice Springs, Cocos Island, Jabiru, Macquarie Island, Tidbinbilla and Yaragadee as constrained stations for Ausclus-1. For Ausclus-2, Alice Springs, Auckland, Bakosurtanal, Casey, Darwin, Davis, Hobart, Mawson, Noumea, Perth and Tidbinbilla are constrained. These stations were selected to

obtain a good geometric configuration in the network solution. However, the repeatability and the coordinate recovery of each station from different constrained station configurations cannot be compared with one other. The only way to see the effects of different constrained stations is directly, by the comparison of integrated precipitable water vapour results. The results of different station fixed configurations can be seen in Section 5.2.1.

5.1.3 Tests on observation sampling intervals

The sampling interval of GPS data observation from the IGS is set at 30 seconds. Previous studies (WAVEFRONT and MAGIC projects) showed that the sampling interval could be decreased to 180 seconds to make the GPS data processing faster. Therefore tests on different sampling intervals were performed to see whether there are changes in the station coordinates when changing the sampling interval of observation selection in GPS data processing.

Tests were performed at 30, 60, 120 and 180 seconds to obtain the best choice of observation sampling interval which gives the best station coordinates quality. The other strategies are set to basic options which are: the elevation cut off angle is set to 10 degrees, apply Niell mapping function, apply elevation dependent weighting, ocean tide loading model not applied, 3 hours tropospheric estimation interval, and the ambiguity is set to ambiguity-free solution.

The coordinate repeatability from 120 days GPS data processing can be seen in Table 5.2 on the next page. The abbreviations of GPS station names are listed in Table 4.1.

From Table 5.2, it can be seen that by using a 30 second sampling interval gives the best station coordinates repeatability. However, there is no big change in the station coordinate repeatability with a change in the sampling interval. Given that processing GPS data in a 180 second sampling interval is faster, the GPS data in Ausclus-1 and Ausclus-2 are processed using this interval. This strategy is applied to perform the next tests: tests on elevation masks, weighting observation, mapping functions, ocean tide loading models, tropospheric estimation interval and relative constraints, ambiguity resolution and different fixed station configurations.

GPS Station	Coordinate Repeatability (mm)											
	30 second			60 second			120 second			180 second		
	N	E	h	N	E	h	N	E	h	N	E	h
ALIC*	–	–	–	–	–	–	–	–	–	–	–	–
AUCK**	–	–	–	–	–	–	–	–	–	–	–	–
BAKO**	–	–	–	–	–	–	–	–	–	–	–	–
BUR1**	7.1	4.4	9.8	7	4.3	10	6.9	4.3	10	6.9	4.4	10.2
CAS1**	–	–	–	–	–	–	–	–	–	–	–	–
CEDU*	5.9	5.3	9.2	5.9	5.3	9.2	5.9	5.3	9.3	5.6	5.2	8.8
COCO*	–	–	–	–	–	–	–	–	–	–	–	–
DARW*	6.3	7.3	15.6	6.4	7.3	15.6	6.4	7.3	15.7	6.5	6.8	17.9
DAV1**	–	–	–	–	–	–	–	–	–	–	–	–
HOB2*	6.7	4.1	8.5	6.6	4.1	8.6	6.6	4.1	8.6	6.4	3.9	8.4
JAB1*	–	–	–	–	–	–	–	–	–	–	–	–
KARR*	4.9	6.9	13.6	5	6.9	13.6	5	6.9	13.7	5	6.2	12.3
MAC1*	–	–	–	–	–	–	–	–	–	–	–	–
MAW1**	–	–	–	–	–	–	–	–	–	–	–	–
NOUM**	–	–	–	–	–	–	–	–	–	–	–	–
PERT*	3.3	4.1	7.8	3.3	4.2	7.7	3.3	4.1	7.7	3.3	4.4	8
STR1**	6.4	4.3	8.4	6.4	4.3	8.6	6.4	4.4	8.7	6.4	4.3	8.7
TID1*	–	–	–	–	–	–	–	–	–	–	–	–
TOW2*	7.2	6.7	11.2	7.2	6.7	11.2	7.3	6.7	11.2	7.2	6.3	10.9
YAR2*	–	–	–	–	–	–	–	–	–	–	–	–
Mean	*5.98*	*5.39*	*10.51*	*5.98*	*5.39*	*10.56*	*5.98*	*5.39*	*10.61*	*5.91*	*5.18*	*10.65*

Table 5.2 Tests on Sampling Interval Observation
(the '-' indicates the fixed station, '*' indicates from Ausclus-1 and '**' indicates from Ausclus-2 data processing)

As can be seen in Table 5.2, the mean coordinate repeatabilities for different sampling interval observation options are almost the same, 6mm, 5mm and 11mm in the north, east and height components respectively. It means that the quality of the GPS data is free from the outliers. The height component repeatability ranges between 8mm to 18mm. The highest quality for the height component is achieved at Perth, whereas Darwin gives the lowest quality. However, Perth only records 30 days GPS data, therefore Hobart station gives the highest quality. Figure 5.4 shows the height component recovery for the Darwin and Hobart stations.

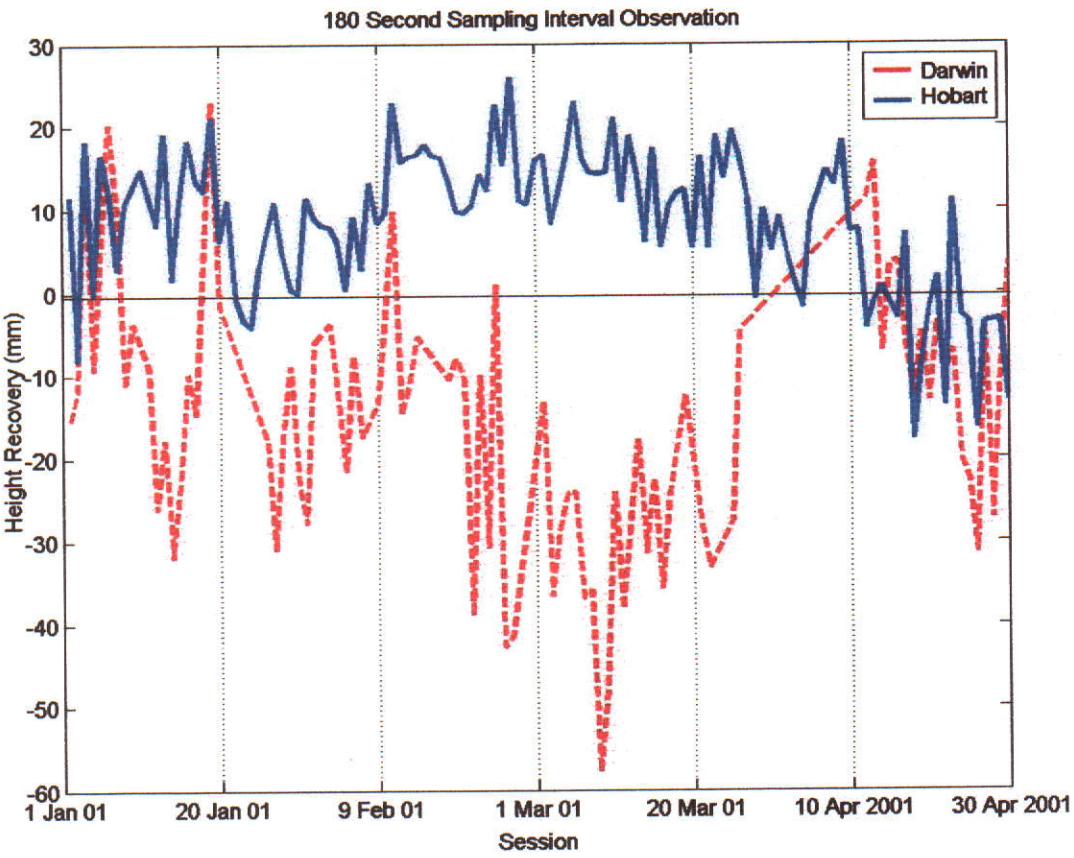

Figure 5.4 Comparison of Height Recoveries for Darwin and Hobart on Applying a 180 Second Sampling Interval Observation

Figure 5.4 shows that the expectations of the GPS data processing quality in this research will be plotted in the maximum range of 100mm. This can be used as a guidance to check the outliers on the following tests.

5.1.4 Tests on elevation mask, weighting observation and mapping function

As was described in Sections 3.4.7 and 3.4.8, elevation mask and mapping functions are tested in strategies to improve the estimation of tropospheric delay. In addition, Bernese 4.2 GPS software enables an elevation-dependent weighting strategy to improve the use of low elevation observations.

This research tests the use of 5, 10 and 15 degree elevation masks in combination with the Niell mapping function, the Hopfield mapping function and the zenith weighted (CosZ) mapping function. The effect of the elevation-dependent weighting

is also assessed in each test. The other options are set to a 180 second sampling interval, ocean tide loading model not applied, 3 hours tropospheric estimation interval, and the ambiguity is set to an ambiguity-free solution.

The coordinate repeatability from 120 days GPS data processing can be seen in Tables 5.3 to 5.8. In these tables, the fixed stations are omitted.

GPS Station	Hopfield Mapping Function			CosZ Mapping Function			Niell Mapping Function		
	N (mm)	E (mm)	h (mm)	N (mm)	E (mm)	h (mm)	N (mm)	E (mm)	h (mm)
BUR1**	6.8	5.8	11.1	6.8	5.8	11.4	6.8	5.8	10.9
CEDU*	6.4	5.5	12.1	6.4	5.5	13.0	6.4	5.6	11.6
DARW*	7.4	7.7	19.3	7.4	7.7	20.0	7.4	7.7	19.0
HOB2*	7.5	4.7	9.4	7.5	4.7	9.6	7.5	4.8	9.4
KARR*	5.8	8.0	13.4	5.8	8.0	14.9	5.8	8.1	12.7
PERT*	3.7	5.2	10.1	3.7	5.3	10.1	3.7	5.2	10.1
STR1**	6.8	5.4	10.2	6.8	5.4	11.1	6.8	5.4	9.7
TOW2*	8.3	7.4	12.5	8.2	7.4	13.2	8.3	7.4	12.3
Mean	*6.59*	*6.21*	*12.26*	*6.58*	*6.23*	*12.91*	*6.59*	*6.25*	*11.96*

Table 5.3 The Repeatability of Tests on 5 Degrees Elevation Mask with No Elevation-Dependent Weighting ('*' indicates from Ausclus-1 and '**' indicates from Ausclus-2 data processing)

GPS Station	Hopfield Mapping Function			CosZ Mapping Function			Niell Mapping Function		
	N (mm)	E (mm)	h (mm)	N (mm)	E (mm)	h (mm)	N (mm)	E (mm)	h (mm)
BUR1**	6.9	4.4	10.1	6.9	4.4	10.3	6.9	4.4	10.1
CEDU*	5.7	5.2	9.4	5.7	5.2	10.0	5.7	5.2	9.1
DARW*	6.5	6.8	18.0	6.5	6.8	18.4	6.5	6.8	17.9
HOB2*	6.4	3.8	8.4	6.5	3.7	8.5	6.4	3.8	8.4
KARR*	5.0	6.3	12.6	5.0	6.3	13.5	5.0	6.3	12.1
PERT*	3.3	4.4	8.0	3.3	4.4	7.9	3.3	4.4	8.1
STR1**	6.4	4.3	8.8	6.4	4.2	9.3	6.4	4.3	8.6
TOW2*	7.2	6.3	10.9	7.2	6.2	11.3	7.2	6.3	10.7
Mean	*5.93*	*5.19*	*10.78*	*5.94*	*5.15*	*11.15*	*5.93*	*5.19*	*10.63*

Table 5.4 The Repeatability of Tests on 5 Degrees Elevation Mask with Elevation-Dependent Weighting ('*' indicates from Ausclus-1 and '**' indicates from Ausclus-2 data processing)

GPS Station	Hopfield Mapping Function			CosZ Mapping Function			Niell Mapping Function		
	N (mm)	E (mm)	h (mm)	N (mm)	E (mm)	h (mm)	N (mm)	E (mm)	h (mm)
BUR1**	6.7	5.7	10.9	6.7	5.7	11.1	6.7	5.7	10.7
CEDU*	6.2	5.5	11.6	6.2	5.4	12.5	6.2	5.5	11.2
DARW*	7.4	7.7	19.3	7.4	7.7	19.9	7.4	7.7	19.1
HOB2*	7.4	4.7	9.3	7.4	4.7	9.5	7.4	4.8	9.3
KARR*	5.7	7.8	13.4	5.7	7.8	14.6	5.7	7.8	12.8
PERT*	3.7	5.3	10.1	3.7	5.3	10.1	3.7	5.2	10.1
STR1**	6.7	5.5	10.1	6.7	5.5	10.9	6.7	5.5	9.8
TOW2*	8.2	7.4	12.5	8.2	7.3	13.2	8.2	7.4	12.3
Mean	*6.50*	*6.20*	*12.15*	*6.50*	*6.18*	*12.73*	*6.50*	*6.20*	*11.91*

Table 5.5 The Repeatability of Tests on 10 Degrees Elevation Mask with No Elevation-Dependent Weighting ('*' indicates Ausclus-1 and '**' indicates Ausclus-2 data processing)

GPS Station	Hopfield Mapping Function			CosZ Mapping Function			Niell Mapping Function		
	N (mm)	E (mm)	h (mm)	N (mm)	E (mm)	h (mm)	N (mm)	E (mm)	h (mm)
BUR1**	6.9	4.4	10.2	6.9	4.4	10.3	6.9	4.4	10.2
CEDU*	5.6	5.2	9.1	5.6	5.2	9.6	5.6	5.2	8.8
DARW*	6.5	6.8	18.1	6.5	6.8	18.4	6.5	6.8	17.9
HOB2*	6.4	3.8	8.4	6.5	3.8	8.5	6.4	4.8	8.4
KARR*	5	6.2	12.7	5	6.2	13.5	5	6.2	12.3
PERT*	3.3	4.4	8	3.3	4.4	7.9	3.3	4.4	8
STR1**	6.4	4.3	8.9	6.4	4.3	9.3	6.4	4.3	8.7
TOW2*	7.2	6.2	11	7.1	6.2	11.4	7.2	6.3	10.9
Mean	*5.91*	*5.16*	*10.80*	*5.91*	*5.16*	*11.11*	*5.91*	*5.18*	*10.65*

Table 5.6 The Repeatability of Tests on 10 Degrees Elevation Mask with Elevation-Dependent Weighting ('*' indicates Ausclus-1 and '**' indicates Ausclus-2 data processing)

GPS Station	Hopfield Mapping Function			CosZ Mapping Function			Niell Mapping Function		
	N (mm)	E (mm)	h (mm)	N (mm)	E (mm)	h (mm)	N (mm)	E (mm)	h (mm)
BUR1**	6.6	5.3	12.3	6.6	5.3	12.4	6.6	5.3	12.3
CEDU*	5.6	5	9.6	5.6	5	9.9	5.6	5	9.5
DARW*	7	7.5	21.6	7	7.5	21.6	7	7.5	21.7
HOB2*	6.5	4.5	10.6	6.6	4.5	10.5	6.5	4.6	10.6
KARR*	5.1	6.7	14.5	5.1	6.7	14.8	5.1	6.8	14.4
PERT*	3.7	5	8.7	3.6	5	8.7	3.6	5	8.7
STR1**	6.3	5.1	10	6.3	5.1	10.2	6.3	5.1	9.9
TOW2*	7.5	6.9	13.6	7.5	6.9	13.7	7.5	6.9	13.5
Mean	*6.04*	*5.75*	*12.61*	*6.04*	*5.75*	*12.73*	*6.03*	*5.78*	*12.58*

Table 5.7 The Repeatability of Tests on 15 Degrees Elevation Mask with No Elevation-Dependent Weighting ('*' indicates Ausclus-1 and '**' indicates Ausclus-2 data processing)

GPS Station	Hopfield Mapping Function			CosZ Mapping Function			Niell Mapping Function		
	N (mm)	E (mm)	h (mm)	N (mm)	E (mm)	h (mm)	N (mm)	E (mm)	h (mm)
BUR1**	6.8	4.5	12.2	6.8	4.5	12.3	6.8	4.5	12.2
CEDU*	5.5	5	9.1	5.5	5	9.3	5.5	5.1	9
DARW*	6.5	6.9	19.8	6.5	6.9	19.6	6.5	6.9	19.9
HOB2*	6.2	3.9	9.9	6.2	3.9	9.8	6.2	4	9.9
KARR*	5	6	14.5	5	6	14.8	5	6	14.4
PERT*	3.5	4.4	9.2	3.5	4.4	9.1	3.5	4.4	9.2
STR1**	6.4	4.5	10.2	6.4	4.5	10.4	6.4	4.5	10.1
TOW2*	7	6.3	12.9	7	6.3	13	7	6.3	12.9
Mean	*5.86*	*5.19*	*12.23*	*5.86*	*5.19*	*12.29*	*5.86*	*5.21*	*12.20*

Table 5.8 The Repeatability of Tests on 15 Degrees Elevation Mask with Elevation-Dependent Weighting ('*' indicates Ausclus-1 and '**' indicates Ausclus-2 data processing)

From Table 5.3 to 5.8, it can be seen that the best repeatability for the height component is given by the Niell mapping function in a 10 degrees elevation mask with elevation-dependent weighting strategy (Table 5.6). Moreover, from these tests, it is shown that the use of elevation-dependent weighting strategy is the most significant factor in improving the coordinate repeatability. As in Section 5.1.3, Hobart gives the highest quality for height repeatability, whereas Darwin is the

lowest. Figure 5.5 and 5.6 show the effect of elevation-dependent weighting to the height recoveries for Darwin and Hobart.

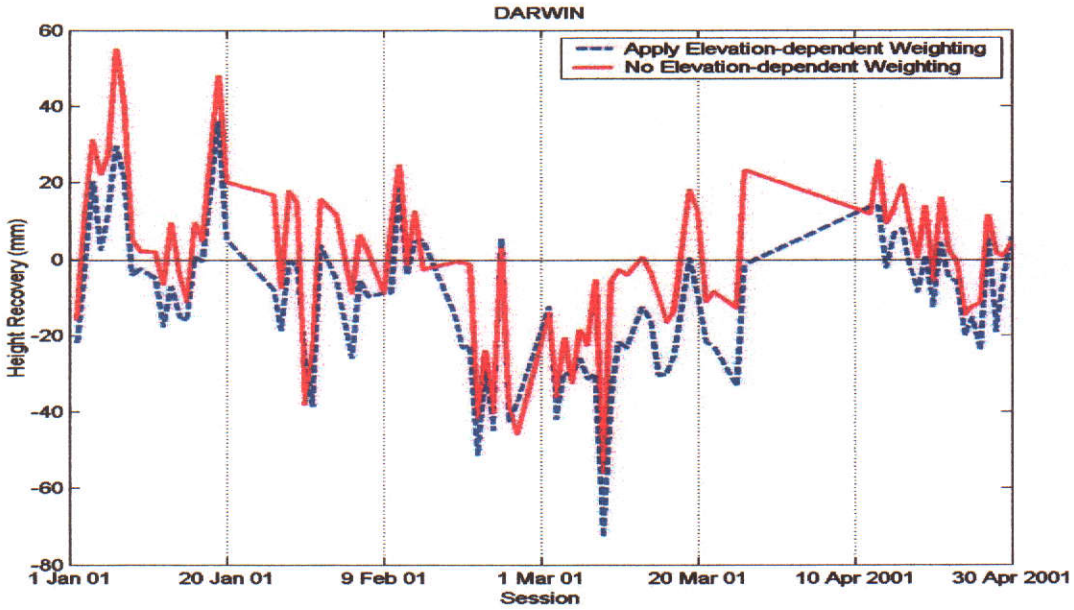

Figure 5.5 Comparison of Height Recoveries for Darwin on Applying Elevation-dependent Weighting

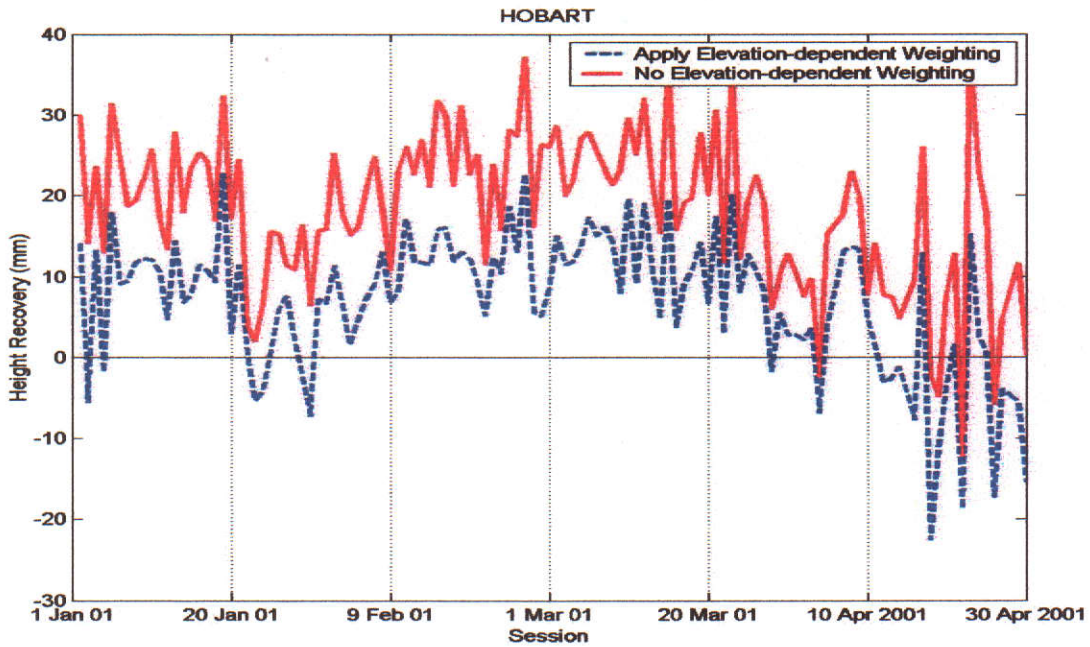

Figure 5.6 Comparison of Height Recoveries for Hobart on Applying Elevation-dependent Weighting

As can be seen in Figures 5.5 and 5.6, by applying elevation-dependent weighting, the height component can be improved by up to 20mm. For the next tests, the strategies of a 180 second sampling interval, a 10 degrees elevation mask in combination with the Niell mapping function and elevation-dependent weighting are applied.

5.1.5 Ocean tide loading

As described in Section 3.4.10, Ocean Tide Loading (OTL) must be taken into account in high accuracy positioning especially for height determination. Moreover, estimating atmospheric water vapour by using GPS is also more closely related to the height or the vertical component, rather than the horizontal component. Therefore, as was mentioned in Section 4.2.6, ten different sets of OTL parameters obtained from Onsala Space Observatory, which are computed by M.S. Bos and H.-G. Scherneck, were applied to process 120 days of GPS data. The OTL models are Schwiderski, FES94.1, FES95.2, FES99, GOT99.2b, GOT00.2, CSR3.0, CSR4.0, NAO99.b and TPXO.5. The other strategies applied are: 180 second sampling interval, a 10 degrees elevation mask in combination with the Niell mapping function and elevation-dependent weighting, 3 hours tropospheric estimation interval, and the ambiguity is set to ambiguity-free solution.

Tables 5.9, 5.10 and 5.11 show the repeatability of the coordinate stations for each component (Northing, Easting and Height in mm) from different OTL model tests.

GPS Station	No OTL	SCWD	FES-94	FES-95	FES-99	GOT-99	GOT-00	CSR-30	CSR-40	NAO 99b	TPXO .5
BUR1**	6.9	6.8	6.9	7.1	6.8	6.9	6.8	6.9	6.9	6.9	6.9
CEDU*	5.6	5.7	5.6	5.6	5.6	5.6	5.6	5.7	5.6	5.6	5.6
DARW*	6.5	6.6	6.7	6.7	6.7	6.7	6.7	6.7	6.7	6.7	6.7
HOB2*	6.4	6.4	6.4	6.3	6.4	6.4	6.3	6.4	6.4	6.3	6.4
KARR*	5.0	5	4.9	4.9	4.9	4.9	4.9	4.9	4.9	4.9	4.9
PERT*	3.3	3.2	3.2	3.2	3.2	3.2	3.2	3.2	3.2	3.2	3.2
STR1**	6.4	6.4	6.4	6.4	6.4	6.4	6.4	6.4	6.4	6.4	6.4
TOW2*	7.2	7.2	7.2	7.1	7.2	7.2	7.2	7.2	7.2	7.2	7.2
Mean	*5.91*	*5.91*	*5.91*	*5.91*	*5.90*	*5.91*	*5.89*	*5.93*	*5.91*	*5.90*	*5.91*

Table 5.9 The Repeatability of the Northing Component from OTL Tests
('*' indicates Ausclus-1 and '**' indicates Ausclus-2 data processing)

GPS Station	No OTL	SCWD	FES-94	FES-95	FES-99	GOT-99	GOT-00	CSR-30	CSR-40	NAO 99b	TPXO .5
BUR1**	4.4	4.4	4.5	4.8	4.5	4.5	4.4	4.5	4.5	4.4	4.4
CEDU*	5.2	5.4	5.3	5.3	5.3	5.2	5.3	5.2	5.3	5.3	5.3
DARW*	6.8	6.9	6.8	6.8	6.7	6.7	6.7	6.7	6.7	6.7	6.7
HOB2*	3.8	3.9	3.9	3.9	3.9	3.9	3.9	3.9	3.9	3.9	3.9
KARR*	6.2	6.1	6.1	6	6	6	6	6	6	6	6.1
PERT*	4.4	4.4	4.4	4.4	4.4	4.4	4.4	4.4	4.4	4.4	4.4
STR1**	4.3	4.3	4.3	4.4	4.4	4.4	4.4	4.4	4.4	4.4	4.3
TOW2*	6.3	6.5	6.4	6.5	6.4	6.4	6.4	6.4	6.4	6.4	6.4
Mean	*5.18*	*5.24*	*5.21*	*5.26*	*5.20*	*5.19*	*5.19*	*5.19*	*5.20*	*5.19*	*5.19*

Table 5.10 The Repeatability of the Easting Component from OTL Tests
('*' indicates Ausclus-1 and '**' indicates Ausclus-2 data processing)

GPS Station	No OTL	SCWD	FES-94	FES-95	FES-99	GOT-99	GOT-00	CSR-30	CSR-40	NAO 99b	TPXO .5
BUR1**	10.2	9.4	9.8	14.3	10	9.4	9.3	9.7	9.4	9.3	9.6
CEDU*	8.8	9.3	9.2	9.2	9.3	9.2	9.2	9.2	9.2	9.3	9.2
DARW*	17.9	16.9	16.8	16.7	16.9	16.9	16.9	16.9	16.9	17	17
HOB2*	8.4	8.2	8.4	8.5	8.4	8.3	8.3	8.4	8.3	8.3	8.3
KARR*	12.3	8.9	8.9	9	9	9.1	9	9	9	9	9.1
PERT*	8.0	8.8	8.8	9.1	9	9	9	9	9	9	8.9
STR1**	8.7	8.3	8.5	9	8.5	8.5	8.5	8.5	8.5	8.5	8.5
TOW2*	10.9	10.8	10.6	10.6	10.6	10.6	10.6	10.6	10.6	10.6	10.6
Mean	*10.65*	*10.08*	*10.13*	*10.80*	*10.21*	*10.13*	*10.10*	*10.16*	*10.11*	*10.13*	*10.15*

Table 5.11 The Repeatability of the Height Component from OTL Tests
('*' indicates Ausclus-1 and '**' indicates Ausclus-2 data processing)

From Tables 5.9, 5.10 and 5.11 above, it is clear that the best repeatability for the height component is given by the Schwiderski model, however, for all GPS data processing, the GOT00.2 model gives the best repeatability for all components and is a much more recent model.

The OTL model gives a big improvement in the height repeatability at Darwin and Karratha. Figure 5.7 and Figure 5.8 show the coordinate recoveries for both stations and the effects of the Schwiderski and GOT00.2 ocean tide loading models.

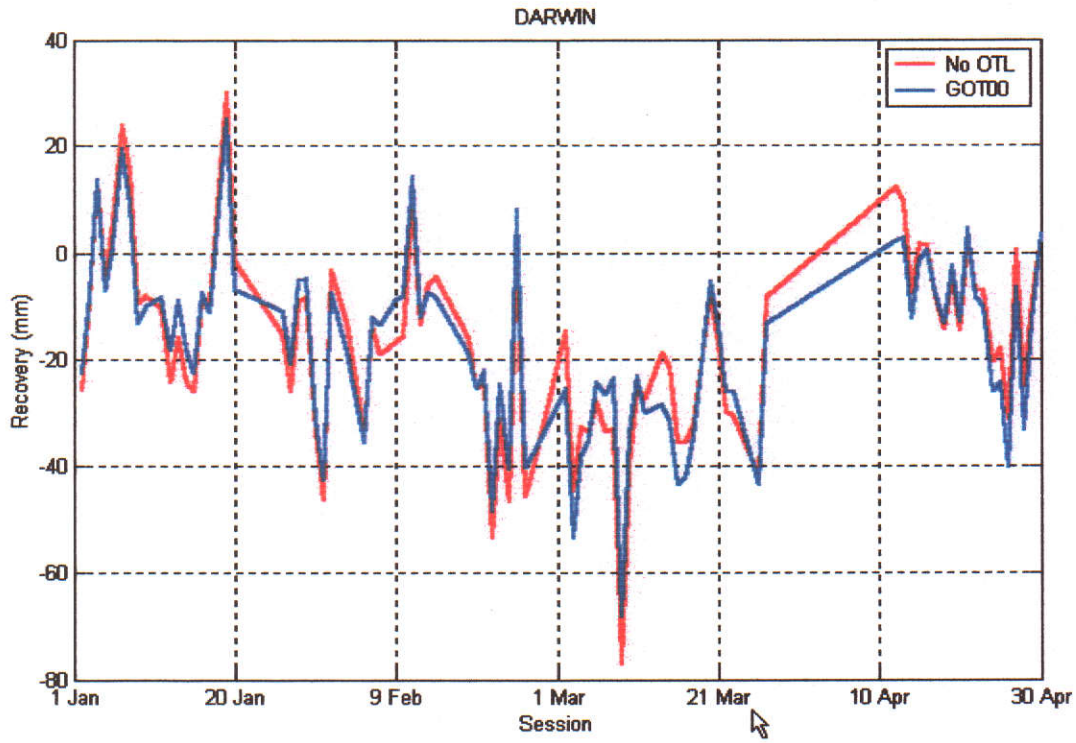

Figure 5.7 The Effects of the OTL models for the Height Recovery at Darwin

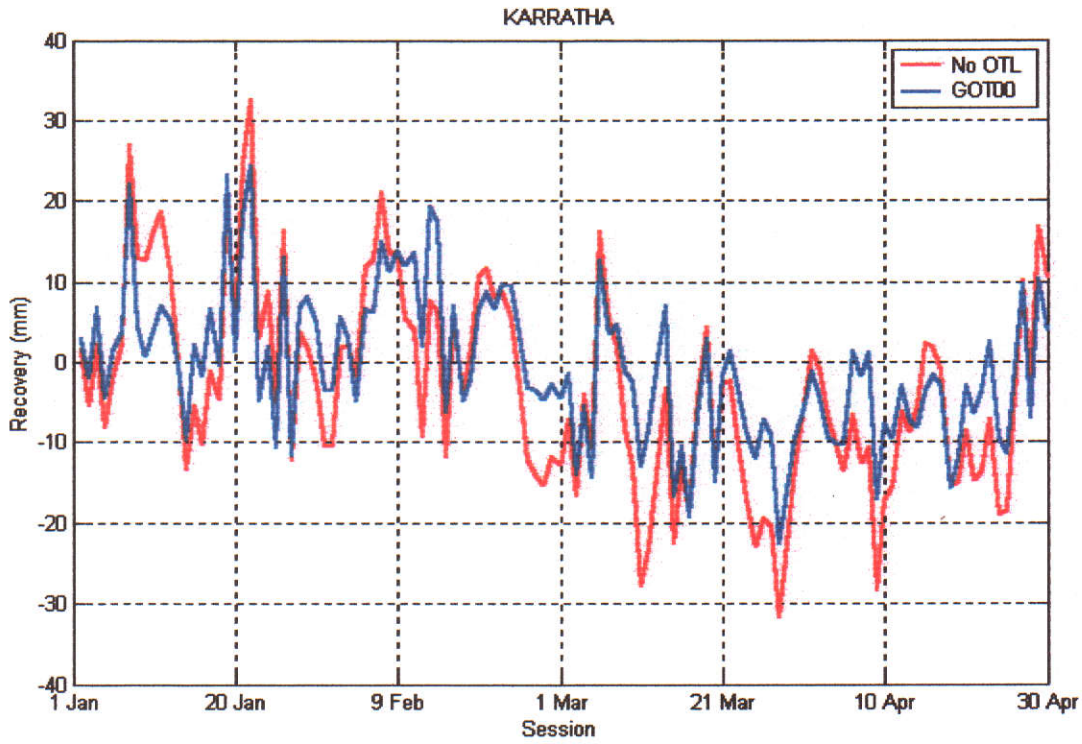

Figure 5.8 The Effects of the OTL models for the Height Recovery at Karratha

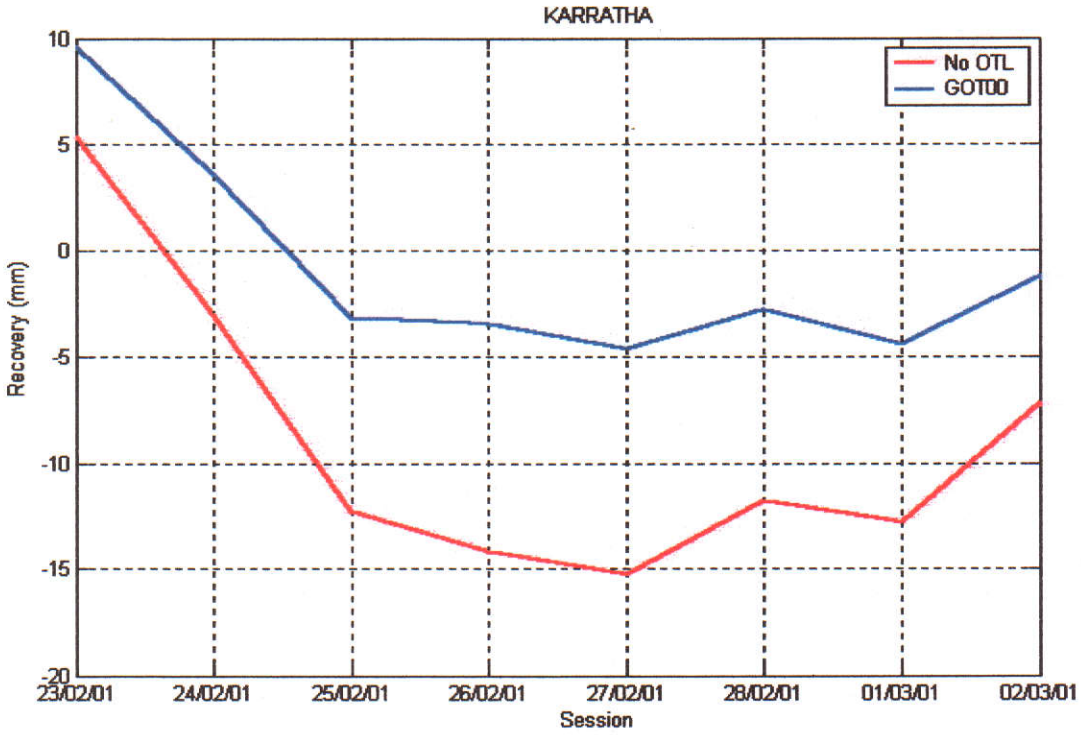

Figure 5.9 Detail Effects of the OTL models for the Height Recovery at Karratha

Figure 5.9 shows that the OTL model can improve the height accuracy by up to 10mm (see Figure 5.9). This fact shows the importance of the OTL model applied in high accuracy data processing and therefore can improve the quality of the tropospheric delay. The GOT00.2 OTL model is therefore used for the next tests.

5.1.6 Tropospheric interval and relative constraint estimates

The solution interval must be short enough to accommodate the time-scale of the variability of the water vapour signal. Rocken *et al.* (1995) suggest that little advantage is found in decreasing the interval to less than 15 minutes. A data set of 120 days of GPS data were tested using different troposphere estimate intervals, such as 15, 30, 60, 120 and 180 minutes; in conjunction with different values of relative a priori sigma (ranging from 1mm to 20mm, and also no constraint). The other strategies are set to a 10 degrees elevation cut-off angle in combination with the Niell mapping function and elevation dependent weighting, apply GOT00.b OTL model, and the ambiguity is set to ambiguity-free solution.

Tables 5.12 - 5.16 show the repeatability of the height component from different tropospheric intervals and tropospheric relative constraints tests. The '*' indicates Ausclus-1 and '**' indicates Ausclus-2 data processing. Due to the number of parameters that can be handled in Bernese, the tropospheric estimation interval for Ausclus-2 can only be estimated at a 30 minutes interval or more.

GPS Station	No Constraint	1mm	2mm	3mm	5mm	10mm	20mm
BUR1**	—	—	—	—	—	—	—
CEDU*	9.2	9.3	9.2	9.2	9.2	9.2	9.2
DARW*	16.9	15.3	16	16.3	16.6	16.8	16.8
HOB2*	8.3	8.1	8.2	8.2	8.2	8.2	8.2
KARR*	9.1	8.9	8.9	8.9	8.9	9	9
PERT*	9	8.8	8.8	8.8	8.8	8.9	8.9
STR1**	—	—	—	—	—	—	—
TOW2*	10.6	10.3	10.3	10.4	10.5	10.5	10.5
Mean	*10.52*	*10.12*	*10.23*	*10.30*	*10.37*	*10.43*	*10.43*

Table 5.12 The Height Repeatability of Tests for a 15 Minute Tropospheric Estimation Interval and Varying Relative Constraint

GPS Station	No Constraint	1mm	2mm	3mm	5mm	10mm	20mm
BUR1**	8.5	9	8.7	8.6	8.6	8.5	8.5
CEDU*	9.3	9.3	9.2	9.2	9.2	9.2	9.2
DARW*	16.6	15	15.6	15.9	16.3	16.5	16.6
HOB2*	8.2	8.2	8.2	8.1	8.1	8.1	8.1
KARR*	9	9	8.9	8.9	8.9	8.9	8.9
PERT*	8.7	8.8	8.8	8.7	8.7	8.7	8.7
STR1**	8.2	8.2	8.2	8.2	8.2	8.2	8.2
TOW2*	10.4	10.3	10.2	10.3	10.3	10.4	10.4
Mean	*9.86*	*9.73*	*9.73*	*9.74*	*9.79*	*9.81*	*9.83*

Table 5.13 The Height Repeatability of Tests for a 30 Minute Tropospheric Estimation Interval and Varying Relative Constraint

GPS Station	No Constraint	1mm	2mm	3mm	5mm	10mm	20mm
BUR1**	8.6	9.2	8.8	8.7	8.6	8.6	8.6
CEDU*	9.3	9.5	9.4	9.3	9.3	9.3	9.3
DARW*	15.7	14.7	15	15.3	15.5	15.6	15.7
HOB2*	8.3	8.3	8.3	8.3	8.3	8.3	8.3
KARR*	9.1	9.2	9.1	9.1	9.1	9.1	9.1
PERT*	9.1	8.9	9	9	9.1	9.1	9.1
STR1**	8	8.1	8.1	8	8	8	8
TOW2*	10.3	10.4	10.2	10.2	10.3	10.3	10.3
Mean	*9.80*	*9.79*	*9.74*	*9.74*	*9.78*	*9.79*	*9.80*

Table 5.14 The Height Repeatability of Tests for a 60 Minute Tropospheric Interval and Varying Relative Constraint

GPS Station	No Constraint	1mm	2mm	3mm	5mm	10mm	20mm
BUR1**	9	9.7	9.2	9.1	9.1	9	9
CEDU*	9.4	9.6	9.4	9.4	9.4	9.4	9.4
DARW*	15.8	15.2	15.4	15.6	15.7	15.7	15.8
HOB2*	8.7	8.5	8.6	8.7	8.7	8.7	8.7
KARR*	9.5	9.7	9.6	9.5	9.5	9.5	9.5
PERT*	9.4	9.5	9.3	9.3	9.4	9.4	9.4
STR1**	8.3	8.3	8.3	8.3	8.3	8.3	8.3
TOW2*	10.8	11	10.8	10.8	10.8	10.8	10.8
Mean	*10.11*	*10.19*	*10.08*	*10.09*	*10.11*	*10.10*	*10.11*

Table 5.15 The Height Repeatability of Tests for a 120 Minute Tropospheric Estimation Interval and Varying Relative Constraint

GPS Station	No Constraint	1mm	2mm	3mm	5mm	10mm	20mm
BUR1**	9.2	9.8	9.4	9.3	9.2	9.2	9.2
CEDU*	9.5	9.8	9.6	9.6	9.6	9.5	9.5
DARW*	14.7	14.7	14.6	14.6	14.7	14.7	14.7
HOB2*	8.3	8.3	8.3	8.3	8.3	8.3	8.3
KARR*	9.8	9.9	9.8	9.8	9.8	9.8	9.8
PERT*	8.7	9.4	8.7	8.7	8.7	8.7	8.7
STR1**	8.3	8.3	8.3	8.3	8.3	8.3	8.3
TOW2*	11	11.3	11.1	11	11	11	11
Mean	*9.94*	*10.19*	*9.98*	*9.95*	*9.95*	*9.94*	*9.94*

Table 5.16 The Height Repeatability of Tests for a 180 Minute Tropospheric Estimation Interval and Varying Relative Constraint

Figure 5.10 shows the mean repeatability over the 120 days of the height component obtained from the tropospheric estimation interval and relative constraint tests.

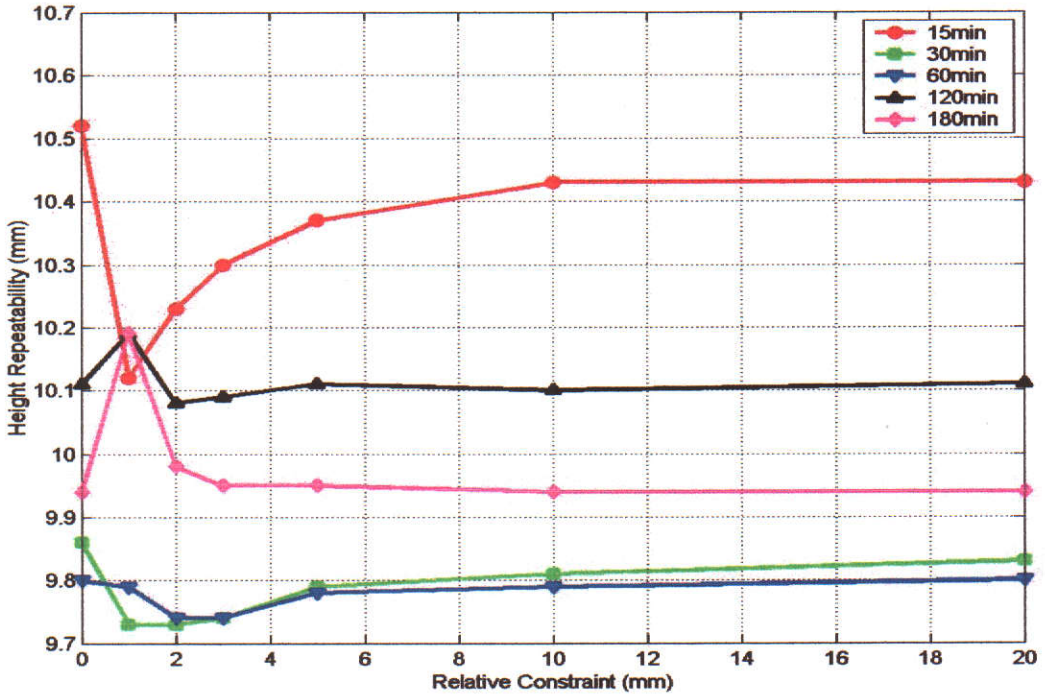

Figure 5.10 The Effect of the Tropospheric Estimation Interval and Relative Constraint to the Mean Repeatability of the Height Component (No constraint is plotted as '0mm' and does not actually indicate a relative constraint of 0mm)

It is seen that the best mean height repeatability can be obtained by estimating the tropospheric delay at a 30 minute interval and applying a relative constraint of 1mm, or a 60 minute interval and relative constraint of 2mm.

5.1.7 Troposphere gradient parameter

Rothacher *et al.* (1997) found that the repeatability of the estimated horizontal station component can be improved by estimating troposphere gradient parameters. The troposphere gradients are estimated to overcome the non-realistic assumption of azimuthal symmetry used by the mapping functions. Troposphere gradient parameters may be estimated in a North-South direction and an East-West direction together with the zenith delay to overcome this. Bernese 4.2 GPS software provides the facility to estimate troposphere gradient parameters.

For this research, only one pair of gradients (1 North-South and 1 East-West) have been estimated per 24 hour session. The effect of the troposphere gradient parameter estimates on the station coordinate repeatabilities for 120 days of data can be seen in Table 5.17.

GPS Station	Coordinate Repeatability					
	No Troposphere Gradient Estimates			Estimate the Troposphere Gradient Parameters		
	N (mm)	E (mm)	h (mm)	N (mm)	E (mm)	h (mm)
BUR1**	6.8	4.4	9.3	7.5	4.3	9
CEDU*	5.6	5.2	8.8	5.6	4.9	7.1
DARW*	6.5	6.8	17.9	5.5	6.9	17
HOB2*	6.4	3.8	8.4	6.3	3.6	7.1
KARR*	5	6.2	12.3	5.1	5.7	10.9
PERT*	3.3	4.4	8	3.4	4.3	8.1
STR1**	6.4	4.4	8.5	6.7	4.2	6.7
TOW2*	7.2	6.3	10.9	5.7	6	10.3
Mean	*5.90*	*5.19*	*10.51*	*5.73*	*4.99*	*9.53*

Table 5.17 The Effect of the Troposphere Gradient Estimates
('*' indicates Ausclus-1 and '**' indicates Ausclus-2 data processing)

This result shows that by considering the troposphere gradient parameters, the coordinate repeatability can be improved marginally.

5.1.8 Ambiguity resolution

The ambiguity resolution strategy was based on three factors (Hugentobler *et al.*, 2001): signal availability (single or dual frequencies), baseline length and session length. Bernese 4.2 GPS software has two basic options for ambiguity resolution: ambiguity free (float) solution and fixed solution. For ambiguity fixed solution, Bernese 4.2 GPS software provides four different techniques which are termed ROUND, SIGMA, SEARCH, and Quasi-Ionosphere Free (QIF) (Hugentobler *et al.*, 2001).

In this research, ROUND and SIGMA algorithms are not used because they work on one carrier (or one linear combination) only, whereas this research is based on using dual frequencies. In addition, Hugentobler *et al.* (2001) found that the SEARCH method has a problem in resolving the ambiguities in long sessions and very long

baselines due to the variations of satellite visibility during the observation session that can affect the selection of the reference ambiguity. Therefore, the SEARCH method was not used. Tests were conducted on ambiguity free (float) and fixed solutions on 120 days of GPS data. The coordinate repeatability from ambiguity solution tests can be seen in Table 5.18.

GPS Station	Repeatability of Ambiguity-free solution (mm)			Repeatability of Ambiguity-fixed solution (mm) using QIF Algorithm		
	N	E	h	N	E	h
BUR1**	7.5	4.3	9	6.6	2.4	8.1
CEDU*	5.6	4.9	7.1	5.8	4.1	10.8
DARW*	5.5	6.9	17	6.8	5.7	17.9
HOB2*	6.3	3.6	7.1	6.7	3.0	9.0
KARR*	5.1	5.7	10.9	5.1	6.2	12.0
PERT*	3.4	4.3	8.1	3.4	4.3	8.4
STR1**	6.7	4.2	6.7	5.9	2.8	7.5
TOW2*	5.7	6	10.3	7.1	5.6	13.9
Mean	*5.73*	*4.99*	*9.53*	*5.93*	*4.26*	*10.95*

Table 5.18 Ambiguity Test Results
('*' indicates Ausclus-1 and '**' indicates Ausclus-2 data processing)

Table 5.19 shows the baseline lengths that were used in this research to compute the non-fixed station coordinates.

GPS Station	Number of Computed Baseline	Baseline Length (km)			Height Repeatability (mm)	
		Min	Max	Mean	Float Solution	Fixed Solution (QIF)
BUR1**	132	232	5405	1257	9	8.1
CEDU*	240	908	2044	1374	7.1	10.8
DARW*	125	192	1838	1213	17	17.9
HOB2*	231	832	1703	1190	7.1	9.0
KARR*	365	910	2354	1702	10.9	12.0
PERT*	29	310	1203	1018	8.1	8.4
STR1**	272	10	4172	1006	6.7	7.5
TOW2*	189	1445	1918	1691	10.3	13.9

Table 5.19 The Average Baseline Length and The Height Repeatability
('*' indicates Ausclus-1 and '**' indicates Ausclus-2 data processing)

This research found that for long baselines (more than 2000 km) and long sessions (minimally a 24 hour data observation session), the ambiguity-free solution gives better coordinate repeatability compared to the ambiguity-fixed solution. In addition, for a long baseline and a long session, the float solution is more reliable, considering the difficulties to fix the ambiguity and the effect of fixing an ambiguity to an incorrect value.

5.1.9 The GPS data processing results from combination of best strategy

Different options for GPS data processing were described in Sections 5.1.3 - 5.1.8. For the data observation sampling interval, since there is no big improvement in the station coordinate repeatability and considering that processing GPS data in a 180 second sampling interval is faster, therefore, networks were processed using this interval. The elevation mask was set to 10 degrees for both networks and the Niell mapping function used with elevation-dependent observation weighting.

Different ocean tide loading models gave similar results for the height repeatability for each station. However, the GOT00.2 OTL model was selected from considering the station coordinate repeatability results, and this model is also more up to date than the others. Relative troposphere constraints of 1mm were used with an estimation interval of 30 minutes, and troposphere gradients in north-south and east-west directions were estimated. The ambiguity-free solution was selected to process both networks based on the results of the ambiguity resolution tests.

The improvement of station coordinate repeatabilities from different strategies for high accuracy GPS data processing and their combination can be seen in Table 5.20.

GPS Station	Sampling Interval Selection Strategy	Elevation Mask, Mapping Function and Weighting Strategy	Ocean Tide loading Model Strategy	Trop. Estimation Interval and Relative Constraint Strategy	Trop. Gradient Estimates Strategy	Ambiguity Resolution Strategy (Float solution)	Combination of Best Strategies
BUR1**	10.2	10.2	9.3	9	9	9	7.3
CEDU*	8.8	8.8	9.2	9.3	7.1	7.1	8.1
DARW*	17.9	17.9	16.9	15	17	17	14
HOB2*	8.4	8.4	8.3	8.2	7.1	7.1	6.8
KARR*	12.3	12.3	9	9	10.9	10.9	7.8
PERT*	8	8	9	8.8	8.1	8.1	9.3
STR1**	8.7	8.7	8.5	8.2	6.7	6.7	9.2
TOW2*	10.9	10.9	10.6	10.3	10.3	10.3	6.3
Mean	*10.65*	*10.65*	*10.10*	*9.73*	*9.53*	*9.53*	*8.60*

Table 5.20 The Improvement of Station Coordinates Repeatability
('*' indicates Ausclus-1 and '**' indicates Ausclus-2 data processing)

The combination of the best strategy is used to derive PW from GPS data processing, and then validated to radiosonde data which will be described in the next section.

5.2 Validation of Post-Processed Strategy with Radiosonde Data

5.2.1 Validation of GPS-PW estimates with radiosonde-PW estimates

Chapter 3 and Chapter 4 have described how to derive PW from GPS data processing. However as mentioned in Section 5.1.2, GPS data were also processed by using different configurations of fixed stations to derive PW. These GPS-PW estimates are validated with radiosonde PW-estimates.

As can be seen in Table 5.1, the strategy to fix the station coordinates can be performed by fixing or tightly constraining the well-established stations and high accuracy station coordinates. Constraining the station coordinates to an a priori sigma of 0.01mm is equivalent to fixing the station coordinates (Hugentobler *et al.*, 2001).

As was explained in Section 4.3.1, the ADDNEQ program has an ability to change the parameter constraints including the station coordinates in rapid and flexible computation without going back to the original observations (Hugentobler *et al.*, 2001). Therefore, tests on different fixed station configurations are performed by setting up the a priori sigma value of the station coordinates in the ADDNEQ program. The GPS processing options were to set the elevation cut-off angle to 10 degrees, to apply Niell mapping function, to apply elevation dependent weighting, not apply ocean tide loading model to reduce processing time, set 3 hours tropospheric estimation interval, and set the ambiguity to an ambiguity-free solution. These strategies are chosen to make sure the tests are purely to assess the effects of different fixed station configuration for the PW estimates.

There are three different tests for station fixed configurations: fix one station, fix some stations and fix all stations. Alice Springs is set to be fixed for the fix one station configuration due to its location in the centre of the Ausclus-1 and Ausclus-2. Alice Springs, Cocos Island, Jabiru, Macquarie Island, Tidbinbilla and Yaragadee are fixed for the fix some stations configuration of Ausclus-1; whereas Alice Springs, Auckland, Bakosurtanal, Casey, Darwin, Davis, Hobart, Mawson, Noumea, Perth and Tidbinbilla are fixed for the fix some stations configuration of Ausclus-2.

As previously mentioned in Chapter 4, only 16 GPS stations can derive PW due to the availability of surface meteorological data. These stations are: Alice Springs, Ceduna, Casey, Cocos Island, Darwin, Davis, Hobart, Jabiru, Karratha, Macquarie Island, Mawson, Perth, Stromlo, Tidbinbilla, Townsville and Yaragadee. From these stations, GPS-PW estimates from Ceduna and Jabiru cannot be validated due to unavailability of radiosonde data around these two stations. The validation results of GPS-PW estimates from different fix station configurations can be seen in Table 5.21 on the next page.

Table 5.21 shows that there is no significant difference between each configuration, however, the best standard deviation of GPS-PW estimates validated to radiosonde data is given by using the fix some stations strategy. Based on this fact, the GPS data for Ausclus-1 and Ausclus-2 were processed by fixing some stations mentioned in Section 5.1.2.

GPS Station	Fix one station		Fix Some Stations		Fix All Stations	
	Std. Deviation (mm)	Bias (mm)	Std. Deviation (mm)	Bias (mm)	Std. Deviation (mm)	Bias (mm)
Alice Springs*	2.32	1.62	2.26	1.50	2.36	1.62
Casey**	2.39	2.14	2.27	2.02	2.53	2.26
Cocos Island*	3.86	0.50	3.78	0.01	3.80	-0.04
Darwin*	7.14	-1.23	7.13	-1.19	7.09	-2.06
Davis**	6.04	3.14	5.97	2.97	6.02	3.13
Hobart*	2.28	1.49	2.30	1.54	2.68	2.08
Karratha*	6.19	0.76	6.18	0.68	6.19	0.51
Macquarie Island*	1.90	0.77	1.82	0.65	1.85	0.69
Mawson**	3.68	1.79	3.51	1.43	3.68	1.62
Perth*	2.02	-0.06	2.03	-0.12	2.23	-0.95
Stromlo**	4.82	1.33	5.11	1.59	4.83	0.98
Tidbinbilla*	4.46	2.02	4.50	2.15	4.58	2.29
Townsville*	2.68	1.11	2.69	1.18	2.58	0.71
Yaragadee*	5.18	0.72	5.10	0.59	5.10	0.65
Mean	*3.93*	*1.15*	*3.90*	*1.07*	*3.97*	*0.96*

Table 5.21 Tests on Different Fixed Station Configurations
('*' indicates Ausclus-1 and '**' indicates Ausclus-2 data processing)

More details about the results of the test on different station fixed configurations are given in Figure 5.11 and Figure 5.12 which illustrate the PW estimates for Perth and Darwin. As can be seen in Table 5.21, the lowest standard deviation of GPS-PW estimates validation is obtain from the Perth GPS station, whereas the highest is obtain from Darwin GPS station. This is because of a climate factor, since Darwin is located in a tropical region which is more humid and has the largest PW content compared to other regions, and also possibly increased ionospheric activity in the tropics. However, as can be seen in Figure 4.2, only 24 percent of GPS data were available and processed for the Perth GPS station from the 120 days selected.

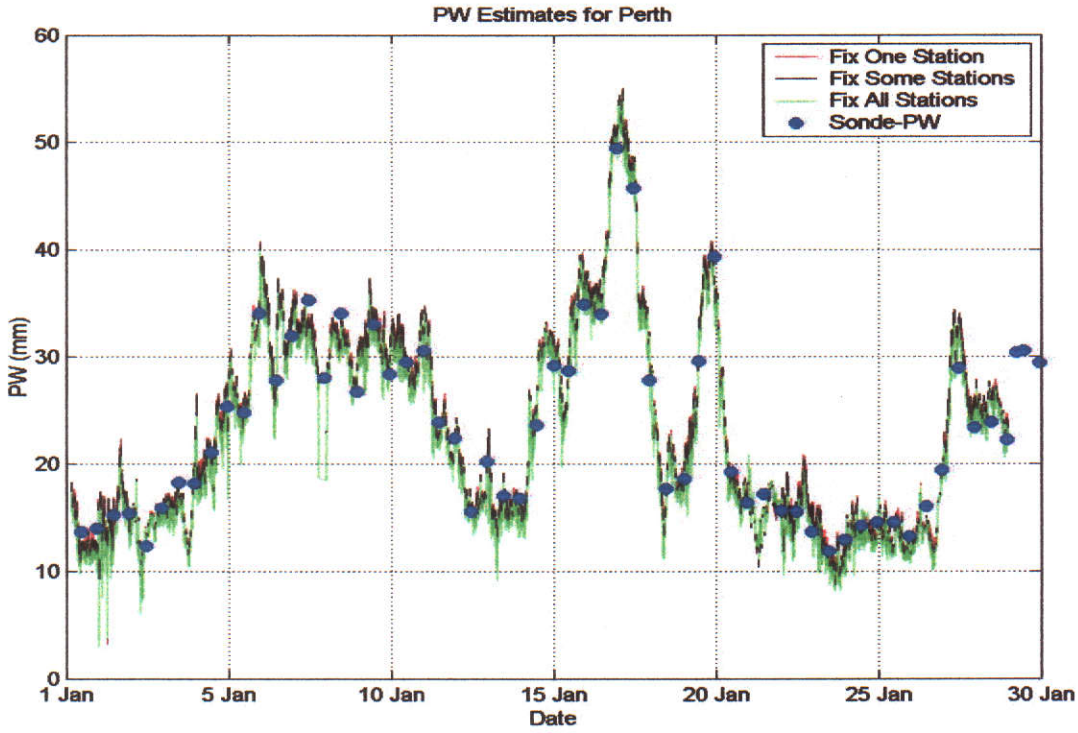

Figure 5.11 GPS-PW Estimates for Perth from Different Fixed Station Configurations

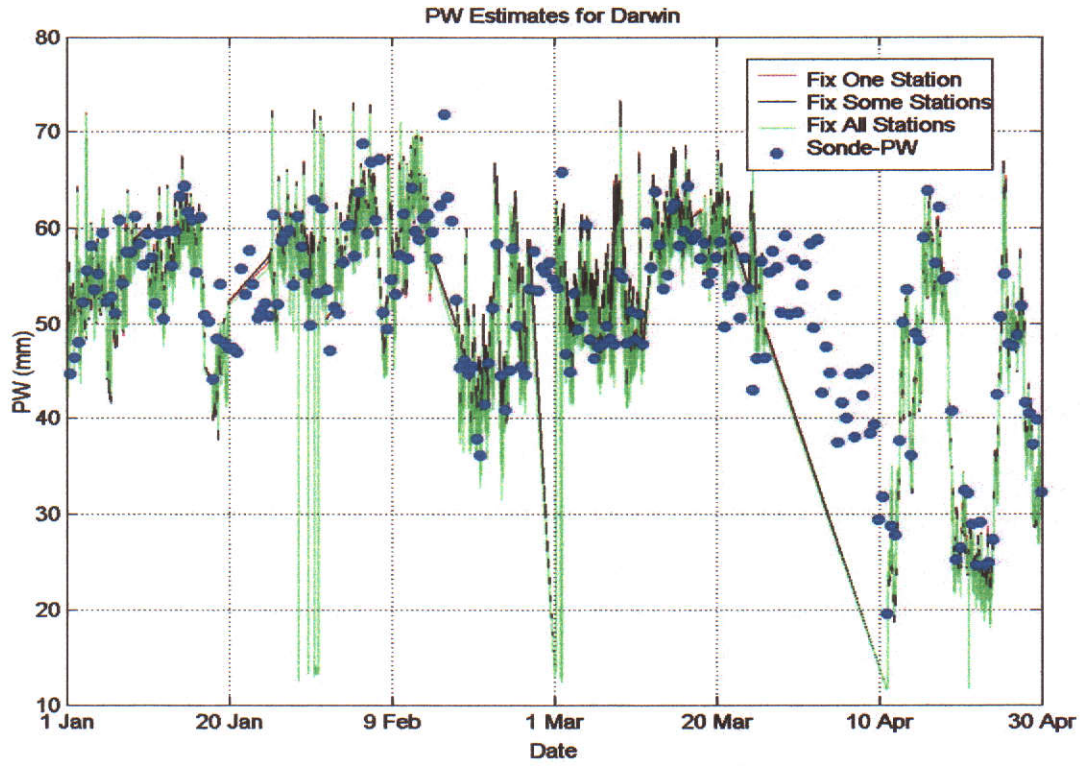

Figure 5.12 GPS-PW Estimates for Darwin from Different Fixed Station Configurations

The validation of the final results for GPS-PW estimates and radiosonde-PW estimates for all GPS stations can be seen in Table 5.22. This result is obtained by using the combination of the best strategies of GPS data processing which have been tested before. These strategies are: applying a 180 second observation data sampling, a 30 minute different troposphere estimates interval, in conjunction with 1mm relative a priori, a 10 degree elevation cut-off angle in combination with Niell mapping function and elevation dependent weighting, applying GOT00.b OTL model, ambiguity-free solution and fixing some stations.

As can be seen in Table 5.22, the GPS-PW estimation agrees with radiosonde-PW estimation in average standard deviation at 2.65mm. The maximum standard deviation is 5.84mm at Karratha, whereas the minimum is 1.13mm at Mawson. The maximum bias is 2.5mm at Tidbinbilla, whereas the minimum bias is 0.18mm at Perth. The validation results are analysed in Section 5.3.

No.	GPS Station	Count	Std. Deviation (mm)	Bias (mm)
1	Alice Springs*	119	2.25	1.52
2	Casey**	233	2.10	1.97
3	Cocos Island*	228	2.03	0.50
4	Darwin*	182	3.70	-0.47
5	Davis**	238	1.65	1.53
6	Hobart*	230	1.81	1.35
7	Karratha*	248	5.84	0.05
8	Macquarie Island*	231	1.57	0.62
9	Mawson**	232	1.13	0.97
10	Perth*	58	1.39	0.18
11	Stromlo**	134	3.91	1.72
12	Tidbinbilla*	134	4.24	2.44
13	Townsville*	122	2.67	1.60
14	Yaragadee*	138	2.81	1.57
		Mean	*2.65*	*1.11*

Table 5.22 Comparison of GPS-PW Estimates and Radiosonde-PW Estimates ('*' indicates Ausclus-1 and '**' indicates Ausclus-2 data processing). Bias is GPS-PW estimates minus Radiosonde-PW estimates. The cause of the bias is not yet fully understood and is a topic of further research.

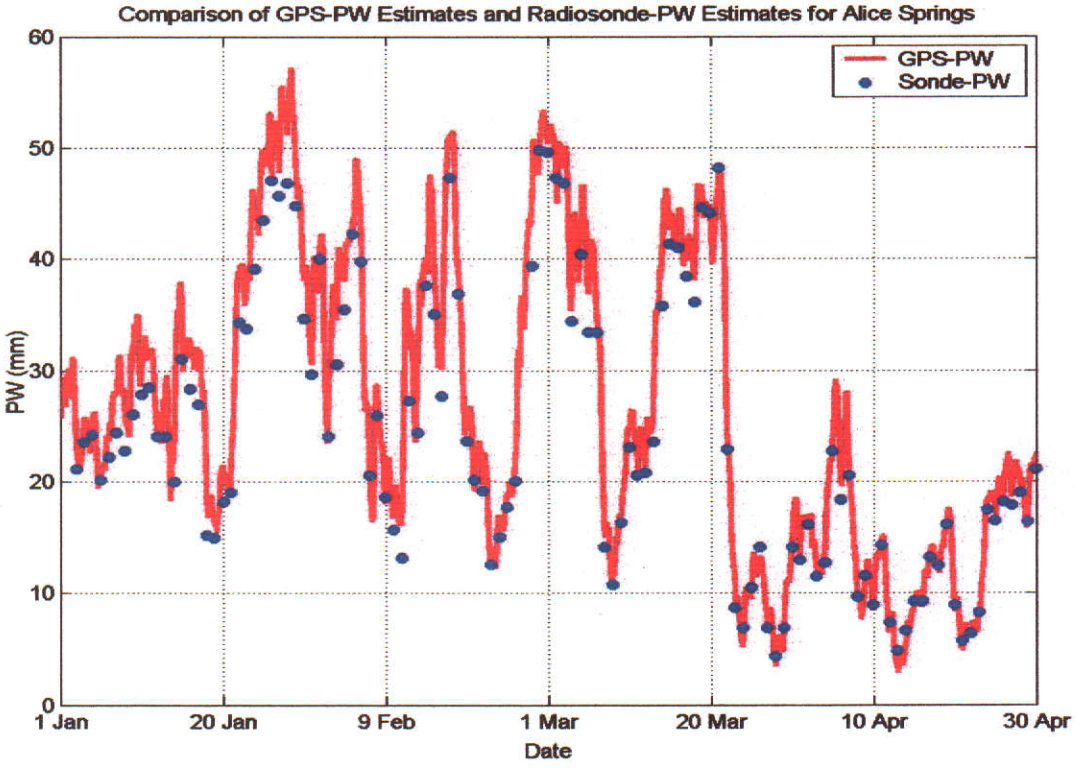

Figure 5.13 GPS-PW Estimates and Radiosonde-PW Estimates for Alice Springs

Figure 5.13 shows a comparison of the final results by using the combination of the best strategies of GPS data processing for GPS-PW estimates and radiosonde-PW estimates for Alice Springs. A validation of GPS-PW estimates to radiosonde-PW estimates for all the GPS stations can be seen in Appendix A.

5.3 Analysis

The research results can be analysed in the quality of the tropospheric delay estimates and the quality of the GPS-PW estimates. The quality of the tropospheric delay estimates is represented by the formal error (σ) of the estimates which is obtained through the GPS data processing using Bernese 4.2 GPS software. This information can be used as an internal quality assessment of the tropospheric parameter estimates. The quality of GPS-PW estimates can be measured by comparing with the radiosonde-PW estimates as the external quality assessment since the radiosonde-PW estimates is assumed as 'the truth value' of the PW estimates. Other factors such as the conversion factor and the distance between GPS stations and meteorological stations are also analysed.

The formal errors for the tropospheric parameter estimates can be seen in Table 5.23.

Station	σ of Tropospheric Parameter Estimates (mm)		
	Mean	Max	Min
Alice Springs*	0.98	1.48	0.67
Casey**	1.00	2.14	0.73
Cocos Island*	1.06	1.67	0.82
Darwin*	1.21	2.5	0.77
Davis**	1.32	3.63	0.86
Hobart*	1.18	4.77	0.79
Karratha*	1.05	1.58	0.72
Macquarie Island*	1.06	2.97	0.75
Mawson**	1.28	2.84	0.88
Perth*	1.38	2.05	1.03
Stromlo**	0.95	1.88	0.69
Tidbinbilla*	0.99	1.49	0.71
Townsville*	1.16	2.26	0.81
Yaragadee*	1.04	3.79	0.73
Mean	*1.12*	*2.50*	*0.78*

Table 5.23 The Quality of Tropospheric Parameter Estimates
('*' indicates Ausclus-1 and '**' indicates Ausclus-2 data processing)

Table 5.23 shows that the quality of tropospheric parameter estimates have an average of 1.12mm. This indicates that the tropospheric parameters are estimated to a high internal quality. However, these indicators are unrealistic and cannot be relied on since the least squares and Kalman filter algorithms depends on correct weighting of the measurements to provide unbiased estimates of the parameters (Barnes *et al.*, 1998).

Validation of GPS-PW estimates and radiosonde-PW estimates shows that the highest standard deviation between GPS-PW estimates with radiosonde-PW estimates occurs in Karratha (5.84mm) and the maximum bias occurs in Tidbinbilla (2.5mm). The average standard deviation of GPS-PW estimates validated to radiosonde-PW estimates is about 2.65mm. This value can be used as the external quality indicator of troposphere parameter estimation from GPS data processing. The summary of post-processed strategy results and the PW comparison can be seen in Table 5.24.

GPS Station	*Surface Met. Station*		*Radiosonde Station*		*Comparison to radiosonde-PW*		
	ΔD (km)	*ΔH (m)*	*ΔD (km)*	*ΔH (m)*	*Count*	*σ (mm)*	*Bias (mm)*
Alice Springs*	13.9	41	13.9	42	119	2.25	1.526
Casey**	0.9	3	0.9	1	233	2.1	1.97
Cocos Island*	0.2	1	0.2	2	228	2.03	0.503
Darwin*	26.2	30	53.9	45	182	3.7	-0.477
Davis**	0.01	5	0.01	11	238	1.65	1.534
Hobart*	6.2	18	6.2	41	230	1.81	1.35
Karratha*	23.3	104	173	111	248	5.84	0.053
Macquarie Island*	1.1	6	1.1	8	231	1.57	0.623
Mawson**	0.4	14	0.4	20	232	1.13	0.976
Perth*	13	20	16.4	30	58	1.39	0.183
Stromlo**	17.4	201	142	569	134	3.91	1.728
Tidbinbilla*	10.7	59	141	435	134	4.24	2.449
Townsville*	30.4	21	30	23	122	2.67	1.603
Yaragadee*	68	4	69	235	138	2.81	1.57
					Mean	*2.65*	*1.11*

Table 5.24 Summary of Post-Processed GPS-PW Estimates
('*' indicates Ausclus-1 and '**' indicates Ausclus-2 data processing)

As has been mentioned, the highest standard deviation is found at Karratha; and Table 5.24, shows that the GPS station at Karratha is located 173km from a radiosonde station, the furthest distance between a GPS station and a radiosonde station used in this research. The PW above Karratha GPS station is different from the PW above Port Hedland Airport, where the radiosonde is launched. This fact is also found at Tidbinbilla and Stromlo GPS stations, where the distances to radiosonde locations are greater than 100km (see Table 4.3).

To find out if there is any relation between the horizontal and the vertical distance between GPS stations with meteorological (radiosonde stations and surface

meteorological stations), the information from Table 5.24 is plotted in Figures 5.14 and 5.15.

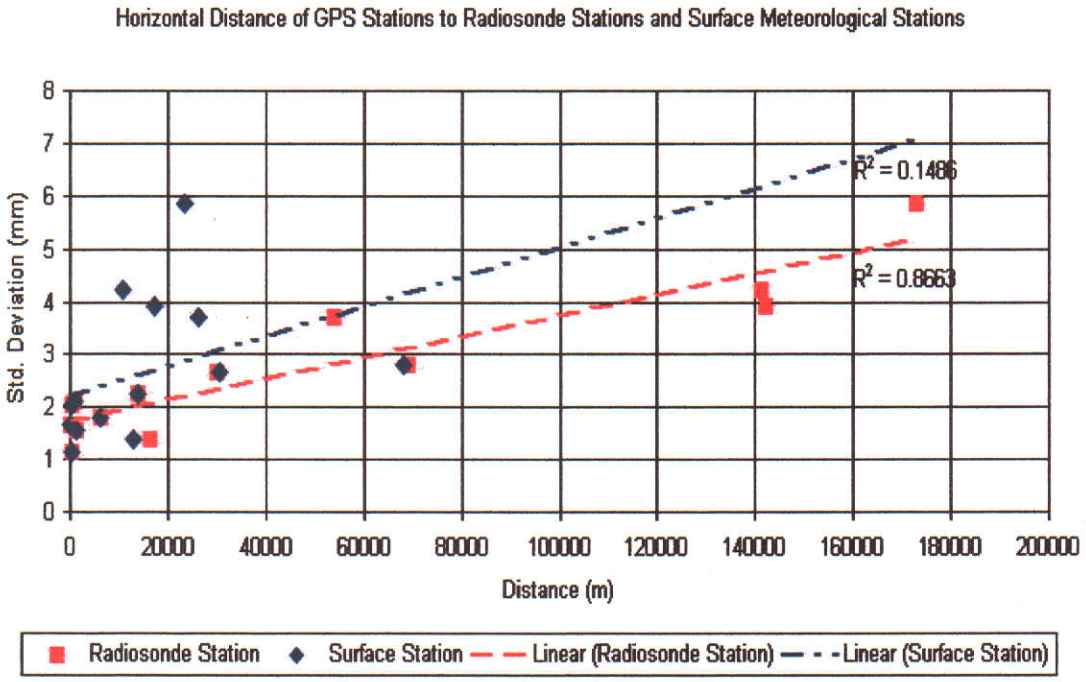

Figure 5.14 Horizontal Distance between GPS stations to Surface Meteorological Stations, Radiosonde Stations and the σ of GPS-Radiosonde PW Estimates

Figure 5.14 plots the distribution of horizontal distances of GPS stations to radiosonde stations and surface meteorological stations. Trendlines can be added to the figure to show the relationships between the horizontal distances of GPS stations to surface meteorological stations and radiosonde stations. The horizontal distances between GPS stations to radiosonde stations affect the σ of GPS-radiosonde PW estimates comparisons, compared to the horizontal distances of GPS stations to surface meteorological stations. It is obtained from the R^2 (coefficient of correlation) value which can be defined as an indicator from 0 to 1 that reveals how closely the estimated values for the trendline correspond to the actual data. Figure 5.10 shows that the R^2 of radiosonde trendline is 0.8663 and it indicates a stronger relationship in linear form compared to only 0.1486 of the R^2 trendline of the surface station.

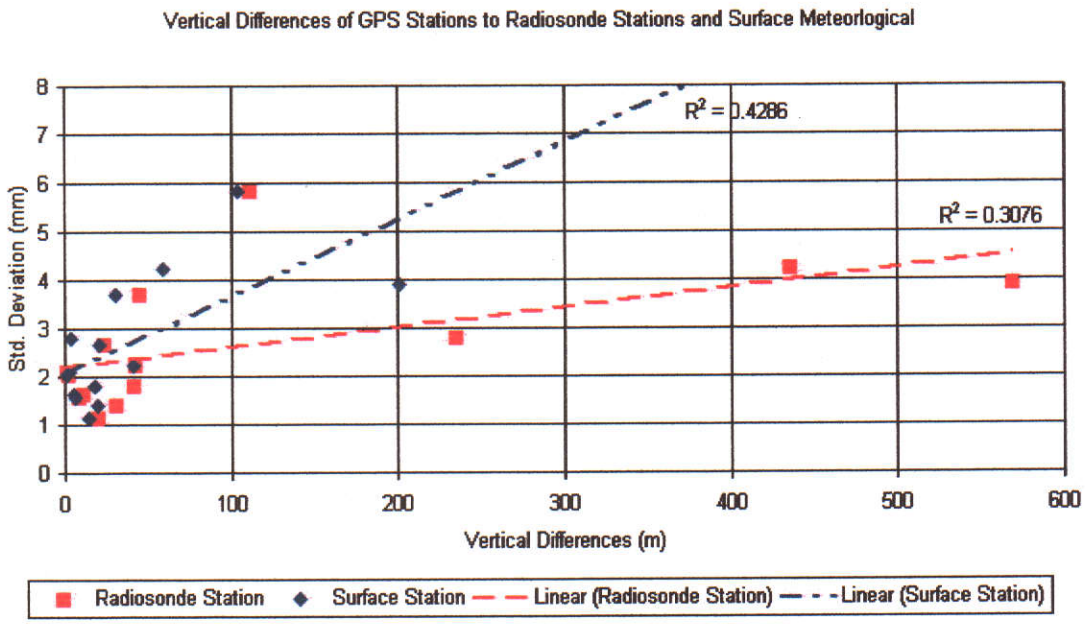

Figure 5.15 Vertical Differences between GPS stations to Surface Meteorological Stations, Radiosonde Stations and the σ of GPS-Radiosonde PW Estimates

In vertical differences between stations, Figure 5.15 shows that the R^2 of surface meteorological trendline is 0.4286 whereas 0.3076 for radiosonde's R^2 trendline. It means there is no strong indicator in linear form to show the vertical differences of GPS stations to radiosonde and surface meteorological stations affect the σ of GPS-radiosonde PW estimate comparisons. Therefore it can be said that the σ of GPS-radiosonde PW estimate comparisons is affected more by the horizontal distance between GPS stations to radiosonde stations.

The surface meteorological stations record the surface temperature and pressure data which are needed to derive the conversion factor (Π) from ZWD to PW. Considering the location of GPS stations in the ARGN configuration vary in latitude (from 12 to 69 degrees South), it can be assumed that the GPS locations represent different conditions in the Australian climate. High temperature and high humidity in tropical regions in the North include Cocos Island, Darwin, Jabiru, Karratha and Townsville. Arid areas in Alice Springs and more temperate zones in the South include Ceduna, Perth, Yaragadee, Stromlo, Tidbinbilla and Hobart. Sub-antarctic in Macquarie Island and Antarctic regions cover Casey, Davis and Mawson.

For that reason, the conversion factor (Π) and the PW from GPS data processing can be analysed further to find the relationship between Π and the individual GPS stations based on the PW values. As explained in section 3.3.2, Π values are calculated using surface temperature and pressure data for each GPS station. Table 5.25 shows the conversion factor comparison for each GPS station.

GPS Station	Latitude	Climate Zones	Mean		Min		Max	
			T (^{0}C)	Π	T (^{0}C)	Π	T (^{0}C)	Π
Cocos Island	-12.188	Tropical	26	6.240	22	6.164	30	6.121
Jabiru	-12.660	Tropical	27	6.254	21	6.151	35	6.043
Darwin	-12.843	Tropical	27	6.310	18	6.163	35	6.032
Townsville	-19.269	Tropical	27	6.308	18	6.169	33	6.074
Karratha	-20.981	Tropical	31	6.349	18	6.123	43	5.942
Alice Springs	-23.670	Arid	24	6.587	2	6.212	42	5.929
Yaragadee	-29.046	Temperate	24	6.605	9	6.205	41	5.918
Perth	-31.802	Temperate	22	6.451	8	6.226	38	6.043
Ceduna	-31.870	Temperate	21	6.567	4	6.268	45	5.905
Stromlo	-35.320	Temperate	18	6.673	-2	6.325	39	5.993
Tidbinbilla	-35.398	Temperate	18	6.645	-1	6.308	38	5.974
Hobart	-42.803	Temperate	16	6.547	4	6.326	34	6.060
Macquarie Island	-54.499	Sub-antarctic	6	6.582	1	6.495	10	6.436
Casey	-66.283	Antarctic	-1	6.820	-10	6.626	28	6.150
Mawson	-67.604	Antarctic	3	6.861	-10	6.551	26	6.172
Davis	-68.577	Antarctic	2	6.843	-10	6.578	23	6.226

Table 5.25 Statistics of Conversion Factor

As can be seen in Table 5.25, the Π values for the tropical region vary from 5.94 to 6.35 with an average of 6.15. For arid and temperate regions, the Π range is from 5.90 to 6.67 with an average of 6.29, and for the Antarctic region, the Π range is from 6.15 to 6.86 with an average of 6.58. It is also shown that the range of Π values is larger when the station location is in the Antarctic region. These findings are also similar to what Emardson *et al.* (1998) found that for the regions with temperature ranges from -38^{0}C to 37^{0}C, the conversion factor also varies from 7.5 to 6. In

addition, the σ of GPS-radiosonde PW estimate comparisons has an average value of 2.65mm.

5.4 Summary

This research found that ambiguity resolution and Ocean Tide Loading models are the main factors tested that affect the quality of station coordinates, especially the height component. For long sessions and very long baselines, it can be said that the float solution is more reliable compared to the fixed solution. Other variables such as the mapping function, elevation mask, tropospheric interval estimation and relative constraints have little influence on improving the quality of GPS data processing results.

The best strategy of GPS data processing obtains the repeatability for the non-fixed station height component ranging from 6.3 to 14mm with an average 8.6mm. The quality of GPS-PW estimates from this research can be assessed by internal and external indicators. The standard deviation of tropospheric parameter estimates is used as an internal quality indicator, whereas for an external quality indicator, the standard deviation of validation of the GPS-PW estimates with radiosonde-PW estimates is used. The internal quality of the tropospheric parameter estimates has an average of 1.1mm level. The standard deviation of the comparisons of the GPS-PW and radiosonde-PW estimates data has an average of 2.65mm, and with a bias of 1.11mm level. The horizontal distances between GPS stations to radiosonde stations have a stronger relation to standard deviation of PW comparison rather than a horizontal distance between GPS stations to the surface stations and the vertical differences between GPS stations and meteorological stations.

Chapter 6

STRATEGY TESTING FOR NEAR REAL-TIME GPS PRECIPITABLE WATER VAPOUR ESTIMATION

This chapter describes GPS data processing strategies for the near real-time estimation of atmospheric water vapour. As was mentioned in Chapter 1, to enable GPS estimated PW to benefit meteorological forecasting, the estimates must be available within near real-time (Baker *et al.*, 2001). The difference between the near real-time strategy and the post-processed strategy for atmospheric water vapour estimation is the estimation time availability. In the near real-time strategy, the aim is to ensure that the PW estimates are available a few hours after data observation, whereas there will be at least 2 weeks latency in the post-processing strategy due to the use of different satellite orbit files.

The IGS final orbit which is used in the post-processing strategy in this research is available after 13 days of data observation and the IGS Ultra-Rapid (IGU) orbit, which is used in the near real-time strategy of this research is available in real time and updated twice a day. This chapter focuses on how to improve the quality of predicted orbits to be used on the GPS data processing since the quality of the IGU orbit is not as good as the IGS final orbit. The coordinate repeatability is used to assess the quality of the GPS data processing results. The results are also compared to radiosonde estimates.

6.1 Near Real-Time GPS-Water Vapour Estimates

The ability of GPS to estimate atmospheric water vapour has been shown in Chapter 5. However, this can not be of use in practical weather forecasting due to the lack of availability of IGS final orbit until after two weeks. The ability of GPS to estimate PW in near real-time becomes an important source of PW for numerical weather prediction (NWP) models and has been assessed in many projects (e.g. Walpersdorf *et al.*, 2001; Cucurull *et al.*, 2002).

To enable near real-time GPS-PW estimation, all input data and data processing must be done in near real-time also. As mentioned in Chapter 2 and Chapter 4, the satellite ephemeris has an important role in the accuracy of GPS data processing results. Dodson and Baker (1998) state that the accuracy of the GPS satellite orbit is an important factor for the accuracy of GPS-PW estimates. Due to IGS final orbits not being available until after two weeks, the IGS produces near real-time ephemerides to address near real-time applications such as meteorology.

6.1.1 Real-time ephemeris

For near real-time applications, the IGS produces a GPS satellite orbit in real time called the *IGS Ultra Rapid Orbit* (IGU). The IGU orbits became IGS official products on 6 November 2000 and are delivered twice a day, at 0300 and 1500 UTC (Springer and Hugentobler, 2001). The IGU orbits contain 48 hours worth of satellite position data. The first 24 hours contain a "real" orbit (an orbit based on actual observations) and the second 24 hours contain a predicted orbit (Springer, 2000). However, the main limitation for IGU orbits is the accuracy. The accuracy of IGU orbits is said to be about 20cm compared with the IGS final orbits accuracy of 5cm (IGS, 2000). Moreover, the IGU orbit accuracy decreases due to the effect of unpredictable non-conservative forces (Rocken *et al.*, 1997) and when satellites are in manoeuvre (Ge *et al.*, 2000).

For estimating water vapour using a near real-time strategy, three methods can be used to improve the accuracy of IGU orbits. The first is by removing the bad satellite data in the GPS data processing (Dodson and Baker, 1998). The second is by applying a weighting strategy to the GPS data according to the satellites' accuracy codes (Kruse *et al.*, 1999). The last method is by improving the quality of the orbits by estimating orbital elements using GPS data (Ge *et al.*, 2001).

In order to estimate water vapour in the Australian atmosphere using GPS in near real-time, these three methods were assessed by using 120 days (1 January 2001-30 April 2001) of GPS data from the Ausclus-1 network which was defined in Chapter 5. The GPS data from the Ausclus-2 network were then processed using the best strategy which was found for deriving the PW estimates. This strategy is based on

the experience gained from Chapter 5, and then the GPS-PW estimates from Ausclus-1 and Ausclus-2 were validated with radiosonde data.

Aside from the orbit, the best strategies found for post-processed GPS estimation of PW strategy were directly applied. These strategies were: set the observation sampling interval to 180 seconds, set 10 degrees for the elevation mask, apply Niell mapping function with elevation-dependent weighting, apply the GOT00.2 Ocean Tide Loading model, constraining the troposphere estimates to 1mm and every 30 minutes, estimate one troposphere gradient per 24hours in north-south and east-west directions and process the GPS data with float ambiguities. Alice Springs, Cocos Island, Jabiru, Macquarie Island, Tidbinbilla and Yaragadee were tightly constrained stations for Ausclus-1; whereas Alice Springs, Auckland, Bakosurtanal, Casey, Darwin, Davis, Hobart, Mawson, Noumea, Perth and Tidbinbilla were tightly constrained for Ausclus-2, following the configuration in Chapter 5.

The results of the GPS data processing were assessed using the repeatability of each station's coordinates. The repeatability of non-fixed station coordinates from 120 days of GPS data processing when using the IGU orbits can be seen in Table 6.1.

GPS Station	Station Coordinates Repeatability (mm)		
	N	E	h
CEDU	5.7	14.1	26
DARW	9.8	71	39.1
HOB2	7.1	14.7	16.6
KARR	6.5	18.6	23.4
PERT	7.8	11.3	21.9
TOW2	9.3	67.4	29.5
Mean	*7.70*	*32.85*	*26.08*

Table 6.1 The Repeatability from GPS Data Processing by Using IGU Orbits

From Table 6.1, it can be seen that the repeatability (especially in Easting component) in Darwin and Townsville is higher compared to other stations. Therefore, it is useful to check the station coordinate recoveries to detect the outlier in the GPS data for each session (24hours). The coordinate recoveries for non-fixed stations are illustrated in Figures 6.1 to 6.6.

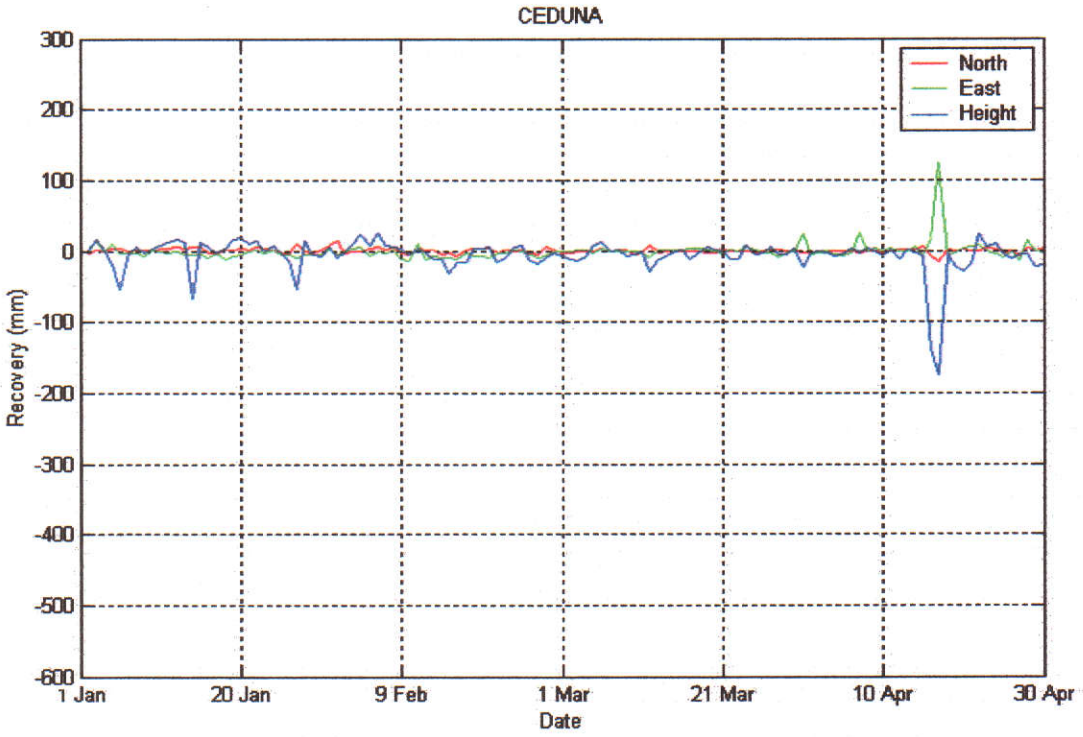

Figure 6.1 Coordinate Recoveries for Ceduna

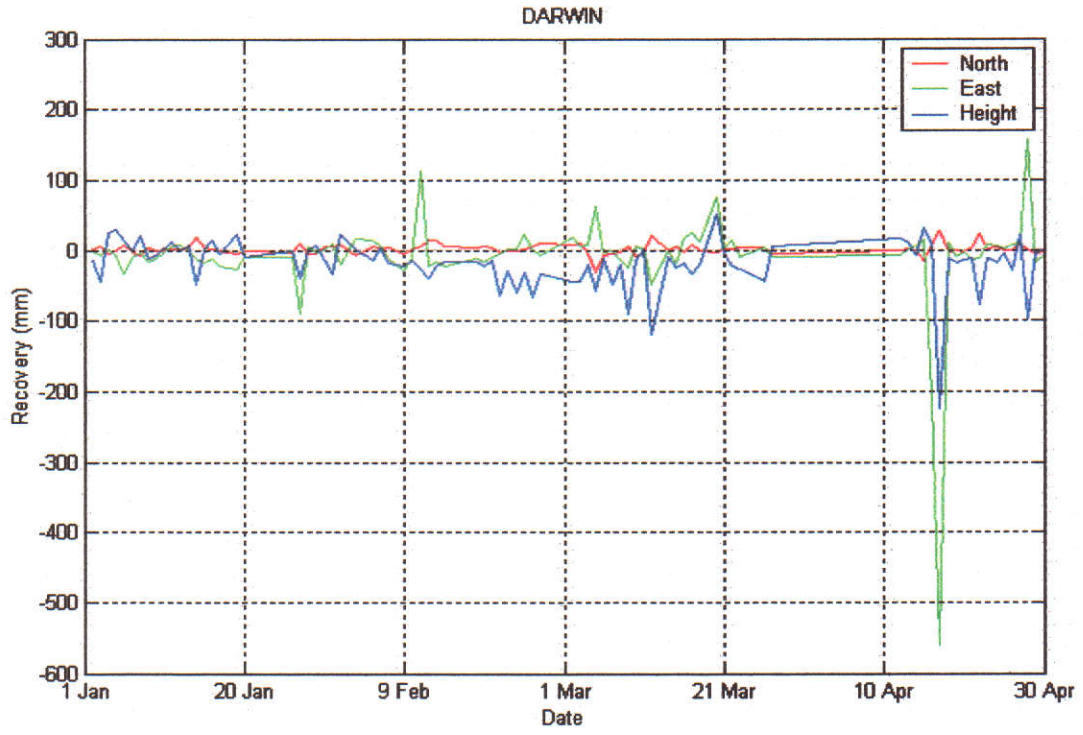

Figure 6.2 Coordinate Recoveries for Darwin

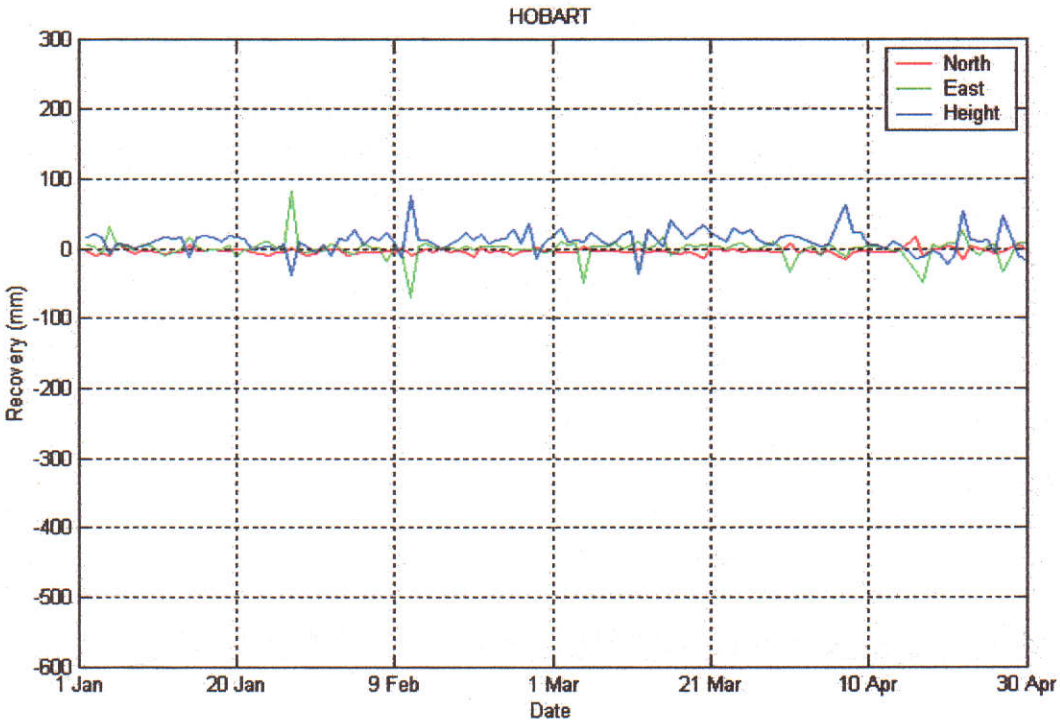

Figure 6.3 Coordinate Recoveries for Hobart

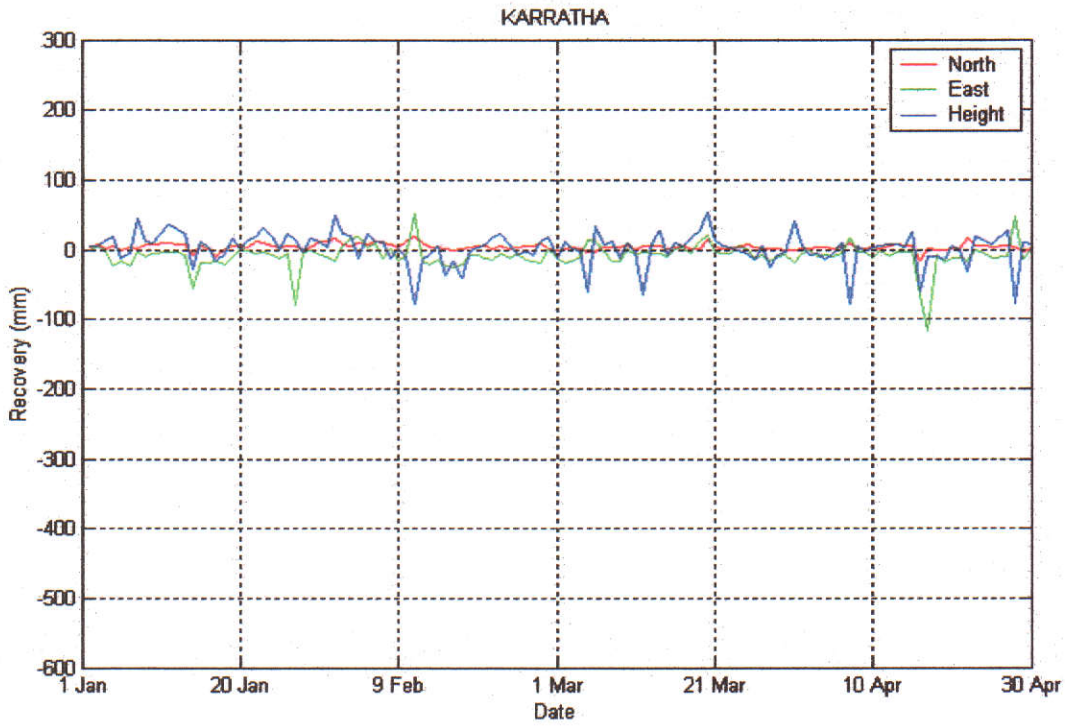

Figure 6.4 Coordinate Recoveries for Karratha

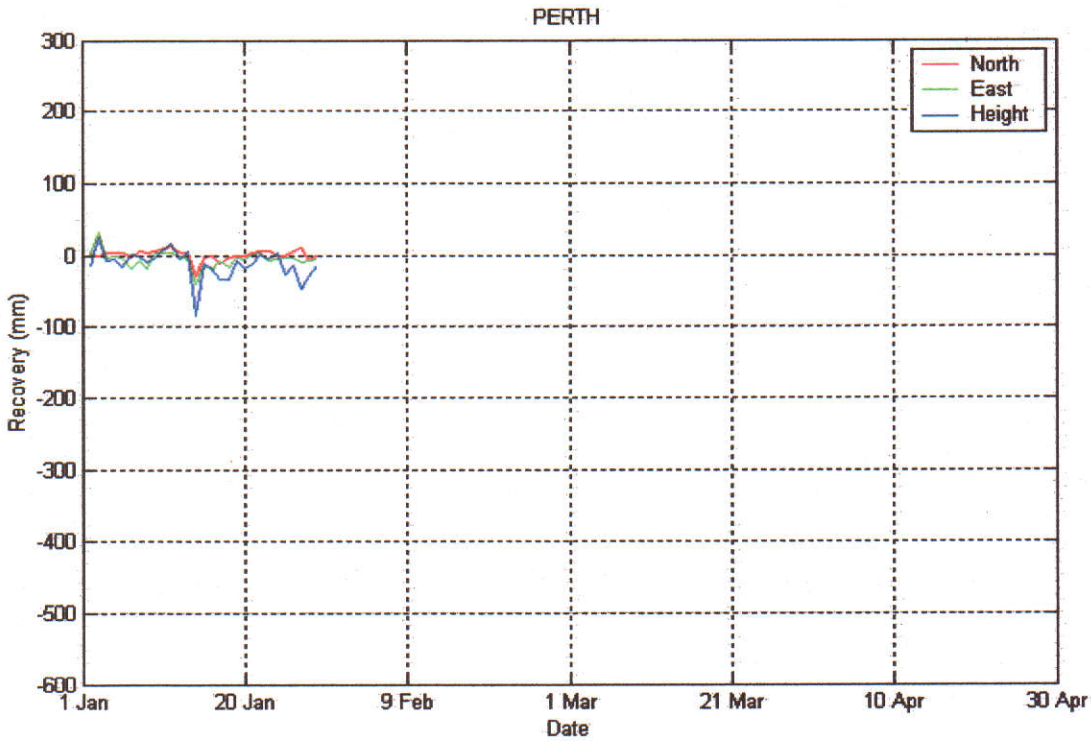

Figure 6.5 Coordinate Recoveries for Perth

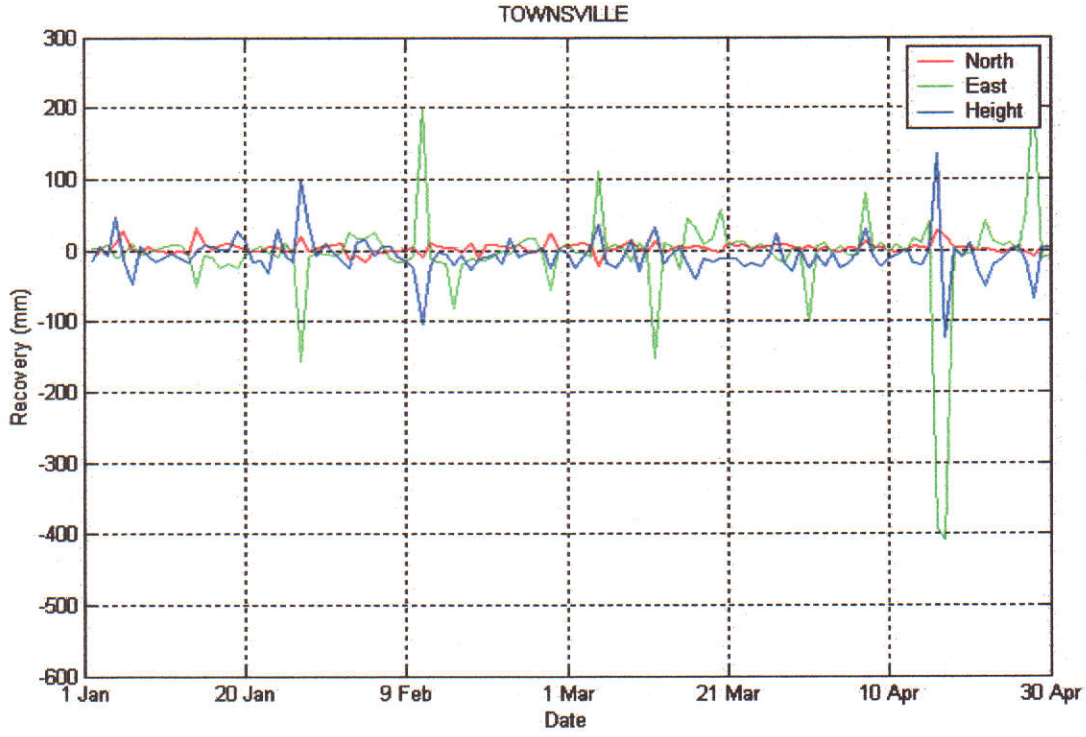

Figure 6.6 Coordinate Recoveries for Townsville

From Figures 6.1 to 6.6, it can be seen that there are some outliers in particular sessions. Table 6.2 listed the particular sessions which contain the outliers for the non-fixed stations.

GPS Station	Bad Session
CEDU	106, 107
DARW	71, 79, 106, 107, 118
HOB2	27, 42, 106, 107
KARR	14, 106, 107
PERT	14
TOW2	14, 27, 42, 46, 64, 71, 79, 90, 97, 106, 107, 118

Table 6.2 Bad Sessions for Non-Fixed GPS Stations

These particular sessions were then assessed by changing the baselines configuration and restarting the data processing. It was found that the orbit factor in performing double-differencing observations is the main factor that causes these outliers. Observations from low accuracy satellites affect the clock offsets which is stored in the phase observation file. To handle this problem, it is necessary to redefine the baselines on these particular sessions which are listed in Table 6.2 by changing GPS station configurations to define the baselines. The coordinate repeatabilities after removing the outliers are listed in Table 6.3.

GPS Station	Station Coordinates Repeatability (mm)		
	N	E	h
CEDU	6.8	20.7	27.9
DARW	8.5	17.7	24.7
HOB2	6.8	12.5	16.3
KARR	6.1	12.4	18.5
PERT	4.8	9.7	23.6
TOW2	9.2	26.2	22.7
Mean	*7.03*	*16.53*	*22.28*

Table 6.3 The Repeatability after Removing the Outliers

By comparing Table 6.1 and Table 6.3, it shows that after removing the outliers by changing baselines in the particular sessions, the coordinate repeatabilities are improved, except for Ceduna.

6.1.2 Removing low accuracy satellites

The GPS satellite orbit files, which were used in this research, are coded in SP3 (Standard Product # 3) format (Spofford and Remondi, 1999). This format contains information about the GPS satellites, for example, the orbit type, number of satellites, the orbit accuracy, and the position.

In the header of IGU orbit files there is information about the accuracy of predicted satellite positions, known as accuracy codes. These provide an indication of the accuracy of each satellite's position along its orbital track (Baker, 1998). The code represents a value of two to the power of the accuracy code, therefore, a bigger value means lower accuracy. For example, an accuracy code of 10 would approximately represent a satellite accuracy of 2^{10} cm or approximately 10.24m.

The accuracy codes of the IGU orbits for 120 days (from 1 January to 30 April 2001) used in this research can be seen in Figure 6.7. The GPS data from satellites which have low accuracy indication are removed from the solution. It can be seen that the range of the accuracy code is from 14 (satellite number 19, it means the accuracy is about 2^{14} cm or 163.84m) to 5 (it means the accuracy is about 2^5 cm or 32cm). Overall, the accuracy code has an average of about 6.9 and the distribution of the satellite accuracy code for 31 satellites for 120 days is illustrated in Figure 6.8.

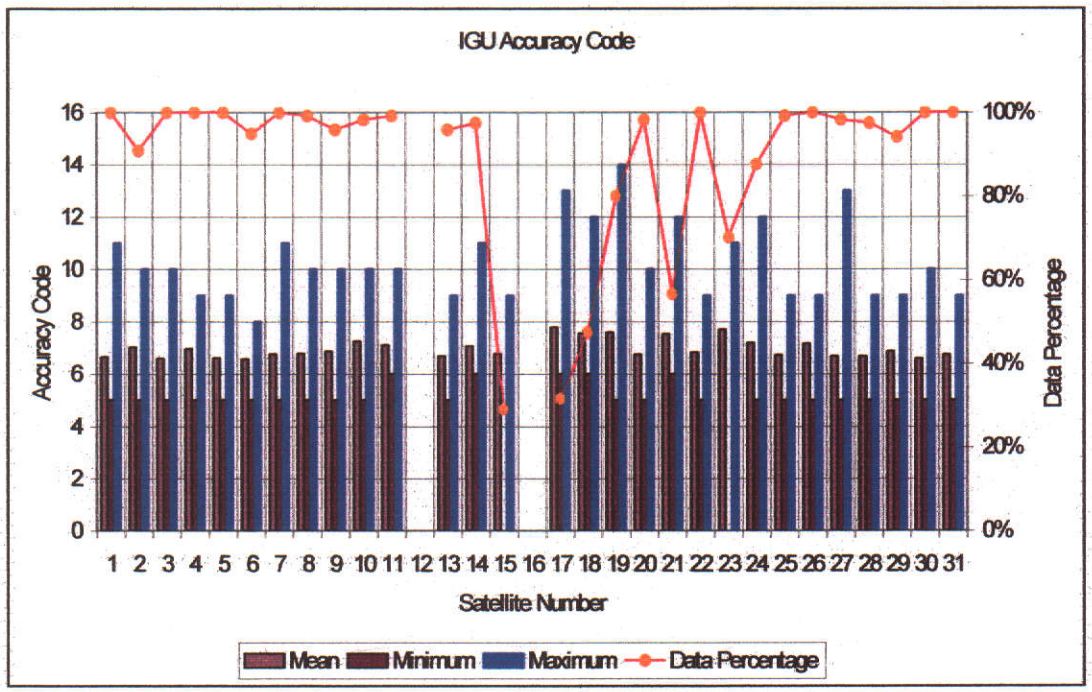

Figure 6.7 The Accuracy Code of the IGU Orbits
(The percentage illustrates the availability of the satellite over 120 days)

Figure 6.7 shows that there are eight satellites (numbers 4, 5, 6, 22, 25, 26, 30 and 31) which have a good quality. As indicators, the data percentage, they are full over 120 days, and the accuracy code maximum is 9. This information is useful to decide the threshold value of the satellite's accuracy code which will be used in data processing.

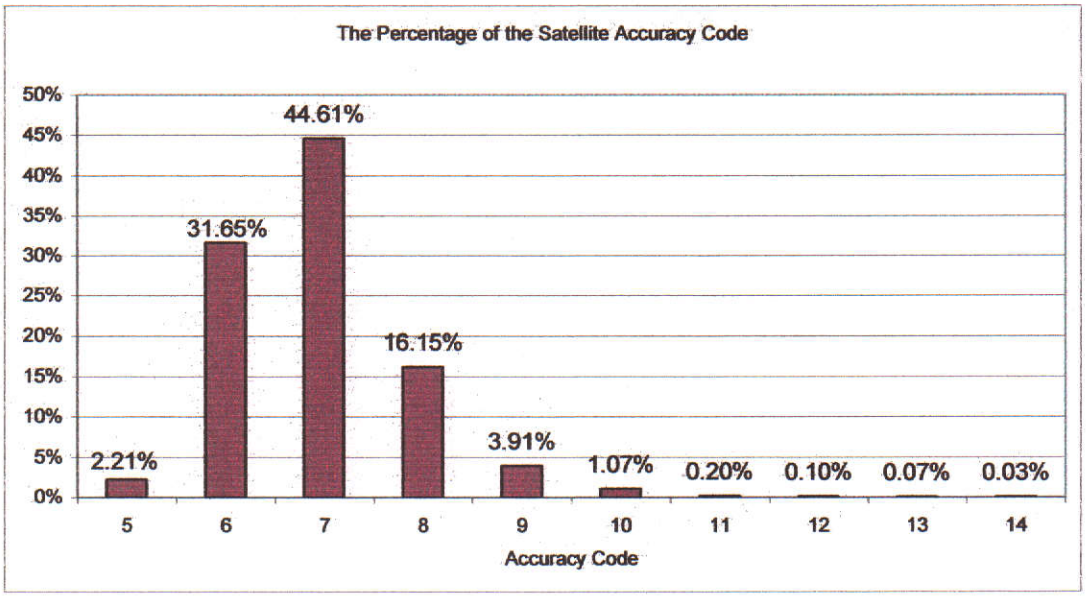

Figure 6.8 The Percentage of the Average Satellite's Accuracy Code over 120 Days

This research used 9 as the maximum value, meaning that satellites with an accuracy code starting from 10 or greater were removed. The repeatability of station coordinates from removing low accuracy satellites from the solution can be seen in Table 6.4.

GPS Station	Repeatability of the Original IGU Orbits (mm)			Repeatability of the Removing Low accuracy satellites (mm)		
	N	E	h	N	E	h
CEDU	6.8	20.7	27.9	6	6.1	12.3
DARW	8.5	17.7	24.7	7.4	13.6	24.1
HOB2	6.8	12.5	16.3	7.3	5.7	11
KARR	6.1	12.4	18.5	4.9	10.1	12.8
PERT	4.8	9.7	23.6	5.8	10.6	17.5
TOW2	9.2	26.2	22.7	6.9	12.7	15.9
Mean	*7.03*	*16.53*	*22.28*	*6.38*	*9.80*	*15.60*

Table 6.4 Comparison of Original IGU Orbits and Removing Low Accuracy Satellites

As can be seen in Table 6.4, the station coordinate repeatabilities have improved. The mean repeatability of the height component for all the stations for the period considered improved from 22.28mm to 15.60mm. As a comparison, Figure 6.9 shows the height repeatability for Townsville.

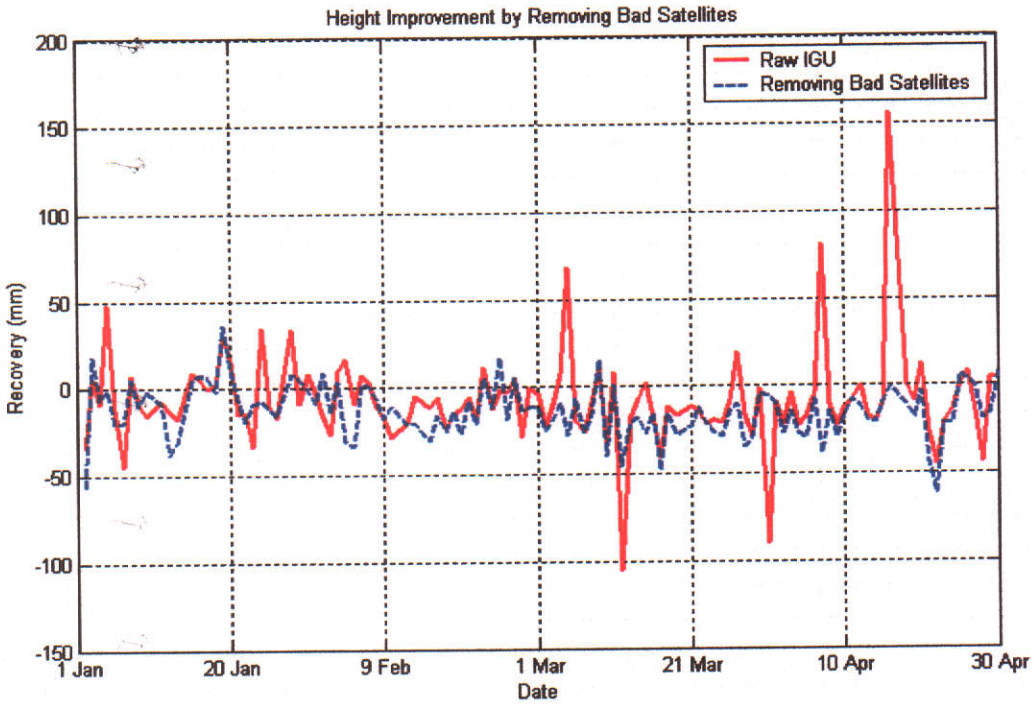

Figure 6.9 The Height Improvement for Townsville by Removing Low Accuracy Satellites

6.1.3 Down-weighting low accuracy satellites

The second strategy to improve upon the IGU orbits is by weighting the GPS data observations based on the satellite accuracy code. The weight of an observation to a satellite which has the highest accuracy code in the orbit file is set to be smaller compared to the satellite which has the lowest accuracy code. For example, satellite number 5 has the accuracy code 5, the lowest accuracy code, whereas satellite number 19 has the accuracy code 12, the highest accuracy code in a particular orbit file. Therefore, satellite number 19 is 'down-weighted' in the solution, based on the accuracy code of satellite number 5. The difference of the accuracy code between satellites number 5 and 19 is the highest accuracy code subtracted the lowest accuracy code (12 – 5 = 7). Therefore the satellite number 19 is weighted 2^7 or 128 times lower than satellite number 5.

Kruse (1999) expresses the satellite weighting strategy in the formula:

$$\left(\frac{\sigma}{\sigma_0}\right)^2 = 2^{(h-l)} \quad \text{.....(6.1)}$$

$$\sigma = \sqrt{2^{(h-l)}.\sigma_0^2} \quad \text{.....(6.2)}$$

Where: σ = satellite sigma weight; σ_0 = satellite a priori sigma;

(h-l) = the difference of the highest (h) and the lowest (l) accuracy code

This research sets the satellite a priori sigma (σ_0) to 0.020m to keep the orbit's weight in a realistic value. However, it is only the relative weight of each satellite that is of interest, so should not affect the answer. The value of the satellite sigma weight can be determined based on the differences of the accuracy code following the Kruse formula. The value of the satellite sigma weight based on the Kruse formula can be seen in Table 6.5.

$(h-l)$	$\sigma_0 = 0.020$m
1	$\sigma = 0.020$m
2	$\sigma = 0.040$m
3	$\sigma = 0.050$m
4	$\sigma = 0.080$m
5	$\sigma = 0.113$m
6	$\sigma = 0.160$m
7	$\sigma = 0.226$m
8	$\sigma = 0.320$m
9	$\sigma = 0.452$m
10	$\sigma = 0.640$m

Table 6.5 Values of Sigma Weight Based on the Kruse Formula

The repeatabilities of the station coordinates from 120 days of GPS data processing by using the down-weighting strategy outlined above are listed in Table 6.6.

GPS Station	Repeatability of the Original IGU Orbits (mm)			Repeatability of the Weighted Satellites (mm)		
	N	E	h	N	E	h
CEDU	6.8	20.7	27.9	5.9	6	14.9
DARW	8.5	17.7	24.7	8.2	14.6	23.8
HOB2	6.8	12.5	16.3	6.9	7.9	12.9
KARR	6.1	12.4	18.5	5.5	12.1	18.6
PERT	4.8	9.7	23.6	4.7	10.9	17.4
TOW2	9.2	26.2	22.7	8.1	15.5	17.7
Mean	*7.03*	*16.53*	*22.28*	*6.55*	*11.17*	*17.55*

Table 6.6 Comparison of Original IGU Orbits and Weighting Low Accuracy Satellites

From Table 6.6, it can be seen that by down-weighting GPS data from low accuracy satellites, the mean repeatability of the height component for all the stations for the period considered is improved from 22.28mm to 17.55mm. However, the improvement is not as good as when removing the observations to the low accuracy satellites. Figure 6.10 illustrates the height recovery for Townsville.

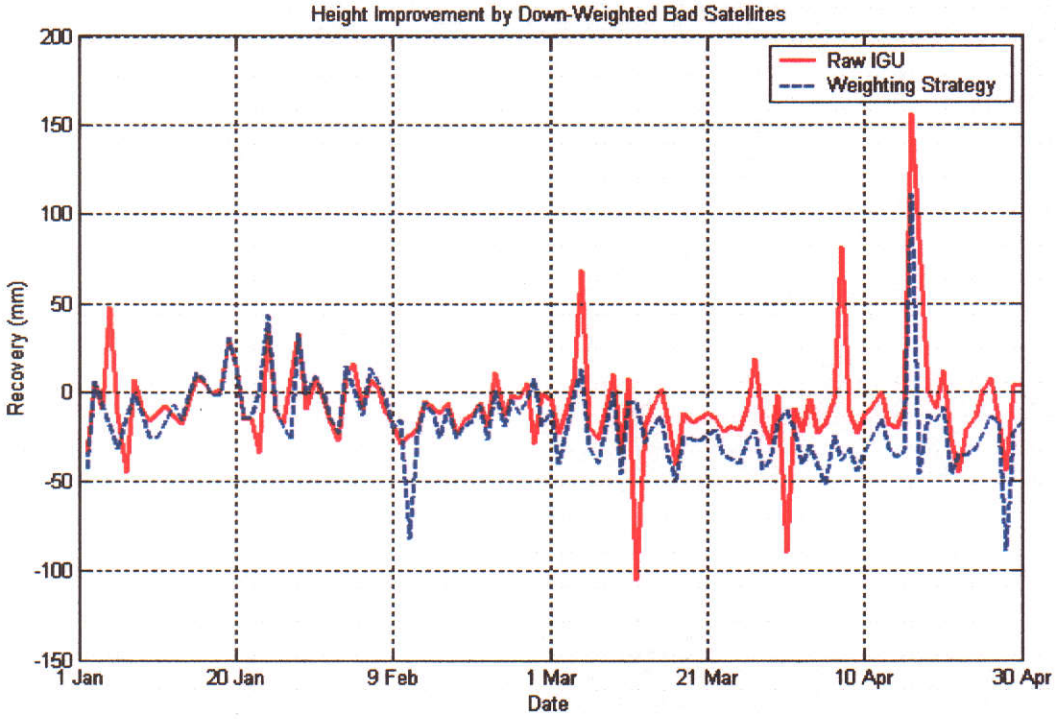

Figure 6.10 The Height Improvement for Townsville by Down-Weighting Strategy

If Figure 6.10 is compared to Figure 6.9, it seems that the height recovery by using down-weighting strategy is not as good by removing low accuracy satellites. It shows that for some sessions, the height repeatability by using down-weighting strategy is worse compared to the original IGU orbits.

The limitation on this strategy is the facility to select only one satellite to be weighted in one session. Therefore, this strategy is not appropriate if there is more than one bad satellite. It means the results of this strategy may still be affected by the error from the satellite orbits which are not accommodated by the down-weighting strategy.

6.1.4 Estimating orbits strategy

The last strategy to improve the quality of IGU orbits is by estimating orbital elements using the GPS data. Six orbital elements may be estimated in GPS data processing, namely (Hugentobler *et al.*, 2001):

Semi major axis of the orbit, which defines the size of the orbit and is represented by the symbol a.

Eccentricity of the orbit, which describes the shape of the orbit and is represented by the symbol e.

Inclination of the orbital plane with respect to the equatorial plane and is represented by the symbol i.

The right ascension of the ascending node, which defines the angle between the direction of the *vernal equinox* and the intersection line of the satellite's orbital plane with the equatorial plane and is represented by the symbol Ω.

Argument of perigee, which defines the angle between the ascending node and perigee and is represented by the symbol ω.

Argument of latitude, which defines the angle between the ascending node and the position of the satellite at the initial time and is represented by the symbol μ_0.

Figure 6.11 illustrates the set of the orbital elements.

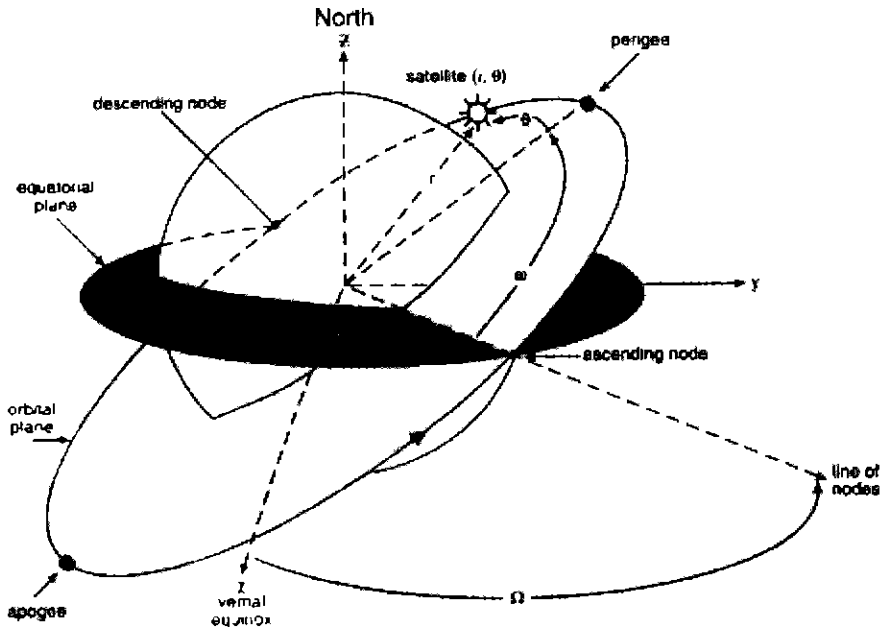

Figure 6.11 The Set of the Orbital Elements (Costulis, 2002)

The quality of the orbits is improved by estimating the orbital elements based on the GPS data. This strategy needs more time as the GPS data processing is performed twice, a first run to estimate the orbital elements and then upgrade the orbits, and the second to estimate the coordinates and the tropospheric delay. Figure 6.12 illustrates the process of this strategy.

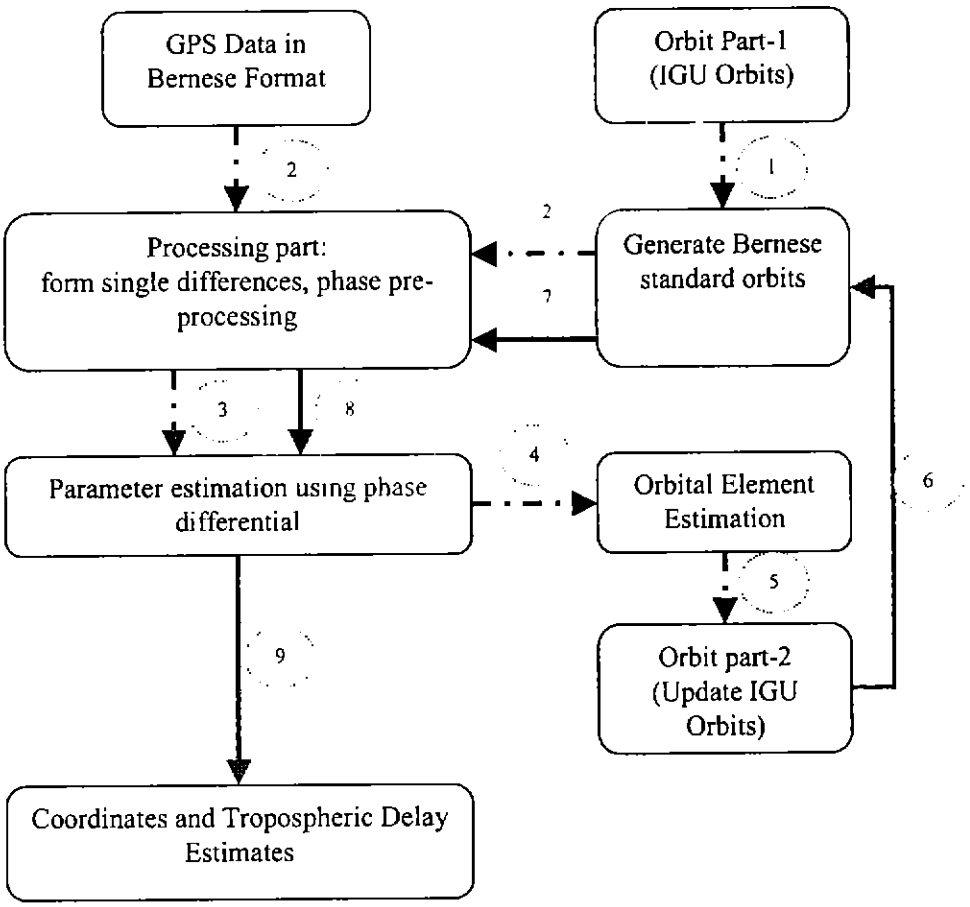

Figure 6.12 The Process of Estimating Orbits Strategy

The GPS data processing stage-1 (illustrated by the dashed line in Figure 6.12) estimates the orbital elements of the satellites to be applied in generating updated IGU orbits. These orbits then are used in GPS data processing stage-2 (illustrated by the solid line in Figure 6.12) to estimate the coordinates and the tropospheric delays. The difference of the original IGU orbits with the updated IGU orbits can be obtained by assessing the precise orbit files and illustrated in Figure 6.13.

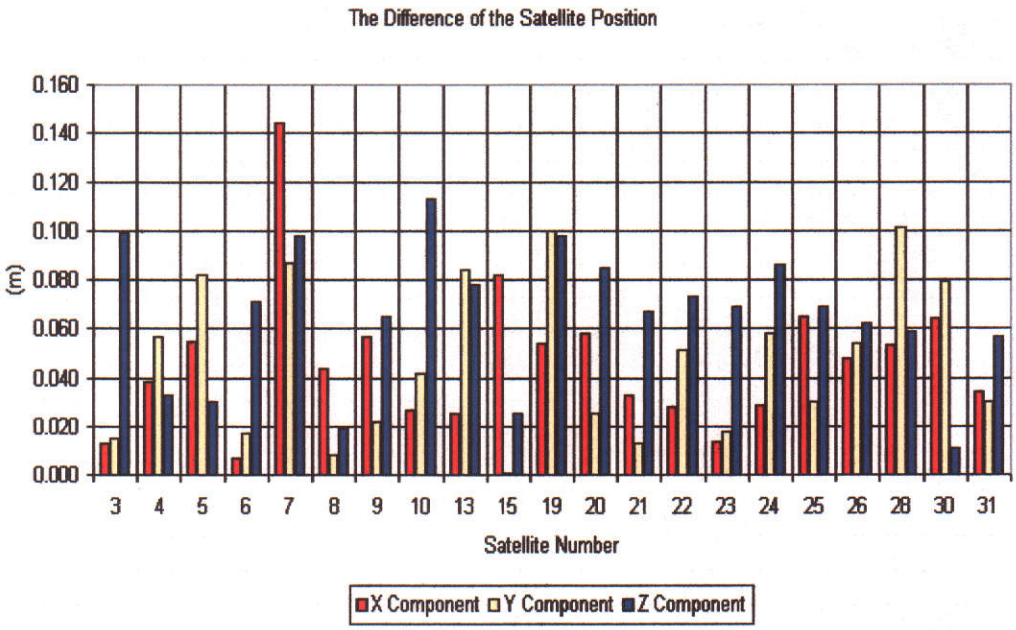

Figure 6.13 Example of the Differences of the Satellite Positions at the Particular Epoch between the Original IGU Orbit and the Estimated IGU Orbit

Figure 6.13 shows that the positions of the satellites between the original IGU orbit with the updated IGU orbit are different by up to 14cm for the X component, 11cm for the Y component and 10cm for the Z component. The results of processing 120 days of GPS data using the estimating orbit strategy can be seen in Table 6.7.

GPS Station	Repeatability of the Original IGU Orbits (mm)			Repeatability of the Estimated Orbits (mm)		
	N	E	h	N	E	h
CEDU	6.8	20.7	27.9	5.8	5.4	11.6
DARW	8.5	17.7	24.7	8.4	13.2	30.3
HOB2	6.8	12.5	16.3	6.7	6.4	9.5
KARR	6.1	12.4	18.5	5.4	11.4	15.1
PERT	4.8	9.7	23.6	4.4	10.1	14.2
TOW2	9.2	26.2	22.7	8	11.7	16.7
Mean	*7.03*	*16.53*	*22.28*	*6.45*	*9.70*	*16.23*

Table 6.7 Comparison of Original IGU Orbits and Estimated Orbits

In general, the estimating orbit strategy can also improve the accuracy of IGU orbits except for Darwin. Figure 6.14 illustrates the height recovery for Townsville.

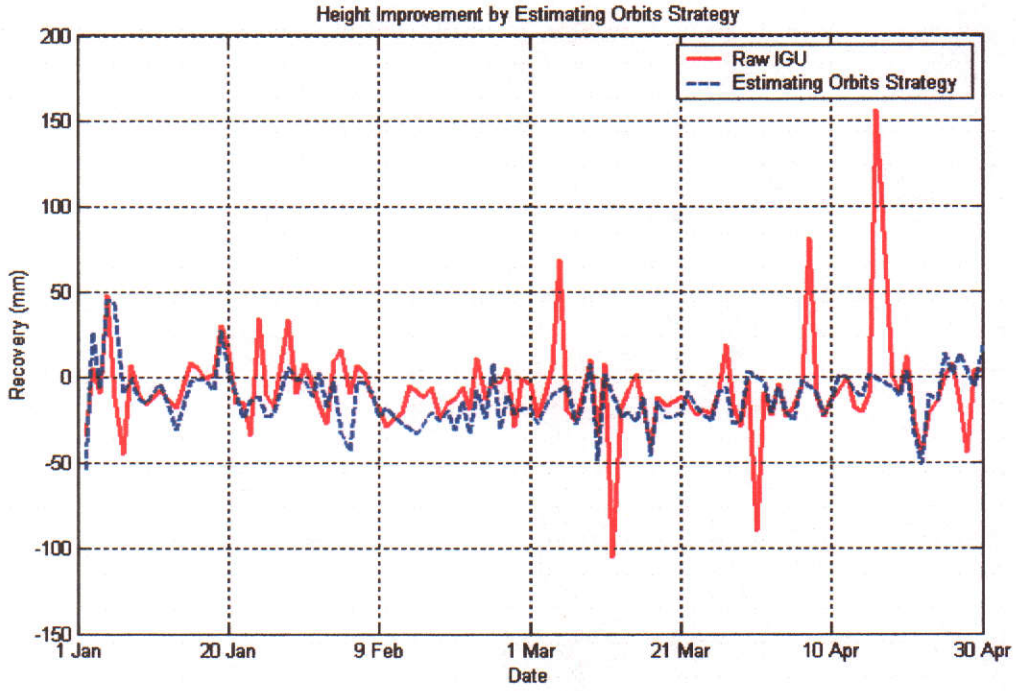

Figure 6.14 The Height Improvement for Townsville by Estimating Orbit Strategy

The results from estimating orbit strategy are better than the down-weighting strategy, however still lower than removing the low accuracy satellites. In general, the comparison results of these three strategies can be seen in Figure 6.15.

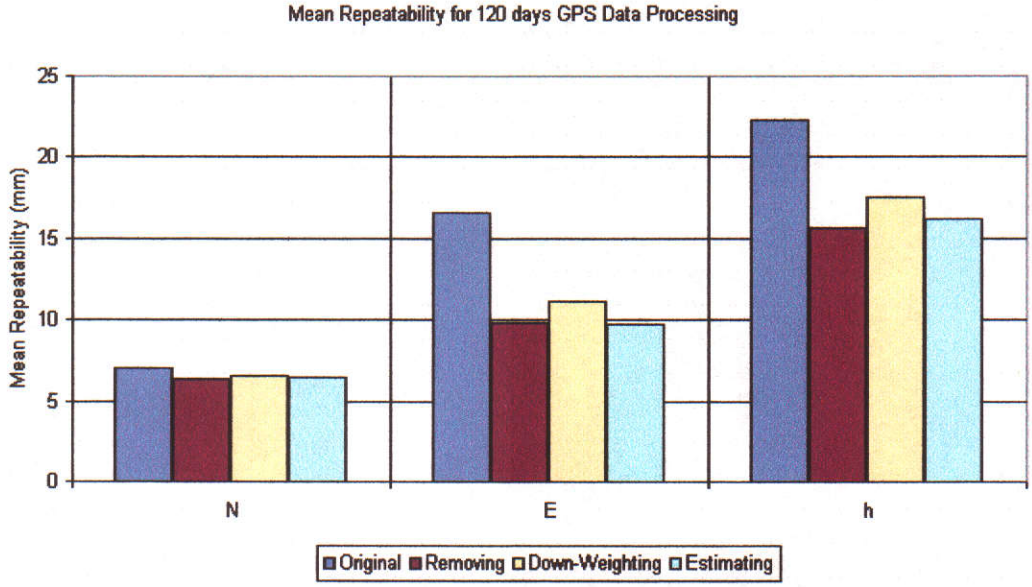

Figure 6.15 Comparisons of Strategies for Improving Orbital Quality

It can be seen from Figure 6.15 that the strategy of removing low accuracy satellites gives the best repeatability for the height component in GPS data processing and it is therefore chosen as the strategy to derive GPS-PW estimates in near real-time mode using GPS data from the Ausclus-1 and Ausclus-2 networks. The strategies to derive PW estimates in near real-time are: set the observation sampling interval to 180 seconds, set 10 degrees for the elevation mask, apply Niell mapping function with elevation-dependent weighting, apply the GOT00.2 Ocean Tide Loading model, constraining the troposphere estimates by 1mm and every 30 minutes, estimate the troposphere gradient in north-south and east-west direction, process the GPS data in ambiguity float solution, fix some stations, and removing low accuracy satellites from the solution. The non-fixed station coordinates repeatability can be seen in Table 6.8.

GPS Stations	N (mm)	E (mm)	h (mm)
BUR1**	6	8.8	10.2
CEDU*	6	6.1	12.3
DARW*	7.4	13.6	24.1
HOB2*	7.3	5.7	11
KARR*	4.9	10.1	12.8
PERT*	5.8	10.6	17.5
STR1**	5.9	7.5	10.1
TOW2*	6.9	12.7	15.9
Mean	*6.28*	*9.39*	*14.24*

Table 6.8 Station Coordinate Repeatability in Near Real-Time Mode
('*' indicates Ausclus-1 and '**' indicates Ausclus-2 data processing)

6.2 Validation of Near Real-Time Strategy GPS-PW Estimates with Radiosondes

GPS data were processed to derive PW estimation in near real-time mode by using IGU orbits after removing low accuracy satellites. The GPS-PW estimates in near real-time mode are compared with radiosonde-PW estimates. The results can be seen in Table 6.9 on the next page.

No.	Stations	Count	Std. Deviation (mm)	Bias (mm)
1.	Alice Springs*	117	2.32	1.56
2.	Casey**	227	2.17	2.05
3.	Cocos Island*	223	2.54	0.69
4.	Darwin*	178	3.72	-0.43
5.	Davis**	231	1.76	1.60
6.	Hobart*	225	1.71	1.09
7.	Karratha*	243	5.91	-0.02
8.	Macquarie Island*	225	1.75	0.65
9.	Mawson**	225	1.29	1.08
10.	Perth*	53	1.65	0.06
11.	Stromlo**	130	3.86	1.99
12.	Tidbinbilla*	132	4.14	2.35
13.	Townsville*	120	2.94	1.72
14.	Yaragadee*	135	2.87	1.51
		Mean	*2.76*	*1.14*

Table 6.9 Comparison of NRT-GPS-PW and Radiosonde-PW
('*' indicates Ausclus-1 and '**' indicates Ausclus-2 data processing)

As can be seen in Table 6.9, the NRT-GPS-PW estimation agrees with Radiosonde-PW estimation with maximum standard deviation of about 5.91mm for Karratha and maximum bias is about 2.35 mm for Tidbinbilla. The validation of the near real-time GPS-PW estimates and the Radiosonde-PW estimates in graphs can be seen in Appendix B.

6.3 Analysis

The quality of the tropospheric parameter estimates which is represented by the standard deviation (σ) of the tropospheric parameter estimates is used for internal precision evaluation. The statistics of the quality of the tropospheric parameter estimates can be seen in Table 6.10.

Station	*σ of Tropospheric Parameter Estimates (mm)*		
	Mean	*Max*	*Min*
Alice Springs*	1.36	10.29	0.77
Casey**	1.27	12.60	0.74
Cocos Island*	1.68	13.38	0.89
Darwin*	1.97	13.01	1.06
Davis**	1.57	19.22	0.81
Hobart*	1.60	21.58	0.86
Karratha*	1.46	10.88	0.81
Macquarie Island*	1.41	15.83	0.85
Mawson**	1.61	14.92	0.92
Perth*	1.80	3.83	1.25
Stromlo**	1.32	10.15	0.75
Tidbinbilla*	1.37	12.02	0.79
Townsville*	1.59	12.38	0.88
Yaragadee*	1.48	11.29	0.80
Mean	*1.54*	*12.96*	*0.87*

Table 6.10 The Quality of the Tropospheric Parameter Estimates in Near Real-Time Mode ('*' indicates from Ausclus-1 and '**' indicates from Ausclus-2 data processing)

As can be seen from Table 6.10, the quality of tropospheric parameter estimates has an average of 1.54mm. On the other hand, for the external quality evaluation, the GPS-PW estimates from near real-time strategy are validated with radiosonde-PW estimates, as summarised in Table 6.9. It can be seen that the RMS of the validation has an average of 2.76mm and a bias of 1.14mm. These statistics show that by using appropriate strategies, the near real-time GPS-PW estimates can be obtained using IGU orbits and the results are good quality which is indicated by the internal and the external quality assessments of the GPS-PW estimates.

6.4 Summary

It is shown that by making some effort to improve the IGU orbits, the quality of GPS-PW in near real-time mode can be improved to almost comparable levels as the post-processed strategy. There are three strategies for improving the IGU orbits, namely: by removing low accuracy satellites, by down-weighting the apriori sigma for a low accuracy satellite and by estimating orbit parameters by using GPS data.

Each of these three strategies has an advantage and a disadvantage. For removing low accuracy satellites, it is possible to lose the solution for one day if the quality of the orbit is low for that day. For example, if the lower limit of the accuracy is set too high and no satellites can satisfy that limitation there is no solution for that day. However, this research shows that removing low accuracy satellites gives the best repeatability for the height component.

The down-weighting strategy has an advantage in terms of flexibility, for example, to determine the appropriate sigma (weight) for the worst satellites. However, it is hard to choose which satellite will be down-weighted if there is more than one satellite with the same accuracy code in one file. Estimating orbit parameters gives a good result, however it is not as good as the satellite removal strategy and it needs more processing time compared to the other strategies.

In summary, the GPS-PW estimates using IGU orbits in near real-time mode achieve high quality results, almost comparable to the post-processed strategy. It is indicated from the standard deviation of the tropospheric parameter estimates as an internal quality indicator, which have an average of 1.54mm. On the other hand, the RMS of the validation of GPS-PW estimates to radiosonde-PW estimates as an external quality indicator has an average 2.76mm and a bias of about 1.14mm.

Chapter 7

CONCLUSIONS AND RECOMMENDATIONS

The GPS application in meteorology as a technique for estimating PW in the Australian region has been investigated in this research which utilized a continuous GPS data set from 1 January 2001 until 30 April 2001, from 20 GPS permanent stations distributed across the Australian region and processed using Bernese GPS Software Version 4.2. These 4 month GPS data were selected to see the PW estimates in a very tropospherically active time of year, summer in the Australian region, when there was more water contained in the atmosphere and also during solar maximum.

This research has shown that by applying high accuracy GPS data processing techniques, the tropospheric delay can be estimated precisely. The precipitable water can be estimated from wet components after separating the tropospheric delay into dry and wet components. High accuracy GPS data processing is dependent on the best choice of processing strategies, the correct application of error-correction models and a priori constraints.

In summary, some conclusions can be made related to estimating atmospheric water vapour content using ground-based GPS receivers in Australia. Firstly concerning GPS-PW estimates in post-processed mode and secondly concerning GPS-PW estimates in near real-time mode.

For the post-processed strategy, the GPS-PW estimation agrees with the radiosonde-PW estimation with an average standard deviation of 2.5mm for the 14 stations and a maximum of 5.8mm. This result quality was achieved by using GPS data processing with the following strategies:

- Using the IGS final orbits as the precise ephemeris,
- Setting the observation sampling interval to 180 seconds,
- Using an elevation mask of 10 degrees,
- Applying the Niell mapping function with elevation-dependent weighting,

- Applying the GOT00.2 Ocean Tide Loading model,
- Using 1mm relative constraints of the troposphere estimates and estimating every 30 minutes (wet delay estimated per station every 30 minutes),
- Estimating one troposphere gradient per 24 hours per station in north-south and east-west directions,
- Processing the GPS data as an ambiguity float solution

For the near real-time mode strategy, the GPS-PW estimation agrees with radiosonde-PW estimation with an average standard deviation of 2.8mm for the 14 stations and a maximum of 5.9mm. This result quality was achieved by using GPS data processing with the following strategies:

- Using IGU orbits and remove low accuracy satellites from the solution,
- Setting the observation sampling interval to 180 seconds,
- Setting 10 degrees as the elevation mask,
- Applying Niell mapping function with elevation-dependent weighting,
- Applying the GOT00.2 Ocean Tide Loading model,
- Using 1mm relative constraints of the troposphere estimates and estimating every 30 minutes (wet delay estimated per station every 30 minutes),
- Estimating one troposphere gradient per 24 hours per station in north-south and east-west directions,
- Processing the GPS data as an ambiguity float solution

The GPS data processing in both strategies (post-processed and near real-time) achieves high quality results, which were assessed by the station coordinate repeatabilities. The mean repeatability for the non-fixed GPS stations has an average of 5.7mm for the northing component, 4.8mm for the easting component and 8.6mm for the height component in the post-processed strategy. On the other hand, for the near real-time strategy, the mean repeatability for the non-fixed GPS stations has an average of 6.3mm for the northing component, 9.4mm for the easting component and 14.2mm for the height component. The accuracy of the post-processed strategy, which uses the IGS final orbits, is almost twice as good as the accuracy of the near real-time strategy, which uses IGU orbits.

Internal and external quality indicators assessed the quality of the GPS-PW estimates. The standard deviation of tropospheric parameter estimates is used as an internal quality indicator, whereas the standard deviation value of the validation of the GPS-PW estimates to the radiosonde-PW estimates is used as an external quality indicator. The standard deviation of tropospheric parameter estimates for the post-processed strategy has an average of 1.1mm and 1.5mm for the near real-time strategy. Moreover, the standard deviation of the GPS-PW estimates validated to radiosonde-PW estimates has an average of 2.5mm for the post-processed strategy and 2.8mm for the near real-time strategy.

This research shows that the agreement of the GPS-PW estimates with the radiosonde-PW estimates is slightly lower than previous studies which agree with an average standard deviation of 1-2mm (i.e. Tregoning *et al.*, 1998; Dodson *et al.*, 1999; Gradinarsky *et al.*, 2002). This is caused by the distance between GPS stations and radiosonde stations. Longer distances between stations will increase the possibility of the different weather conditions above the stations.

This research shows that the ARGN has the potential to be used as a water vapour observation system. Potentially this could be used in operational weather forecasting, and similar techniques used if new stations were added at locations where GPS may be most beneficial.

REFERENCES

Altamimi, Z., Boucher, C., Sillard, P. and Feissel, M. (2000) in Dick, W.R. and Richter, B. (eds) *IERS Annual Report 2000*, International Earth Rotation Service, Central Bureau. Frankfurt am Main: Verlag des Bundesamts für Kartographie und Geodäsie, 152 p.

American Geophysical Union (1995) *Water Vapor in Climate System*, Special Report, http://www.agu.org/sci_soc/mockler.html.

Baker, H.C. (1998) GPS Water Vapour Estimation for Meteorological Applications, *PhD Thesis*, Institute of Engineering Surveying and Space Geodesy, The University of Nottingham, 268p.

Baker, T.F., Curtis, D.J. and Dodson, A.H. (1995) Ocean Tide Loading and GPS, *GPS World*, Vol. 6, No. 3, pp 54-59.

Baker, H.C., Dodson, A.H., Penna, N.T. Higgins, M. and Offiler, D. (2001) Ground-Based GPS Water Vapour Estimation: Potential for Meteorological Forecasting, *Journal of Atmospheric and Solar Terrestrial Physics*, Vol. 63, pp. 1305-1314.

Barnes, J.B., Ackroyd, N. and Cross, P.A. (1998) Stochastic Modelling for Very High Precision Real-Time Kinematic GPS in an Engineering Environment, *XXI Congress of the International Federation of Surveyors (FIG)*, Part 6, Paper TS13, pp. 61-76.

Barry, R.G. and Chorley, R.J. (1989) *Atmosphere, Weather and Climate*, Routledge, London, 460p.

Becker, M., Franke, P., Weber, G., Ineichen, D. and Mervart, L. (2000) EUREF Contribution to ITRF2000 and Analysis Coordinator Report for 8/99 - 6/00, *Reports of the EUREF Technical Working Group*, International Association of Geodesy / Section I – Positioning; Subcommission for Europe (EUREF), Vol. 9, pp. 31-36.

Bevis, M., Businger, S., Herring, T.A., Rocken, C., Anthes, R.A. and Ware, R.H. (1992) GPS Meteorology: Remote Sensing of Atmospheric Water Vapour Using the Global Positioning System, *Journal of Geophysical Research*, Vol. 97, No. D14, pp. 15787-15801.

Bock, O. and Doerflinger, E. (2001) Atmospheric Modeling in GPS Analysis for High Accuracy Positioning, *Physics and Chemistry of the Earth, Part A: Solid Earth and Geodesy*, Vol. 26, No. 6-8, pp. 373-383.

Bock, O., Flamant, C. and Duquesnoy, T. (2001) Integrated Water Vapor Estimated by GPS Compared to Independent Observations during MAP, *presented in 8th International Symposium on Remote Sensing*, Toulouse, France, September.

Boucher, C., Altamimi, Z., Sillard, P and Feissel-Vernier, M. (2004) *The ITRF2000*, IERS Technical Note No. 31, Verlag des Bundesamts für Kartographie und Geodäsie, Frankfurt am Main, 289p.

Bureau of Meteorology (2001) *Climate Activities in Australia 2001*, Bureau of Meteorology, Melbourne, 221p.

Bouma, H.R. and Stoew, B. (2001) GPS Observations of Daily Variations in the Atmospheric Water Vapor Content, *Physics and Chemistry of the Earth, Part A: Solid Earth and Geodesy,* Vol. 26, No. 6-8, pp. 389-392.

British Atmospheric Data Centre (2002) *Radiosonde Apparatus*, http://www.badc.rl.ac.uk/data/radiosonde/figures/figone.html

Brock, F.V. and Richardson, S.J. (2001) *Meteorological Measurement Systems*, Oxford University Press, New York, 290p.

Brockmann, E. (1996) Combination of Solutions for Geodetic and Geodynamic Applications of the Global Positioning System (GPS), *PhD Dissertation*, Astronomical Institute, University of Berne, Switzerland, 211p.

Bussinger, S., Chiswell, S.R., Bevis, M., Duan, J., Anther, R.A., Rocken, C., Ware, R.H., Exner, M., VanHove, T. and Solheim, F.S. (1996) The Promise of GPS in Atmospheric Monitoring, *Bulletin of the American Meteorological Society*, Vol. 77, No. 1, pp. 5-18.

Chao, C.C. (1973) A New Method to Predict Wet Zenith Range Refraction from Surface Measurements of Meteorological Parameters, *DSN Progress Report*, No. 32-1526, Vol. XIV, Jet Propulsion Laboratory, Pasadena, California, pp. 33-41.

Costulis, P.K. (2002) *Glossary of Term*, http://asd-www.larc.nasa.gov/asd-over/gloassary/k.html.

Crowder, B. (2000) *The Wonders of the Weather*, Bureau of Meteorology, Griffin Press Pty Ltd., Second Edition, Canberra, 270p.

Cucurull, L., Sedo, P., Behrend, D., Cardellach, E. and Rius, A. (2002) Integrating NWP Products into the Analysis of GPS Observables, *Physics and Chemistry of the Earth,* Vol. 27, pp. 377-383.

Dach, R. and Dietrich, R. (2001) The Ocean Loading Effect in the GPS Analysis: A Case Study in the Antartica Peninsula Region, *Marine Geodesy*, Vol.24, pp. 13-25.

Davis, J.L. and Elgered, G. (1998) The Spatio-Temporal Structure of GPS Water-Vapor Determinations, *Physics and Chemistry of The Earth,* Vol. 23, No. 1, pp. 91-96.

Davis, J.L., Herring, T.A., Shapiro, I., Rogers, A.E.E. and Elgered, G. (1985) Geodesy by Radio Interferometry: Effects of Atmospheric Modelling Errors on Estimates of Baseline Length, *Radio Science*, Vol. 20, pp.1593-1607.

Dick, G., Gendt, G. and Reigber, C. (2001) First Experience with Near Real-Time Water Vapor Estimation in a German GPS Network, *Journal of Atmospheric and Solar-Terrestrial Physics*, Vol. 63, No. 12, pp. 1295-1304.

Dodson, A., Buerki, B., Elgered, G., Rius, A. and Rothacher, M. (1999) GPS Water Vapour Experiment For Regional Operational Network Trials (WAVEFRONT), *Final Report to European Commission Framework IV Environment and Climate Work Programme*, Institute of Engineering Surveying and Space Geodesy, University of Nottingham, Nottingham, UK.

Dodson, A.H. and Baker, H.C. (1998) Accuracy of Orbits for GPS Atmospheric Water Vapour Estimation, *Physics and Chemistry of the Earth*, Vol. 23, No. 1, pp. 119-124.

Dodson, A.H., Shardlow, P.J., Hubbard, L C.M, Elgered, G. and Jarlemark, P.O.J. (1996) Wet Tropospheric Effects on Precise Relative GPS Height Determination, *Journal of Geodesy*, No. 70, pp. 188-200.

Droegemeier, K. K. (2002) *Ground-Based GPS Meteorology Demonstration Network*, http://kkd.ou.edu/

Duan, J., Bevis, M., Fang, P., Bock, Y., Chiswell, S., Businger, S., Rocken, C., Solheim, F., Van Hove, T., Ware, R., McClusky, S., Herring, T.A. and King, R.W. (1996) GPS Meteorology: Direct Estimation of the Absolute Value of Precipitable Water, *Journal of Applied Meteorology*, Vol. 35, No. 6, pp. 830-838.

Eanes, R.J. and Bettadpur, S.V. (1996) The CSR 3.0 Global Ocean Tide Model, *Technical Memorandum CSR-TM-96-05*, Center for Space Research, University of Texas at Austin, 25pp.

Eanes, R.J. and Shuler, A. (1999) An Improved Global Ocean Tide Model from TOPEX/Poseidon Altimetry: CSR4.0, presented in European Geophysical Society (EGS) 24th General Assembly, The Hague, The Netherlands, April.

Egbert, G.D., Bennett, A.F. and Foreman, M.G.G. (1994) TOPEX/POSEIDON Tides Estimated Using a Global Inverse Model, *Journal of. Geophysical Research*, Vol. 99, No. C12, pp. 24821-24852.

Emardson, R., Johansson, J. M. and Elgered, G. (1998) Three Months of Continuous Monitoring of Atmospheric Water Vapour with a Network of Global Positioning Receivers, *Journal of Geophysical Research*, Vol. 103, D2, pp. 1807-1820.

Elgered, G., Davis, J.L., Herring, T.A. and Shapiro, I.I. (1991) Geodesy by Radio Interferometry: Water Vapor Radiometry for Estimation of the Wet Delay, *Journal of Geophysical Research*, Vol. 96, pp. 6541-6555.

Elgered, G., Johansson, J.M., Ronnang, B.O. and Davis, J.L. (1997) Measuring Regional Atmospheric Water Vapour Using the Swedish Permanent GPS Network, *Geophysical Research Letters*, Vol. 24, No. 21, pp. 2663-2666.

Feng, Y., Bai, A., Fang, P. and Williams, A. (2001) GPS Water Vapour Experimental Results from Observations of the Australian Regional GPS Network (ARGN), *presented in 2001-A spatial Odyssey: 42nd Australian Surveyor Congress*, Brisbane. Available Online at http://www.isaust.org.au/innovation/2001-Spatial_Odyssey/abstracts_6D.htm#feng

Gabor, M. (1997) *Water Vapor from Satellite Based GPS Receiver*, http://www.csr.utexas.edu/texas_pwv/midterm/gabor/gpsspace.html.

Ge, M., Calais, E. and Haase, J. (2000) Reducing Satellite Orbit Error Effects in Near Real-Time GPS Zenith Tropospheric Delay Estimation for Meteorology, *Geophysical Research Letter*, Vol. 27, pp. 1915-1918.

Ge, M., Calais, E. and Haase, J. (2001) Automatic Orbit Quality Control for Near Real-Time GPS Zenith Tropospheric Delay Estimation, *Physics and Chemistry of the Earth, Part A: Solid Earth and Geodesy*, Vol. 26, No. 3, pp. 177-181.

Gendt, G., Reigber, C. and Dick, G. (2001) Near Real-Time Water Vapor Estimation in a German GPS Network-First Results from the Ground Program of the HGF GASP Project, *Physics and Chemistry of the Earth, Part A: Solid Earth and Geodesy*, Vol. 26, No. 6-8, pp. 413-416.

Glover, D.R. (2001) *Dictionary of Technical Terms for Aerospace Use*, http://roland.lerc.nasa.gov/~dglover/dictionary/

Gradinarsky, L.P., Johansson, J. M., Bouma, H. R., Scherneck, H.-G. and Elgered, G. (2002) Climate Monitoring using GPS, *Physics and Chemistry of the Earth*, Vol. 27, pp. 335-340.

Guidry, M.W., Riedinger, M. and Barnes, T (2001) *Online Journey Through Astronomy*, http://csep10.phys.utk.edu/astr161/lect/earth/atmosphere.html.

Gurtner, W. (2001) *RINEX: The Receiver Independent Exchange Format Version 2.10*, http://www.ngs.noaa.gov/CORS/Rinex2.html.

Haase, J., Calais, E., Talaya, J., Rius, A., Vespe, F., Santangelo, R., Huang, X. Y., Davila, J. M., Ge, M., Cucurul, L., Flores, A., Sciarretta, C., Pacione, R., Boccolari, M., Pugnaghi, s., Vedel, H., Mogensen, K., Yang, X. and Garate, J. (2001) The Contributions of the MAGIC Project to the COST 716 Objectives of Assessing the Operational Potential of Ground-Based GPS Meteorology on an International Scale, *Physics and Chemistry of the Earth, Part A: Solid Earth and Geodesy*, Vol. 26, No. 6-8, pp. 433-437.

Herring, T.A. (1992) Modeling Atmospheric Delays in the Analysis of Space Geodetic Data, in de Munck, J.C. and Spoelstra, T.A.Th. (eds) *Proceedings of the Symposium on Refraction of Transatmospheric Signals in Geodesy*, Netherlands Geodetic Commission, Publications on Geodesy, Delft, The Netherlands, No. 36, New Series, pp. 157-164.

Hofman-Wellenhof, B., Lictenegger, H. and Collins, J. (2001) *Global Positioning System: Theory and Practice*, 5th ed., Springer-Verlag, 382p.

Hopfield, H.S. (1969) Two-Quartic Tropospheric Refractivity Profile for Correcting Satellite Data, *Journal of Geophysical Research*, Vol. 74, No. 18, pp. 4487-4499.

Hopkins, E.J. (1996) *Weather Satellite Platform*, http://www.aos.wisc.edu/~hopkins/aos100/satpltfm.htm.

Hugentobler, U., Schaer, S. and Fridez P. (2001) *Bernese GPS Software Version 4.2*, Astronomical Institute, University of Berne, 515p.

Ifadis, I. (1986) The Atmospheric Delay of Radio Waves: Modelling The Elevation Dependence on a Global Scale, *Technical Report No 38L*, Chalmers University of Technology, Gothenburg, Sweden.

IGS (2002) *IGS Products*, http://igscb.jpl.nasa.gov/components/prods.html

IGS (2002) *Monitoring Global Change by Satellite Tracking*, http://igscb.jpl.nasa.gov

Infrared Measurements Group (2002) *Infrared Measurements and Water Vapor Studies Group*, http://www.ghcc.msfc.nasa.gov/irgrp/index.html.

Iwabuchi, T., Naito, I. and Mannoji, N. (2000) A Comparison of Global Positioning System Retrieved Precipitable Water Vapour with the Numerical Weather Prediction Analysis Data Over the Japanese Islands, *Journal of Geophysical Research*, Vol. 105, No. 4, pp. 4573-4585.

Jacobson, M.Z. (1999) *Fundamentals of Atmospheric Modeling*, Cambridge University Press, United States of America, 656p.

Jaegle, J., Jacob, D.J., Brune, W.H., Faloona, I.C., Tan, D., Kondo, Y., Sachse, G. W., Anderson, B., Gregory, G.L., Vay, S., Singh, H.B., Blake, D.R. and Shetter, R. (1999) Ozone Production in the Upper Troposphere and the Influence of Aircraft during SONEX: Approach of NO_x-Saturated Conditions, *Geophysical Research Letter*, Vol. 26, pp. 3081-3084.

Jerrett, D. and Nash, J. (2001) Potential Uses of Surface Based GPS Water Vapour Measurements for Meteorological Purposes, *Physics and Chemistry of The Earth*, Vol. 26, No. 6-8, pp. 457-461.

Johansson, J.M., Emardson, T.R., Jarlemark, P.O.J., Gradinarsky, L.P. and Elgered, G. (1998) The Atmospheric Influence on the Results from the Swedish GPS Network, *Physics and Chemistry of the Earth*, Vol. 23, No. 1, pp. 107-112.

Kaplan, E. (1996) *Understanding GPS: Principles and Applications*, Artech House Publishers, Boston London, 554pp.

Kempler, S. (2000) *Atmospheric Structure*, http://daac.gsfc.nasa.gov/CAMPAIGN_DOCS/ATM_CHEM/exosphere.html

King, R.W. and Bock, Y. (1997) *Documentation for the GAMIT GPS Analysis Software*, Release 9.66, Massachusetts Institute of Technology, Cambridge Massachusetts.

Kruse, L., Sierk, B., Springer, T. and Cocard, M. (1999) GPS Meteorology: Impact of Predicted Orbits on Precipitable Water Estimation, *Geophysical Research Letter*, Vol. 26, pp. 2045-2048.

Kruse, L.P. (1999) *Personal E-mail to Nigel Penna on March, 19th 1999.*

Lee, L.C., Rocken, C. and Kursinski, E.R. (eds) (2001) *Applications of Constellation Observing System for Meteorology, Ionosphere and Climate*, Springer-Verlag, Hong Kong, 384p.

Leick, A. (1995) *GPS Satellite Surveying*, 2nd ed., John Wiley and Sons, New York, 560p.

Lefevre, F., Le Provost, C., Lyard, F.H. and Schrama, E.J.O. (2000) FES98 and FES99: Two New Versions of the FES' Global Tide Finite Element Solutions, presented in *Joint TOPEX/POSEIDON and Jason-1 Science Working Team Meeting*, Radisson Deauville Resort, Miami Beach, Florida, USA, November.

Le Provost, C., Genco, M.L., Lyard, F., Vincent, P. and Canceil, P. (1994) Spectroscopy of the World Ocean Tides from a Finite-element Hydrodynamic Model. *Journal of Geophysical Research*, Vol. 99, No. C12, pp. 24777-24797.

Le Provost, C., Lyard, F., Molines, J.M., Genco, M.L., and Rabilloud, F. (1998) A Hydrodynamic Ocean Tide Model Improved by Assimilating a Satellite Altimeter-Derived Data Set. *Journal of Geophysical Research*, Vol. 103, No. D14, pp. 5513-5529.

Linacre, E. and Geerts, B. (1997) *Climates & Weather Explained*, Routledge, London, 432p.

Liou, Y-A., Teng Y-T., van Hove, T. and Liljegren, J.C. (2001) Comparison of Precipitable Water Observations in the Near Tropics by GPS, Microwave Radiometer, and Radiosondes, *Journal of Applied Meteorology*, Vol. 40, pp. 5-15.

MAGIC (1999) *Online Resources*, Available at: http://kreiz.unice.fr/magic/THEORY/data_processing.html.

Marini, J.W. (1972) Correction of Satellite Tracking Data for an Arbitrary Atmospheric Profile, *Radio Science*, Vol. 7, pp. 223-231.

Marquardt, C, Labitzke, K., Reigber, Ch., Schmidt, T. and Wickert, J. (2001) An Assessment of the Quality of GPS/MET Radio Limb Soundings during February 1997, *Physics and Chemistry of the Earth, Part A: Solid Earth and Geodesy*, Vol. 26, No. 3, pp. 125-130.

Matsumoto, K., Takanezawa, T. and Ooe, M. (2000) Ocean Tide Models Developed by Assimilating TOPEX/POSEIDON Altimeter Data into Hydrodynamical Model: A Global Model and a Regional Model Around Japan, Journal of Oceanography, Vol. 56, pp. 567-581.

McCarthy, D. D. (1996) IERS Conventions (1996), *IERS Technical Note 21*, Observatoire de Paris, July 1996.

Mendes, V.B. and Langley, R.B. (1994) A Comprehensive Analysis of Mapping Functions Used in Modeling Tropospheric Propagation Delay in Space Geodetic Data, *Proceedings of the International Symposium on Kinematic Systems in Geodesy, Geomatics and Navigation*, 30 August-2 September 1994, The University of Calgary, Calgary, Alberta, pp. 87-98.

Mendes, V.B. and Langley, R.B. (1998) Optimization of Tropospheric Delay Mapping Function Performance for High-Precision Geodetic Applications, *Proceedings of DORIS Days*, 27-29 April 1998, Toulouse, France.

Merriam-Webster (1936) *Collegiate Dictionary*, Online Resources, Available at: http://www.m-w.com/home.htm

NetCent Communication (2003) *Weather and Climate Terminology, Glossary Data and Reference Services*, Online Resources, Available at: http://weather.ncbuy.com/glossary.html?action=LETTER&term=U

Niell, A.E. (1996) Global Mapping Functions for the Atmospheric Delay at Radio Wavelengths, *Journal of Geophysical Research*, Vol. 101, No. B2, pp. 3227-3246.

NOAA Forecast Systems Laboratory (2001) *Ground-Based GPS Meteorology Demonstration Network*, http://gpsmet.fsl.noaa.gov/jsp/index.jsp

Ohtani, R. (2001) Detection of Water Vapour Variations Driven by Thermally-induced Local Circulations Using the Japanese Continuous GPS array, *Geophysical Research Letters*, Vol. 28, No. 1, pp. 151-154.

Pacione, R. Fionda, E., Ferrara, R., Lanotte, R., Sciarretta, C. and Vespe, F (2002) Comparison of Atmospheric Parameters Derived from GPS, VLBI and A

Ground-Based Microwave Radiometer in Italy, *Physics and Chemistry of the Earth*, Vol. 27, No. 4-5, pp 309-316.

Penna, N.T. (1997) Monitoring Land Movement at UK Tide Gauge Sites Using GPS, *PhD Thesis*, University of Nottingham, 233p.

Penna, N.T. and Baker, T.F. (2002) Ocean Tide Loading Considerations for GPS Processing around Australia, *Submitted to Geomatics Research Australasia*.

Petrov, L. and Boy, J-P. (2004) Study of Atmospheric Pressure Loading Signal in Very Long Base Interferometry Observations, *Journal of Geophysical Research*, Vol. 109, B03405.

Pugnaghi, S., Boccolari, M., Fazlagic, S., Pacione, R., Santangelo, R., Vedel, H. and Vespe, F (2002) Comparison of Independent Integrated Water Vapour Estimates from GPS and Sun Photometer Measurements and a Meteorological Model, *Physics and Chemistry of the Earth*, Vol. 27, pp. 355-362.

Ray, R.D. (1999) A Global Ocean Tide Model From TOPEX/POSEIDON Altimetry: GOT99.2, *NASA Technical Memorandum 209478*, Goddard Space Flight Center, 58 pp.

Ray, J.R. (2000) New Timing Products from the IGS: IGS/BIPM Time Transfer Pilot Project and UT1-like Estimates from GPS, *IVS 2000 General Meeting Proceedings*, International VLBI Service for Geodesy and Astrometry, Kötzting, Germany, May.

Rizos, C. (1999) *Principle and Practice GPS Surveying*, Online Resources, Available at: http://www.gmat.unsw.edu.au/snap/gps/gps_survey/principles_gps.htm.

Rocken, C., Sokolovskiy, S., Johnson, J.M. and Hunt, D. (2001) Improved Mapping of Tropospheric Delays, *Journal of Atmospheric and Oceanic Technology*, Vol. 18, pp. 1205-1213.

Rocken, C., van Hove, T. Johnson, J., Solheim, F., Ware, R.H., Bevis, M., Businger, S. and Chiswell, S.R. (1995) GPS/STORM – GPS Sensing of Atmospheric Water Vapor for Meteorology, *Journal of Atmospheric and Oceanic Technology*, Vol. 12, pp. 468-478.

Rocken, C., van Hove, T. and Ware, R.H. (1997) Near Real-Time GPS Sensing of Atmospheric Water Vapor, *Geophysical Research Letter*, Vol. 24, No.24, pp. 3221-3224.

Rocken, C., Ware, R.H., van Hove, T., Solheim, F., Alber, C., Johnson, J., Bevis, M. and Businger, S. (1993) Sensing Atmospheric Water Vapor with the Global Positioning System, *Geophysical Research Letter*, Vol. 20, No. 23, pp. 2631-2634.

Rothacher, M., Schaer, S, Mervart, L. and Beutler, G. (1995) Determination of Antenna Phase Centre Variations Using GPS Data, in *Proceedings of IGS Workshop 'Special topics an New Directions' in Postdam, May, 1995.*

Rothacher, M., Springer, T.A., Schaer, S. and Beutler, G. (1997) Processing Strategies for Regional GPS Network, in *Proceedings of the IAG General Assembly in Rio, September, 1997*, Springer.

Roy, A. (2002) *Water-Vapour Radiometer*, http://www.mpifr-bonn.mpg.de/staff/aroy/wvr.html

Scherneck, H.-G. (1991): A Parametrized Solid Earth Tide Model and Ocean Tide Loading Effects for Global Geodetic Baseline Measurements, *Geophysical Journal International*, Vol. 106, No. 3, pp. 677-694.

Schuler, T. (2001) On Ground-Based GPS Tropospheric Delay Estimation, *Dr.-Ing Dissertation*, Universitat der Bundeswehr Munchen, Munchen, 364p.

Schwiderski, E.W. (1980) On Charting Global Ocean Tides, *Reviews of Geophysics and Space Physics*, Vol. 18, pp. 243-268.

Seeber, G. (1993) *Satellite Geodesy-Foundations, Methods and Applications*, Walter de Gruyter, Berlin New York, 531pp.

Shum, C.K., Woodworth, P.L., Andersen. O.B., Egbert, E., Francis, O., King, C., Klosko, S., Le Provost, C., Li, X., Molines, J.M., Parke, M., Ray, R., Schlax, M., Stammer, D., Thierney, C., Vincent, P. and Wunsch, C. (1997) Accuracy Assessment of Recent Ocean Tide Models, *Journal of Geophysical Research*, Vol. 102, C11, pp. 25173-25194.

Spofford, P.R. and Remondi, B.W. (1999) *The National Geodetic Survey Standard GPS Format SP3*, http://igscb.jpl.nasa.gov/igscb/data/format/sp3_docu.txt

Springer, T. (2000) *IGS Ultra Rapid Products.*
http://igscb.jpl.nasa.gov/mail/igsmail/2000/msg00435.html

Springer, T.A. and Hugentobler, U. (2001) IGS Ultra Rapid Products for (Near-) Real-Time Applications, *Physics and Chemistry of The Earth*, Vol. 26, No. 6-8, pp. 623-628.

Stewart, M.P. (1998) How Accurate is the Australian National GPS Network as a Framework for GPS Heighting?, *The Australian Surveyor*, Vol. 43, No. 1, pp. 53-61.

Takiguchi, H., Kato, T., Kobayashi, H. and Nakaegawa, T. (2000) GPS Observations in Thailand for Hydrological Applications, *Earth Planets Space*, Vol. 52, No. 11, pp. 913-919.

Teunissen, P.J. G. (1998) GPS Observation Equations and Positioning Concepts, in P.J.G. Teunissen and Kleusberg, A. (eds) *GPS for Geodesy*, 2nd ed., Springer-Verlag, Berlin-Heidelberg-New York.

Thayer, G.D. (1974): An improved equation for the radio refractive index of air. *Radio Science*, 9, 803- 807

Tregoning, P., Boers, R., O'Brien, D. and Hendy, M. (1998) Accuracy of Absolute Precipitable Water Vapour Estimates from GPS Observations, *Journal of Geophysical Research*, Vol. 103, No. D2, pp. 28701-28710.

Tsuda, T., Heki, K., Miyazaki, S., Aonashi, K., Hirahara, K., Nakamura, H., Tobita, M., Kimata, F., Tabei, T., Matsushima, T., Kimura, F., Satomura, M., Kato, T. and Naito, I. (1998) GPS Meteorology Project of Japan-Exploring Frontiers of Geodesy, *Earth Planet Space*, Vol. 50, No. 10, pp. i-v.

Twilley, R.J. and Digney, P.W. (2001) The Australian Regional GPS Network, *Physics and Chemistry of The Earth*, Vol. 26, No. 6-8, pp. 629-635.

UNESCO. (2000) *The Hydrological Cycle*, http://www.unesco.org/science/ waterday2000/Cycle.htm

Van Dam T.M., Blewitt, G. and Heflin, M.B. (1994) Atmospheric Pressure Loading Effects on Global Positioning System Coordinate Determination, *Journal of Geophysical Research*, Vol. 99, No. B12, pp. 23939-23950.

Walpersdorf, A., Calais, E., Haase, J., Eymard, L., Desbois, M. and Vedel, H. (2001) Atmospheric Gradients Estimated by GPS Compared to a High Resolution Numerical Weather Prediction (NWP) Model, *Physics and Chemistry of the Earth, Part A: Solid Earth and Geodesy,* Vol. 26, No. 3, pp. 147-152.

Ware, R., Alber, C., Rocken, C. and Solheim, F. (1997) Sensing Integrated Water Vapour Along GPS Ray Paths, *Geophysical Research Letters,* Vol. 24, No. 4, pp. 417-420.

Ware, R., Exner, M., Feng, D., Gorbunov, M., Hardy, K., Herman, B., Kuo, Y., Meehan, T., Melbourne, W., Rocken, C., Schreiner, W., Sokolovskiy, S., Solheim, F., Zou, X., Anthes, R., Businger, S. and Trenberth, K. (1996) GPS Sounding of the Atmosphere from Low Earth Orbit: Preliminary Results, *Bulletin of the American Meteorological Society*, Vol. 77, No. 1., pp.19-40.

Ware, R.H., Fulker, D.W., Stein, S.A., Anderson, D.N., Avery, S.K., Clark, R.D., Droegemeier, K.K., Kuettner, J.P., Minster, J.B. and Sorooshian, S. (2000) SuomiNet: A Real-Time National GPS Network for Atmospheric Research and Education, *Bulletin of the American Meteorological Society*, Vol. 81, No. 4, pp. 677-691.

Ware, R.H., Fulker, D.W., Stein, S.A., Anderson, D.N., Avery, S.K., Clark, R.D., Droegemeier, K.K., Kuettner, J.P., Minster, J.B. and Sorooshian, S (2001)

Real-Time National GPS Networks for Atmospheric Sensing, *Journal of Atmospheric and Solar-Terrestrial Physics*, Vol 63, No. 12, pp. 1315-1330.

WAVERONT (1999) GPS Water Vapour Experiment For Regional Operational Network Trials (WAVEFRONT), *European Commission Framework IV Environment and Climate Work Programme Final Report*, EC Contract No. ENV4-CT96-0301, 137p.

Webb, F.H. and Zumberge, J.F. (1993) *An Introduction to the GIPSY/OASIS-II*, JPL Publication D-11088, Jet Propulsion Laboratory, Pasadena.

World Meteorological Organization (1968) *Method in Use for the Reduction Atmospheric Pressure*, Technical Note. No. 91, Geneva

Yoshihara, T., Tsuda, T. and Hirahara, K. (2000) High Time Resolution Measurements of Precipitable Water Vapor from Propagation Delay of GPS Signals, *Earth Planets Space*, Vol. 52, pp. 479-493.

Yunck, T.P., Liu, C.H. and Ware, R. (2000) A History of GPS Sounding, *Terrestrial, Atmospheric and Oceanic Science*, Vol. 11, pp. 1-20.

APPENDIX A

POST-PROCESSED GPS-PW ESTIMATES

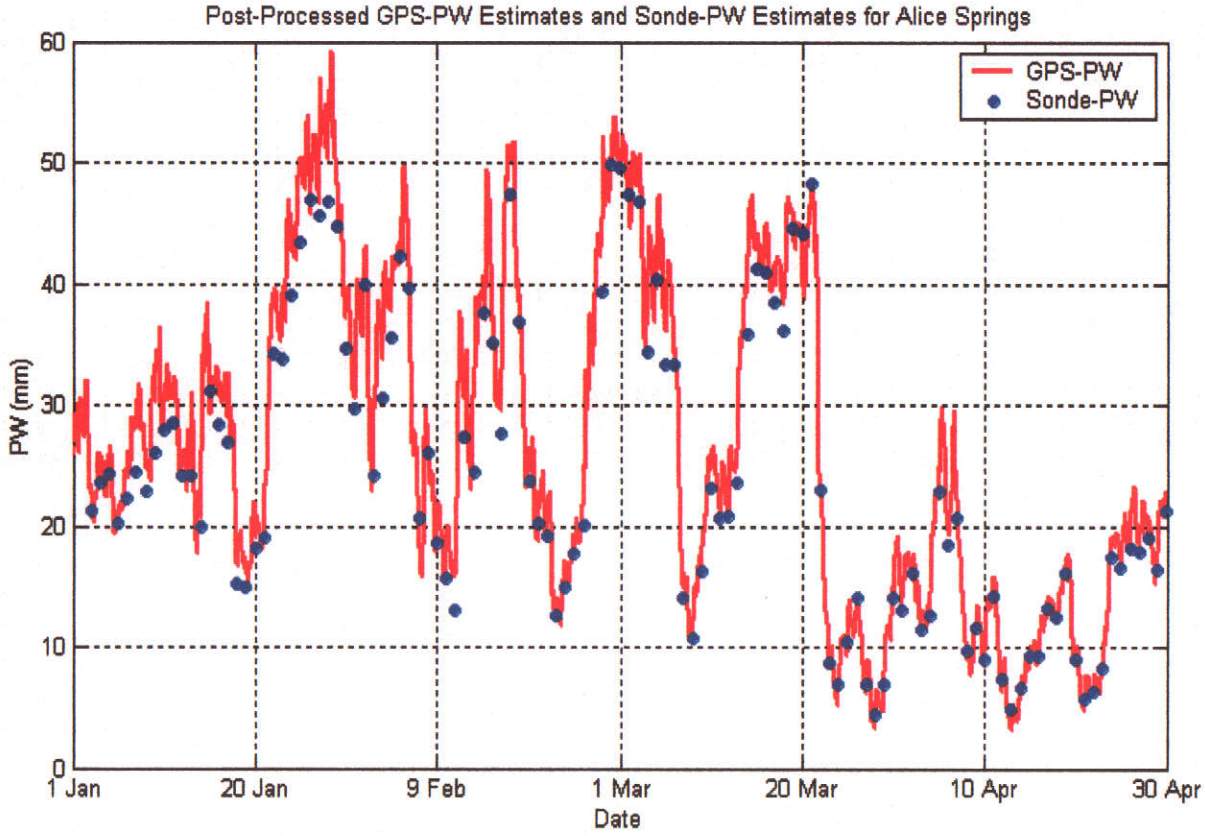

Comparison of GPS-IPW and Radiosonde-IPW at Alice Springs

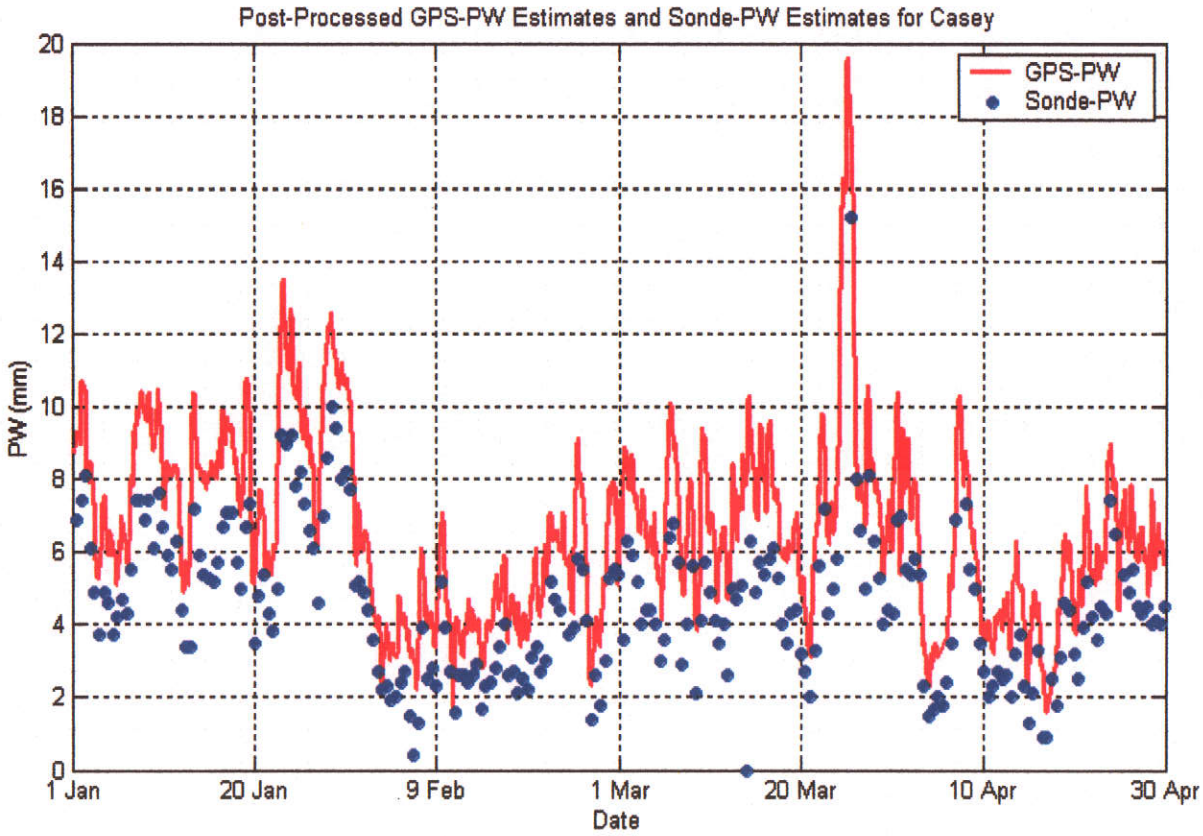

Comparison of GPS-IPW and Radiosonde-IPW at Casey

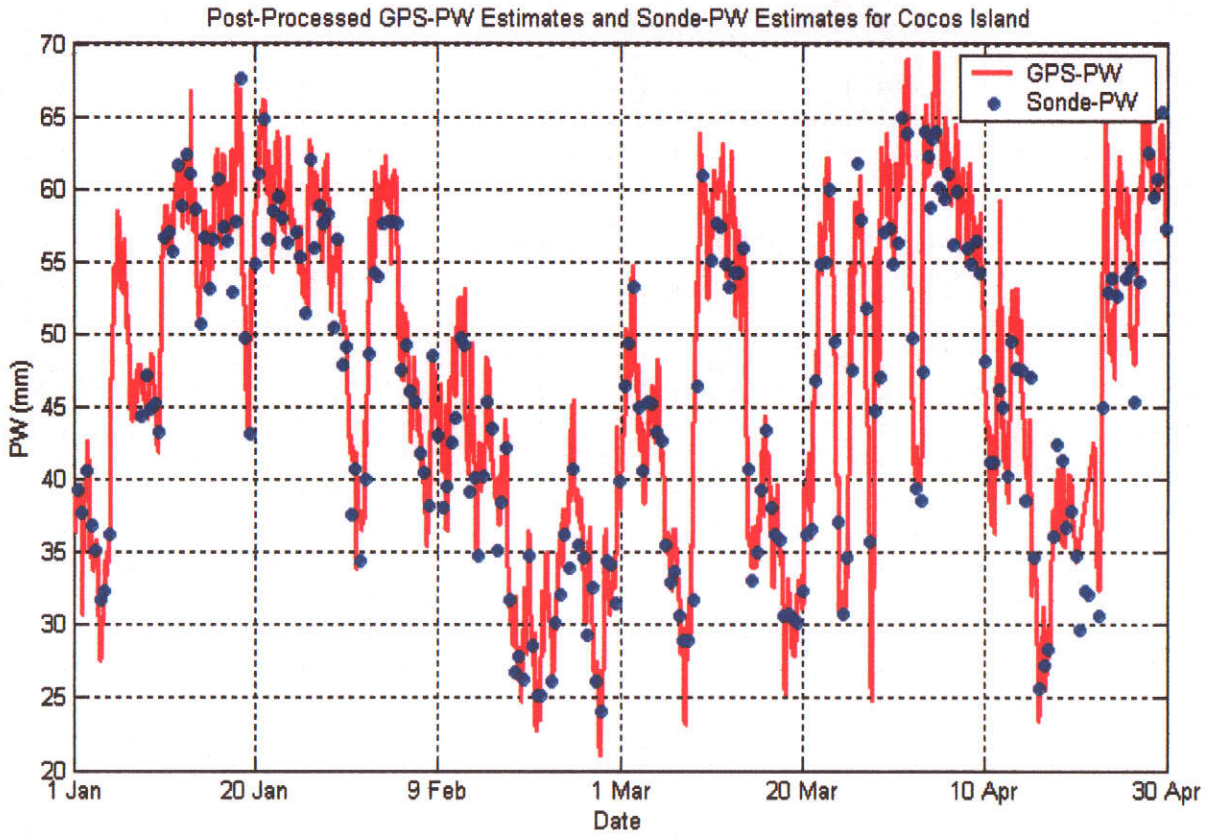

Comparison of GPS-IPW and Radiosonde-IPW at Cocos Island

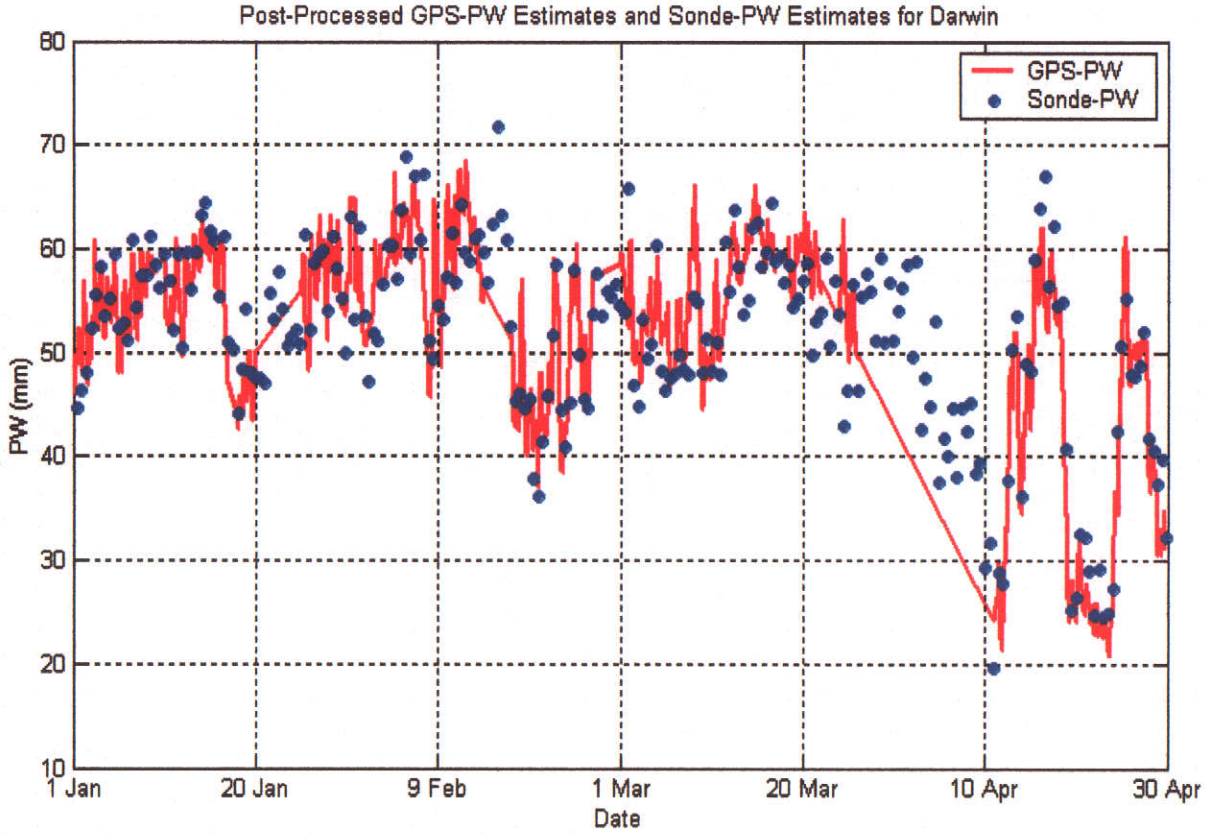

Comparison of GPS-IPW and Radiosonde-IPW at Darwin

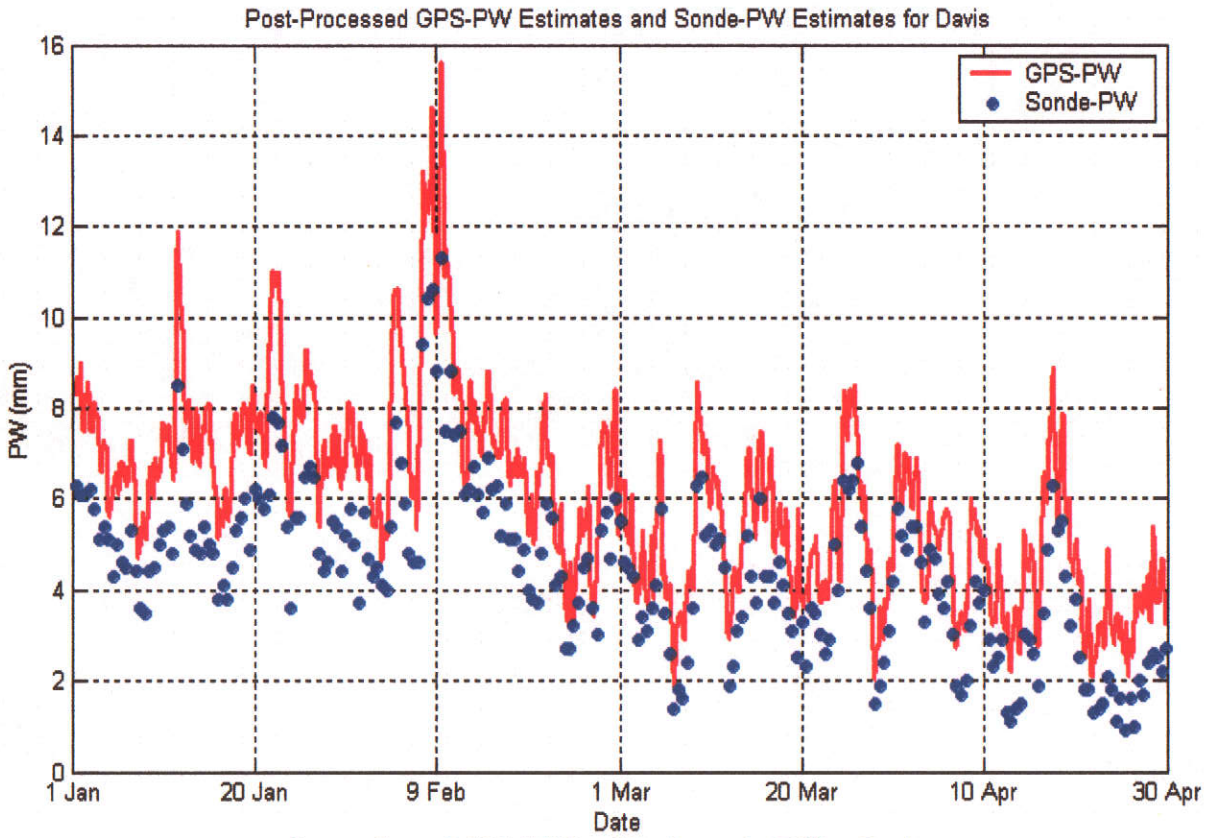

Comparison of GPS-IPW and Radiosonde-IPW at Davis

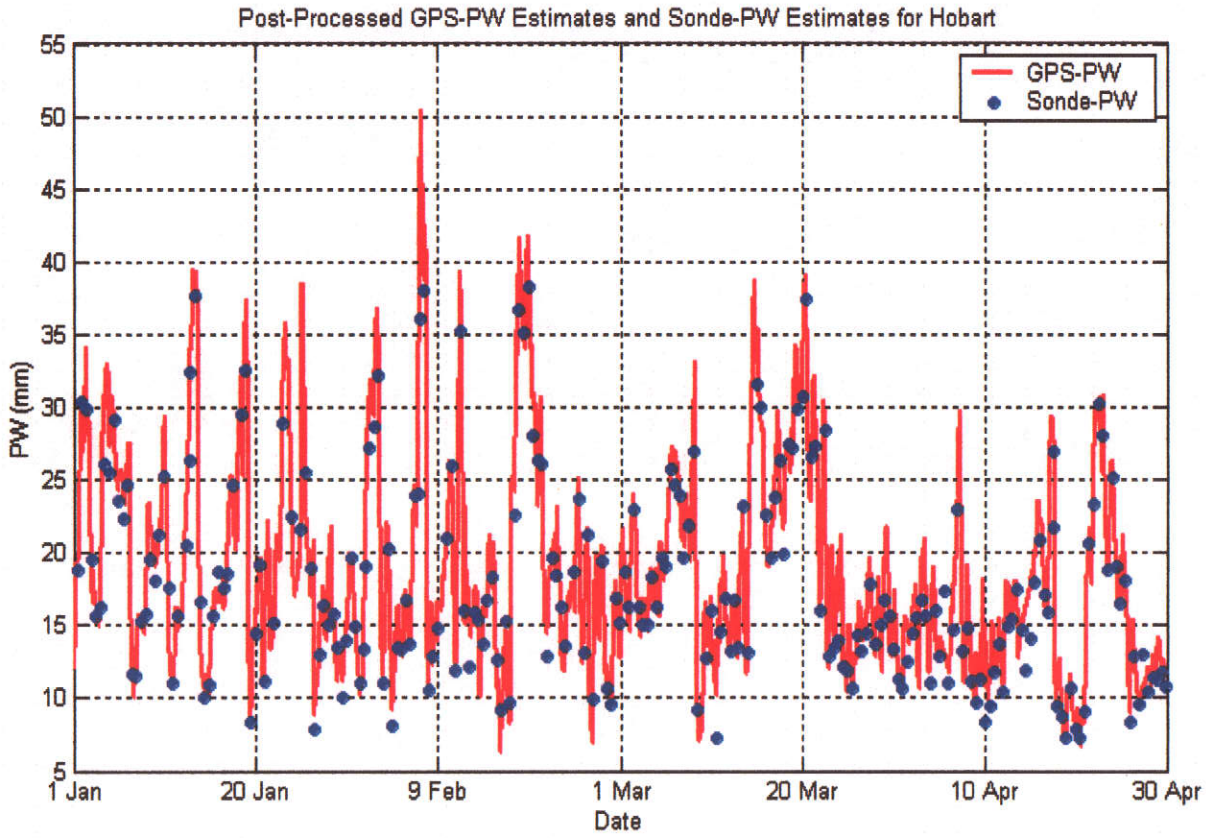

Comparison of GPS-IPW and Radiosonde-IPW at Hobart

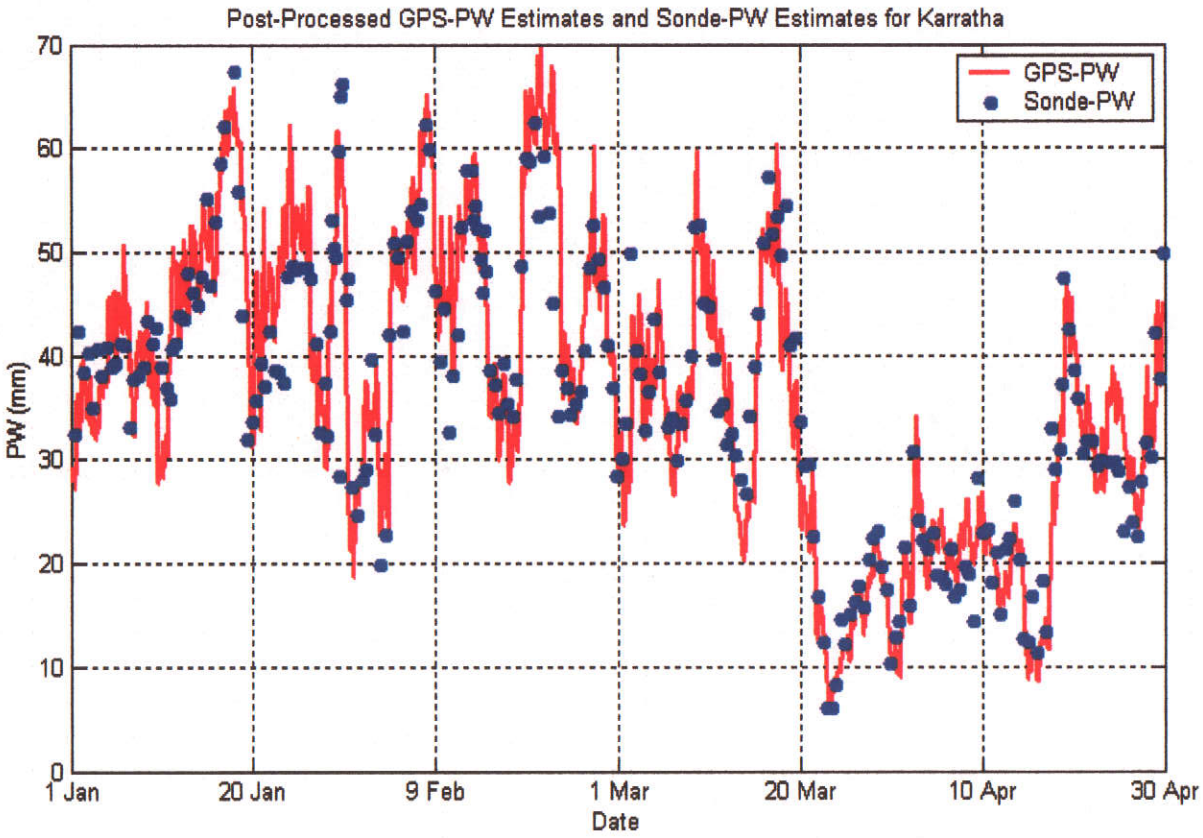

Comparison of GPS-IPW and Radiosonde-IPW at Karratha

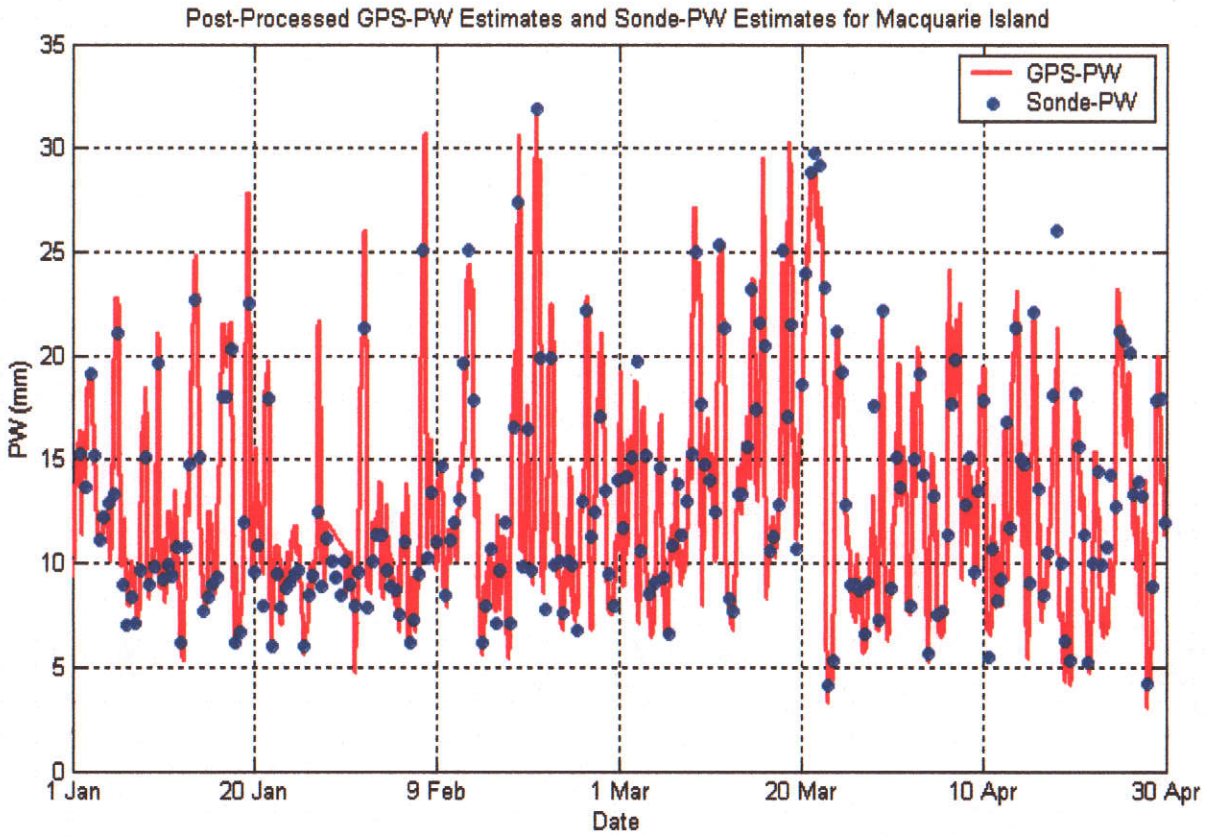

Comparison of GPS-IPW and Radiosonde-IPW at Macquarie Island

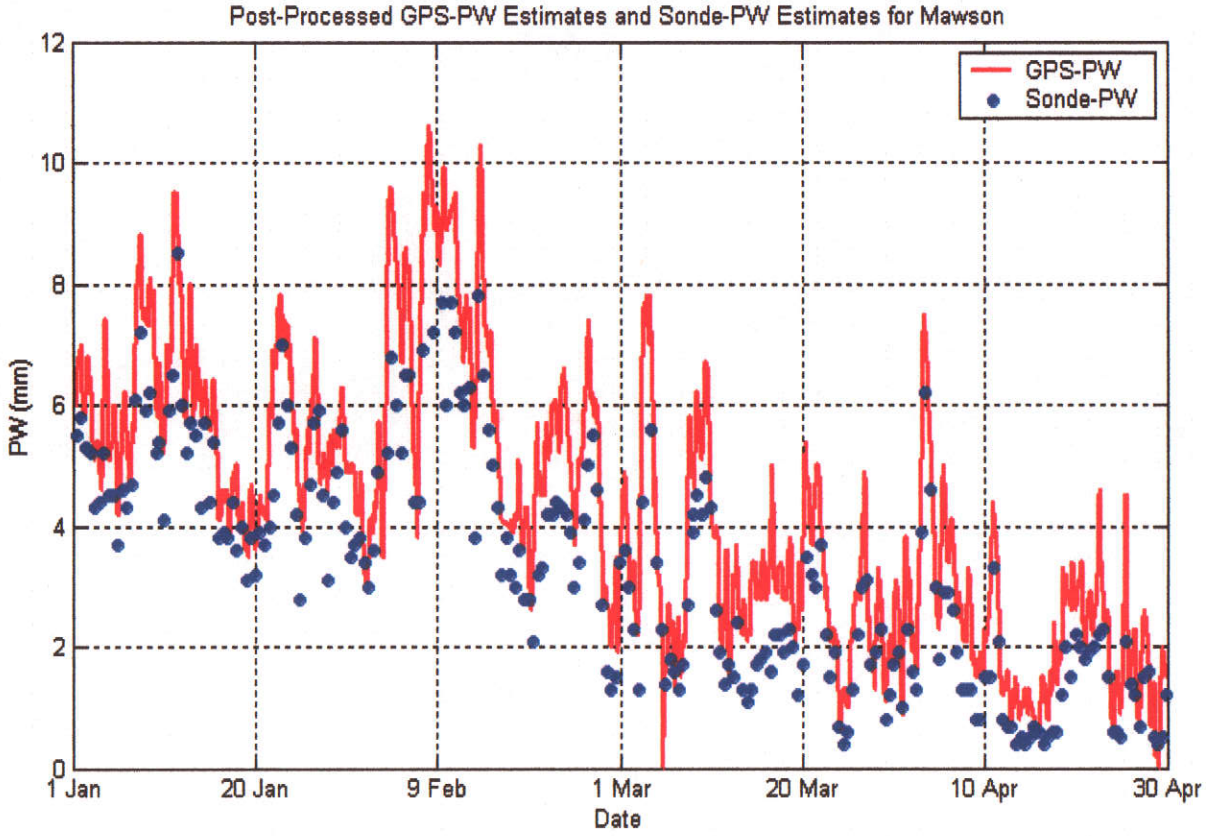

Comparison of GPS-IPW and Radiosonde-IPW at Mawson

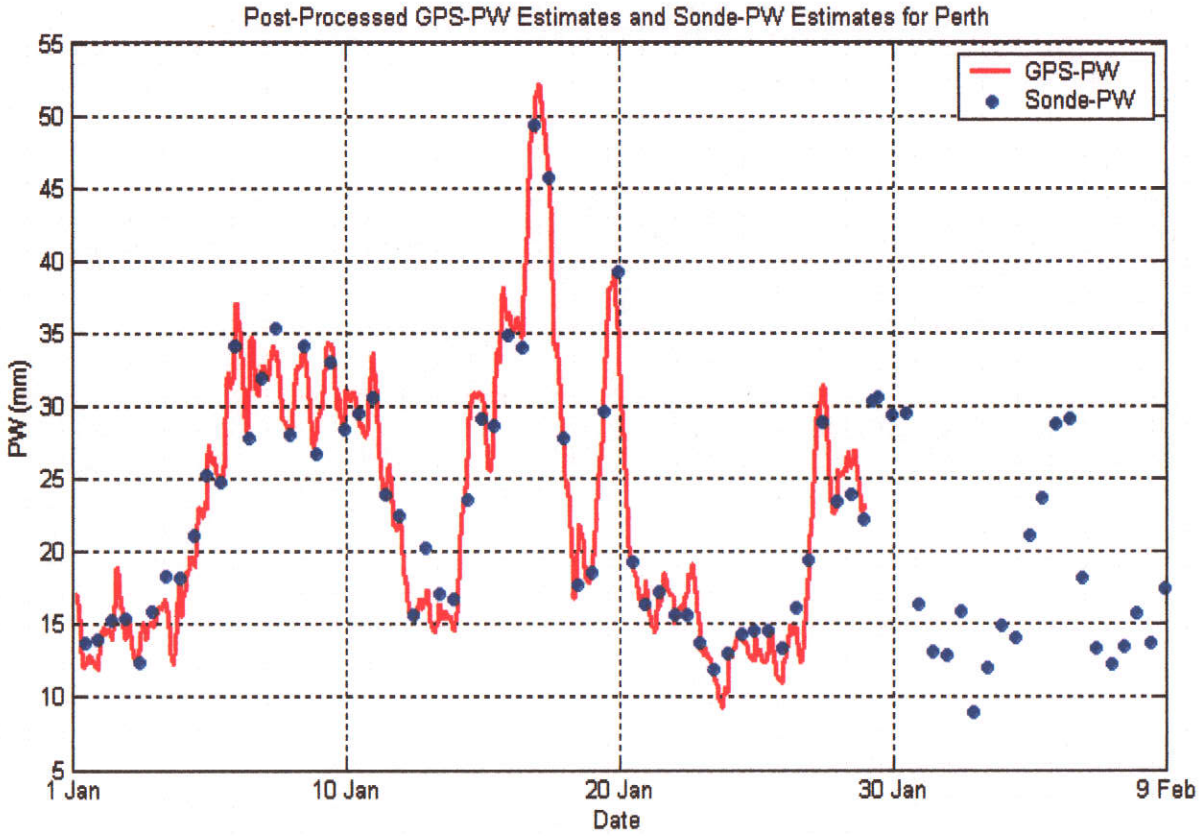

Comparison of GPS-IPW and Radiosonde-IPW at Perth

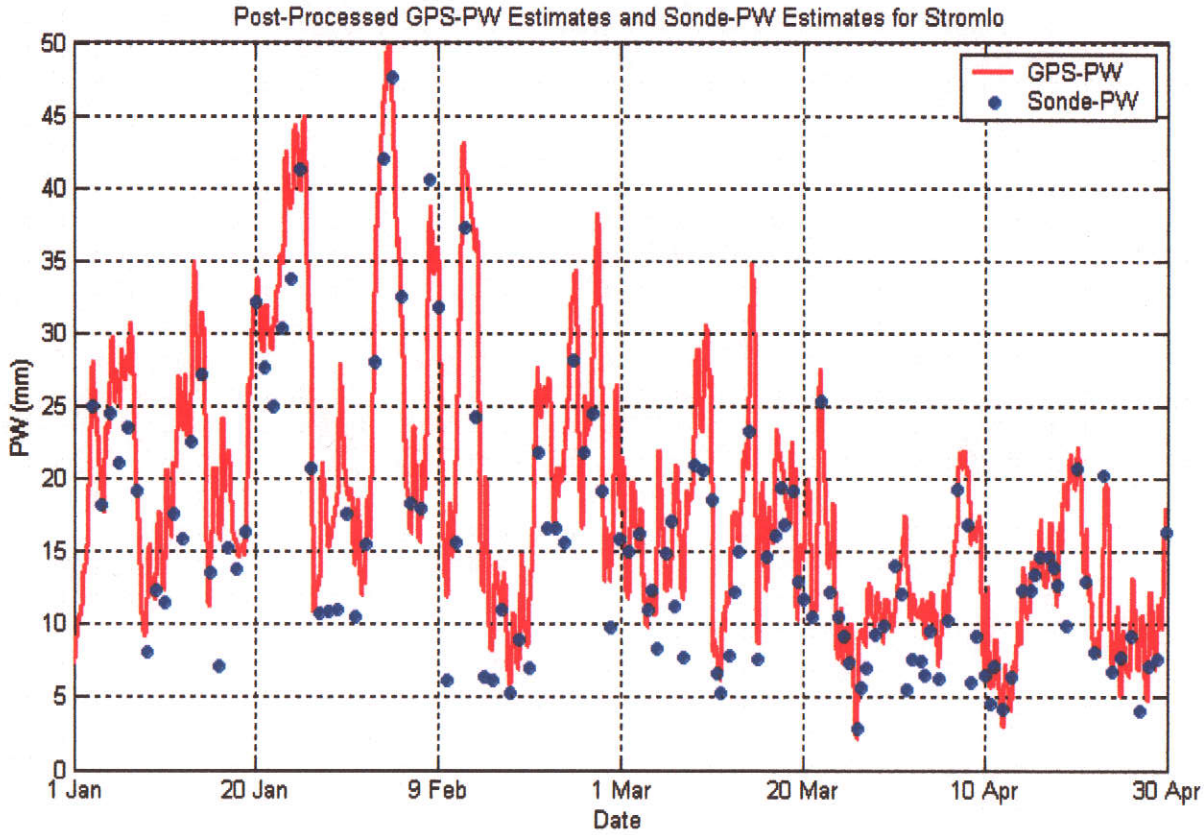

Comparison of GPS-IPW and Radiosonde-IPW at Mt. Stromlo

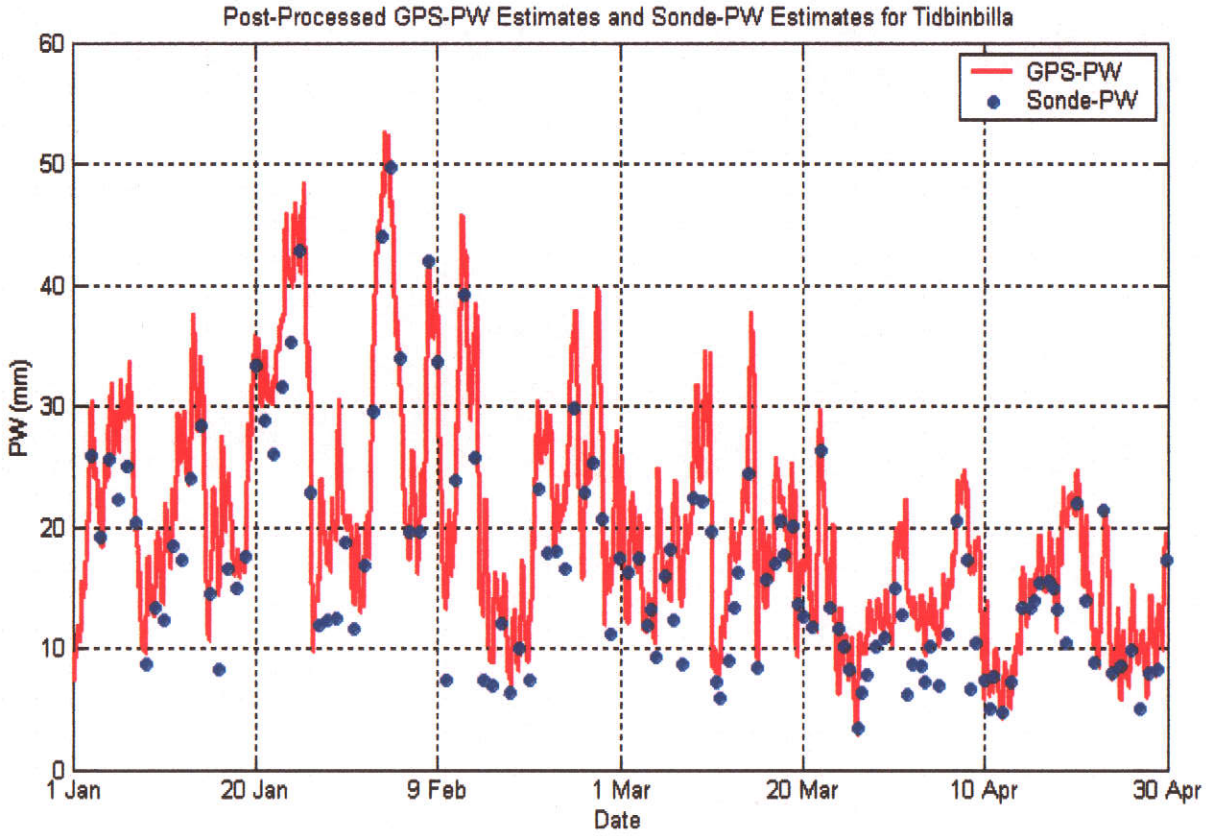

Comparison of GPS-IPW and Radiosonde-IPW at Tidbinbilla

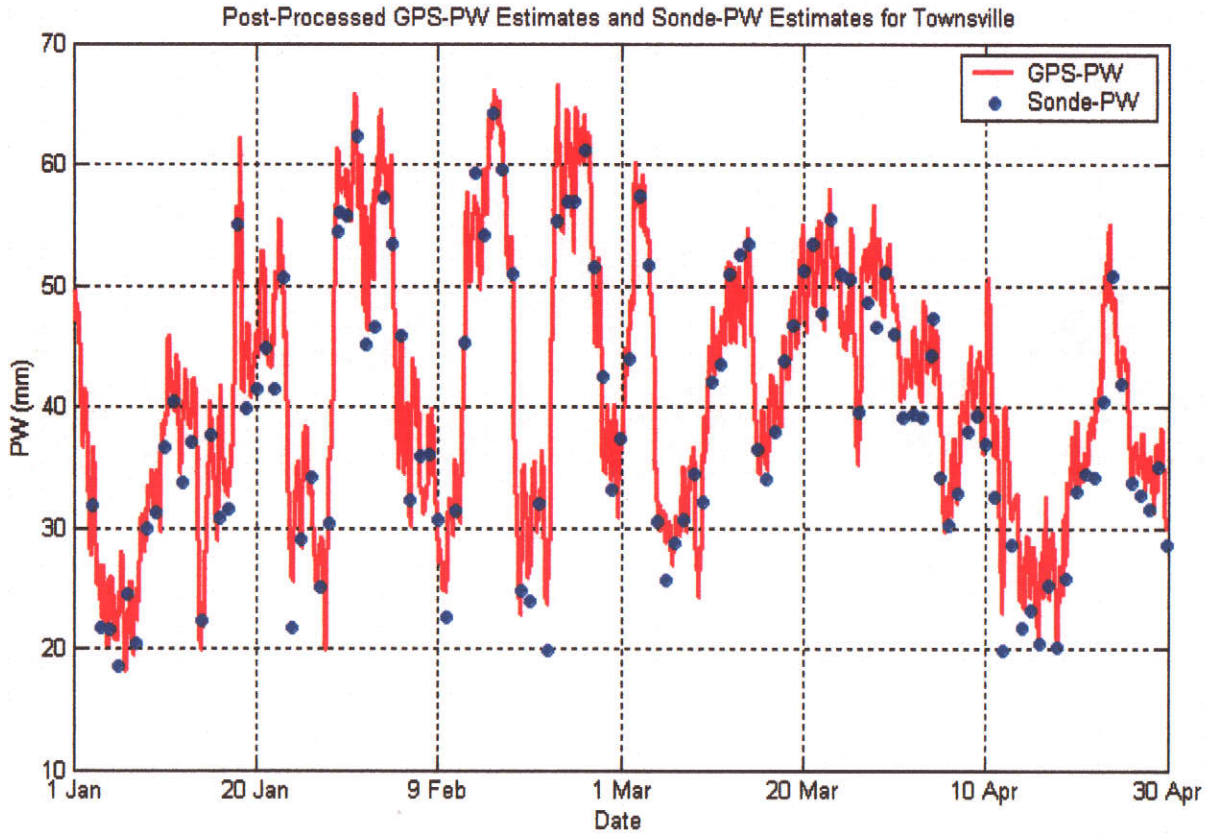

Comparison of GPS-IPW and Radiosonde-IPW at Townsville

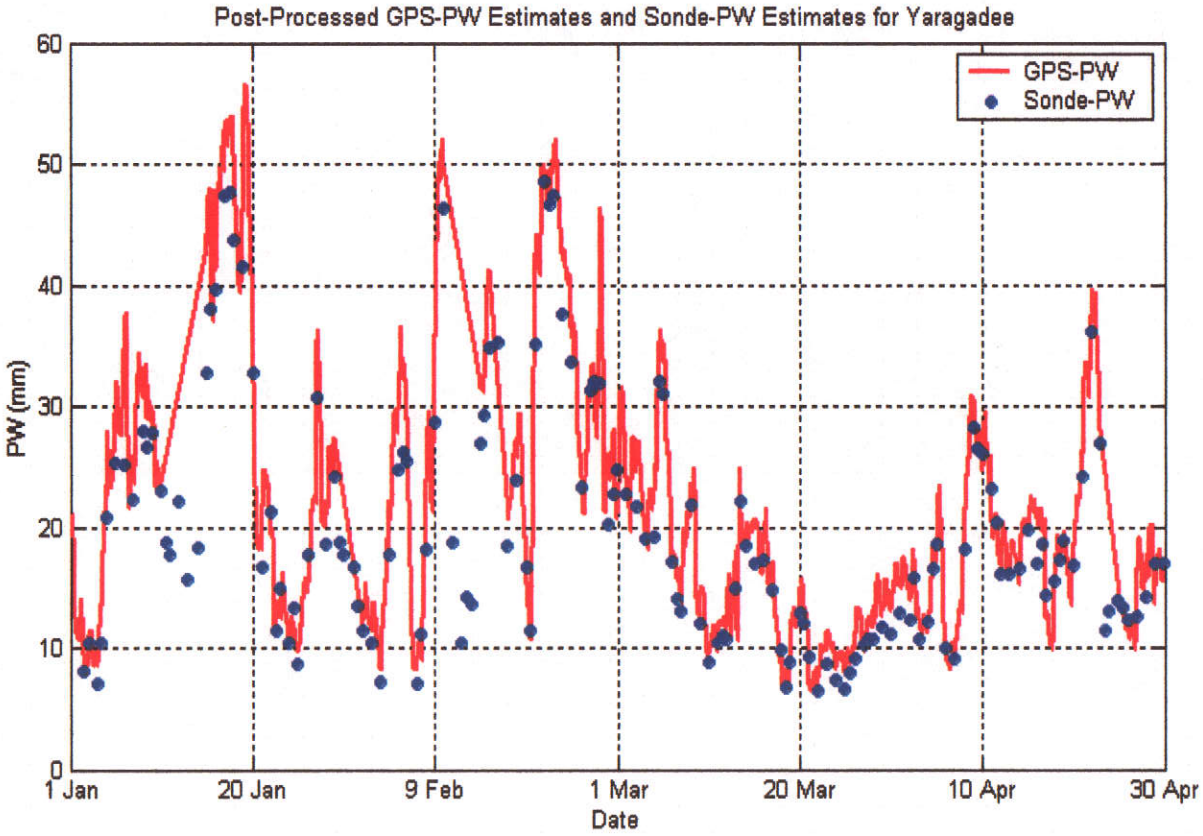

Comparison of GPS-IPW and Radiosonde-IPW at Yaragadee

APPENDIX B

NEAR REAL-TIME GPS-PW ESTIMATES

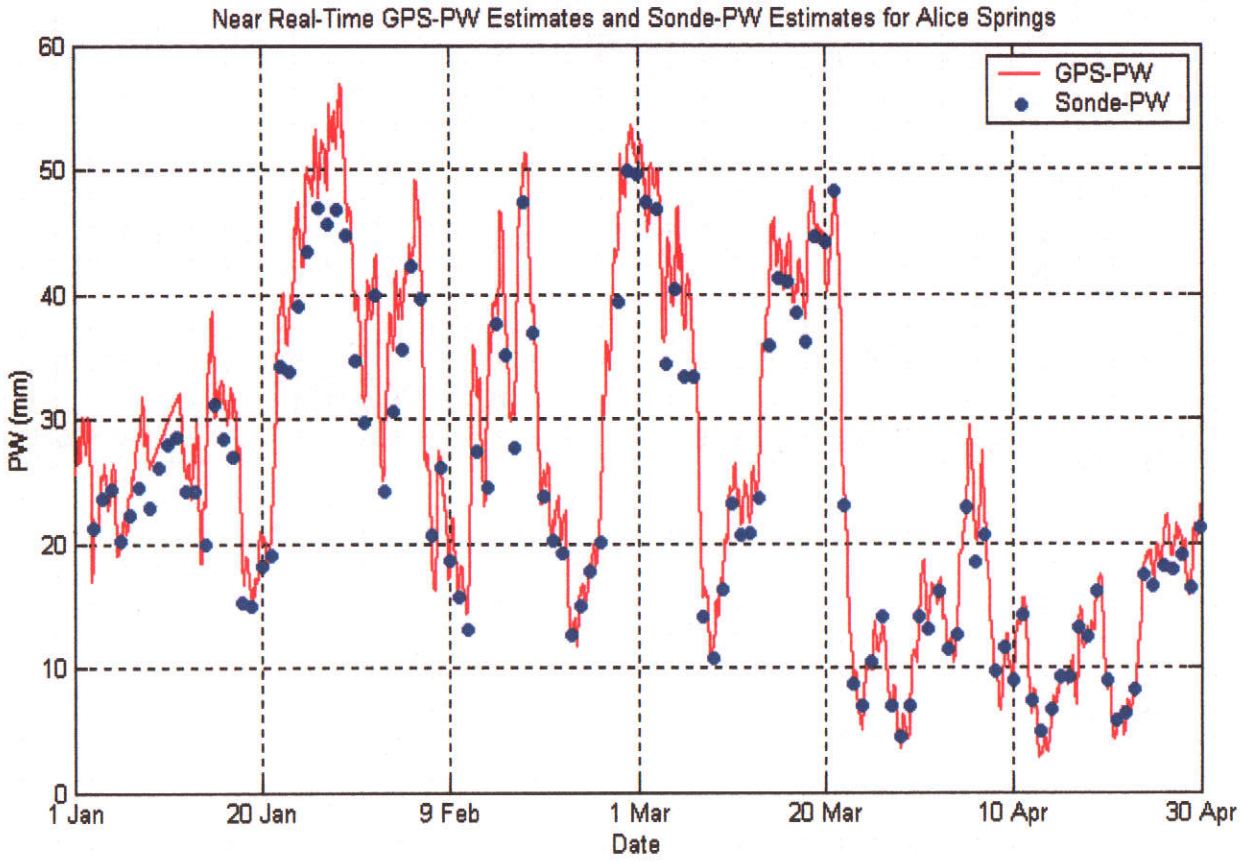

Comparison of GPS-IPW and Radiosonde-IPW for Alice Springs

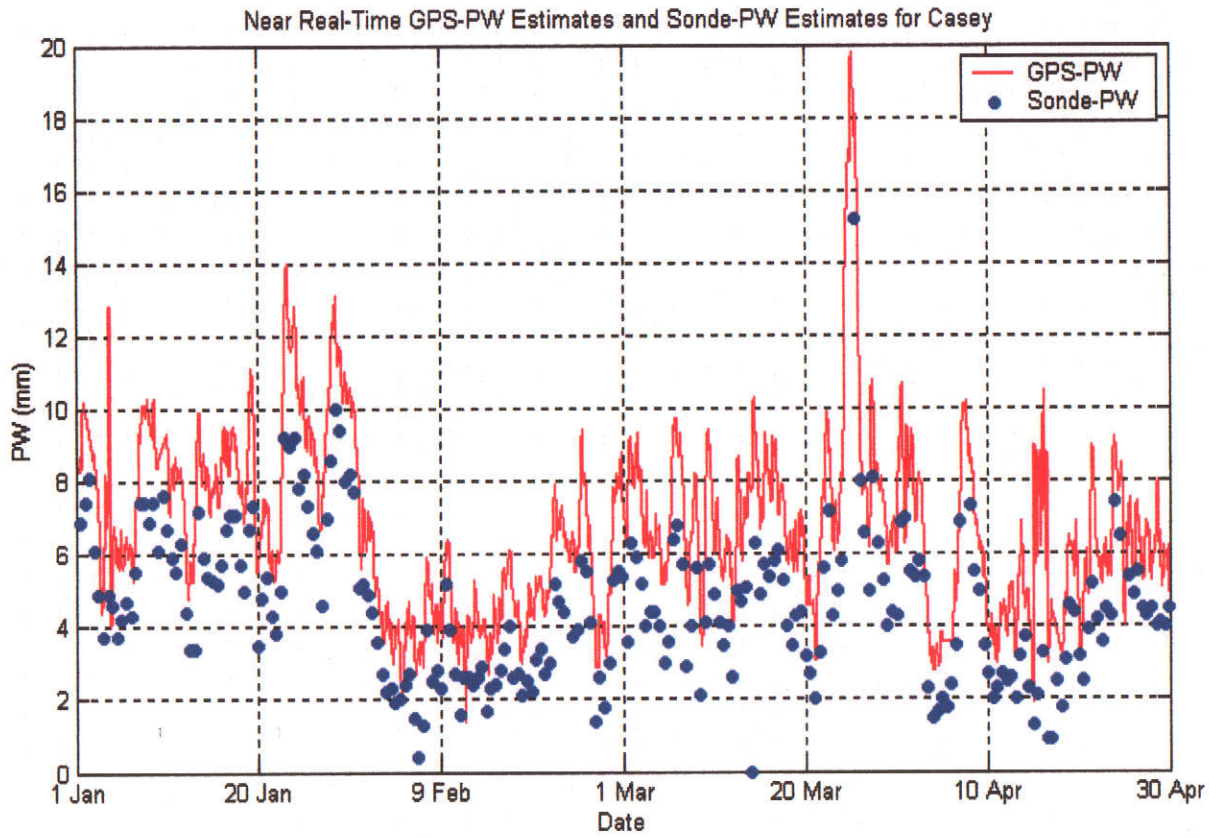

Comparison of GPS-IPW and Radiosonde-IPW for Casey

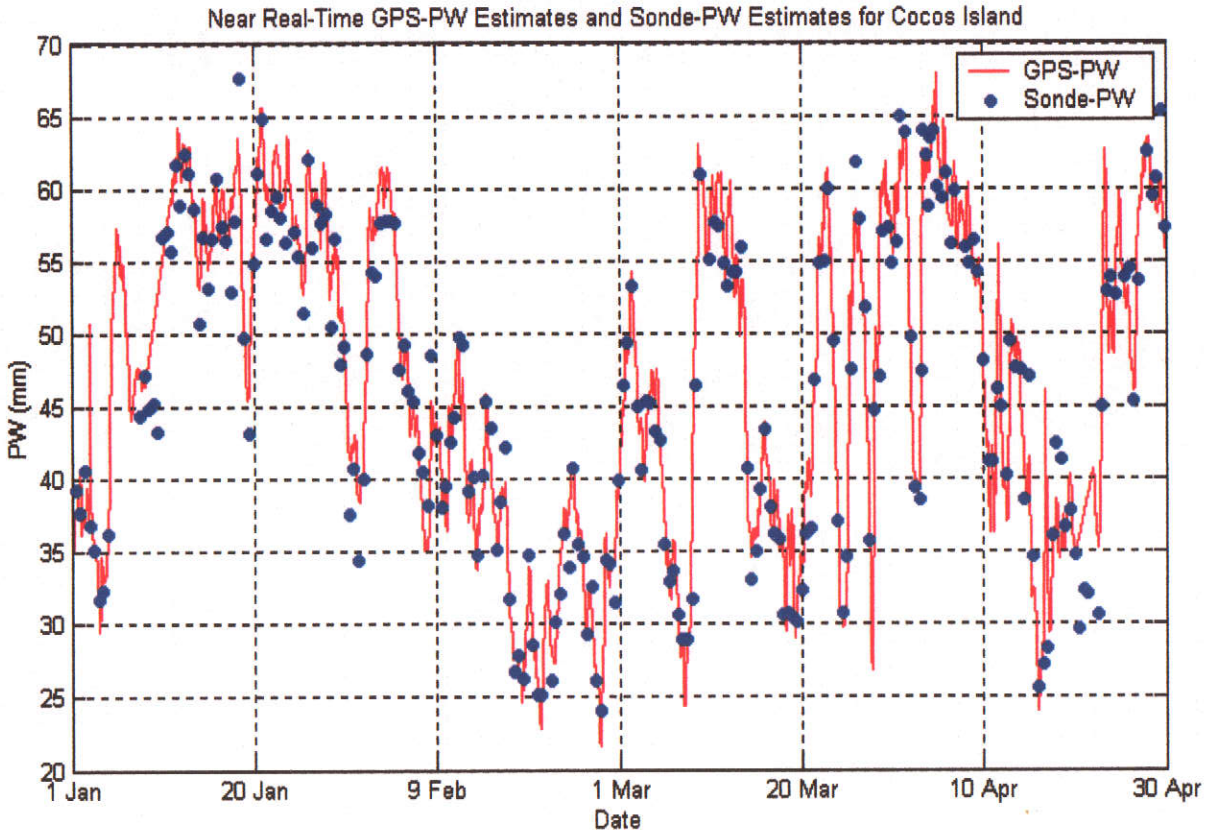

Comparison of GPS-IPW and Radiosonde-IPW for Cocos Island

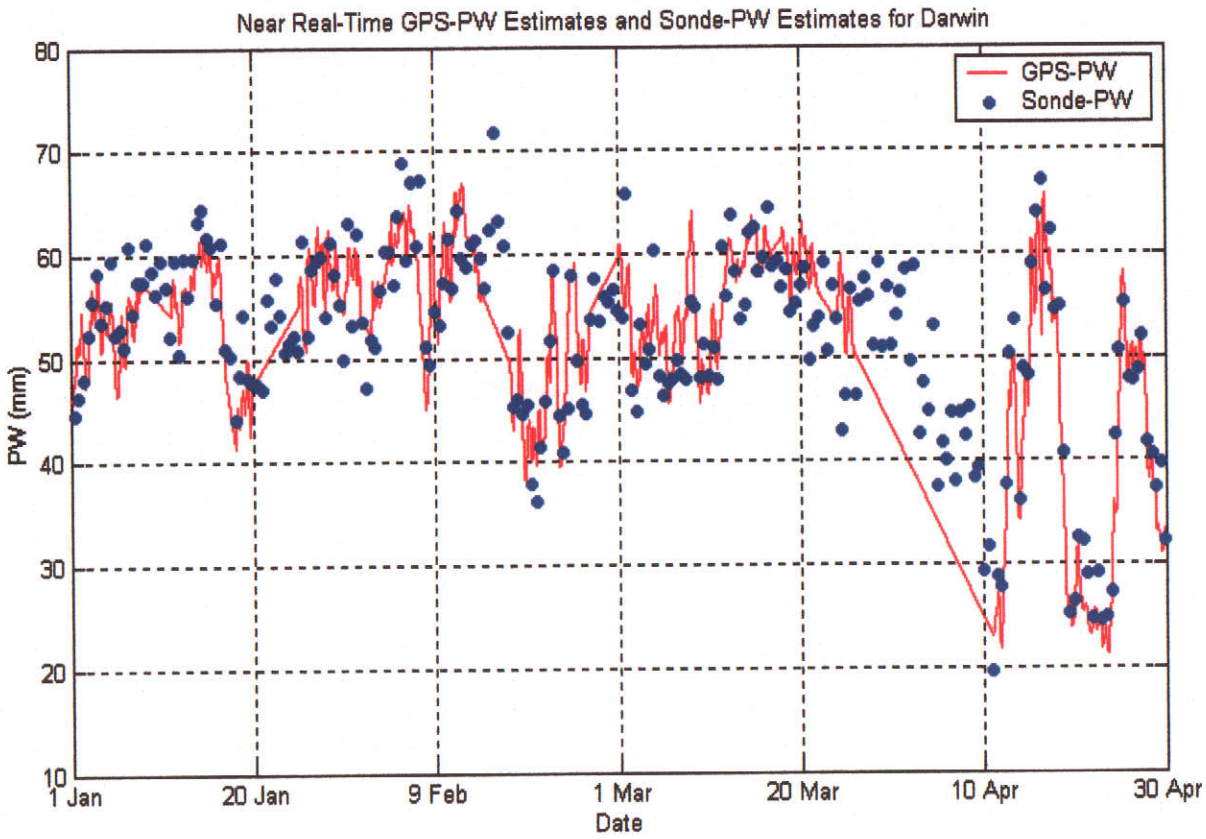

Comparison of GPS-IPW and Radiosonde-IPW for Darwin

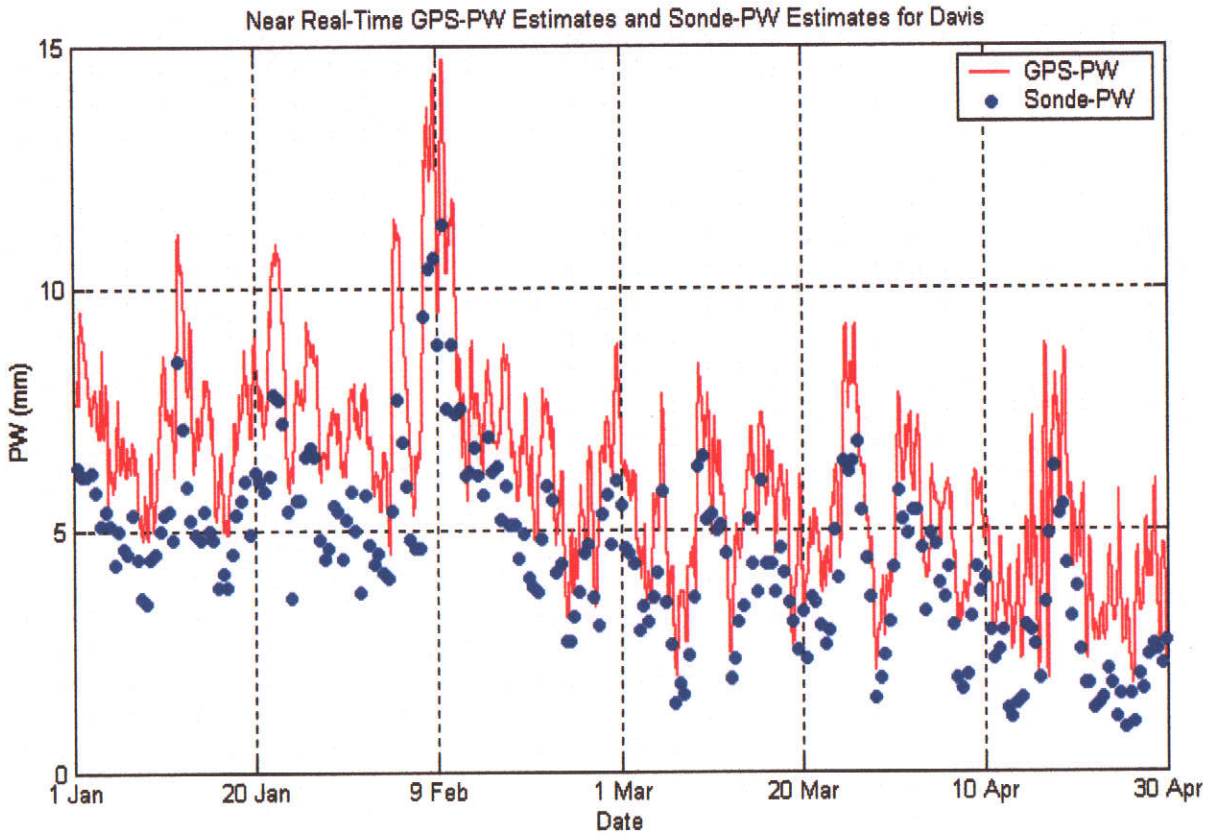

Comparison of GPS-IPW and Radiosonde-IPW for Davis

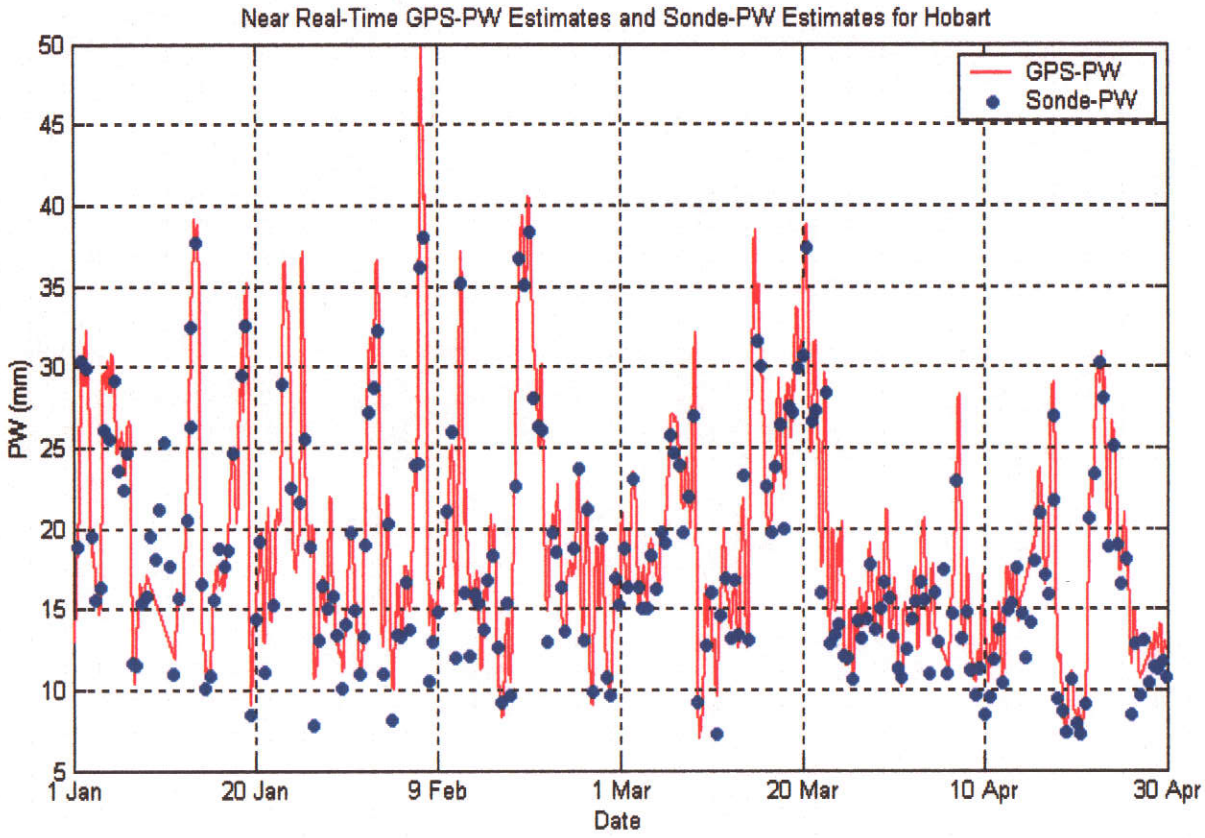

Comparison of GPS-IPW and Radiosonde-IPW for Hobart

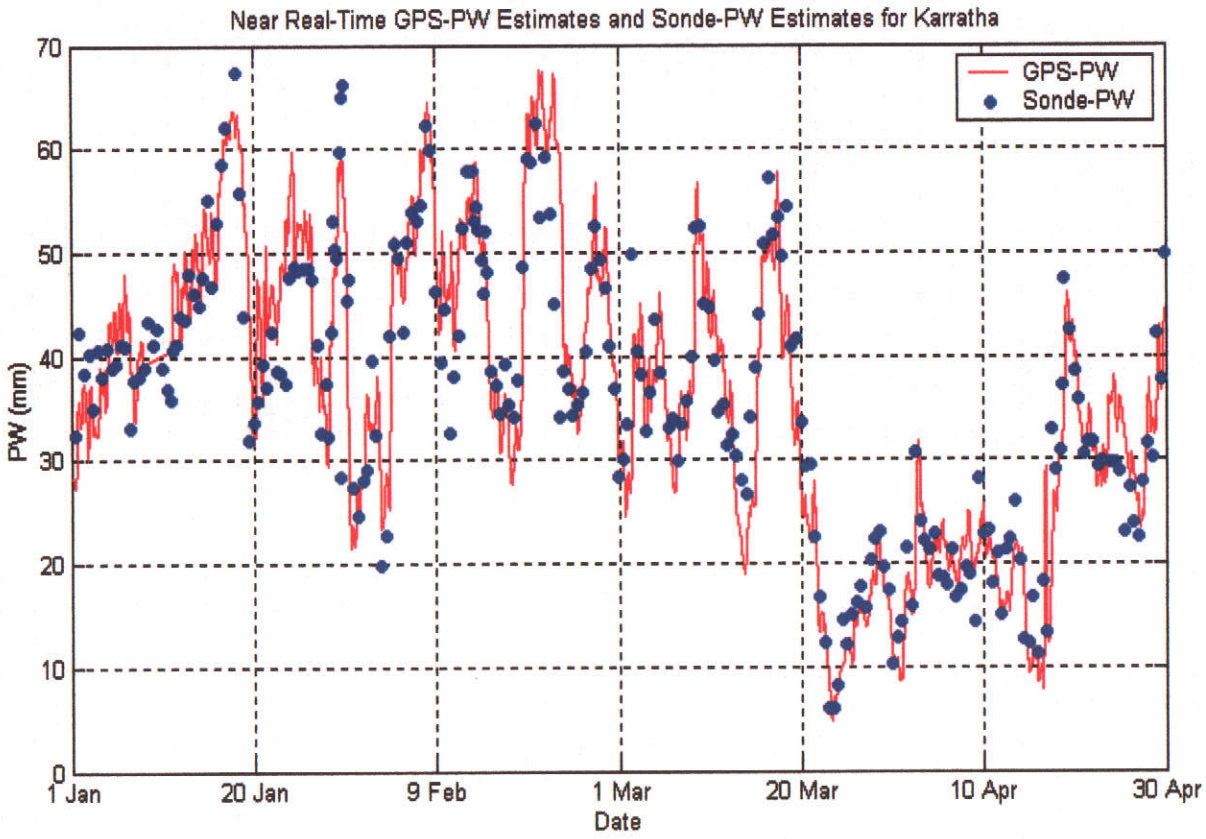

Comparison of GPS-IPW and Radiosonde-IPW for Karratha

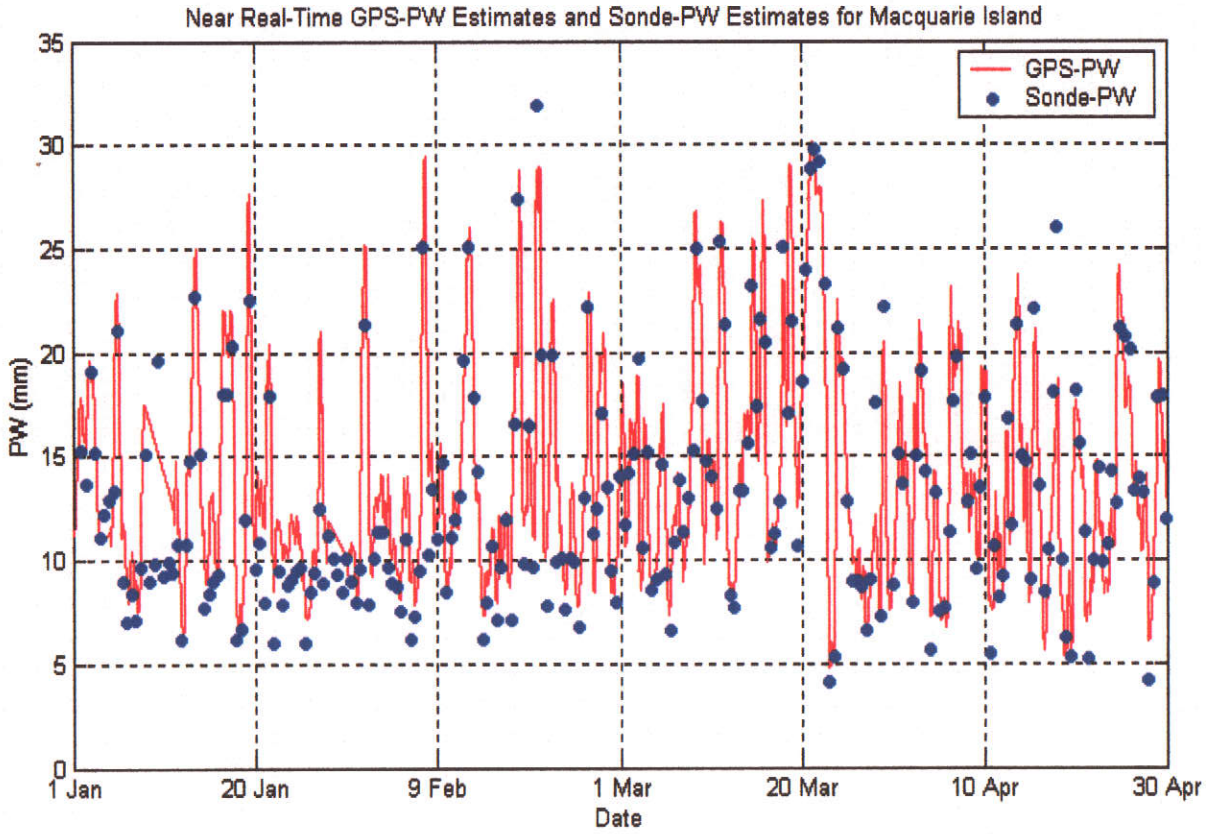

Comparison of GPS-IPW and Radiosonde-IPW for Macquarie Island

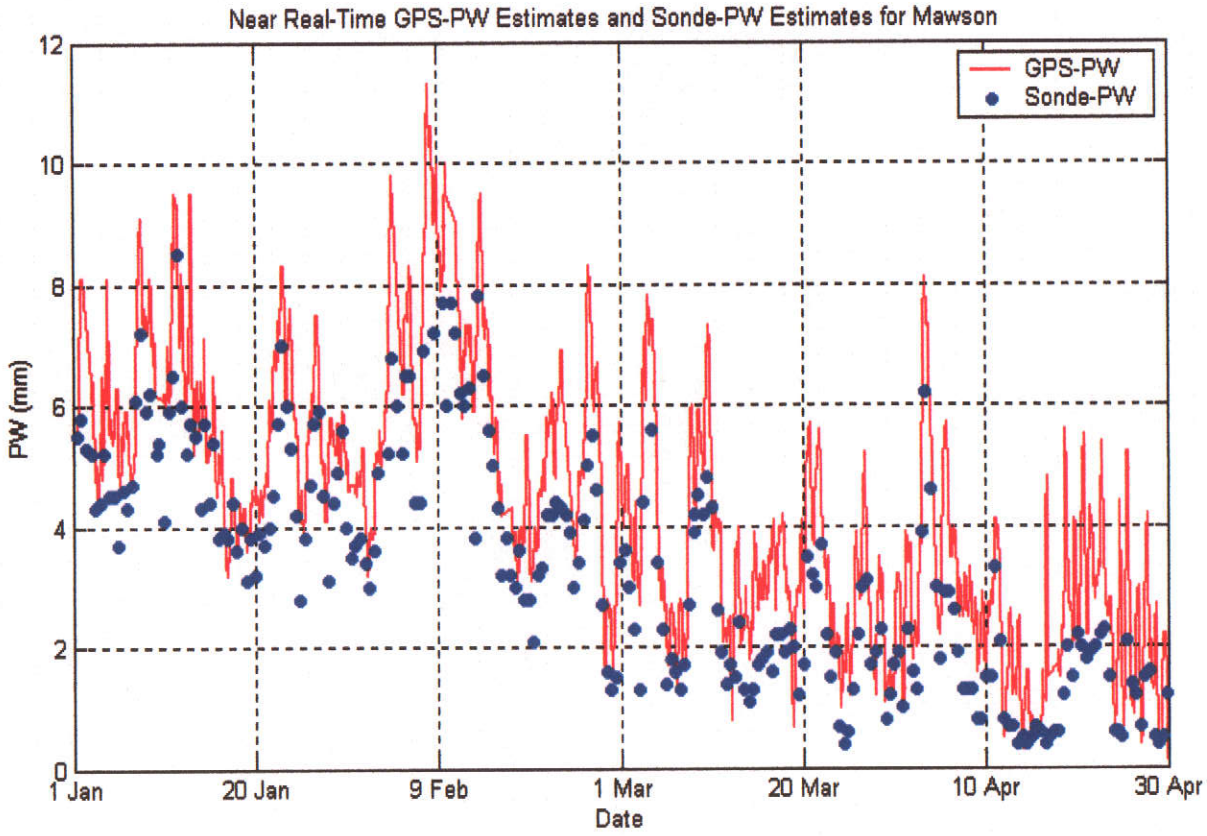

Comparison of GPS-IPW and Radiosonde-IPW for Mawson

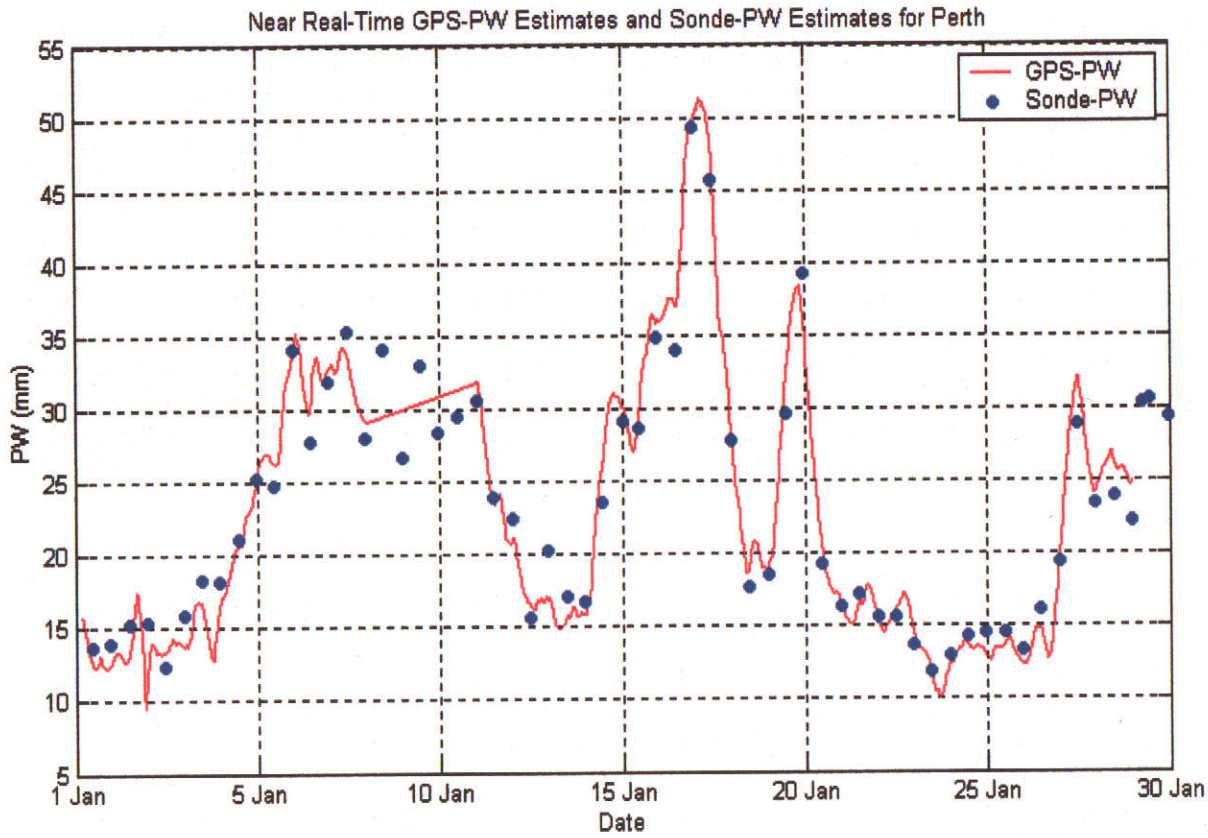

Comparison of GPS-IPW and Radiosonde-IPW for Perth

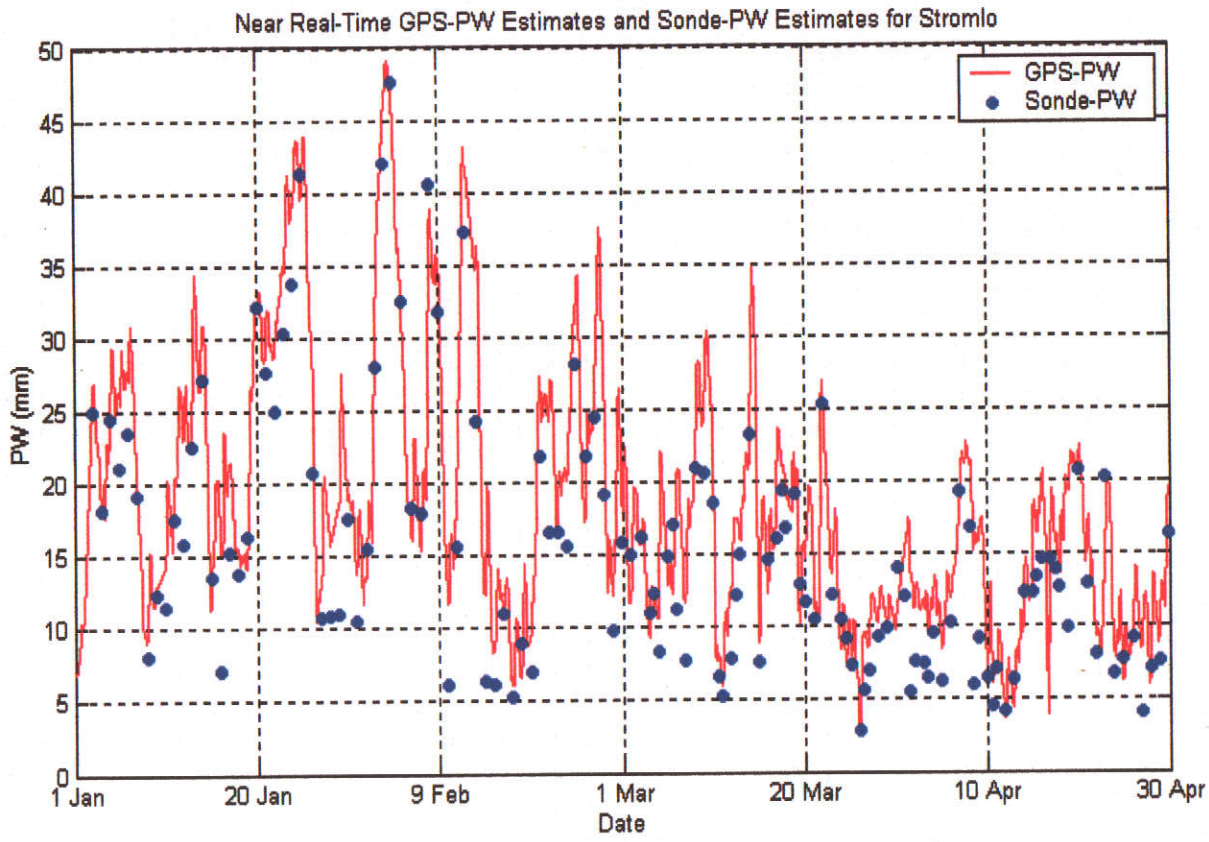

Comparison of GPS-IPW and Radiosonde-IPW for Stromlo

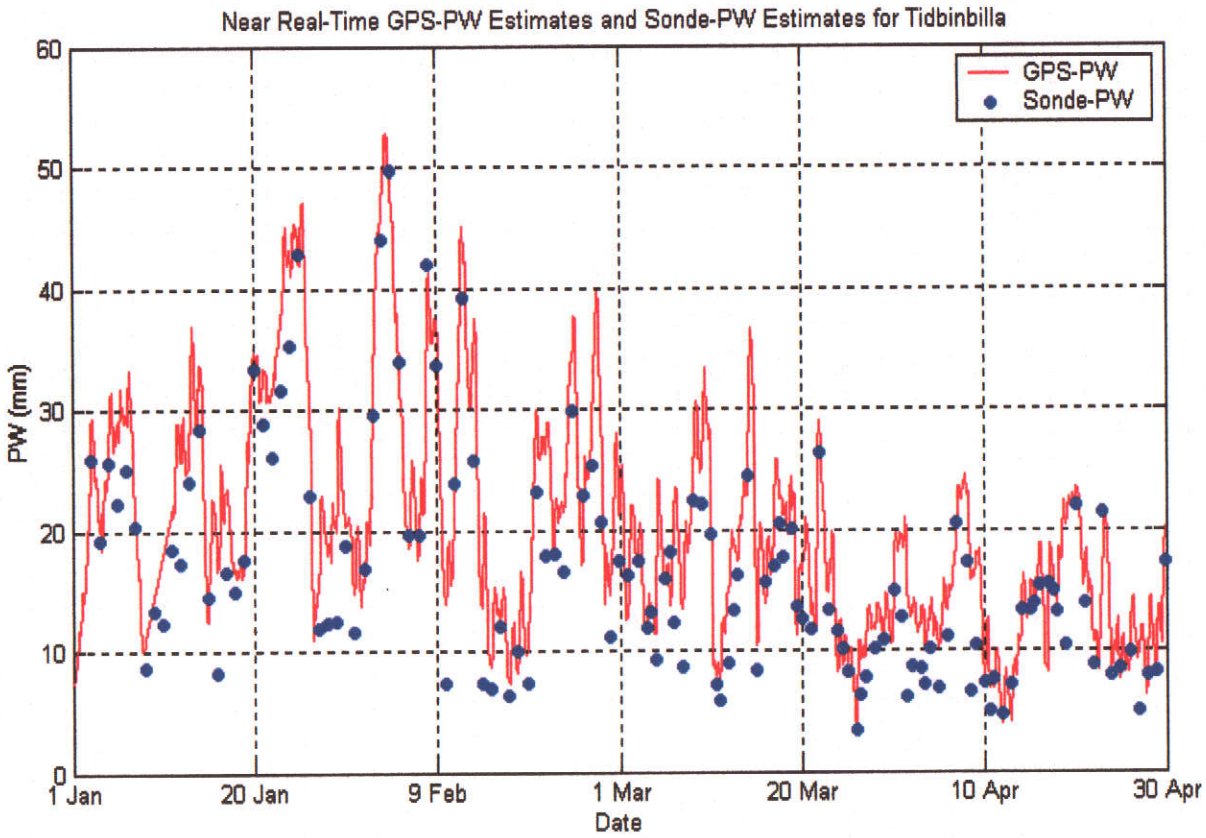

Comparison of GPS-IPW and Radiosonde-IPW for Tidbinbilla

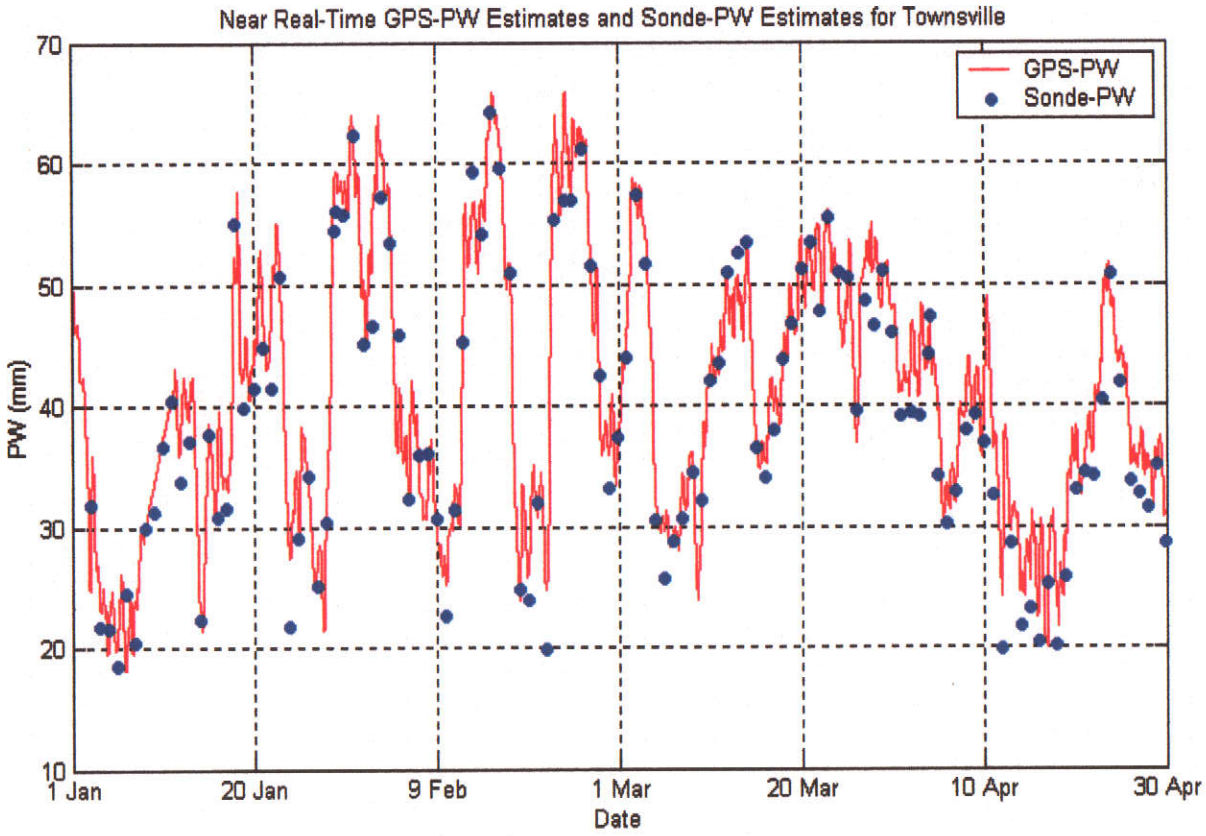

Comparison of GPS-IPW and Radiosonde-IPW for Townsville

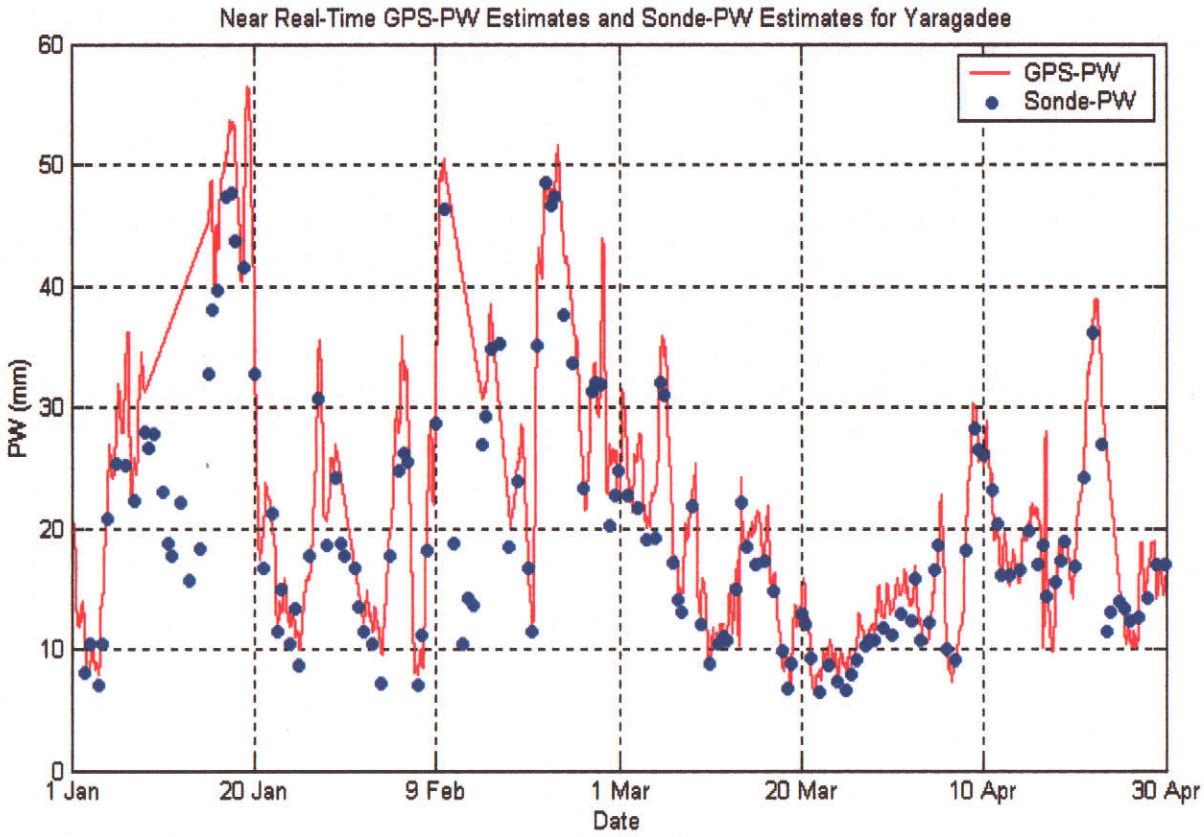

Comparison of GPS-IPW and Radiosonde-IPW for Yaragadee

APPENDIX C

SATELLITE APRIORI SIGMA FOR DOWN-WEIGHTING STRATEGY

Date	Satellite Number (PRN)																											PRN
	1	2	3	4	5	6	7	8	9	10	11	13	14	15	17	19	20	21	22	23	24	25	26	27	28	29	30	31	and σ
1-Jan	7	7	8	8	6	7	10	8	6	7	7	7	8	7		7	8	6	7	9	6	8	8		7		6	8	7=0.05
2-Jan	8	7	8	7	6	8	8	7	7	8	7	7	7	7	6	6	8	7	7	8	7	6	7	6	8	7	7	8	
3-Jan	7	6	6	7	7	7	7	6	7	7	8	7	7	0	7	8	8	6	6	8	6	7	8	6	6	7	6	6	
4-Jan	8	7	7	6	6	6	8	5	7	6	7	7	6	0	6	11	7	6	5	7	7	7	6	6	7	9	6	7	19=0.16
5-Jan	6	7	6	7	5	7	8	7		7	7	7	7	6	6	11	7	7	7	6	12	7	8	7	6		6	7	24=0.23
6-Jan	8	7	6	7	7	7	7	6		9	6	7	7	7		7	8	6	6	8	10	6	8	6	6	7	6	7	24=0.08
7-Jan	7	7	6	7	6	5	7	7		8	8	8	7	7		6	6	6	7	8	8	7	7	7	7	6	6	7	
8-Jan	8	9	6	7	7	6	8	7		9	7	8	7	6	7	7	6	7	7	8	9	7	7	7	6	7	7	6	24=0.05
9-Jan	6	6	6	7	6	6	7	6	6	7	7	7	7	6	6	6	7	6	6	9	9	7	7	6	7	8	5	6	24=0.08
10-Jan	6	7	6	7	6	7	8	6	7	9	8	7	7	6	7	8	6	6	7	8	9	6	7	8	6	6	6	7	24=0.05
11-Jan	8	7	6	6	6	7	6	7	7	9	7	8	7	6	8	7	7	6	7	7	7	7	7	7	7	7	7	6	10=0.05
12-Jan	7	7	7	6	6	7	7	6	6	8	7	7	8	8	7	7	7	6	7	7	7	6	8	7	7	9	7	7	29=0.05
13-Jan	7	7	7	8	7	7	6	7	7	8	8	7	8	7	9	7	8	8	7	7	7	8	8	7	6		6	8	17=0.05
14-Jan	7	6	5	7	6	6	6	7	6	8	7	7	8		8	7	7	6	6	7	7	6	7	6	7		6	6	
15-Jan	8	6	6	7	7	7	7	6	6	7	6	7	7			6	8	6	7	7	6	6	8	6	8		7	7	
16-Jan	8	6	6	7	7	6	6	8	7	6	7	8	7	7		7	7	6	7	7	8	6	6	6	7		6	6	
17-Jan	8	6	5	9	7	6	6	7	6	8	6	8	7				7	10	7	7	8	6	7	7	6		6	7	21=0.11
18-Jan	8	6	6	7	6	6	6	7	7	5	6	8	7				6	7	6	8	8	7	7	6	7	7	5	7	
19-Jan	8	8	6	6	5	8	6	6	7	7	7	7	8	8		7	7		7	8	7	6	8	6	6	8	5	5	
20-Jan	8	7	6	7	6	6	5	7	5	6	8	8	7	8	8	7	7		6	8	6	7	7	6	6	8	6	6	
21-Jan	7	7	6	6	5	6	6	6	5	6	7	8	6		7	5	6		6	8	6	6	6	5	6	7	5	6	
22-Jan	7	7	5	6	6	7	6	6	6	8	8	8	7		7	7	7		7	7	7	6	6	6	6	6	6	6	
23-Jan	7	7	6	7	7	6	7	8	6	8	8	8	7	8	7	6	7	8	6	8	7	6	7	7	6	7	6	6	
24-Jan	8	7	6	7	7	6	6	7	7	9	6	7	9		10	10	10	9	6	6		8	7	7	7	6	7	7	19=0.04
25-Jan	7	7	6	7	7	6	7	6	6	9	7	7	11		8	10			7	9	7	7	8	7	8	7	6	6	14=0.11
26-Jan	11	8	7	7	7	7	8	8	7	9	7	7	8		9	8	9	9	9			9	7	8	7	8	7	8	17=0.04
27 Jan	7	6	6	6	7	7	6	6	7	7	6	7	7		13	10	6	7	7	8	8	8	8	7	7	7	6	7	17=0.23
28 Jan	7	7	7	6	6	6	7	6	6	7	7	6	8			6	7	7	6	7	7	6	7	6	7	7	6	7	
29 Jan	7	7	6	6	6	5	5	7	6	7	7	6	7		8	6	7		6	9	7	5	8	6	7	7	6	6	
30-Jan	7	6	6	7	5	6	6	6	6	5	7	7	7		7	6	8		6		7	6	7	6	5	7	5	7	
31-Jan	8	7	10	7	6	6	6	7	6	6	8	6	6		6	7	7	8	7	6	6	6	7	6	6	6	6	7	3=0.08
1-Feb	7	8	7	7	6	6	6	7	7	7	8	7	7		7		8	6	6	8	8	6	7	6	6	7	5	7	
2-Feb	7	6	7	7	7	6	7	6	7	7	7	7	6		6		8		6		7	6	7	6	6	6	6	6	
3-Feb	7	7	7	7	6	7	8	6	6	9	7	7	7		6	7	7		7	8	7	7	8	6	7	6	6	7	10=0.05
4-Feb	8	7	7	7	7	8	7	7	7	10	8	7	7		7	7	8	7	7	7	7	7	7	7	7	7	6	7	10=0.08
5-Feb	8	7	7	7	7	7	6	7	7	8	7	6	8		8	8	7	8	6	7	8	7	8	8	7	8	8	6	
6-Feb	7	7	7	8	7	7	8	7	7	8	7	7	8			7	8		8	8	8	7	8	8	7	7	7	7	
7-Feb	5	6	6	7	6	6	6	6	6	7	7	6	7			8	7		6	6	7	6	5	6	6	6	6	7	
8-Feb	5	5	6	7	7	6	6	6	7	8	8	6	6		7	6	6		7	7	7	6	7	6	6	7	6	7	
9-Feb	6	8	6	7	5	6	7	7	6	6	7	7	6		9		7	7	6		7	6	6	7	7	6	6	6	17=0.05
10-Feb	7	8	9	8	7	6	8	7	8	9	8	7	7		8	7	8	10	8		9	7	7	8	8	7	7	6	21=0.08
11-Feb	9	8	8	7	8	8	8	8	7	7	9	8	7		9	9	8		9	9	7	7	7	8	9	8	7	8	17=0.04
12-Feb	6	6	5	7	6	6	7	7	6	8	7	7	8			7	6		7	7	8	6	9	7	6	7	6	7	26=0.08
13-Feb	7	7	7	7	6	7	7	6	8	8	7	7	7			8	7	6	7	7	8	6	7	7	7	6	6	7	
14-Feb	7	7	8	7	7	6	7	7	7	7	7	7	7			8	6		7	8	8	6	7	7	8	7	7	7	
15-Feb	7	8	8	8	7	6	7	8	7	7	6	8	7		10	8	7	12	8	7	7	7	7	8	7	8	7	7	21=0.16
16-Feb	6	8	7	8	6	6	7	7	7	8	8	6	7			7	7	7	7	7	8	7	8	7	7	7	6	7	
17-Feb	7	8	6	7	5	7	6	7	7	8	8	7	7				6	7	7	8	9	7	8	7	7	8	7	8	24=0.08
18-Feb	7	8	7	7	7	8	7	8	7	8	9	6	7			10	7		7			8	7	7	6	7	8	8	19=0.08
19-Feb	5	6	7	7	7	7	6	6	7	8	7	6	7			10	6	8	7	8	8	7	7	7	7	6	7	6	19=0.08
20-Feb	7	7	6	7	6	6	7	6	7	8	7	7	6			7	7	7	7	7	9	6	8	6	6	6	5	6	23=0.08
21-Feb	7	7	7	8	6	7	7	8	8	7	7	7	7				7		7	7		7	6	7	7	7	7	7	

22-Feb	7	7	7	7	7	7	7	7	8	7	7	7	7				7		6	9		7	7	7	6	7	7	7	23=0 05
23-Feb	8	7	6	7	7	6	7	10	7	7	8	7	7				6	7	7	8		7	7	7	7	7	7	7	8=0 08
24-Feb	7	7	7	7	6	6	7	7	8	8	7	7	7				6		8	7		7	7	7	7	6	6	7	
25-Feb	6	7	6	7	6	7	7	8	7	9	7	6	6			8	6		6			7	7	7	7	6	7	7	10=0.05
26-Feb	6	8	6	7	7	6	6	8	7	6	7	6	6				6	7	7	7		7	6	7	7	6	6	7	
27-Feb	6	7	6	7	6		7	7	8	7	8	7	7				6	8	6	8		8	7	8	6	7	6	6	18=0.16
28-Feb	7	7	7	8	7		6	8	7	7	7	7	8				7		7	8		8	8	8	7	8	6	7	
1-Mar	7	7	6	7	7		7	7	7	6	7		6				7	8	6	7		7	7	8	7	7	6	6	18=0.05
2-Mar	6	6	6	7	6		6	7	7	7	7		7			8	7		6	8	9	7	6	8	5	7	6	7	18=0.05
3-Mar	6	6	7	8	6		6	7	8	7	8		7		10	9	7		7	7	7	6	6	6	6	6	7	7	17=0.08
4-Mar	8	8	7	8	7	7	7	8	7	6	7	8	6			7	6	8	7	7	7	7	7	7	6	5	7	7	
5-Mar	6	7	6	8	6	8	7	7	8	8	7		6			7	6	8	6	9		7	8	7	6	6	6	7	18=0.05
6-Mar	7	7	6	7	6	7	6	8	8	6	7	8	7				6		6		9	7	9	8	7	6	6	7	18=0 05
7-Mar	6	6	6	8	6	6	8	7	8	7	8	6	7				6		6		8	7	9	7	5	7	6	7	26=0 08
8-Mar	6	7	7	8	6	7	6	8	7	7	8	7	7		7		6		6	9	7	7	9	7	6	6	6	7	26=0 08
9-Mar	6	7	7	8	7	7	7	7	7	8	6	7	6			8	6	9	7	7		6	8	6	6	7	6	7	21=0 05
10-Mar	6	7	6	7	7	6	7	8	7	7	7	6	6			8	7	7	6			6	7	7	7	7	6	6	
11-Mar	6	7	7	7	6	8	7	7	7	7	7	6	7			7	6		6		7	7	7	7	6	6	6	7	
12-Mar	7	7	7	7	6	7	8	8	8	8	7	7	7			9	6	9	7	8	7	7	8	9	8	8	7	8	19=0.05
13-Mar	6	7	7	7	6	7	7	7	7	6	7	7	7			7	7		6	10	7	7	7	7	7	6	6	6	24=0.08
14-Mar	6	7	8	8	6	6	6	7	7	7	7	6	7			7	7		7	8	7	7	6	7	7	6	6	7	
15-Mar	6	7	7	8	7	6	7	7	7	7	7	6	7			7	6	6	7	7	7	7	8	8	7	7	7	6	
16-Mar	5	7	7	7	6	7	7	7	7	7	7	6	7			8	7	8	6	8	7	7	7	8	6	7	6	6	
17-Mar	6	7	8	7	6	6	6	8	7	7	7	6	7			7	6	9	6	8	7	6	7	6	6	7	6	7	21=0.05
18-Mar	6	6	7	8	6	7	6	8	7	6	6	6	7			9	6	7	6	9	7	7	8	6	6	6	6	6	23=0.05
19-Mar	6	7	7	6	6	6	6	7	7	8	7	6	8			9	6		7	7	7	6	6	7	6	7	6	7	19=0.05
20-Mar	8	8	8	8	8	8	9	9		8	8	9	8			8	9		8		10	8	8	10	8	8	8	8	24=0.04
21-Mar	6	7	7	7	6	6	7	6	6	7	6	6	7			9	7		7	8	8	6	7	6	6	7	6	6	19=0.05
22-Mar	5	7	6	6	7	7	7	8	7	6	6	7	6			7	6	9	6	8	7	6	8	7	7	6	9	6	20=0.05
23-Mar	6	7	7	7	7	7	5	7	7	6	6	6	7			8	6	9	6		7	7	6	7	6	7	7	6	20=0.05
24-Mar	6	6	6	6	6	6	6	7	7	7	6	6	6			7	6	7	6		6	6	7	6	6	6	7	6	
25-Mar	6	6	6	6	7	6	6	6	6	7	7	7	7			6	7		6		6	7	8	6	6	7	6	6	
26-Mar	6	7	6	7	7	7	7	6	7	8	9	6	7			9	6	8	6	9	7	7	7	6	6	8	7	6	23=0.05
27-Mar	6	7	7	7	6	7	6	6	7	8	6	6	6			7	6	8	7	9	6	7	7	5		7	7	6	23=0.05
28-Mar	6	8	6	7	6	7	6	6	7	7	7	6	7			7	7	7	7		6	6	8	7		7	6	6	
29-Mar	6	6	7	6	6	6	6	6	6	7	6	6	6			10	6		6		5	6	9	6		6	6	6	19=0.11
30-Mar	6	6	6	5	6	7	5	7	7	7	6	6	7			14	6		6		6	7	6	7	7	5	7	6	19=0.45
31-Mar	6	7	6	8	7	7	7	6	7	7	10	6	8				8	10	6	9	6	7	9	6	6	8	7	7	21=0.08
1-Apr	6	6	6	6	7	7	5	5	7	8	10	6	6				6		6		7	7	7	5	6	6	7	6	11=0.11
2-Apr	7	6	6	6	6	7	7	7	7	6	6	6	6			7	6		6		6	7	7	5	7	7	7	7	
3-Apr	6	7	9	7	6	6	6	7	6		6	6	7			6	6	8	7		7	6	8	6	6	6	6	7	3=0.05
4-Apr	6	7	5	7	6	6	6	6	6		10	6	6			7	5	7	8		6	7	5	6	6	6	6	7	11=0.11
5-Apr	8	7	7	7	6	6	6	7	8	9	7	7	7			7	7		7	9	7	8	7	6	6	8	6	7	18=0.08
6-Apr	6	8	6	7	8	7	8	6	7	6	7	6	9			7	6		7		7	8	6	6	7	9	7	6	14=0.05
7-Apr	6	7	6	6	8	6	7	6	7	6	6	6	8			6	7	8	7		7	6	7	6	6	7	7	6	
8-Apr	5	7	7	5	7	6	6	6	7	6	7	7	7			7	6		7		7	7	7	6	7	7	7	7	
9-Apr	6	7	7	6	8	7	7	6	6	7	6	6	6			7	6		7		6	5	7	6	7	8	8	7	
10-Apr	6	7	6	7	7	6	6	6	7	7	6	6	7			7	6		7		6	6	6	6	7	7	8	6	
11-Apr	5	7	6	6	6	6	6	6	6	7	6	6	6	7		7	6		7		6	6	6	6	6	7	7	7	
12-Apr	6		7	7	7	6	6	7	6	6	7	6	6	7		7	6	7	7	9	6	7	7	6	8	6	7	7	23=0.05
13-Apr	7	10	8	7	8	7	6	6	8	7	6	6	8	7		8	6		7		6	8	7	6	8	7	7	7	2=0.08
14-Apr	6	8	8	6	8	6	6	6	6	6	6	6	8	6			6		7	6	6	7	7	5	7	7	7	7	
15-Apr	6		5	6	8	7	6	6	6	6	7	6	7	6			6	9	7	9	7	7	7	6	6	6	7	7	23=0.05
16-Apr	8		8	7	8	7	7	7	9	7	7	7	8	6			7	9	8		8	8	9	13	7	8	7	8	27=0.23

17-Apr	6		6	6	8	6	7	5	6	6	7	5	7	9		7	9		8		6	6	7	6	7	7	7	6	**15=0.08**
18-Apr	5	8	6	6	8	7	7	6	7	6	6	6				7	7	8	8		6	7	6	6	6	6	7	7	
19-Apr	6	7	6	7	7	7	6	7	8	7	6	6		9		7	8		8	7	6	6	7	6	6	6	7	6	**15=0.08**
20-Apr	6	8	7	7	9	7	7	7	7	7	8	6	10	9	9	8	7	8	8	8	7	8	6	6	8	6	9	7	**14=0.08**
21-Apr	8	9	8	8	9	8	9	8	9	8	7	7	7	8			6	7	8	9	8	7	8	7	8	7	10	8	**30=0.05**
22-Apr	8	10	8	8	9		10		10	9								9	9	11	10		8		9	9	10	9	**23=0.05**
23-Apr	5		7	6	7	7	7	5	6	7	7	6	8	8		9	6		8		6	7	6	6	8	7	8	7	**19=0.05**
24-Apr	6		5	7	8	6	7	6	7	7	7	7	8	7		7	7		8		7	7	6	6	7	7	8	6	
25-Apr	6	7	6	5	7	6	6	6	7	7	6	6	7	8		7	6		8		6	6	7	7	7	7	8	7	
26-Apr	7		7	7	7	7	7	7	7	9	8	6	7	8		9	8	7	8	0	8	6	8	7	6	7	8	7	**10=0.05**
27-Apr	6		7	7	7	7	8	6	6	7	7	7	6	7	9	9	6	7	8	9	7	8	7	6	7	6	8	8	**17=0.05**
28-Apr	6		6	7	6	7	6	6	6	7	7	6	7	6		7	6	8	7	7	7	6	7	7	7	6	6	7	
29-Apr	7		6	7	7	6	8	7	6	7	7	6	7	7	9	7	7		6	8	6	6	7	7	7	7	7	7	**17=0.05**
30-Apr	7		8	8	8	7	11	7	8	8	9	7	9	8	8	8	7		8		7	7	7	7	8	8	8	7	**7=0.08**

APPENDIX D

VISUALISATION OF INTERPOLATION GPS-PW ESTIMATES

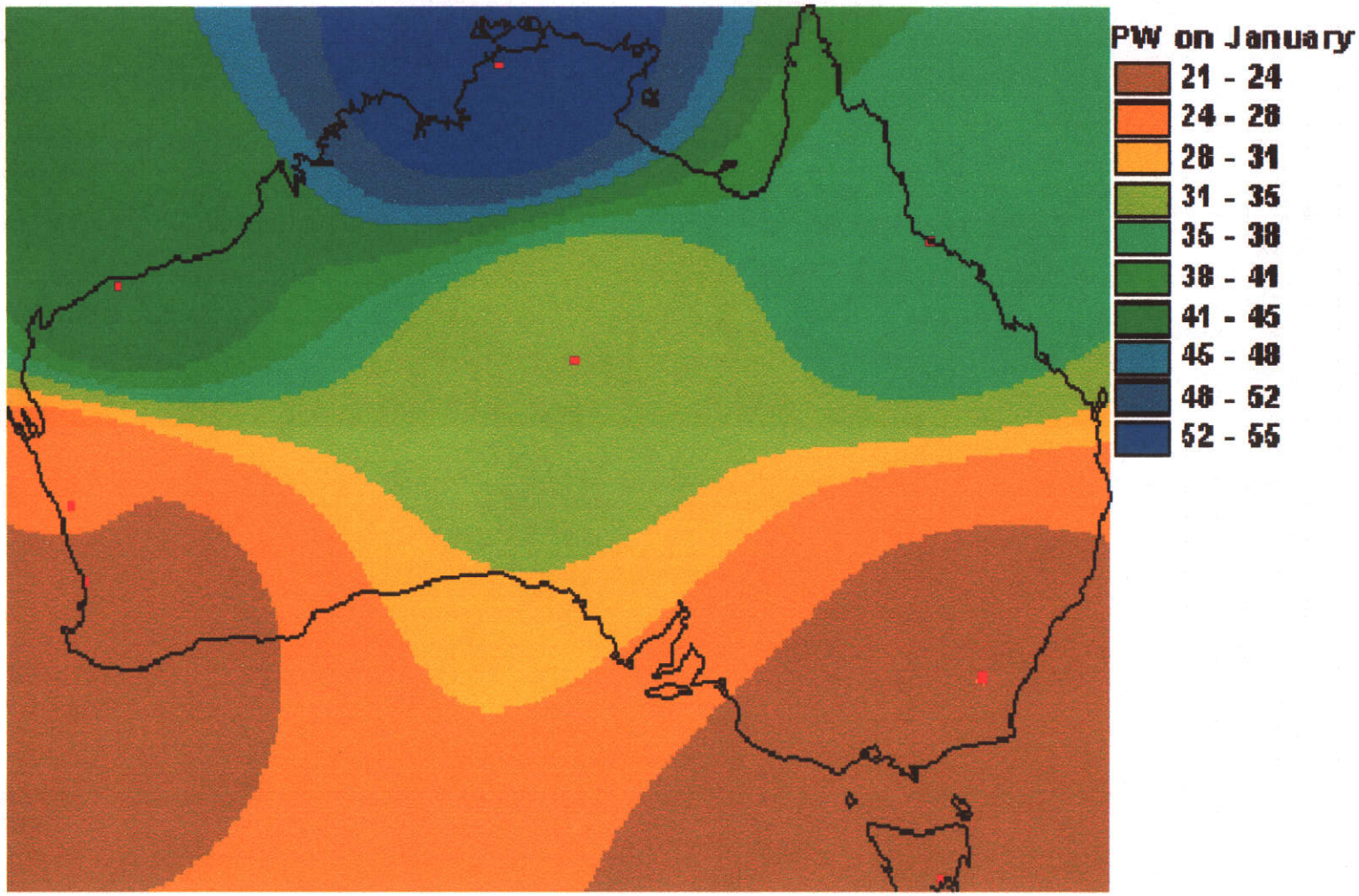
PW on January
21 - 24
24 - 28
28 - 31
31 - 35
35 - 38
38 - 41
41 - 45
45 - 48
48 - 52
52 - 55

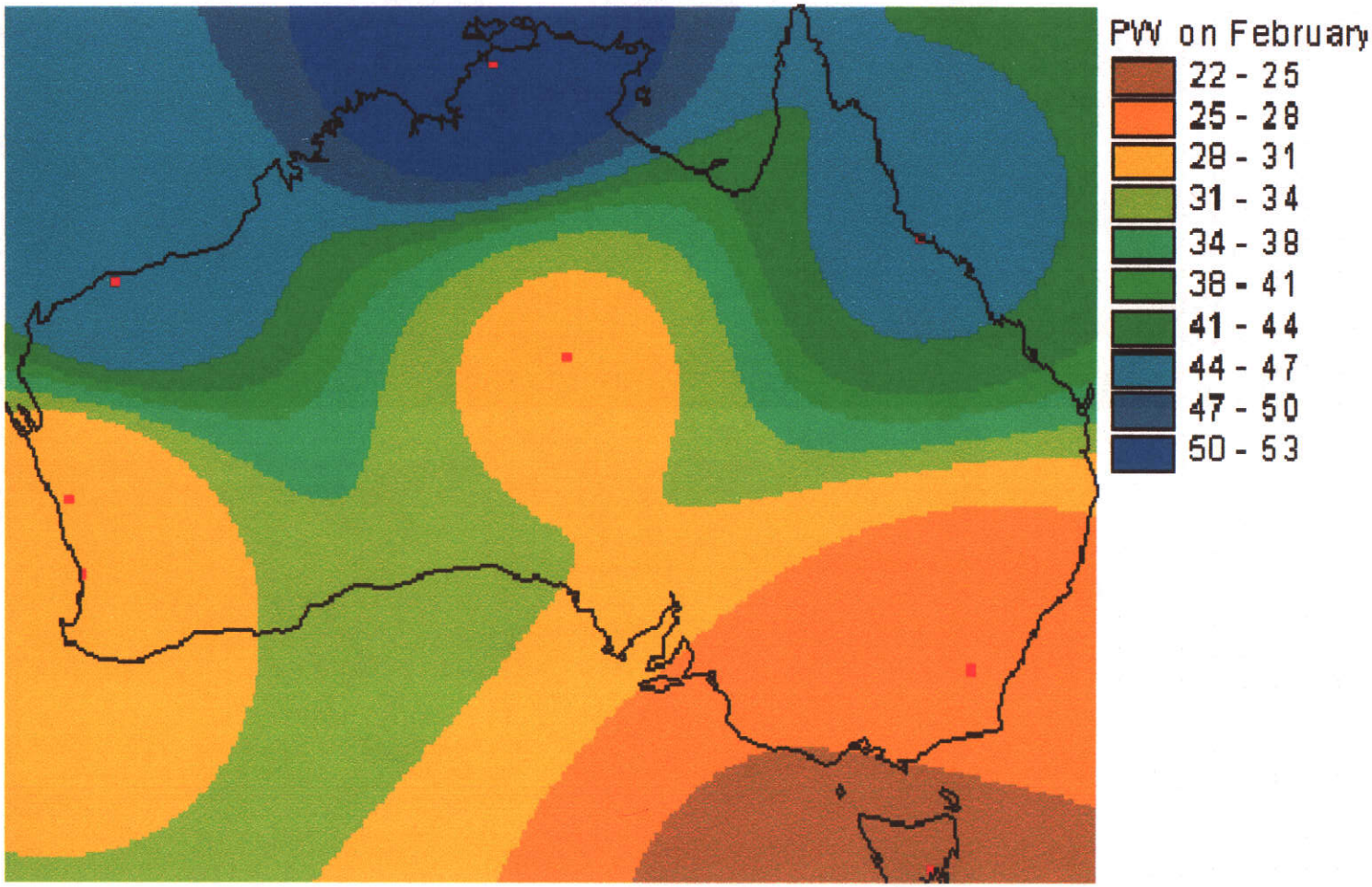
PW on February
22 - 25
25 - 28
28 - 31
31 - 34
34 - 38
38 - 41
41 - 44
44 - 47
47 - 50
50 - 53

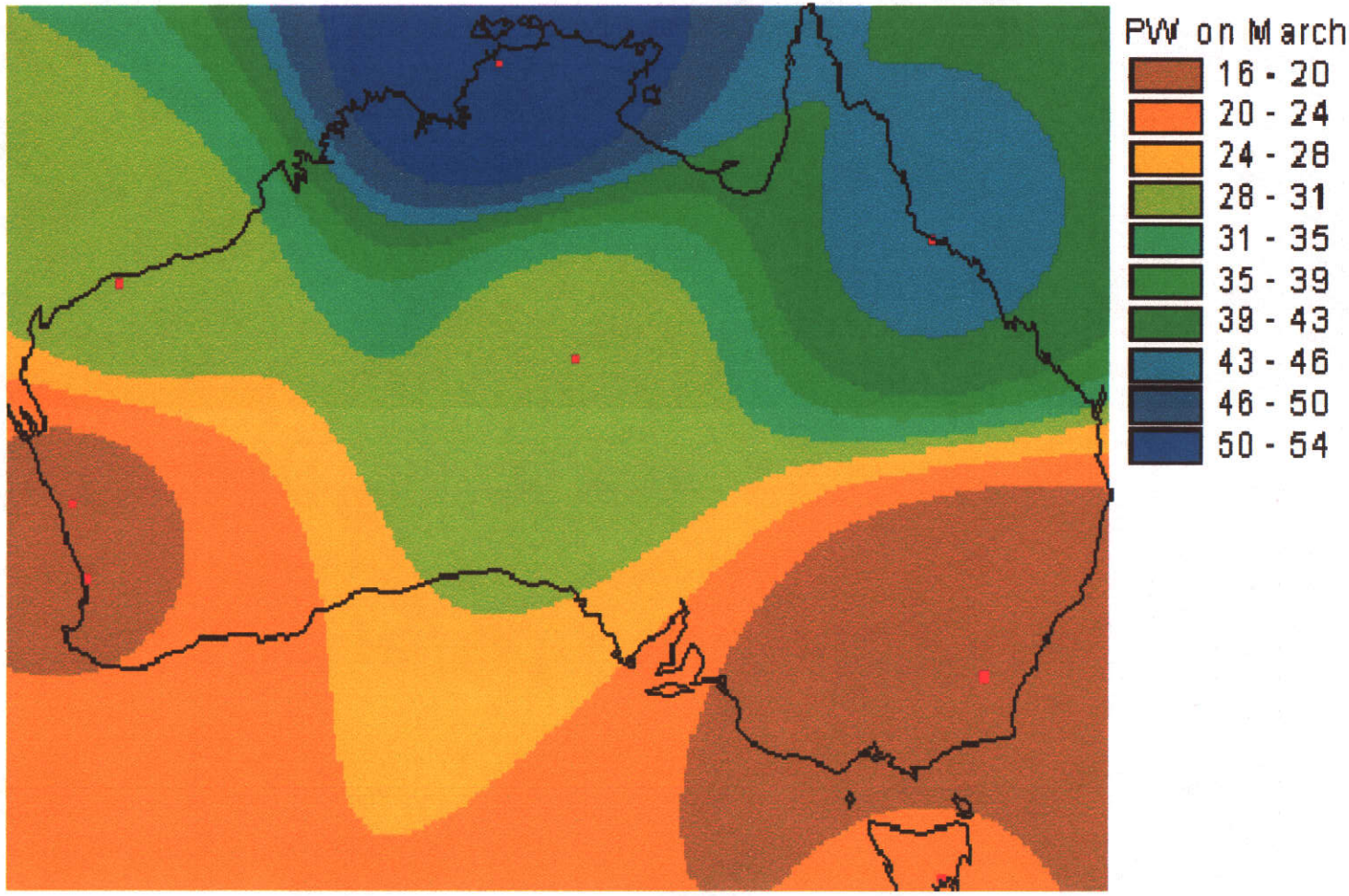
PW on March
16 - 20
20 - 24
24 - 28
28 - 31
31 - 35
35 - 39
39 - 43
43 - 46
46 - 50
50 - 54

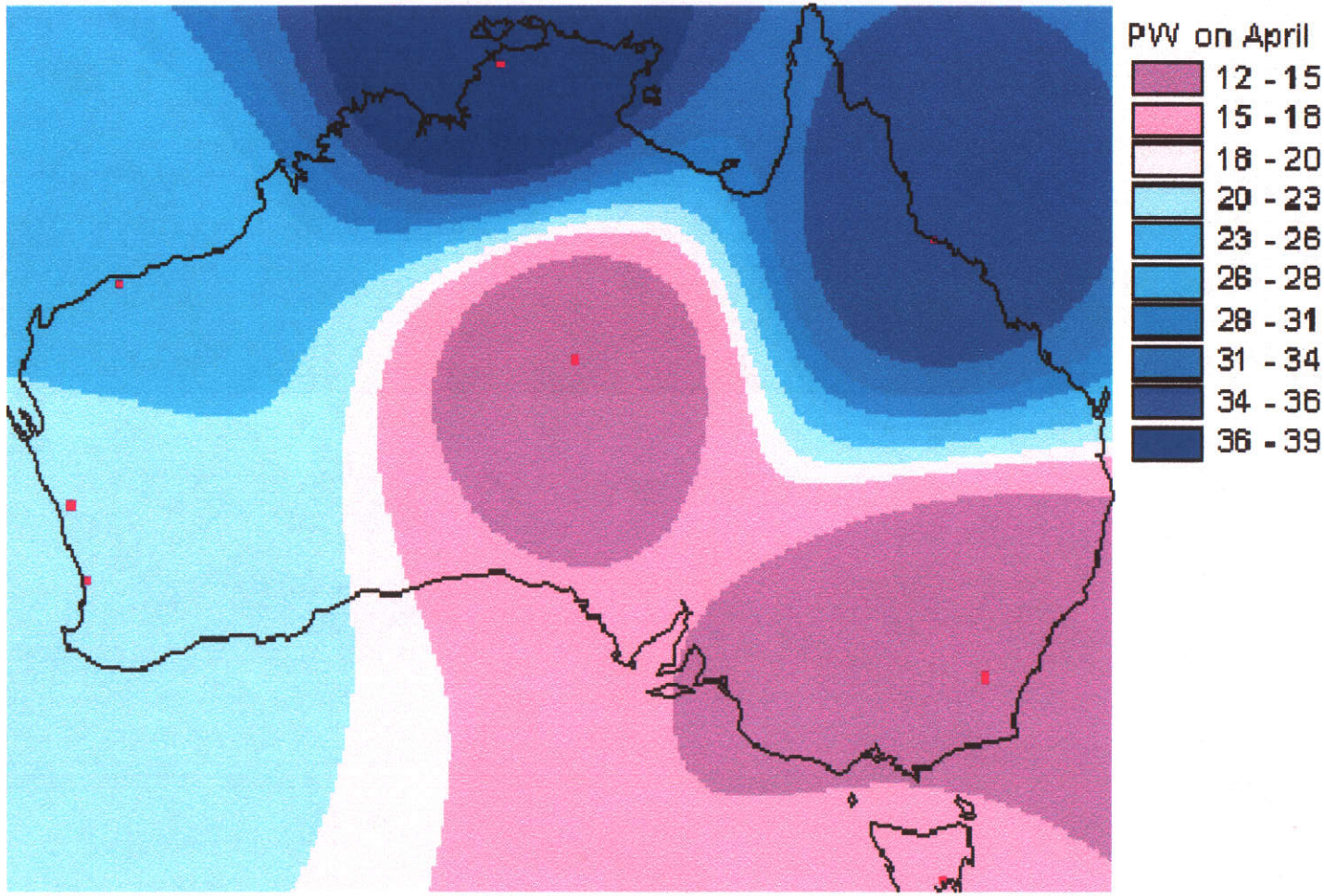
PW on April
12 - 15
15 - 18
18 - 20
20 - 23
23 - 26
26 - 28
28 - 31
31 - 34
34 - 36
36 - 39